Geochemical Perspectives

Volume 1, number 1 | January 2012

Robert Raiswell
Donald E. Canfield

The Iron Biogeochemical Cycle Past and Present

Geochemical Perspectives

Each issue of ***Geochemical Perspectives*** presents a single article with an in-depth view on the past, present and future of a field of geochemistry, seen through the eyes of highly respected members of our community. The articles combine research and history of the field's development and the scientist's opinions about future directions. We welcome personal glimpses into the author's scientific life, how ideas were generated and pitfalls along the way. *Perspectives* articles are intended to appeal to the entire geochemical community, not only to experts. They are not reviews or monographs; they go beyond the current state of the art, providing opinions about future directions and impact in the field.

ISSN 2223-7755 (print)
ISSN 2224-2759 (online)

Principal Editor in charge of this issue
Liane G. Benning
Reviewers
Tim Lyons, University of California, Riverside, USA
Simon Poulton, Newcastle University, UK
Robert Newton, University of Leeds, UK

Cover Layout **Pouliot Guay Graphistes**
Typesetter **Info 1000 Mots**
Printer **J.B. Deschamps**

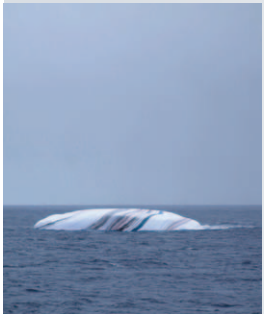

ABOUT THE COVER
Sediment-laden iceberg from Antarctica showing bands of reddish, iron-rich subglacial debris.
Photo credit: Øyvind Tangen

Welcome to ***Geochemical Perspectives***, a new concept in publications. The journal will be issued quarterly and the single, peer reviewed articles will be written by internationally renowned leaders. Each paper will present an overview of a major research area, written at a level that is accessible to people who are not experts in that field. However, in addition, we encourage authors to express personal perspectives and to recount their experiences about how ideas were generated and developed through time, and then, to go beyond the current state of the art, providing opinions about future directions and impact of their field.

Geochemical Perspectives has been created by the European Association of Geochemistry, for the benefit of our community. In contrast to most journals in our field, which are produced to generate profit for publishing houses, ***Geochemical Perspectives*** has the single goal of promoting the communication of high level science – but with a twist. It also aims to show the humanity of scientists and to paint pictures of the pathways trodden and the triumphs and frustrations that scientists meet along the way. ***Geochemical Perspectives*** will be mailed free of charge to all members of the European Association of Geochemistry and attendees of the most recent European Goldschmidt Conference. The journal format has been chosen to make it readily portable and easy to read, even on a crowded train or plane. Once you have finished it, we encourage you to lend it to friends and graduate students. If for some reason it's not returned, or if you want to send an electronic copy to colleagues, back issues are always online **www.geochemicalperspectives.org**.

The production of ***Geochemical Perspectives*** has only been possible through the efforts of several people. Marie-Aude Hulshoff accepted to manage the journal – all, from organising publishers and graphic designers to keeping the editors just ahead of deadlines. Pierrette Tremblay and Kevin Murphy guided us through the nuts and bolts of publishing. We are deeply indebted to our first authors, who wrote manuscripts on faith, for a journal that was still only an idea: Rob Raiswell, Don Canfield, Wally Broecker, Bruce Yardley, Gordon Brown, Georges Calas, Charlie Langmuir, Bjørn Jamtveit, Øyvind Hammer and Fred MacKenzie.

We invite you to share in welcoming ***Geochemical Perspectives*** to our community.

CONTENTS

DEDICATION

"We dedicate this volume to Bob Berner,
mentor, colleague and friend.
In reading the pages that follow, Bob Berner's influence on us,
and on this story, will become abundantly obvious.
Indeed, without Bob's inspiration and guidance,
this story would be unwritten."

Rob Raiswell and Don Canfield

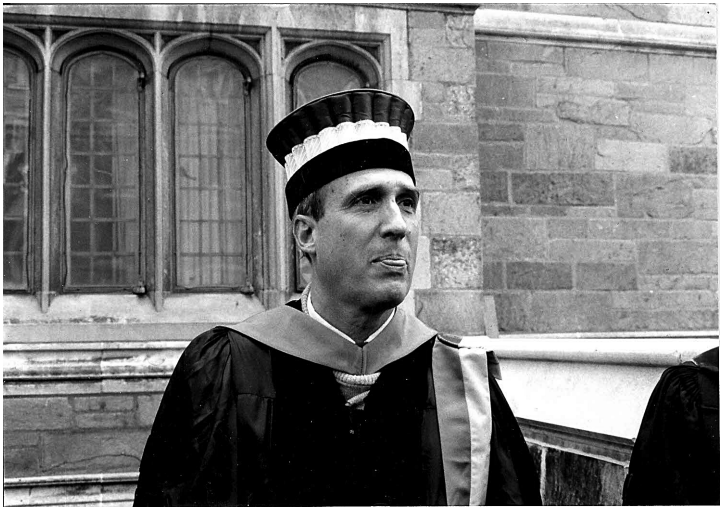

Bob Berner

PREFACE

Over the past many years, the biogeochemical Fe cycle has gained prominence in discussions ranging from controls on primary production in the oceans and their impact on climate change (as expressed in the Iron Hypothesis) to the evolution of ocean chemistry through time. Much of this awareness is relatively recent, and indeed, little was known of the Fe cycle when the two authors of this first Geochemical Perspectives *volume met in 1982 in the laboratory of Bob Berner at Yale University in New Haven, Connecticut. At the time, Rob Raiswell was a visiting scientist, preparing to return to Yale the following Spring for a one-year sabbatical leave, and Don Canfield was beginning as a graduate student. During Rob's sabbatical, and for many years to follow, Rob and Don worked both closely together, and separately, on various aspects of the Fe cycle. Through this time, there were many laughs, a few heated discussions, and numerous beers in different New Haven pubs and elsewhere.*

Since their first encounter at Yale nearly 30 years ago, knowledge of the Fe cycle has expanded enormously. This contribution, the first in a series of Geochemical Perspectives*, follows the development of our understanding of the Fe cycle through the eyes of both Rob and Don. In various parts, the story converges, and in others, the authors explore their own current research interests and place them in the context of the developing field. This monograph is somewhat unusual in that its first-person perspective allows the story to develop both personally and professionally. Throughout, the first-person voice stays the same, but the narrator changes.*

Rob Raiswell tells his story through the first 7 sections. In these sections, Rob outlines his early days at Yale and discusses the developments of various palaeoenvironmental indicators. Mostly, however, he focuses on the modern Fe cycle and provides a comprehensive accounting of sources of bioavailable Fe to the oceans and the various factors controlling iron's bioavailability. This is a current interest of Rob's. Don Canfield's story begins in Section 8, also with his early Yale years. He continues to discuss how the Fe cycle interacts with various other biogeochemical cycles. This sets the stage for Section 9, where Don discusses how the Fe cycle, and its interactions with the cycles of carbon and sulphur, have changed through time. Section 10 offers a quick synopsis of the main points offered through the text as well as some ideas as to future avenues of research.

The authors hope that you enjoy this journey.

Robert Raiswell
School of Earth and Environment,
University of Leeds
Leeds LS2 9JT, United Kingdom

Donald E. Canfield
Nordic Center for Earth Evolution (NordCEE)
Institute of Biology,
University of Southern Denmark
Campusvej 55, 5230 Odense M, Denmark

Acknowledgements: *The ideas presented in this volume have grown over many years. We must acknowledge all of our good friends and colleagues who have contributed to these ideas and to the development of our careers. Many of you are named directly in the text; many are not, but we hope you know who you are, as a list would be very long, and we would run the risk of forgetting someone important. The authors are both exceptionally grateful to Tim Lyons, Simon Poulton and Liane G. Benning, who provided valuable scientific and editorial reviews of the complete manuscript; a heavy burden, which is much appreciated. We are also grateful to Tim Jickells, Rob Newton, Zonbo Shi, Tais Dahl, Peter Statham and Martyn Tranter for commenting on parts of this manuscript. Rob Raiswell's postgraduate geochemical career at Liverpool University was encouraged and supported by Mike Atherton, without whose help none of this would have been possible. Rob Raiswell also thanks Sheila Aiken for Norwegian translation and his trekking partners (Maia in Peru and Debbie in Mongolia) who provided valuable diversions. The principal editor Liane G. Benning of this first* Geochemical Perspectives *issue and the editorial manager Marie-Aude Hulshoff were both very helpful and supportive throughout the pathway to the finished manuscript. These are much needed qualities in producing such a large document. Juan Diego Rodriguez Blanco (University of Leeds) is thanked for redrawing some of the figures. Our work has also required resources, and we are grateful to those agencies that have funded our work over the years including: NERC, the Leverhulme Trust, NSF, NASA, the Max Planck Society, the Danish National Research Foundation and the Agouron Institute.*

THE IRON BIOGEOCHEMICAL CYCLE PAST AND PRESENT

ABSTRACT

Presented here is a combined historical account, current synthesis and a perspective of how the modern Fe cycle functions, and how this cycle has evolved through geologic time. We begin by highlighting how new developments in nanogeoscience demonstrate the importance of nanoparticulate Fe (oxyhydr) oxide aggregates in the modern iron cycle. We further document how these aggregates are supplied from shelf sediments, aeolian dust and icebergs to the global ocean. Based on these observations, we present a kinetic model evaluating the supply of bioavailable Fe to surface seawater by ferrihydrite dissolution, photoreduction and siderophore-aided dissolution. The model indicates that the rate of delivery of bioavailable Fe from icebergs to the Southern Ocean is at least as large as that by wind-blown dust. However estimates of all the main aqueous, nanoparticulate and colloidal (and potentially bioavailable) Fe inputs to the ocean are poorly-constrained.

We provide a historical perspective on the evolution of ideas as to how sedimentary pyrite formation is controlled and how these ideas led to the development of the Fe-based palaeoenvironmental proxies widely used today. This provides a springboard into our discussion of the ancient Fe cycle, which begins

with a survey of how Fe interacts with a variety of other elements of biogeochemical interest including sulphur, oxygen and nitrogen. We highlight how interactions between these elements have evolved through geologic time, and how these interactions define the evolution of ocean and atmospheric chemistry. It is clear that the Fe cycle has gained a prominent role in regulating the biogeochemical function of the oceans through time. We offer, in the end, suggestions and a geochemical perspective as to how recent momentum in our understanding of the Fe cycle may be harnessed into catalysing future progress in the field.

1. INTRODUCTION

1.1 Retrospective: In the Beginning

Where did it all begin? For me it started with carbonate concretions in the pyritiferous black shales at Whitby. Pyrite provided the impetus for my association with Bob Berner (Fig. 1.1a). Then I began to combine my passion for mountains with fieldwork, so starting my long-standing interest in glaciers and the polar regions (Fig. 1.1b). Over my career geochemical research and geochemical techniques have changed beyond belief. What would you have found in a geochemical laboratory fifty years ago? The geochemical laboratory then was a primitive place compared to present day (Fig. 1.2). Many laboratories were equipped only with balances, spectrophotometers and glassware. In the Geology Department at Liverpool we carried out analyses (Atherton *et al.*, 1971) by the so-called 'rapid wet chemical' methods (Riley, 1958), based mainly on colorimetry, which represented a huge improvement in speed and simplicity from the classical gravimetric methods that they replaced. Gravimetric methods required skill and experience, as demonstrated dramatically by the results from the inter-laboratory comparison (Fairburn *et al.*, 1951) of the standard rocks G1 (a granite) and W1 (a diabase), where the ranges of some analytical data were disturbingly large. Some of the largest errors appeared in the measurement of Fe_2O_3 (with coefficients of variation >36%) and this error then carried over into Al_2O_3 which was determined by subtracting the separate determinations of Fe_2O_3, TiO_2 and P_2O_5 from the weight of precipitate of these components plus Al_2O_3. Salutary lessons were learnt about the need to improve analytical precision.

Figure 1.1a Fieldwork with Bob Berner on the Jet Rock at Whitby, Yorkshire.

Photo from Martyn Tranter.

Figure 1.1b Glaciological fieldwork in Norway.

The new rapid methods were able to produce a whole rock analysis for SiO_2, Al_2O_3, CaO, MgO, Na_2O, K_2O, Fe_2O_3, FeO, P_2O_5 and MnO in a batch of six rocks in approximately 10 days. Important lessons had been learnt from the G1 and W1 exercise, and considerable emphasis was placed on precision in pipetting (all without bulbs!), dilutions to volume using volumetric flasks, and in reactant additions to ensure reproducible colour development for colorimetry. However sedimentary geochemistry was still learning that the whole rock analyses that

were routine in igneous and metamorphic geochemistry were not necessarily the best approach. Crucially, it was realised that sediments were mixtures of minerals that were often genetically unrelated, in contrast to igneous and metamorphic geochemistry. New analytical approaches had to be developed that stressed specificity to enable selected components of the sediments to be analysed. This is still a major aim of sedimentary geochemistry in the present day.

Figure 1.2 The Chairman was delighted to have recruited in an area which required no set-up money.

Along with the changes in analytical techniques, geochemistry had started to develop quantitative tools, initiated by the application of thermodynamics and landmarked by the publication of *Mineral Equilibria* (Garrels, 1960). However, thermodynamics predicts an equilibrium state that is realised only where reactions are relatively fast and reversible, whereas many geochemical reactions are slow and irreversible, and time provides a measure of progress towards an equilibrium which may never be reached. Quantifying the role of time required a second step that was landmarked by the introduction of kinetics, which describe the rates at which chemical systems approach an equilibrium state that is defined by thermodynamics, but is controlled by transport processes or reaction

mechanisms. Four decades ago hugely significant texts presented kinetic views on all scales in geochemistry. For us those that shaped geochemistry through the early 1970's were *The Evolution of Sedimentary Rocks* (Garrels and Mackenzie, 1971) and *Chemical Cycles and the Global Environment* (Garrels *et al*., 1973) on a global scale, *Principles of Chemical Sedimentology* (Berner, 1971) for sedimentary environments, *Chemical Oceanography* (Broecker, 1974) for the oceans, and *Aquatic Chemistry* (Stumm and Morgan, 1970) on the micro-scale.

Change occurs in dynamic geochemical systems through the continuous transport of chemical components from one place to another. The kinetics of these systems can be formulated as box models where the system being studied is divided into a series of storage units (termed reservoirs) which have inputs and outputs of material (termed fluxes). Reservoirs can be defined at different scales; at a global scale the atmosphere and the oceans can each be defined as reservoirs but it is equally valid to define reservoirs at a smaller scale, such as a lake or even an individual microorganism. It is also possible to sub-divide reservoirs to isolate the behaviour of different components but careful thought is needed because a reservoir should only be sub-divided as accurately as it can be measured. In the biogeochemical cycle of iron there is a major on-going problem in that the specificity of our measurement techniques depends on size fractionation to discriminate between aqueous and solid phases. However iron, unfortunately, often occurs as colloids that are intermediate in size between aqueous and particulate species. Simply put, such measurements of dissolved iron do not solely represent aqueous species.

1.2 Perspective: The Iron Biogeochemical Cycle

A curious conundrum lies at the heart of the iron cycle: iron is all around us but is biologically scarce. All the main redox states, Fe(0), Fe(II) and Fe(III), are able to persist as solids almost indefinitely in oxygenated environments although only the Fe(III) state is thermodynamically stable. Persistence in part arises from the low solubility of iron phases in oxygenated surface environments which effectively inhibits solid-liquid reactions and so limits bioavailability. By contrast, Fe is the most abundant trace element in marine and terrestrial organisms, where it is required to form metalloenzymes used in many essential life processes, including photosynthesis (Section 8). Biological demand exceeds supply in many parts of the ocean and iron thus limits photosynthesis. This anaemia can be relieved where external sources enhance photosynthesis so effecting the removal of CO_2 from the atmosphere. Thus fluctuations in external sources of Fe to the oceans can influence climate by mitigating or enhancing the 'Greenhouse Effect', potentially making the iron biogeochemical cycle a key regulator of climate change.

Ocean-atmosphere box models of the iron cycle may be complex (see for example Lefevre and Watson, 1999) but still rely on the same basic kinetic principles that will be outlined in Section 1.3. However kinetic models of the iron biogeochemical cycle present unusual difficulties. Fluxes cannot be described

solely in terms of aqueous components because iron is also transported as colloids (defined as <1 µm diameter), nanoparticles (defined as <0.1 µm or 100 nm diameter) and aqueous species (operationally defined as passing through a 0.02 µm filter). These size definitions of colloidal, nanoparticulate and aqueous species use precise boundaries although in fact the different species represent a size continuum (Fig. 1.3). Unfortunately these definitions do not correspond with the filtrate that is commonly collected following passage through membrane filters that have cut off values of 0.02, 0.2 and 0.45 µm (Fig. 1.3). Further difficulties arise where the cutoff values may be altered because material may be trapped due to electrostatic interactions, aggregation and clogging effects as filtration progresses (Howard, 2010). The pragmatic solution adopted here assumes that filtrates through 0.02 µm mainly represent aqueous species and that 0.2 µm filtrates are mainly nanoparticulate.

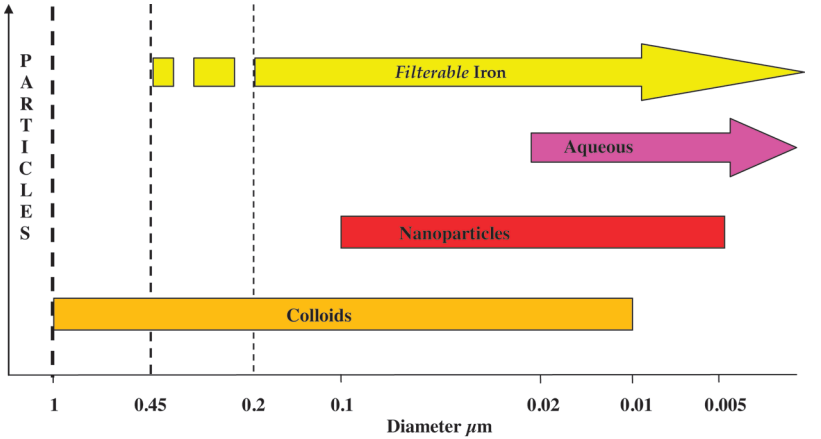

Figure 1.3 Size ranges of particles, colloids, nanoparticles and aqueous species in relation to *filterable* iron.

However measurements are commonly made following filtration through filters with a nominal pore size of 0.45 µm which represent a variety of species including smaller colloids and nanoparticles (not attached to coarser sediment grains nor present as large aggregates) as well as aqueous Fe. These measurements are here termed *filterable*, which is italicised to emphasise that this fraction includes colloids, nanoparticles and aqueous species. *Filterable* iron measurements are usually described as 'dissolved' and, truth be told, 'dissolved' is often assumed to represent aqueous species. This assumption is flawed because *filterable* iron measurements represent an unpredictable and variable proportion of the aqueous and particulate fractions (Howard, 2010). Unfortunately colloids and nanoparticles measured as *filterable* Fe behave differently to aqueous Fe species (Raiswell, 2011a). In fact colloidal and nanoparticulate forms of iron lie between two extremes where physical and chemical properties are determined

on the one hand by aqueous reactivity and on the other hand by the reactivity of macroscopic particles. For example nanoparticles are several orders of magnitude more soluble and more reactive than larger particles because they possess a high proportion of atoms at their surface which have bonding deficits and are therefore labile (Section 2.2).

Clearly box models of the iron cycle may need to distinguish between colloidal, nanoparticulate and aqueous iron (see also Breitbarth *et al*., 2010), which may be difficult where data are mostly collected as *filterable* iron measured as the fraction passing through 0.2 or 0.45 μm filters. Measurements so made cannot be simply interpreted in the context of aqueous chemical reactions but mineralogy needs to be considered, as well as size-related physical effects such as surface charge and aggregation. The influence of colloid and interface effects has been given insufficient attention in iron biogeochemical cycles where *filterable* iron is considered to equate to aqueous iron. This article will demonstrate the need to re-evaluate current iron biogeochemical cycles from the perspective of nanomineralogy.

1.3 Back to Basics: Kinetics and Global Cycles

We all associate time with change, but the earth surface system seems to be able to remain largely unchanged for hundred of millions of years. How is it that complex earth systems can remain so static? Geoscientists rationalise this observation by envisioning that stability results from the operation of processes which are counter-balanced to produce no overall change, which they term a steady state (see below). For example it is easy to see that river flow can only be maintained by the continued precipitation of water derived from evaporating the oceans, because the processes involved are readily observable and occur on a timescale which is short relative to the human lifespan. This balance between precipitation input and river runoff suggests the idea of a water cycle, where water is transferred successively between reservoirs, from the atmosphere to land and then on to the sea, before returning to the atmosphere via evaporation. In this cycle there is no identifiable starting point and no overall change, thus time and progress are decoupled. This is the basis of geological cycling.

Reservoirs are used in geological cycles to represent a mass of material which possesses characteristic physical, chemical or biological properties, and is normally considered to be well-mixed and thus homogeneous. Global cycles are frequently constructed with separate reservoirs for the atmosphere, ocean and crust because of the very different properties of gases, liquids and solids. For example mixing gases and liquids is relatively easy whereas mixing solids is much more difficult. Thus homogeneity is a reasonable approximation for some reservoirs (e.g. the atmosphere) but is clearly a very poor approximation for any solid reservoir. Problems of homogeneity may be resolved in some cases by sub-dividing reservoirs where compositional variations arise because different processes operate in different parts of the reservoir.

Fluxes represent earth surface processes that transfer material from one reservoir to another, and are expressed in units of mass per unit time. Fluxes usually involve the transfer of gases or liquids which occur relatively easily by steady state processes whereas the movement of solids is much more difficult and often occurs episodically. It is often the case that a cycle may be simplified by omitting some reservoirs in order to focus attention on a single box, and its input and output fluxes.

The simplified iron biogeochemical cycle shown in Figure 1.4 shows all the principal reservoirs (the crust, atmosphere and oceans) and fluxes (aeolian dust, atmospheric precipitation, rivers and hydrothermal activity) that transfer material around the earth's surface. However this cycle is not a simple circuit, from which it differs in two important ways. First, the cycle is not uni-directional. For example the transfer of aeolian dust from the crust to the atmosphere may be reversed when dust is scavenged from the atmosphere by precipitation on to land. Second, the cycle is not completely closed. Small amounts of new material are introduced to the cycle from meteorites and larger amounts are added by magma and hydrothermal activity and lost by subduction. Strictly speaking these additions constitute a change such that passage around the cycle may not allow a return to precisely the same starting point. Progression in this manner can be envisaged by representing the cycle in three dimensions as a coil made up of loops of exactly the same diameter. Viewed end on, effectively in two dimensions, progression down the length of the coil would not be apparent and only a circular movement would be seen. Nevertheless progress around the cycle does not result in a return to precisely the original state, and thus there may be a linear progression (or global change component) to cyclicity.

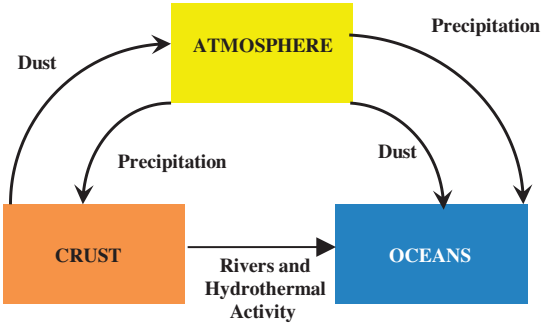

Figure 1.4 A simplified global iron cycle.

A cycle approach, although an over-simplification, does possess the advantage of giving a good over-view of the relationships between different reservoirs and their connecting fluxes. This can sometimes be useful in identifying those parts of the cycle which are poorly-understood, but there are disadvantages in that this approach provides no information on the processes which occur within reservoirs, or on the exact nature of the fluxes between them. Furthermore, on a large scale, it is clearly necessary to use average values which may have to account for considerable spatial variability (as is in any solid reservoir). Such averages are difficult to make accurately, and may therefore be a poorly-recognised source of

uncertainty. This is certainly the case in the Fe biogeochemical cycle, as I will show later (see Table 7.1 and Section 7.8). Nevertheless cycles do encourage a quantitative view of geological processes and quantifying the reservoirs and fluxes provides a valuable insight into the timescales over which the cycle operates. Discussions of geochemical cycles commonly use the following principles:

Residence Time. A Residence Time (R) can be calculated as:

$$R = \frac{\text{Mass in Reservoir (M)}}{\text{Flux or Fluxes (F)}} \tag{1.1}$$

The Residence Time represents the average time spent by a component in a reservoir or the time it would take to empty the reservoir (if all the input fluxes ceased) or the time it would take for the reservoir to double in mass (if all the output fluxes ceased).

Steady State. Many geological cycles are considered to represent a steady state, in which the fluxes in and out of a particular reservoir are exactly balanced. Any reservoir which is not in a steady state must increase or decrease with time. Thus the atmosphere reservoir in Figure 1.4 is balanced because the flux of material brought in by aeolian dust equals that removed by precipitation to the crust and oceans. Geological cycles are usually assumed to be in a steady state because the rock record seems to be remarkably similar for long periods during Phanerozoic time (~600×10^6 years) whereas continuous non-steady state conditions would have produced observable changes. The existence of a steady state allows a balance sheet to be drawn up comparing the sum of all the input fluxes to the output fluxes. The absence of a balance in a steady state system may indicate the existence of an unknown flux. Such budgets are thus extremely valuable, although it must be remembered that there can be considerable errors in estimating an unknown flux as the difference between two comparatively large figures which represent the sums of the input and output fluxes.

Kinetics. Cycles are assumed to operate by first order kinetics: that is the flux (F_o) out of a reservoir is assumed to be linearly and directly proportional to the reservoir mass (M). In many instances this is a reasonable approximation (Lasaga and Berner, 1998). Thus

$$F_o = k\,M \tag{1.2}$$

where k is a first order rate constant. Writing $1/k = M/F_o$ shows from equation (1.2) that Residence Time is the reciprocal of the first order rate constant. Furthermore the rate of change of any reservoir with time (dM/dt) is given by:

$$dM/dt = F_i - F_o$$

where F_i is the input flux. At a steady state $dM/dt = 0$ and so $F_i = F_o$, as defined above. However for a reservoir which is not in a steady state:

$$dM/dt = F_i - F_o = F_i - k\,M$$

This differential equation can be solved with the initial conditions that $M = M_o$ at $t = 0$, $M = M_t$ at any time t, which on integrating gives:

$$M = M_t - (M_t - M_o)\, e^{-kt} \qquad (1.3)$$

The term e^{-kt} becomes very small (~0.05) when t = 3/k or 3R and equation (1.3) then shows that M closely approaches the new value M_t after the passage of three residence times. This represents the time taken by a reservoir to respond to change by reaching a new steady state.

Some of the features described above can be recognised in the more detailed iron cycle (Fig. 1.5) which provides a framework for the discussions which follow. This cycle differs from Figure 1.4 by sub-dividing the ocean into a continental shelf and open ocean reservoir but the crust reservoir is not represented in detail, although the fluxes from the crust into the continental shelf reservoir are shown. The continental shelf reservoir is restricted to water depths of less than 200 m, and the open ocean reservoir is used for water depths greater than 200 m. Most of the reservoirs in Figure 1.5 contain multiple input and/or output fluxes, reflecting a complex suite of processes that affect iron in surface environments as recognised by de Baar and de Jong (2001), Raiswell *et al.* (2006), Aumont and Bopp (2006), Moore and Braucher (2008), Tagliabue *et al.* (2009; 2010). I shall consider the fluxes of iron into the open ocean as being derived from rivers, icebergs (and subglacial runoff), aeolian dust (including that scavenged by precipitation), hydrothermal activity and export from shelf sediments by the iron shuttle (Section 4).

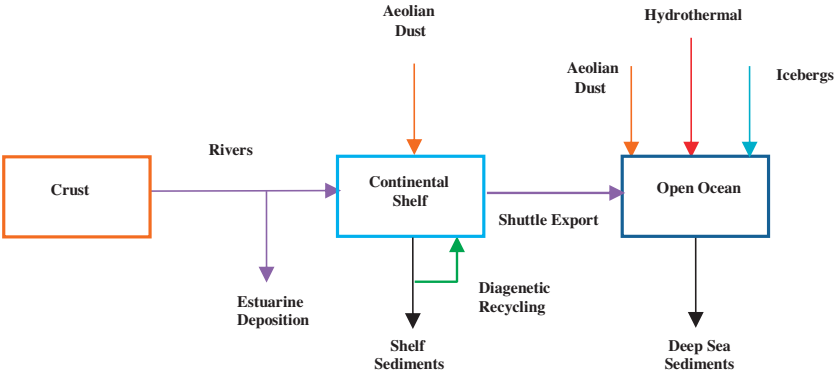

Figure 1.5 Inputs and outputs to marine reservoirs in the iron biogeochemical cycle.

2. THE IRON CYCLE: BIOGEOCHEMISTRY AND MINERALOGY

2.1 Perspective

Iron is delivered to the open ocean mainly by rivers, aeolian dust, icebergs (and subglacial runoff), hydrothermal activity and by recycling from shelf sediments (Fig. 1.5). It is believed that only rivers and hydrothermal activity supply iron in a dissolved form but neither source is effective at reaching surface waters in the open ocean. Most dissolved iron in rivers is removed in estuaries and most dissolved iron in hydrothermal sources is supplied to deep waters (Section 7). However iron is an essential nutrient for the growth of marine plankton in surface waters and, in some regions of the open ocean, the bioavailability of iron limits photosynthesis which in turn influences atmospheric CO_2 levels and has implications for global climate. These links are expressed in the 'Iron Hypothesis' (Martin, 1990; see Section 5).

The critical questions at the heart of the Iron Hypothesis relate to how plankton take up iron delivered to the oceans. All the sources in Figure 1.5 supply far more iron as (oxyhydr)oxides than in a dissolved form (Poulton and Raiswell, 2002) but iron (oxyhydr)oxides are only poorly soluble and concentrations of aqueous Fe in seawater are therefore low. Cellular uptake requires iron as an aqueous species and, especially in iron limited conditions, the (oxyhydr)oxides represent a potential resource. How this resource may become bioavailable requires a knowledge of the aqueous chemistry of iron, the behaviour of different iron (oxyhydr)oxide minerals in seawater and the interactions between (and photochemical reactions of) aqueous and mineral species with organic ligands (see Fig. 2.1 and Breitbarth *et al.*, 2010). Mineralogy has only been peripheral in this research agenda (Fig. 2.2) but understanding the role of iron (oxyhydr)oxides requires that it assume a leading role.

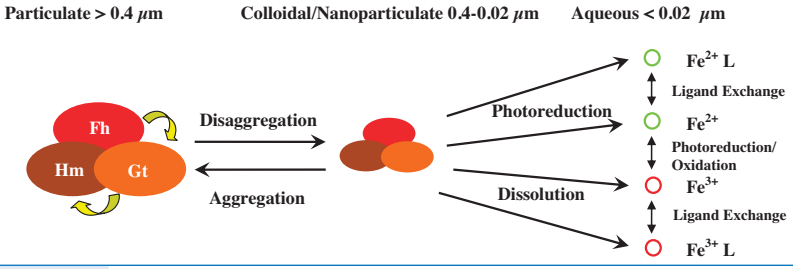

Figure 2.1 Interactions and transformations between aqueous, colloidal (and nanoparticulate) and particulate Fe (oxyhydr)oxides in surface seawater. Yellow arrows show transformation pathways from ferrihydrite to goethite and haematite.

Figure 2.2 And best of all you don't need any mineralogy to read this lot.

2.2 Iron in Seawater: a Beginners Guide

The following section represents a simplified view of iron behaviour in seawater, which is aimed only at providing a necessary background for discussion of the iron biogeochemical cycle and the formation of bioavailable Fe. This background relies on primary literature and is introduced here via a brief question and answer format. More details and full references are summarised in the **Supplementary Information (SI)**.

What Forms of Iron in Seawater are Bioavailable?

Inorganic aqueous Fe(III) (and Fe(II) produced by reduction) is more readily bioavailable than their organic complexes. Eukaryotic phytoplankton directly take up Fe either by photochemical reduction (external to the cell) and/or by the reduction of iron (oxyhydr)oxide colloids adsorbed to the cell surface. Prokaryotes excrete siderophores (low molecular weight organic ligands with a high affinity and specificity for iron) that bind with aqueous Fe(III) species and solubilise iron (oxyhydr)oxides. Further details are given in **SI-1**.

What is the Speciation of Aqueous Iron in Seawater?

Fe(III) is the thermodynamically stable form of iron and predominates in oxic, surface seawater. The main inorganic Fe(III) species in seawater at pH 8 is the $Fe(OH)_3^0$ complex, which constitutes 92% of the aqueous iron pool if organic ligands are absent. Fe(II) is stable under anoxic conditions where the inorganic aqueous speciation at pH 8 is dominated by the Fe^{2+} ion (76%) and the aqueous $FeCO_3^0$ complex (23%).

Table 2.1 The abundance of aqueous inorganic iron species in seawater at pH 8 in the absence of organic complexing species (from Millero et al., 1995).

Inorganic Fe^{2+} Species and Abundance in Anoxic Seawater		Inorganic Fe^{3+} Species and Abundance in Oxic Seawater	
Fe^{2+}	75.8%	$Fe(OH)^0_3$	91.8%
$FeCO_3^0$	22.6%	$Fe(OH)_4^-$	4.5%
$Fe(OH)^+$	1.0%	$Fe(OH)_2^+$	3.6%
$Fe(HCO_3)^+$	0.5%		

However measurements of dissolved iron in seawater are typically made after filtering through 0.2 or 0.45 µm membrane filters and concentrations obtained when filtering oxic seawater are typically up to an order of magnitude larger than the solubility of freshly precipitated ferrihydrite (~0.06 nM). Hence *filterable* Fe(III) in seawater is considered to be mainly complexed to organic ligands.

What is *Filterable* Iron in Seawater?

Filterable iron (<0.2 or 0.45 µm) in seawater includes aqueous species as well as colloids and nanoparticles (Section 1.2). The use of smaller pore size filters (0.02 µm) can produce a filtrate with a greater proportion of aqueous species but colloids and nanoparticles are still present (Fig. 1.3). These filtrates show considerable variability in the distribution of Fe between aqueous and colloidal/nanoparticulate forms in surface seawater. A pragmatic view is that no more than ~50% of the *filterable* Fe is <0.02µm (assumed to be aqueous but actually includes nanoparticles) and no less than ~50% lies between 0.02 µm and 0.2-0.45 µm (and is colloidal/nanoparticulate). See **SI-2** for more details.

What are the Organic Complexes of Iron in Seawater?

Almost all the *filterable* Fe in seawater appears to be complexed with organic ligands. Two types of organic ligands are present; a strong iron-binding ligand is found in surface seawater and a weaker iron-binding ligand is found throughout the water column. The stronger ligand has an affinity for *filterable* Fe which is similar to siderophores (which are produced by prokaryotic organisms to aid in iron acquisition). The weaker ligand has an iron affinity at the lower end of the siderophore range but could be mainly polysaccharides. Most of the <0.02 µm fraction of Fe is complexed (assumed to be aqueous but actually also nanoparticulate) which probably indicates that all the truly aqueous Fe is complexed. A substantial fraction (probably ~50%) of the colloidal/nanoparticulate fraction in surface seawater also appears to be complexed or associated with organic matter. See **SI-1** and **SI-2** for further details.

What are the Colloidal/Nanoparticulate Species in Seawater?

A limited number of high resolution microscopy studies of the <0.1µm particles in surface seawater have shown the presence of nanoparticulate aggregates composed of 2-5 nm sub-units, with Fe-rich grains that resemble ferrihydrite and organic-rich aggregates of 30-60 nm sub-units. Furthermore, up to ~50% of the colloidal/nanoparticulate fraction in surface seawater is inert towards ligand exchange, indicating occurrence as an iron (oxyhydr)oxide. The iron (oxyhydr)oxides may be coprecipitated with organic matter or organic matter may be adsorbed on the mineral surfaces. Coprecipitated aggregates have a different surface charge to mineral aggregates coated with adsorbed organic matter because the former has more mineral exposed at the surface (Fig. 2.3). See **SI-3** and **SI-4** for further details.

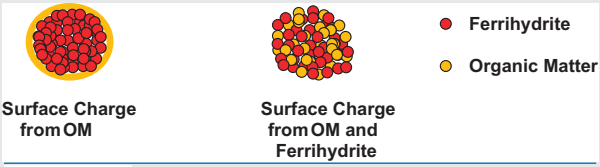

Figure 2.3 End-member characteristics of Fe-organic matter (OM) nanoparticulate aggregates with surface characteristics conveyed by OM alone and a mixture of OM and ferrihydrite.

What is the Origin of Nanoparticulate Iron (Oxyhydr)oxides in Seawater?

Nanoparticles of Fe (oxyhydr)oxides are believed to form at high degrees of supersaturation. Aqueous Fe(III) (plus rapidly oxidised Fe(II)) forms clusters of octahedral $Fe(O, OH, OH_2)_6$ that slowly aggregate to nanoparticles and then to colloids. Nanoparticles of Fe (oxyhydr)oxides form in seawater where (a) porewater Fe(II) in reducing sediments is mixed into the overlying oxic waters and the iron is oxidised to nanoparticulate Fe (oxyhydr)oxides and, (b) oxidation of Fe^{2+}-bearing rock minerals (carbonates, sulphides and silicates) can occur. Nanoparticulate (oxyhydr)oxides may also form by the transformation of the most reactive phases to more stable forms. For example the transformation of ferrihydrite to goethite/haematite has a half-life of approximately 500 days at pH 8 and 5°C (Fig. 2.4). Further details are given in SI-3.

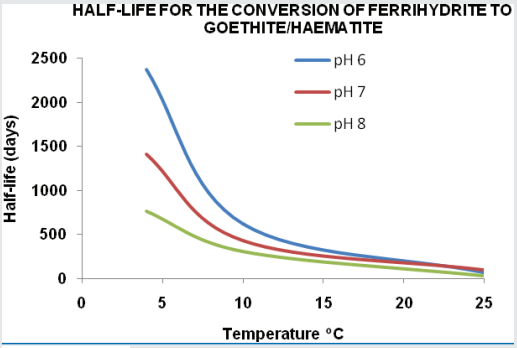

Figure 2.4 Variation in the half-life for the conversion of ferrihydrite to goethite/haematite mixtures (from Raiswell, 2011a, with permission from Elements; data from Schwertmann *et al.*, 2004).

What are the Distinctive Properties of Nanoparticulate Iron (Oxyhydr)oxides?

Nanoparticles represent the smallest 10% of the colloid size range, but these particles, which are <100 nm, exhibit the most dramatic deviations in chemical properties as compared to larger particles. A 10 nm cubic nanoparticle has a large proportion (~16%) of its atoms near the surface, and their reactivity produces novel properties which differ significantly from the bulk mineralogy. Inside this size range the influence of surface area and surface charge are strongest but these effects become progressively less important with increasing grain size.

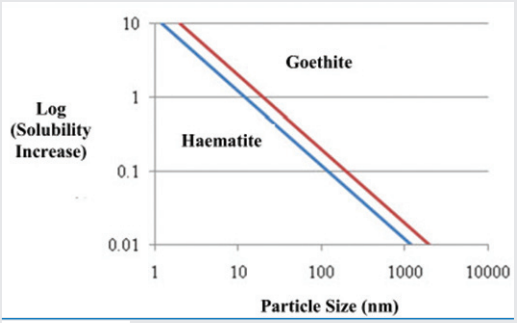

Figure 2.5 Effect of particle size on the solubility products of goethite and haematite (after Cornell and Schwertmann, 2003).

Surface area has a significant effect on the solubility of goethite and haematite once particle size decreases below ~100 nm, and below ~10 nm solubility is increased by more than an order of magnitude (Fig. 2.5). The size distribution of a suite of nanoparticles may increase due to aggregation, which decreases solubility and the rate of dissolution because aggregates possess internal microporosity which inhibits the access of reactants. Further details are given in SI-4.

What Photochemical Reactions Affect Aqueous and Nanoparticulate Iron in Seawater?

Fe(II) can be transiently present in seawater as a result of photochemical reactions (Fig. 2.6) and is kinetically labile and highly bioavailable. Many aqueous Fe(III) inorganic and organic complexes can be photoreduced to Fe(II) but organic complexes are considered to be the most important. Photochemical reactions can occur either by the direct photolysis of Fe(III) complexes or indirectly by reactions with other photochemically produced species. Rates of photoreduction of iron (oxyhydr)oxides depend on the wavelength and intensity of the incident light, on the concentration and type of any reductants that are present, the concentration, surface area and crystallinity of the solid Fe(III) phases, and the pH and ionic strength of the media. The efficiency of photoreduction is thought to be controlled by the rates of Fe(II) release from the mineral surface (and thus decrease with increasing thermodynamic stability) because slow detachment allows in situ re-oxidation. Further details are given in SI-5.

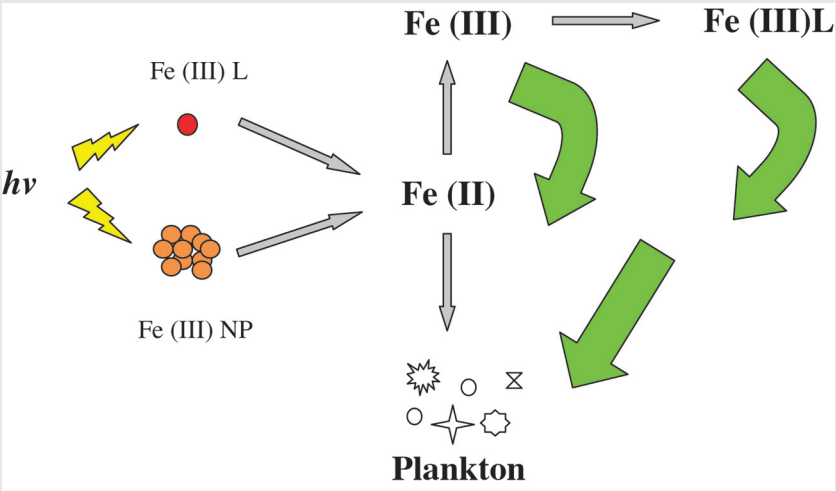

Figure 2.6 A schematic model for the formation of bioavailable Fe(II) by photochemical reduction of ligand complexed (L) and nanoparticulate (NP) Fe(III); photons represented as hv (after Barbeau, 2006).

Which Iron Minerals are Important in the Iron Biogeochemical Cycle?

Iron exists in mineral form primarily in the oxidation states Fe(II) and/or Fe(III). Iron (oxyhydr)oxide, sulphide, carbonate, phosphate and silicate minerals play a crucial role in a variety of processes that will be discussed in the following sections of this paper. Here only the names and formulas are given (Table 2.2) and more detailed information about their occurrence, composition and structure are provided in the **SI-6**.

Table 2.2 Iron minerals involved in biogeochemical cycling.

Mineral Class	Mineral Name	Formula
(Oxyhydr)oxides	Ferrihydrite	$Fe_4HO_8.4H_2O$
	Lepidocrocite	γ-FeOOH
	Goethite	α-FeOOH
	Haematite	Fe_2O_3
	Magnetite	Fe_3O_4
(Oxy)hydroxyl-sulphate	Schwertmannite	$Fe_3O_8(OH)_{1\text{-}1.8}.\ 8H_2O$
Sulphides	Pyrite	FeS_2
	Mackinawite	FeS
	Greigite	Fe_3S_4
Carbonates	Siderite	$FeCO_3$
Phosphates	Vivianite	$Fe_3(PO4)_2.\ 8H_2O$
Silicates : 7 Å Minerals	Kaolinite	$Al_2\ Si_2\ O_5\ (OH)_4$
Silicates: 10 Å Minerals	Illite	$(K, H_3O)\ (Al, Mg, Fe)_2\ (Si, Al)_4\ O_{10}\ (OH)_2\ (H_2O)$
Silicates: 14 Å Minerals	Smectite	$(Ca, Na)\ (Al, Mg, Fe)_2\ (Si, Al)_4\ O_{10}\ (OH)_2.\ x\ H_2O$
	Chlorite	$(Mg, Fe, Mg)_6\ (Si, Al)_4\ O_{10}\ (OH)_8$

What Determines the Supply of Bioavailable Fe from Nanoparticulate (Oxyhydr)oxides into Seawater?

Iron must be solubilised to become bioavailable. The most important mineralogical influences on the solubility and thus bioavailability of nanoparticulate Fe (oxyhydr)oxides (particularly ferrihydrite) are summarised in Figure 2.1. Ferrihydrite is thermodynamically the least stable iron (oxyhydr) oxide in seawater and is the most likely source of bioavailable Fe. However, its aggregation, growth or transformation to more geologically stable phases (e.g., goethite, hematite etc) can all decrease its bioavailability by decreasing its solubility and rates of dissolution. Conversely, the rates of bioavailable Fe supply from ferrihydrite to the oceans can be increased by disaggregation, photochemical reduction, siderophore-aided dissolution and grazing. It follows that the rate of supply of bioavailable Fe to seawater will be affected by the residence time of nanoparticulate ferrihydrite in surface seawater, which in turn will be influenced by sinking and scavenging. These kinetic factors can be integrated into a model that determines how much Fe can be solubilised from nanoparticulate ferrihydrite before removal from the photic zone in surface seawater (see **SI-7**). This model is later also used for evaluating the Fe supply to the oceans by icebergs or by windblown dust (Sections 5.5 and 6.4).

3. IRON DIAGENESIS AND THE C-S-Fe GEOCHEMICAL INDICATORS

3.1 Retrospective: Early Days at Yale

It is a warm summer evening, I have just arrived in the US and I am sitting on Bob Berner's porch drinking beer and listening to his stories. I mention names of people that I had only known from the literature; people whose reputations have reached me across the Atlantic. I have just started as a visiting scientist on study leave from the University of East Anglia and I feel rather like an actor in a first night production; lights are coming on, the stage is being set and the audience is gathering. The evening gets steadily later; much wine has been consumed and we have reached the scotch finale. The project is discussed. We will drive around the US (I like the sound of that), visiting museums that have fossil collections (I have never done any palaeontology but I expect that someone will be able to help), then remove pieces of the shale attached to any marine specimens and analyse the shale for organic C and pyrite sulphur (S) so enabling us to describe variations in the marine C/S ratio through the Phanerozoic. It all seems breathtakingly simple and, with a flash of alcohol-fuelled insight, I realise that this must be how world-class geoscience is done! In fact the sampling scheme turns out to be flawed and the project runs into difficulties right from the start. It took us many years to complete (Raiswell and Berner, 1986) but along its way this collaboration unexpectedly produced the important C-S-Fe indicators. These indicators are amongst our best windows into ancient earth sediment depositional environments (Section 9) and their development is described here. As Hans Eugster said, 'If you work on interesting problems, something interesting always turns up.' Turning up the geochemical indicators relied on the diagenetic groundwork provided by the Bob and the Yale group, especially Joe Westrich (whose work is described below) and Marty Goldhaber (whose review of pyrite formation was our platform; see Goldhaber and Kaplan, 1974). This groundwork will now be briefly discussed.

3.2 Perspective: Kinetics in Diagenesis

Diagenesis refers to the chemical, physical and biological changes that occur in a sediment after deposition but before temperatures increase sufficiently to produce metamorphism. There is no precise boundary between diagenesis and metamorphism but this contribution will only be concerned with diagenesis in near surface sediments where temperature is not the principal driving force for reactions and metamorphism is absent. During the early 1980's the time Don and I spent at Yale spanned the halcyon days where kinetic studies utilising Diagenetic Equations, as formulated by Bob Berner, were starting to play a prominent

part in the study of modern sediments, most notably at the Friends of Anoxic Mud (FOAM) site in Long Island Sound, the acronym for which is now part of the language of geochemistry.

Recognition of diagenetic changes requires that changes in sediment composition with time can be isolated from changes brought about by processes occurring in the sediment after burial. A particular case of steady state diagenesis is defined where the sediment input remains uniform in terms of both mass and composition so that changes with increasing depth can be attributed solely to time-dependent chemical processes. At the other extreme, sediments may constitute an historical archive where there are variations in the input composition with time but no compositional changes occur after deposition. Steady state diagenesis may seem an idealised concept but many sediments approximate to a steady state, at least over short timescales. This assumption has provided a valuable basis for the interpretation of depth variations in terms of time using kinetic models, as initially expounded in the texts by Berner (1971, 1980).

Many important redox reactions occur during early diagenesis because marine sediments contain mixtures of oxidised and reduced, terrestrial and marine components that are inherently reactive. Diagenetic reactions represent the approach of this assemblage towards equilibrium. The most rapid reactions arise from the deposition of reduced carbon (as organic matter) with dissolved and solid phase oxidants (oxygen, nitrate, Fe and Mn oxides and sulphate). The kinetics of the redox reactions between these components are, however, often slow unless mediated by microorganisms that exploit the energy to be gained by using the oxidants as terminal electron acceptors to oxidise organic matter. One of the most important pathways of organic matter oxidation in marine sediments is sulphate reduction which may ultimately produce pyrite.

Pyrite formation plays an important role in global cycles, notably those of iron and sulphur, but also oxygen and carbon (Section 9). In view of this it is hardly surprising that pyrite formation has been intensively studied for more than a century. However, there are still significant gaps in our understanding because an extraordinarily detailed suite of reactions apparently catalyse, participate in, or contribute to the different mechanisms of sedimentary pyrite formation. Figure 3.1 shows a simplified view of the main pyrite formation reactions; the green arrows delineate processes involving dissolved sulphide that form iron monsulphides and/or pyrite, the brown arrows delineate pathways by which partially or fully oxidised species are produced from dissolved sulphide and are then used in other pyrite-forming pathways. Further details about the pathways of iron sulphide formation can be found in valuable reviews of the mechanisms of pyrite formation by Rickard *et al*. (1995), Schoonen (2004) and Rickard and Luther (2007), but the perspective of the present contribution is rather different. Here we will focus less on mechanistic details and instead focus on the ideas that provided the groundwork for the C-S-Fe indicators, discuss their limitations, and present some recent developments.

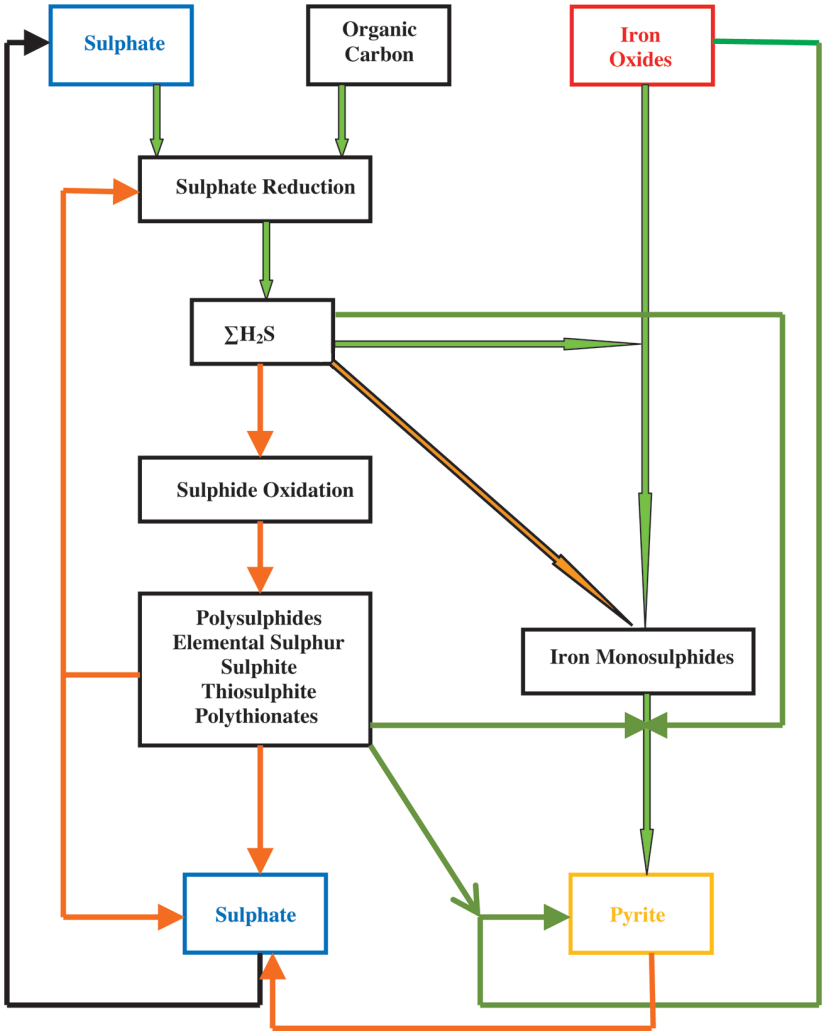

Figure 3.1 Pyrite formation. Green arrows show main reactions by which pyrite is formed, brown arrows show pathways using partially or fully oxidised sulphur species (after Kasten and Jorgensen, 2000). The black bordered brown arrow shows the FeS reaction with H_2S discussed in Section 8.7.

3.3 The C-S-Fe Geochemical Indicators

Accurate recognition of depositional environments is a fundamental goal in the study of sedimentary rocks. For example, identifying how depositional environments varied through time provide the background against which we evaluate the evolution of life. There are four commonly-used C-S-Fe geochemical indicators (C/S, Degree of Pyritisation, Highly Reactive Fe/Total Fe and Total Fe/Aluminium) which developed logically from early work that attempted to quantify the influence of organic carbon, dissolved sulphate and reactive iron on the amounts of pyrite formed in different modern sediment environments. These indicators have evoked contradictory responses in the literature ranging from adverse scrutiny through uncritical acceptance to appreciative and successful usage. Detailed study has revealed limitations on the use of these indicators (see Lyons and Severmann, 2006). As a consequence of these healthy challenges, however, comes refined and greater utility – in part because the indicators have been thoroughly calibrated against modern and ancient sediments where the depositional environments have well-constrained palaeoecological and sedimentological characteristics. This is an important point to grasp; more detailed study of pyrite formation has revealed increasing layers of mechanistic complexity (see review by Rickard and Luther, 2007), that make it difficult to understand how simple empirical indicators can be diagnostic. However calibration against known depositional environments allows the influence of many different and poorly-quantified processes to be integrated into reliable signatures, at least for stable depositional environments.

The groundwork for these indicators was provided by Berner (1964, 1974) who explored the mechanisms by which seawater sulphate was microbially reduced under anoxic conditions to H_2S which reacted with Fe oxides to form pyrite, as expressed schematically in the following equations:

$$2CH_2O + SO_4^{2-} \rightarrow H_2S + 2HCO_3^- \quad (3.1)$$

$$2FeOOH + 3\,H_2S \rightarrow 2FeS + S^o + 4H_2O \quad (3.2)$$

$$FeS + S^o \rightarrow FeS_2 \quad (3.3)$$

where CH_2O represents organic matter as a simple carbohydrate and FeS is an intermediate product that is typically (but not necessarily) precipitated before pyrite (Rickard and Luther, 2007). This reaction scheme is hugely over-simplified (see reviews cited above and Fig. 3.1) but it provides a suitable starting point in that it clearly shows that an anoxic sediment needs to contain three ingredients (organic matter, seawater sulphate and iron oxides; but see Section 3.7) in order to form pyrite. Resolving the mystery of pyrite formation is in part a story of the attempts to discover which of these ingredients exerts the main control on pyrite formation in typical continental margin sediments, and, as in all good mystery stories, the identity of the true culprit was not immediately obvious.

Berner (1964, 1974) set the scene by proposing that the rate of sulphate reduction was proportional to the concentration of organic matter and, on this basis, was able to model the depth changes in porewater sulphate that resulted from sulphate removal by reduction and re-supply by burial advection and diffusion from the overlying seawater. Kinetic models had been introduced to diagenesis and increasingly complex diffusion-advection-reaction models were to be routinely applied to the diagenesis of C, N, O, S, Fe and Mn (see Berner, 1980; Boudreau, 1997). The kinetic models have shown that the rate of sulphate reduction is related to the concentration of metabolisable organic matter and so at first it seemed reasonable to conclude that the amount of diagenetic pyrite that can be formed would be related in some way to the organic matter content of a sediment. From this position it is only a small step to imagine that concentrations of organic matter, sulphate and reactive iron might each, in different sedimentary environments, exert the principal control on the amounts of pyrite formed. This premise turns out to be too simple, but it nevertheless provides a useful starting point.

3.4 The C/S Palaeoenvironmental Indicator

The use of C/S ratios to distinguish between marine and freshwater environments (Berner and Raiswell, 1984) depended on the observation that modern, fine-grained normal marine (oxygenated overlying water and with normal ocean salinity) siliciclastic sediments exhibit a reasonably well-defined linear relationship between organic C and sulphide sulphur with a mean C/S = 2.8 ± 0.8 (Berner, 1982). This was the starting point for my work at Yale. The definition of normal marine sediments excludes sediments where the concentrations of organic matter are too low for anoxic conditions to develop below the sediment-water interface (e.g. deep sea sediments and coarse clastic or $CaCO_3$-rich sediments). Bob and I found that the C/S relationship in normal marine sediments contrasted with the much higher C/S ratios (5 to >100) found in freshwater sediments (Berner and Raiswell, 1984). We thought that these high ratios occurred because the low concentrations of sulphate limited pyrite formation, and thus organic C-rich sediments (up to 10% org C) are associated with low concentrations of pyrite sulphur (Fig. 3.2). Hence C/S ratios provide a method for distinguishing marine and non-marine sediments. Note however that there has been no rigorous examination of C/S variations as a function of

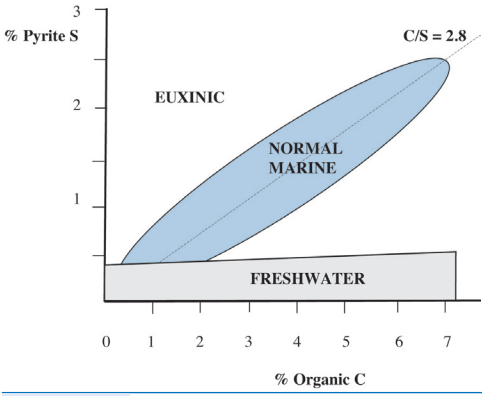

Figure 3.2 C/S relationships in normal marine, freshwater and euxinic sediments.

sulphate concentrations and the C/S ratio cannot therefore be used as a palaeosalinity indicator beyond a very general distinction between marine and freshwater systems. Unfortunately evaluating the effects of sulphate concentrations through an estuary is difficult because of the pronounced temporal and spatial variability in salinity (and hence also sulphate concentrations).

Actually it seems counter-intuitive that the C/S ratios in normal marine sediments should be constrained. To start with, equation (3.1) seemingly suggests that there should be an inverse relationship between the organic matter and pyrite sulphur contents since organic matter is consumed to form pyrite. However not all organic matter can be metabolised by sulphate reduction and, in fact, a large proportion of organic matter is poorly-metabolisable or essentially inert (written below as C_{inert}.) and is preserved during burial so that equation 3.1 is better expressed as:

$$2\ [C_{inert}\ CH_2O] + SO_4^{2-} \rightarrow 2\ C_{inert} + H_2S + 2HCO_3^- \qquad (3.4)$$

There can only be a direct relationship between organic matter and pyrite sulphur if the residual C_{inert} scales positively with the initial amount of labile organic matter (CH_2O). Westrich and Berner (1984) showed that the organic matter in Long Island Sound sediments could be modelled as comprising two components: one that was metabolisable towards sulphate reduction (with a half-life of ~0.7 yr) and one was essentially inert on the timescales studied. These components comprised approximately 65% and 35% respectively of the total organic matter and it appears that the fraction of organic matter that is sufficiently inert to be buried in typical continental margin sediments can vary widely (1-90%) but is crudely related to sedimentation rate, with faster deposition inhibiting the degradation of labile organic matter. Faster rates of deposition with less degraded organic matter also produce higher rates of pyrite burial (Canfield, 1988) and thus, to a first approximation, the amount of carbon preserved and buried as C_{inert} correlates roughly with the amount used to form pyrite. Hence the amount of organic carbon is directly, rather than inversely related, to the amount of pyrite sulphur. Many C/S studies of marine and non-marine sediments followed our initial work (see below) but it took a decade before there was any attempt (Fig. 3.3) to use these understandings of pyrite formation to quantify the controls on the marine C/S signature (Morse and Berner, 1995), as described below.

Theoretical Background. Morse and Berner (1995) developed a simple model using the following parameters:

(a) The total amount of organic C content added by sedimentation (C_T),

(b) The amount of organic C that is metabolisable by all microbial processes including oxic respiration and anaerobic processes using nitrate, Fe and Mn oxides as well as sulphate (C_M),

(c) The amount of organic C metabolised by sulphate reduction (C_S),

(d) The total amount of reduced sulphur produced by sulphate reduction (S_T) and

(e) The amount of reduced sulphur that is buried as pyrite (S_P).

The model is based on the assumption that only organic carbon limits pyrite formation and that neither reactive iron nor dissolved sulphate are limiting (but see below). The above parameters can be assembled into three factors: the ratio of the total organic carbon to that which can be metabolised (C_T/C_M), the fraction of metabolised organic matter used by sulphate reduction (C_S/C_M), and the fraction of reduced sulphur buried as pyrite (S_P/S_T). Morse and Berner (1995) concluded that the limited range of C/S ratios in marine sediments can only occur if these three factors are closely coupled, as expressed below where R represents the molar ratio of organic carbon to pyrite sulphur:

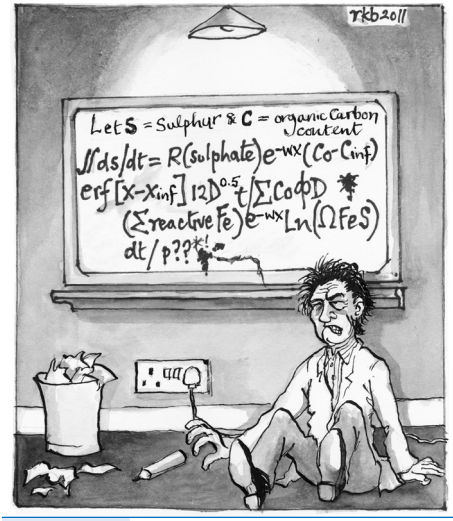

Figure 3.3 Deriving the normal marine C/S ratio from first principles had seemed to be a trivial problem at first...

$$R = \frac{2(C_T/C_M - 1)}{(C_S/C_M)\ (S_P/S_T)} \qquad (3.5)$$

The model is briefly examined below because it provides some useful general insights into all the C-S-Fe palaeoenvironmental indicators.

Equation 3.5 is deceptively simple as the three ratios must each integrate a wide range of different processes (see Fig. 3.1), as discussed below. Table 3.1 uses data from Berner and Westrich (1985), Canfield and Thamdrup (1994) and Lin and Morse (1991) to show the variations in C/S ratios with S_P/S_T and sedimentation rate.

These sediments display a range in C/S ratios from 1.4 to 16 that are not simply related to the ratio S_P/S_T or to sedimentation rate, presumably reflecting the influence of the ratios C_T/C_M and C_S/C_M. However, a plot (Fig. 3.4) of S_P/S_T against log (sedimentation rate) shows the following features:

(a) Low sedimentation rates are associated with low ratios of S_P/S_T. These normal marine sediments lose exceedingly large proportions of sulphide (Table 3.1) mainly by oxidation, which is promoted by sediment disturbance, either by bioturbation or physical re-working

(Berner and Westrich, 1985). Bioturbation minimises the preservation of sulphide both by mixing dissolved and solid phase sulphide into overlying seawater and by introducing oxygen into the sediment which also oxidises sulphides. Slower sedimentation rates also allow more time for organic matter to be degraded at the sediment surface prior to the onset of sulphate reduction leaving smaller amounts of organic carbon (Canfield, 1993, 1994) for sulphate reduction (thus decreasing C_S/C_M).

Intense physical re-working can produce still more extreme effects as can be seen in the normal marine 'fluid mud' sediments of the Amazon Inner Shelf (Aller *et al.*, 1986), which are characterised by C/S ratios (3 to 100) approaching those typical of freshwater sediments. High C/S ratios arise here because physical re-working periodically re-suspends anoxic sediments into oxygenated seawater and thus promotes the extensive oxidation of solid sulphides. Relatively high concentrations of iron (oxyhydr)oxides (partly enhanced by re-working), and low concentrations of re-worked, poorly-metabolisable organic matter, also favour iron reduction over sulphate reduction. Thus diagenetic conditions on the Amazon Inner Shelf are relatively unfavourable to sulphate reduction and the preservation of iron sulphides, and unusually high C/S values result. These sediments typically contain less than 1% organic C and their low sulphide contents therefore produce high C/S ratios that are typical of freshwater sediments. This study shows us that geochemical indicators should always be used in conjunction with sedimentological evidence and not merely in isolation.

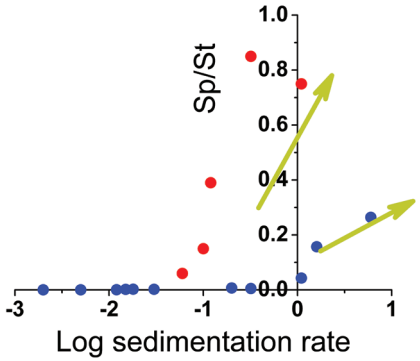

Figure 3.4 Fraction of sulphur buried compared to total sulphur reduced as a function of sedimentation rate. Blue circles are Texas-Louisiana Shelf sediments (after Morse and Berner, 1995).

(b) Fig. 3.4 also shows two trends of increasing S_P/S_T as sedimentation rates increase. The trends differ in that the increase in S_P/S_T starts at higher sedimentation rates in the Texas-Louisiana shelf sediments, as compared to the remaining sediments. Morse and Berner (1995) conjecture that this difference arises because the Texas-Louisiana shelf sediments contain a greater proportion of metabolisable organic matter (higher C_M/C_T).

The Role of Iron. Throughout the first few years of my work at Yale, reactive iron had been an unconsidered player. We measured reactive iron using a boiling HCl extraction (Berner, 1970) which completely dissolved fine-grained haematite, goethite and chlorite. It was unclear whether some or any of these minerals could react with dissolved sulphide; that work was begun by Don (Canfield, 1989) who showed that the content of reactive iron was a major factor in controlling the amounts of pyrite formed. The techniques used by Don divided sediment reactive iron into two different mineralogical pools: a highly reactive pool of ferrihydrite plus lepidocrocite, and a rather less reactive pool of goethite plus haematite (see Section 8.7). Simply put, the results showed that dissolved sulphide was absent from porewaters when these two pools of iron oxides were present, but once the (oxyhydr)oxides were consumed dissolved sulphide was present. Thus the abundance of iron (oxyhydr)oxides placed an upper limit on the amounts of pyrite that could be formed during shallow burial.

Table 3.1 Relationship between C/S ratio, sulphur buried as pyrite as a fraction of total sulphur reduced and sedimentation rate. Data from Berner and Westrich (1985), Canfield and Thamdrup (1994) and Lin and Morse (1991).

Sediment	C/S	S_P/S_T	Sedimentation Rate (cm/yr)
Sachem Harbour	5.8	0.75	1.1
FOAM	1.7	0.15	0.1
North West Control	2.0	0.06	0.06
Santa Barbara Basin	3.1	0.39	0.12
Aarhus Bay	4.0	0.85	0.32
Texas-Louisiana Shelf G1-14	1.5	0.26	6.0
Texas-Louisiana Shelf G1-15	7.1	0.16	1.6
Texas-Louisiana Shelf G1-16	10	0.04	1.1
Texas-Louisiana Shelf G1-17	16	0.0020	0.03
Texas-Louisiana Shelf G1-18	6.8	0.007	0.02
Texas-Louisiana Shelf T4-16	4.7	0.0023	0.018
Texas-Louisiana Shelf T4-17	2.1	0.002	0.03
Texas-Louisiana Shelf T4-18	1.5	0.0019	0.015
Texas-Louisiana Shelf T4-19	1.4	0.0005	0.012
Texas-Louisiana Shelf T1-6	4.4	0.0004	0.005
Texas-Louisiana Shelf T1-7	3.7	0.0003	0.002

Consistent with these observations I had found (Raiswell *et al.*, 1988) that high C/S ratios can also result in normal marine sediments, and in sediments deposited under oxygen-deficient and/or sulphidic bottom water conditions, as a result of iron limitation. These results from ancient sediments were also confirmed in modern sediments where Lyons and Berner (1992) showed that high C/S ratios result from reactive iron limitations in the organic-rich euxinic sediments of the Black Sea. High C/S ratios were also reported (Morse and Emeis, 1990) in hemipelagic sediments from areas of high productivity in sediments with up to 9% organic C. However, in this case the increased C/S ratios were attributed to higher concentrations of organic matter that were poorly-metabolisable towards sulphate reduction (due to more degradation prior to sulphate reduction, i.e. low C_S/C_M) and lower concentrations of pyrite sulphur (due to increased bioturbation promoting sulphide loss from the sediment).

Figure 3.5 shows sulphate reduction rates (and maximum potential sulphate reduction rates) plotted as a function of sedimentation rates for a variety of normal marine, deep sea and euxinic sediments (Canfield, 1988; Canfield and Raiswell, 1991; with updates from Canfield *et al.*, 2005). Superimposed on this plot is a pair of parallel lines that show the amounts of sulphur that could be formed assuming that a reactive iron content of 0.6 to 1.5% (typical of that found in continental margin sediments) was completely pyritised. In deep sea sediments sulphate reduction rates do not reach high enough levels to convert all the highly reactive iron to pyrite and iron oxides are preserved. By contrast, even at low sedimentation rates in continental margin sediments (where sulphate reduction rates are relatively low), the sulphide production rates are still higher than the delivery rates of highly reactive iron. Hence all iron is pyritised and iron oxides are not preserved. This is also true at the intermediate sedimentation rates typical of continental margin sediments and in euxinic sediments. Clearly sulphate reduction rates in continental margin and euxinic sediments are always high enough to pyritise all the reactive iron or, in other words, that reactive iron limits pyrite formation. This was an unexpected twist to the pyrite mystery that raised a question as to how these data could be reconciled with the seemingly robust evidence for organic carbon limitation. The answer is that iron limitation is mostly the key factor in organic-rich sediments (where C_M concentrations are high) and that C/S covariation is defined largely by sediments that have limited concentrations of labile organic matter (C_M). Don essentially solved this mystery which required understanding the role of reactive iron in pyrite formation, as is explored in more detail in the following section.

Final Thoughts. The influence of variations in the relative proportions of metabolisable organic carbon can also be used constructively. We have seen that normal covariance in C/S results from C_S limitations on the formation of pyrite sulphur. Careful collection of normal marine sediments can therefore be used to track historical variations in the nature of organic matter supply, provided the variations in C_S/C_T are large relative to the effects of iron limitation. Comparisons of modern and Precambrian C/S ratios are affected by such historical changes; for example, modern sediments receive a significant supply of

terrestrial organic matter which is only poorly metabolised by sulphate reduction. However terrestrial organic matter was not available in Pre-Silurian sediments. Bob and I found that the effects of this change in carbon supply were significant (Raiswell and Berner, 1986) since normal marine shales (see Section 3.5) from the Cambrian and Ordovician had C/S ratios (0.5±0.1), lower than expected for their measured thermal maturity (see below). We attributed this change to the absence of terrestrial carbon, possibly aided by a lower bioturbation (and thus smaller losses of sulphide).

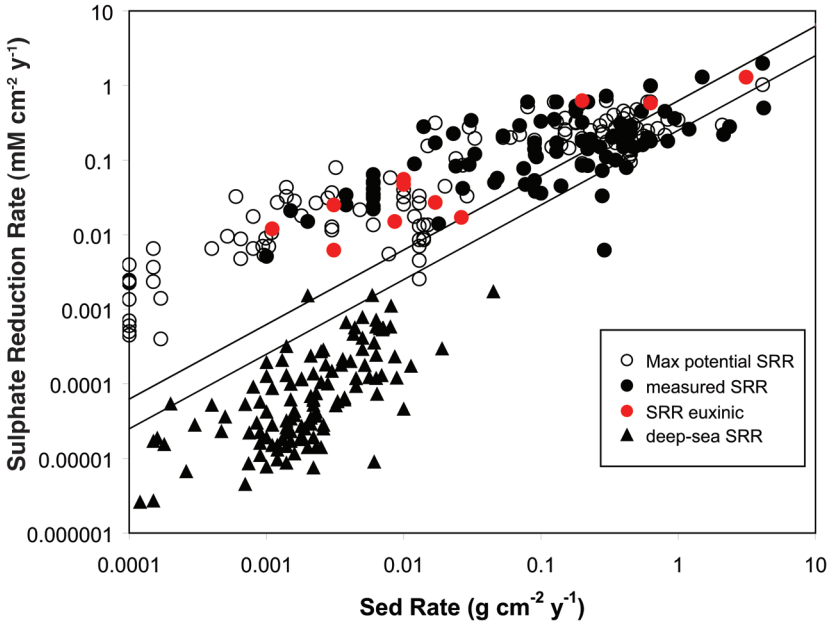

Figure 3.5 Depth-integrated sulphate reduction rates (SRR) as a function of sedimentation rate for normal marine, deep sea and euxinic sediments. Also shown are potential maximum rates of sulphate reduction determined as half the rate of oxygen uptake in a host of marine sediments, assuming that oxygen uptake rate approximates total carbon mineralisation rate and that there is a 1 to 2 stoichiometry between rates of sulphate reduction and rates of total carbon oxidation. The parallel lines define the maximum rate of pyrite burial assuming pyrite formation is limited by the availability of highly reactive iron. Updated from Canfield and Raiswell (1991) with additional data as presented in Canfield *et al.* (2005).

Clearly these differences mean that the C/S ratio cannot provide unambiguous evidence for the sulphate concentrations of the Precambrian oceans. There are also other difficulties that arise because C/S ratios are also considerably modified by organic C losses during diagenetic reactions which occur after sulphate reduction, including methanogenesis, organic matter maturation and

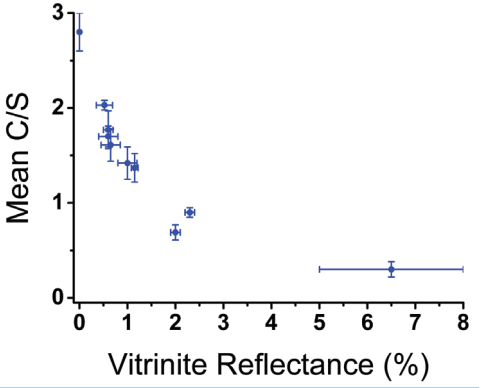

Figure 3.6 Variation in mean C/S ratio with vitrinite reflectance (%) for Palaeozoic sediments. Holocene sediments are plotted at zero reflectance for comparison (after Raiswell and Berner, 1986).

metamorphism. Bob and I were able to show (Fig. 3.6; Raiswell and Berner, 1987) that C/S ratios in normal marine sediments decline as a function of their thermal history, using vitrinite reflectance (R) as an indicator of more intense heating through burial. Depositional C/S values of approximately 2.8 in modern sediments decrease to approx 1.9 (equivalent to a carbon loss of ~30%) at the onset of thermal maturity (R ~ 0.5%), and then to 0.6 (~70% carbon loss) during the anthracite grade of metamorphism (R ~ 2%). The C/S ratio finally reached 0.5 (~80% loss) during greenschist facies metamorphism (R ~ 5-8%). However attempts to quantify carbon losses require a measure of the level of organic matter maturation, and such measures are often imprecise and are rarely performed in ancient C/S studies.

Attempts have been made to apply C/S ratios to Precambrian sediments (Holland, 1984a; Kakegawa *et al.*, 1999) but the variations we have documented above indicate that there are five areas of difficulty (see Canfield and Raiswell, 1999; Shen *et al.*, 2002):

(a) The absence of bioturbation must have increased the degree of sulphide retention

(b) Abundant reactive iron may have enhanced sulphide fixation in iron-rich sediments, such as the banded iron formations (BIFs)

(c) The effects of variable sulphate concentrations on C/S ratios have not been quantified

(d) Increasing thermal maturity produces significant losses in organic C which can be only crudely quantified.

(e) Changes in the metabolisability of organic matter due to the absence of land plants prior to the Silurian.

The modern sediment studies of C/S ratios have provided valuable insights into the influences of organic matter metabolisability, physical re-working, bioturbation and iron limitations on pyrite formation. The C/S ratio remains a valuable tool, but careful sample collection with regard to sedimentological context is necessary so that these sources of variation are constrained. This, in general, applies to all the geochemical indicators.

3.5 Degree of Pyritisation (DOP)

The Degree of Pyritisation (DOP) was originally developed to explore the effects of iron limitation on pyrite formation (Berner,1970), and only subsequently used to recognise the degree of bottom water oxygenation in organic C-bearing rocks. It is now regarded as one of the most dependable indicators of sulphidic (euxinic) bottom waters in ancient fine-grained siliciclastic sediments (Lyons and Severmann, 2006). DOP was defined by Berner (1970) as:

$$\text{DOP} = \frac{\text{Pyrite Fe}}{(\text{Pyrite Fe} + \text{HCl-soluble Fe})} \tag{3.6}$$

Reactive Fe, as measured by Berner (1970) was the amount of iron dissolved during a two minute treatment (one minute to reach boiling plus a one minute boil) with concentrated HCl, which completely dissolved fine-grained haematite, goethite and chlorite (and iron carbonates; Raiswell *et al*., 1994) . At the time we believed that this HCl – soluble iron provided a rough measure of the sediment iron that was reactive towards sulphide. In this way DOP represents the proportion of the original sediment reactive iron that has been converted to pyrite. In fact we did not know how much of this HCl-soluble iron could actually be utilised to form pyrite. However, I thought that DOP might increase in depositional environments where there was increased opportunity for exposure to dissolved sulphide.

Calibration of DOP. We therefore calibrated DOP (Raiswell *et al*., 1988) against a range of Jurassic, Cretaceous and Devonian sediments with depositional environments that were well-constrained from palaeoecological and sedimentological criteria. The sediments were grouped into three categories that represented a range of bottom water oxygenation:

(a) Aerobic (normal marine): homogeneous bioturbated sediments with trace fossils and an abundant and diverse benthic fauna dominated by epifaunal bivalves. These sediments were deposited from bottom waters that were fully oxygenated. Here we prefer to term these sediments oxic.

(b) Restricted (normal marine): poorly laminated sediment with sparse bioturbation and bivalves mainly comprising infaunal deposit feeders. Bottom waters were poorly oxygenated.

(c) Inhospitable Bottom Water: finely laminated sediments with little or no bioturbation and a benthic fauna, if present, that only comprised epifaunal suspension feeders. Bottom water contained no dissolved oxygen.

I was delighted to find that aerobic normal marine sediments had values of DOP < 0.45 and were clearly separated from restricted samples with DOP values ranging from 0.45-0.8. There was some overlap between restricted and

inhospitable bottom water samples (DOP values of 0.55-0.93) but I could see that a boundary at 0.75 separated more than 90% of these sets of samples. Later I was able to show that this boundary could also be recognised in early Palaeozoic samples (Raiswell and Al-Biatty, 1989). At this point I assumed that the relatively high DOP values in inhospitable bottom water arose from the increased opportunity for detrital iron minerals to react with dissolved sulphide in the water column and for long periods after deposition. In other words I thought that these high DOP values were the result of nearly complete pyritisation of reactive iron minerals under prolonged exposure to suphidic conditions.

Iron Limitations and Iron Mineralogy. The hypothesis that pyrite formation would be iron-limited in euxinic sediments seemed to be supported by the occurrence of DOP values that approached unity in the ancient sediments that we studied (Raiswell *et al*., 1988), but the devil was in the detail. Which minerals actually reacted with dissolved sulphide? Pyzik and Summer (1981) observed that amorphous iron (oxyhydr)oxide (most probably ferrihydrite) reacted very rapidly with dissolved sulphide and that goethite reacted much more slowly. More mineralogical detail emerged only after publication of the DOP indicator when Don (Canfield; 1989) investigated the reactivity of a range of synthetic iron oxides towards sulphide, showing that all the main iron (oxyhydr)oxides (ferrihydrite, goethite, lepidocrocite and haematite) reacted rapidly with dissolved sulphide on a timescale of days (see Section 8.7 for a more complete discussion). Now there was a mineralogical definition of reactive iron and, based on this, Don (Canfield; 1989) utilised a citrate-dithionite buffer to extract all the iron (oxyhydr)oxides. His study of modern sediments using the dithionite extraction is a classic and it showed that dissolved sulphide began to accumulate in porewaters only when dithionite-extractable fine-grained, poorly-crystalline iron (oxyhydr)oxides had been reacted from the sediment to form iron sulphides (Canfield, 1989).

The dithionite-extractable iron (oxyhydr)oxides typically contributed 75-85% of the iron for pyrite formation and their presence in a sediment ensured that sulphide was rapidly reacted from the porewaters. Don's study (Canfield; 1989) also showed that dithionite-extractable sediment Fe consisted of two pools; one pool comprised fast-reacting ferrihydrite and lepidocrocite and the other the rather slower-reacting minerals haematite and goethite. The iron (oxyhydr)oxides that dissolved in dithionite were also dissolved in the boiling HCl extractions but so too were a wide range of other iron minerals, including silicates (see above). Did silicate minerals continue to react slowly with dissolved sulphide during deep burial as I believed (Raiswell *et al*., 1988)? The answer turned out to have surprising implications.

In further work we found (Canfield *et al*., 1992) that the FOAM sediments only reached intermediate DOP values (~0.4) despite exposure to porewater sulphide concentrations of up to 6 mM for thousands of years. Furthermore Scanning Electron Microscopy observations of these deeply buried samples showed the formation of only tiny amounts of pyrite in association with iron-bearing silicates. The FOAM sediments were clearly not euxinic but the data identified

a problem and the unavoidable conclusion was that the boiling HCl extraction overestimated the amount of reactive iron that could be pyritised. Subsequently we showed that this was indeed the case (Raiswell *et al*., 1994) as the boiling HCl extraction quantitatively dissolved significant amounts of iron from nontronite and chlorite and rather smaller amounts from glauconite and biotite, as well as dissolving all the main iron (oxyhydr)oxide minerals. By comparison, the dithionite extraction dissolves iron (oxyhydr)oxide minerals with negligible effects on the silicates that are partially dissolved in boiling HCl. At last reactive iron had been defined mineralogically and an extraction identified for its measurement. Finally, and conclusively, Don and I showed (Raiswell and Canfield; 1996) that even extraordinarily long exposure times to dissolved sulphide (up to several million years) were only able to pyritise 30-60% of the HCl-soluble iron. It then follows that the high pyrite contents and high DOP values found in euxinic sediments must be due to a mineralogical control. To put it simply; euxinic sediments must contain larger amounts of the easily pyritised iron (oxyhydr)oxide minerals than do normal marine sediments.

Now we needed to compare the contents of dithionite-extractable Fe and the iron present in sulphide minerals in euxinic sediments with typical continental margin sediments. The euxinic sediments of the Black Sea were the obvious research target and these were already under detailed investigation by the Yale group (Lyons and Berner, 1992). Together with Tim Lyons (Canfield *et al*., 1996) Don and I were able to show that the microlaminated deep basin, euxinic sediments formed sulphides from a pool of 2-3 times more reactive iron, as compared to the reactive iron contents of typical continental margin sediments. Euxinic sediments did therefore contain large concentrations of readily pyritised iron minerals (see Section 4) that produced high DOP values. DOP was placed on a much sounder foundation as a result of this new understanding. There were, however, important cautionary observations from Lyons and Berner (1992) who found that Black Sea turbidites deposited rapidly under euxinic conditions only reached intermediate DOP values. This was attributed partly to their rapid deposition and partly to the presence of smaller amounts of reactive iron minerals than in the euxinic sediments. Lyons and Berner (1992) therefore confirmed that reactive iron enrichments (and not sulphide exposure) were necessary for high DOP values, whilst also re-asserting the need to consider the sedimentological context.

The situation is now understood to be that high values of DOP almost universally reflect euxinic conditions and low values generally typify oxic depositional conditions. However intermediate values are not necessarily diagnostic of restricted bottom water conditions but can also occur where there is exposure to high concentrations of dissolved sulphide in normal marine conditions, or from high rates of sedimentation (sufficiently high to dilute the additional reactive iron) under euxinic conditions (Werne *et al*., 2002; Cruse and Lyons, 2004; Lyons and Severmann, 2006). Rapid deposition swamps the iron enrichment (see Section 4) and continued exposure to dissolved sulphide has relatively little effect because the reactive iron pool is exhausted (Lyons, 1997; Hurtgen *et al*., 1999).

Final Thoughts. Don's iron study (Canfield; 1989) changed our perspective on the controls of pyrite formation in normal marine sediments. Originally it was thought that organic matter was the main control, but the clear links between the consumption of iron (oxyhydr)oxides, the formation of iron sulphides, and the accumulation of dissolved sulphide in the porewaters indicate instead a control by reactive iron content. These views are not inconsistent because in sediments of the continental margin, rates of sulphate reduction correlate with sediment accumulation rates and, therefore, with rates of reactive iron accumulation (Fig. 3.5). Thus complete pyritisation of reactive iron also produces a roughly constant C/S ratio (see above) because the deposition of fine-grained organic matter and iron (oxyhydr)oxides can be closely coupled (Aplin and MacQuaker, 1993). With the benefit of hindsight, a control on pyrite abundance by reactive iron content also explains why the same DOP boundary exists between oxic and euxinic sediments in the Cambrian and the Ordovician as compared to younger sediments (Raiswell and Al-Biatty, 1989) even though the younger sediments contain less readily metabolisable organic C due to the later advent of terrestrial plants in the Silurian. This change in organic C composition would have been expected to produce a different DOP boundary if pyrite formation were instead controlled by the content of metabolisable organic C. The absence of any change in the DOP boundary is, however, entirely consistent with control by reactive iron content.

It is possible to use different techniques to determine reactive iron content and one popular approach has been to utilise a 24 hr cold 1M HCl extraction (e.g. Leventhal and Taylor, 1990) instead of the boiling HCl extraction that Bob and I had used (Berner, 1970; Raiswell *et al*., 1988). Cold 1M HCl is undoubtedly a better measure of the reactive iron content of the sediment than the boiling HCl extraction (although not as good as dithionite; see Raiswell *et al*., 1994) but DOP values so-derived have never been calibrated against sediments with known depositional environments. Thus the extraction of different mineral pools by different extractions will inevitably produce cases where the resulting DOP values produce inaccurate interpretations of iron limitation. A better approach to recognising iron limitation is to use the ratio (pyrite Fe)/Fe_{HR} with Fe_{HR} defined as the iron removed in a dithionite extraction (but see Section 3.7).

3.6 The Anoxicity Indicator

The enrichment of pyrite we observed in the euxinic sediments of the Black Sea (Canfield *et al*. (1996) resulted from an additional source of reactive iron that was decoupled from the main siliciclastic sediment source. We hypothesised that the additional iron was added in association with settling biogenous debris. Euxinic and/or anoxic environments, like the Black Sea, contain stratified water columns that are well-oxygenated at the surface but become progressively depleted in oxygen with depth. Once conditions are anoxic, iron can be reductively dissolved from clastic iron (oxyhydr)oxide-bearing grains and a water layer rich in dissolved iron is established. Below this layer sulphate reduction

occurs in euxinic environments, and dissolved sulphide accumulates through the remaining water column down to the sediment surface. The solubilities of iron sulphides are sufficiently low (Rickard *et al.*, 1995) that significant concentrations of iron and sulphide cannot coexist and bottom waters are dominated either by dissolved sulphide or dissolved iron (Canfield and Raiswell, 1991). Settling, organic C-rich biogenous debris can decompose by sulphate reduction in both the dissolved sulphide and dissolved iron-rich regions of the water column, but the hydrogen sulphide so generated can only be fixed as iron sulphides in the iron-rich water layer. This suggested to us (Canfield *et al.*, 1996) that the formation of pyrite from decomposing biogeneous material in the Fe-rich portion of the water column was the source of the additional pyrite. This source was over and above siliclastic sources of oxide iron (plus silicate iron) in the dissolved sulphide water column and in the sediments. We also considered that the additional iron might be derived from the chemocline and/or the basin margin. It was to be some time before the role of settling biogenous debris was finally refuted by Lyons and Severmann (2006) and, by then, replaced by the idea of enrichment by iron transported from the shelf (Wijsman *et al.*, 2001, see Section 4).

Quantifying Sediment Reactive Iron Contents. The stage was now set for a detailed comparison of the abundances of reactive iron in modern continental margin and euxinic sediments (Raiswell and Canfield, 1998), especially as evidence was also appearing of iron enrichments in ancient sediments (Schieber, 1995). Don and I approached this by examining nearly 150 oxic (continental margin and deep sea) and dysoxic (low bottom water oxygenation) sediments (Raiswell and Canfield, 1998). We found a wide variation in their contents of highly reactive iron (Fe_{HR}), defined as iron that was dithionite-extractable (and could potentially form pyrite, see above) plus iron actually present as pyrite. The Fe_{HR}/FeT ratios for these sediments were quite variable (0.26 ± 0.09) but the Fe_{HR}/FeT ratio was limited to a range from 0.08 to 0.4 (Fig. 3.7).

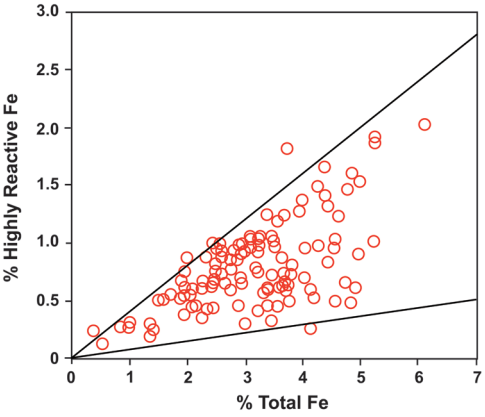

Figure 3.7 Variation in highly reactive Fe with total Fe for continental margin, deep sea and dysoxic sediments (modified from Raiswell and Canfield, 1998). The data fall within an envelope defined by ratio values of 0.08 and 0.4.

Our data also showed that Fe_{HR}/FeT ratios covaried with inorganic C contents for samples from modern anoxic/euxinic environments, i.e. with bottom waters that are oxygen-free and contain either dissolved iron and/or dissolved sulphide (Raiswell and Canfield, 1998). High inorganic C contents indicate a relatively large

contribution of biogenous sediment. Samples from the Cariaco Basin, and Black Sea samples high in inorganic C, have ratios of $Fe_{HR}/FeT > 0.5$, but samples from Kau Bay, the Orca Basin and Black Sea samples of probable turbiditic origin plot with distinctly lower ratios of Fe_{HR}/FeT and low inorganic C content. This latter group of samples has similar Fe_{HR}/FeT ratios to modern sediments deposited under fully or weakly oxygenated bottom waters. This situation presents few difficulties because turbidite sediments are easily recognised by their sedimentological characteristics. Note that sediments from the euxinic Framvaren have high Fe_{HR}/FeT ratios with low carbonate contents, but are very organic C-rich (>15%).

Our study clearly showed that high proportions of highly reactive iron occurred only in euxinic sediments, and also seemed to suggest that enrichment was related to the delivery of biogenous material. However the amounts of additional pyrite formed from decomposition of biogenous material appear to be relatively small and relatively high sedimentation rates mean that Fe_{HR}/FeT ratios may not be significantly enriched compared to sediments deposited in oxygenated bottom waters. Nevertheless, it was clear that ratios of $Fe_{HR}/FeT > 0.4$ indicate enrichments of highly reactive iron are associated with the existence of a stratified anoxic and/or euxinic water column. We had found a potential Anoxicity Indicator for the recognition of stratified water columns in the ancient record.

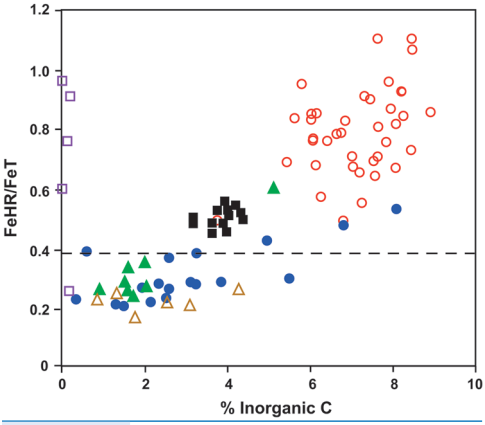

Figure 3.8 Variation in the ratio of highly reactive Fe to total Fe with inorganic C content for anaerobic/euxinic sediments from the Black Sea (open circles data from Raiswell and Canfield, 1998; filled circles from Rozanov *et al*., 1974), Cariaco Basin (filled squares), Orca Basin (filled triangles), Kau Bay (open triangles) and Framvaren (open squares). Dashed line indicates maximum ratio found in Figure 3.7 (modified from Raiswell and Canfield, 1998).

Validation of the Anoxicity Indicator. My next step (Raiswell *et al*., 2001) was to validate the application of the Anoxicity Indicator in ancient sediments. This exercise was carried out in the Kimmeridge Clay (Jurassic, UK) in which careful palaeoecological studies (Wignall and Hallam, 1991) had recognised five categories of oxygen-restricted biofacies (ORB; see Wignall, 1994). Note that the palaeoecology only monitors the presence and absence of oxygen (rather than dissolved sulphide), and thus the ORB categories define the degree of anoxicity but not euxinicity. However ORB 1 and 2 are persistently anoxic and probably euxinic, and the extent of bottom water oxygenation increases through ORB 3 and 4 (which fluctuated between oxygenated and anoxic) to ORB

5 (rare anoxic events) to ORB 6 (persistently oxygenated). All the sediments in the ORB 1, 2 and 3 categories had Fe_{HR}/ FeT > 0.4 and all the ORB 6 sediments had Fe_{HR}/ FeT < 0.4. Furthermore the proportion of sediments with Fe_{HR}/ FeT > 0.5 decreased progressively from ORB 1 and 2 through to 6. Hence a threshold value of 0.4 seemed to enable the Anoxicity Indicator to distinguish euxinic from non-euxinic sediments. The Kimmeridge Clay data also showed a similar relationship between Fe_{HR}/ FeT and inorganic C content as had been seen for the modern euxinic sediments in Figure 3.8, which was also consistent with a source of iron that was coupled to the biogenous sediment supply. However evidence for a basinal source for iron enrichments (Canfield *et al.*, 1996) was emerging from Wijsman *et al.* (2001) who showed that the iron enrichments in the euxinic Black Sea sediments were balanced by an equivalent loss of reactive iron from the shelf. This intrabasinal transfer of iron was later termed the Shelf-to-Basin Shuttle (Lyons and Severmann, 2006) and is discussed in more detail in Section 4.

3.7 The FeT/Al Ratio

The idea that euxinic sediments became enriched through the addition of shelf sources of highly reactive iron that were de-coupled from siliciclastic sediment sources rapidly gained credence, even though details of the source and transport mechanisms were initially obscure (see Section 4). Enrichment can clearly be recognised by the Fe_{HR}/FeT ratio but alternative methods for detecting iron enrichment came from Werne *et al.* (2002) who used the FeT/Ti ratio, which was shortly superseded by FeT/Al mass ratio (Lyons *et al.*, 2003). The FeT/Al ratio is more widely used than the FeT/Ti ratio (see Lyons and Severmann, 2006), and only the former is considered hereon.

Both the Fe_{HR}/FeT and FeT/Al ratios assume that the enrichment of highly reactive iron is sufficient to produce a measurable increase when normalised against FeT or Al as a measure of the proportion of siliciclastic sediment (thus correcting for any dilution by carbonate or silica-bearing biogenous sediment). The Fe_{HR}/FeT and FeT/Al indicators both detect iron enrichment but the former includes enrichments that arise from the addition of highly reactive iron by export from the shelf as well as enrichments that arise from the conversion of an unreactive portion of FeT to Fe_{HR}. Tom Anderson and I wondered (Anderson and Raiswell, 2004) whether this conversion might be effected by microbial activity in oxic and/or anoxic conditions, or by fractionation of the siliciclastic sediment supply but neither mechanism has been verified in a euxinic basin. However observations on modern euxinic sediments (Lyons and Severmann, 2006) including the Black Sea, the Orca Basin and Effingham Inlet, indicate that enrichment cannot result from conversion of unreactive FeT to Fe_{HR}. This study also confirmed, as suggested by Canfield *et al.* (1996), that the enrichment mechanisms, whatever they were, are swamped at high siliciclastic sedimentation rates that produce FeT/Al ratios typical of shelf sediments. High sedimentation rates also produce similar effects on DOP and Fe_{HR}/FeT ratios as already discussed (Sections 3.5 and 3.6).

The use of FeT/Al ratios to detect iron enrichments requires a base-line against which enrichment can be detected. Base-line data are commonly derived from FeT/Al ratios in average shale, which range from 0.5 to 0.56 (e.g. Clarke, 1924; Ronov and Migdisov, 1971; Taylor and McLennan, 1985). However there is a small potential error in that these averages include data from both oxic and euxinic shales, and the latter may have enhanced FeT/Al ratios. More critically there are no errors on these averages and hence simple statistical tests cannot be used to assess the probability that an observed enrichment is significant. These problems are reduced by using the mean FeT/Al ratio (0.53±0.11) from Palaeozoic normal marine sediments (Raiswell *et al.*, 2008c). The message, as elsewhere, is that boundary values are not prescriptive.

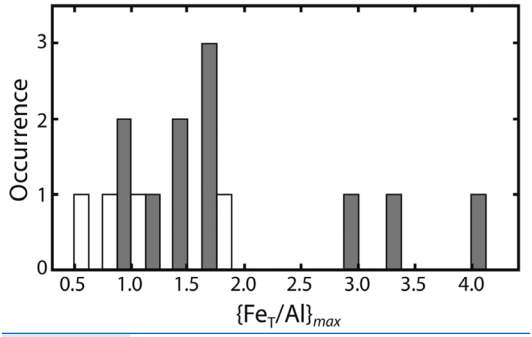

Figure 3.9 Variations in maximum FeT/Al values for modern (white) and ancient (gray) euxinic sediments (after Raiswell *et al.*, 2011).

The FeT/Al ratio possesses an important advantage over the Fe_{HR}/FeT ratio in that it is unaffected by deep burial and/or high degrees of metamorphism where losses of Fe_{HR} may occur that decrease the Fe_{HR}/FeT ratio (Section 3.8). However the FeT/Al ratio cannot distinguish between euxinic and ferruginous bottom waters, which is a crucial requirement for detailing changes in ocean chemistry during the Precambrian (see Poulton and Canfield, 2011 and Section 9). Precambrian ferruginous sediments can result from iron added by hydrothermal activity, upwelling from deep Fe-rich waters or iron released from sediment porewaters (with volcanogenic sediments a potentially important source; Homoky *et al.*, 2011). A recent literature survey of modern and ancient euxinic sediments in collaboration with the Tim Lyons group (Raiswell *et al.*, 2011) has shown that maximum FeT/Al ratios rarely exceed 2 (Fig. 3.9) unless Al contents are <0.5% (a requirement that excludes sediments with minimal siliciclastic contents). Thus values of FeT/Al > 2 seem unlikely to occur as a result of typical euxinic processes and alternative sources are probable. Ambiguity can be avoided by considering the geological context along with complimentary data.

3.8 Recent Developments

The definition of highly reactive iron has been refined by Poulton *et al.* (2004) who realised that Proterozoic rocks often contained diagenetic iron minerals other than pyrite (particularly magnetite, siderite and ankerite) which must have been

formed from the original pool of highly reactive iron. A new analytical scheme was developed by Simon Poulton with Don (Poulton and Canfield, 2005) which could measure Fe present in these minerals and the definition of highly reactive Fe (here italicised as Fe_{HR} to distinguish it from Fe_{HR} based on the dithionite extraction, see Sections 3.4 and 3.6) was thus extended to differentiate Fe present as carbonate (Fe_{carb}), magnetite (Fe_{mag}), oxides (Fe_{ox}) and pyrite (Fe_{py}). The new definition of Fe_{HR} (as Fe_{carb} + Fe_{ox} + Fe_{mag} + Fe_{py}) has formed the basis for an indicator defined by Fe_{py}/Fe_{HR} (Poulton *et al.*, 2004), which is complimentary to the DOP indicator and has a euxinicity threshold recognised at >0.8 based on the Black Sea data of Anderson and Raiswell (2004). This indicator has been widely used in the study of Precambrian sediments (Section 9) and may also provide useful insights in the Phanerozoic (see below).

Does this new definition of Fe_{HR} require that a different threshold is used for oxic sediments, as our original data did not include Fe_{mag} and Fe_{carb}? In other words, did the modern oxic sediments that Don and I used (Raiswell and Canfield, 1998) to define the Fe_{HR}/FeT < 0.4 threshold also contain significant concentrations of Fe_{mag} and Fe_{carb}? Probably not, but this might not necessarily be the case throughout the Phanerozic record. Simon Poulton and I (Poulton and Raiswell; 2002) examined the iron speciation of oxic sediments ranging in age from Ordovician to Jurassic that were originally characterised as normal marine (Raiswell and Berner, 1986) on the basis of palaeoecology and DOP values <0.57. The mean Fe_{HR}/FeT values for these Cretaceous, Jurassic, Silurian, Ordovician and Cambrian sediments were found to range from 0.13±0.06 to 0.17±0.11; values that are significantly lower (at the <0.1% level) than for modern sediments (0.26±0.08). We attributed (Poulton and Raiswell, 2002) these low Fe_{HR}/FeT values to the reductive removal of residual iron oxides remaining after pyrite formation during subsequent deep burial into reducing conditions. The unanswered question is whether these sediments behaved as open systems (with the iron removed by fluids, as Simon and I thought (Poulton and Raiswell, 2002) or closed systems, with the products of reductive dissolution fixed as Fe_{mag} and Fe_{carb}, or even used to form clay minerals (Taylor and Macquaker, 2011). Closed system behavior may not occur in normal marine sediments but is certainly observed in some euxinic sediments. For example, Marz *et al.* (2008) used the Poulton and Canfield (2005) methodology to measure Fe_{HR} in Cretaceous euxinic sediments and found significant concentrations of Fe_{mag} and Fe_{carb}.

Another important development has been to combine the use of the Fe geochemical indicators. Shen *et al.* (2002) introduced the plot of Fe_{HR}/FeT against DOP for Proterozoic black shales from the McArthur Basin. This plot (Fig. 3.10) used the Black Sea sediments to define a euxinic field with DOP > 0.45 and Fe_{HR}/FeT > 0.4. This DOP boundary is lower than that we had originally proposed (Raiswell *et al.*, 1988) and was chosen to include some rapidly-deposited euxinic sediments whose DOP values overlapped with those found in low oxygen depositional environments (see Section 3.5). Li *et al.* (2010) used a cross-plot of Fe_{py}/Fe_{HR} against Fe_{HR}/FeT to separate anoxic, iron-rich depositional environments from euxinic environments (Fig. 3.11). This is a robust approach for distinguishing

anoxic and euxinic environments but the use of these precise boundary conditions to identify oxic deposition requires care due to the potential for Fe_{HR} enrichments to be masked during rapid sedimentation beneath an anoxic water column (e.g. during turbidite deposition; Canfield *et al.*, 1996; Raiswell and Canfield, 1998), and due to the possibility that some unsulphidised Fe_{HR} may be lost to clay minerals during diagenesis. To address this, Simon and Don have come up with a better approach (Poulton and Canfield, 2011) that recognises that the two indicators should be used separately, with Fepy/Fe_{HR} only being applied to samples that show robust evidence for anoxic deposition. Thus, as shown in Figure 3.12, it is important to note that the boundary values are not prescriptive and that areas of doubt exist. The Poulton and Canfield (2011) plot in Figure 3.12 is the recommended approach for Precambrian and Phanerozoic rocks, with samples that fall in the areas of doubt requiring additional detailed consideration to evaluate the water columns under which they deposited.

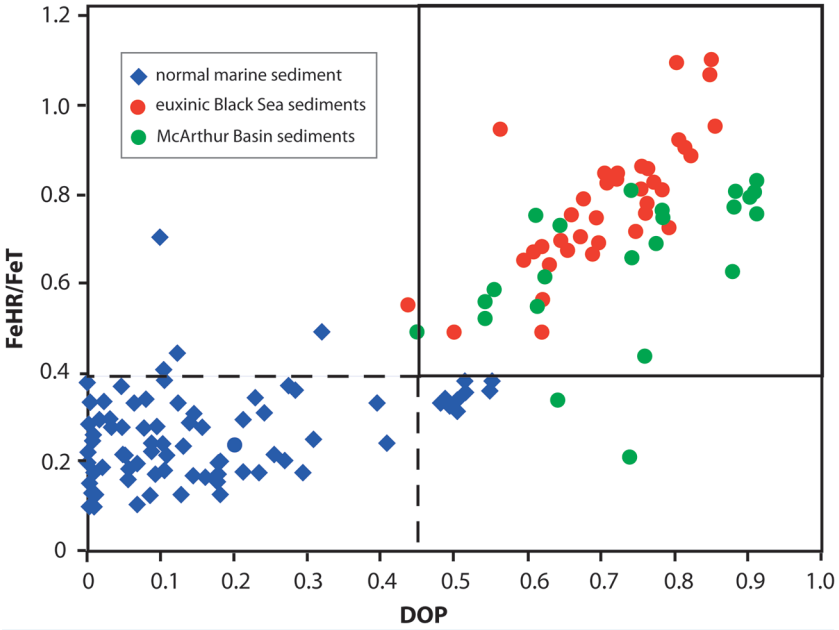

Figure 3.10 Cross-plot ratio of the ratio of highly reactive Fe to total Fe against DOP for iron speciation results from McArthur Basin Sediments, showing oxygenated (normal marine) and sulphidic (euxinic) fields (after Shen *et al.*, 2002).

Final Thoughts. We now believe that the Poulton and Canfield (2005) methodology is the best option for study of Phanerozoic and Proterozoic sediments, although extraction of siderite (and ankerite) can be incomplete in some cases and residual siderite then carries over to the subsequent extractions (Reinard *et*

al., 2009; Raiswell *et al.*, 2011). This siderite may not be fully dissolved in the subsequent extractions of Fe_{ox} and Fe_{mag}, which then compromises the estimation of Fe_{HR}. Resolving this problem is difficult. Measurements of carbonate C by CO_2 evolution include Ca and Mg associated with calcite, siderite and ankerite, as well as Fe_{carb}. Alternatively measurements of carbonate metals by dissolution with cold 10% HCl include Fe from reactive silicates (Raiswell *et al.*, 2011), but may still be the best approach to determine Fe_{carb} in these situations. Ideally a check on the efficiency of carbonate extraction should be routinely made and the iron speciation methodology validated independently in each and every case. Additionally the C-S-Fe geochemical indicators should always be interpreted within a broad sedimentological and palaeoecological context, taking particular account of rates of deposition and the extent of reworking by physical or biological processes (Lyons and Severmann, 2006). Within this context the indicators are robust, although ambiguous signals may still occur in marginal or fluctuating environments.

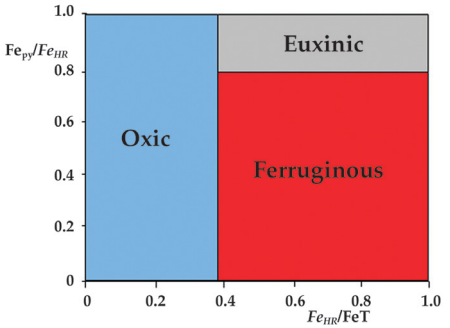

Figure 3.11 Cross-plot of the ratios of pyrite Fe to highly reactive Fe against highly reactive Fe to total Fe (modified after Li *et al.*, 2010).

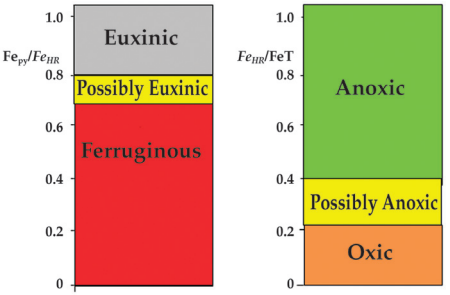

Figure 3.12 Variations in the ratios of pyrite Fe to highly reactive Fe against highly reactive Fe to total Fe in diffferent ocean redox conditions. Boundaries should be treated with caution and areas of doubtful interpretation shown in yellow (after Poulton and Canfield, 2011).

4. IRON TRANSPORT BY THE SHELF-TO-BASIN SHUTTLE

4.1 Retrospective: My Graduate Geochemical Training

My PhD supervisor, Mike Atherton, was a metamorphic geochemist who ran a geochemical training 'boot camp.' There was an initiation rite at the start of this programme with neophyte geochemists being tested on their pipetting skills. The exercise seemed deceptively simple: pipette successive one ml increments of distilled water into a beaker until 20 successive increments achieved a precision of ~0.2% (as measured by the coefficient of variation). Many students spent hours in the weighing room through failing to realise that evaporation had to be prevented by placing a watch glass over the open beaker. Boot camp training was underpinned by a firm belief in the value of mineralogy and Mike was fond of saying 'Geochemistry is only dynamic mineralogy.' I was never entirely sure what this meant but it certainly sounded profound – and it left a lasting impression. Mineralogy, sadly, is now an important skill that no longer appears at the core of some of the larger scientific agendas (Fig. 2.2) and instead only plays supporting roles for a variety of other science communities (Ewing, 2009). Recent studies of natural particulates in seawater have not routinely encompassed mineralogy but have the potential to make significant contributions to the study of particulate Fe transport from shelf to basin (see below and Lam *et al.*, 2012). Even the smallest solid phases, such as colloids and nanoparticles, are now amenable to study via high resolution microscopy, specifically Transmission Electron Microscopy (TEM; for morphology), Selected Area Diffraction (SAED; for mineralogy) and Energy Dispersive X-ray Spectrometry (EDS; for elemental composition). Descriptions of TEM, SAED and EDS techniques are beyond the scope of this article but further details can be found in Williams and Carter (2009).

4.2 Perspective: Ironing Out the Enrichment Problem

What mechanisms produce the Fe enrichment measured by the Anoxicity Indicator? Oceanographers have long been aware that oxic deep sea sediments with low clastic sedimentation rates contain high proportions of an authigenic sediment component enriched in Fe. Estimates of the rate of accumulation of authigenic Fe in these sediments range from 0.8 to 2.7 μg cm^{-2} yr^{-1} (Chester, 2003) but the concentration of authigenic Fe in oxic sediments is usually overwhelmed by the clastic sediment flux, unless sedimentation rates are extremely low (<1 cm 1000 yr^{-1}). Thus oxic sediments do not show enrichment in Fe_{HR}/FeT. However, as discussed in Section 3.6, significant authigenic Fe enrichments (recognised by Fe_{HR}/FeT > 0.4) do occur in euxinic sediments such as the Black Sea (Lyons and Berner, 1992; Canfield *et al.*, 1996; Lyons and Severmann, 2006). Indeed the

enrichment of Fe in deep basinal sulphidic sediments is a persistent feature of euxinic sediments throughout the Phanerozoic record (Poulton and Raiswell, 2002) and likely also the Precambrian (Section 9). It is thought that this enrichment in Phanerozoic sediments generally results from the recycling of iron from shallow shelf sediments followed by lateral transport from the basin margin to the deep basin (Fig. 4.1) where the mobilised iron can be precipitated as syngenetic pyrite in a sulphidic water column (Canfield *et al.*, 1996; Lyons, 1997; Wijsman *et al.*, 2001; Lyons *et al.*, 2003; Raiswell and Anderson, 2005; Lyons and Severmann, 2006). Lyons and Severmann (2006) have termed this process the shelf-to-basin shuttle. The existence of enrichments that are recognised by the Anoxicity Indicator requires that the shuttle source and transport mechanisms must have been persistent through geological time.

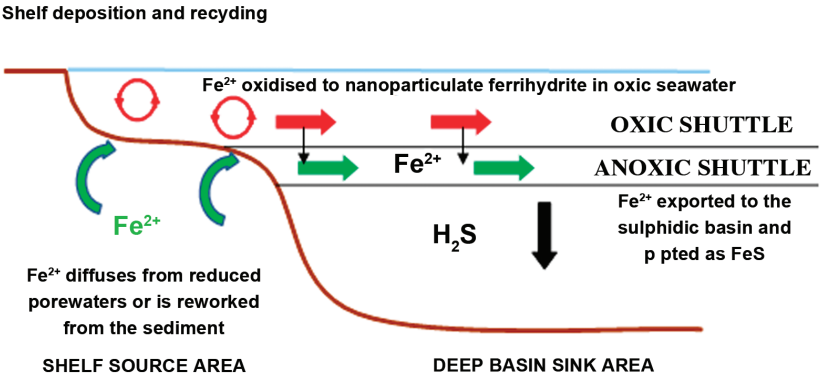

Figure 4.1 The shelf-to-basin shuttle, showing the operation of oxic and anoxic transport in a euxinic basin.

We (Canfield *et al.*, 1996) originally envisaged that the shuttle Fe was precipitated as a consequence of sulphate reduction associated with biogenous material in an anoxic water column which contained Fe derived from shelf sediments (see Section 3.6). However, removal of Fe by the sulphidation of biogenous material is not now thought to be of major significance (Lyons and Severmann, 2006). We also suggested that Fe could be derived from shelf sediments in two ways:

(a) Where Fe(II) from shelf porewaters diffused into, or mixed with, oxic seawater. This Fe(II) is oxidised and then transported as Fe (oxyhydr) oxides (Fig. 4.1) that are subsequently reduced (in anoxic water column) or precipitated (in a sulphidic water column). This oxic shuttle is consistent with the occurrence of authigenic Fe in deep sea sediments (Fig. 4.2).

(b) Where Fe(II) from shelf porewaters is supplied to, and transported in, the chemocline to the deep basin (Fig. 4.1). Anderson and Raiswell (2004) and Lyons and Severmann (2006) have argued that anoxic transport in the chemocline makes only a minor contribution to enrichment in euxinic Black Sea sediments.

Figure 4.2 Is this the oxic shuttle? It doesn't say it takes in-Solubles.

There is, however, the intriguing possibility that the two mechanisms may operate together in euxinic basins . Thus Fe (oxyhydr) oxides in oxic seawater may be transferred by sinking, scavenging or mixing into an underlying chemocline. This oxic shuttle may thus enhance the delivery potential of the anoxic shuttle such that their combined effects produce the enhanced values of Fe_{HR}/FeT in euxinic sediments (Fig. 4.1).

4.3 Shuttle Reactive Iron Species: Constraints Imposed by Basinal Reactivity

Enrichment in euxinic sediments requires that iron must be mainly transported in a form that is reactive on very rapid timescales in the water column. Half-lives for the reactivity of iron in different minerals (Table 4.1) show that only the (oxyhydr)oxides can react sufficiently quickly with sulphide, or be rapidly reduced and dissolved in an anoxic water. Hence these minerals (present as nanoparticles or colloids), together with aqueous Fe(II) or Fe(III) (present as organic complexes; see Supplementary Information SI-2), are the most likely sources. Transport of reactive Fe in an oxic shuttle will be predominantly as colloidal/nanoparticulate Fe (oxyhydr)oxides along with dissolved (and complexed) Fe(III) species, whereas dissolved (and complexed) Fe(II) species will predominate in an anoxic shuttle.

4.4 Particulate Sources of Reactive Fe Eroded from Shelf Sediments

Evidence for shelf sediment sources of particulate reactive iron derived by erosion from the shelf has come from studies of suspended sediments by solid phase analytical methods. Erosion is likely to be most effective on an oxic (or poorly oxygenated) shelf and is likely to be relatively ineffective in anoxic waters where

Table 4.1 Half-lives of sedimentary iron minerals with respect to their sulphidation (after Canfield *et al*., 1992 and Raiswell and Canfield, 1996) and reductive dissolution (after Poulton *et al*., 2004).

Iron Mineral	Half-life with respect to Sulphidation	Half-life with respect to Reductive Dissolution
Fresh 2-line Ferrihydrite Aged 2-line Ferrihydrite	– 2.8 hours	5.0 min 12.3 hr
Lepidocrocite	<3 days	10.9 hr
Goethite	11.5 days	63 days
Haematite	31 days	182 days
Magnetite	105 years	72 days
'Reactive' Silicates	230 years	–
Sheet Silicates	84000 years	–
Poorly reactive silicates	$2\text{-}4 \times 10^6$ years	–

the chemocline impinges on the shelf. Lam *et al*. (2006) examined size-fractionated (1-53 µm and >53 µm) samples from the subarctic Pacific Ocean in the upper 200 m of the oxic water column approximately 900 km from the shelf. The samples were mainly comprised of coccolith aggregates containing iron-rich hot spots with diameters of 0.8-3 µm. X-ray absorption spectroscopy indicated the hot-spot mineralogy to be ~63% goethite and 37% ferrihydrite. These iron (oxyhydr) oxide aggregates were most abundant in the 1-53 µm size fraction. Depth profiles showed hot spot maxima at depths that corresponded to a potential shelf sources, and modelling results suggested transport over ~1000 km in approximately 14 months (~0.4 cm s^{-1}). Next Lam and Bishop (2008) collected size-fractionated samples through a depth profile in the Western Subarctic around 2000 km from the adjacent Kamchatka Shelf. X-ray absorption spectroscopy showed the presence of Fe^{2+} -bearing minerals from volcanogenic sediments which, along with redox-mobilised iron (oxyhydr)oxides, were also present on the shelf. Once again the peak concentrations of acid-leachable iron in the particulates occurred at a density surface just above the oxygen minimum, which was consistent with a supply from the Sea of Okhotsk (see also Nishioka *et al*., 2007). Subsequently Lam *et al*. (2012) studied the mineralogical composition of the 1-51 µm fraction of suspended sediments collected over a 1000 km transect in the eastern tropical north Atlantic. Particulate Fe(III) predominated over Fe(II) and was present mainly in clays, iron (oxyhydr)oxides and an Fe-Organic Matter aggregate (Fig. 4.3). Fe(II) was present as detrital minerals (biotite, hornblende, magnetite and augite) that were characteristic of the weathered Precambrian rocks on the continent. These minerals were also accompanied by small concentrations of pyrite that could only have been derived from the continental shelf (Fig. 4.3). Pyrite appeared to have been transported in an oxygen minimum zone along with the other Fe(II)-bearing minerals.

The disappearance of pyrite from samples more than 500 km from the coast (Fig. 4.3) provides a time constraint on transport, assuming oxidation alone was responsible. Lam *et al.* (2012) use the empirical rate laws of Williamson and Rimstidt (1994) to provide a rough estimate of the time needed to oxidise pyrite by dissolved oxygen, as in eq (4.1) below (see also Section 8.7).

$$\text{Rate of pyrite oxidation (mol}^2\ \text{m}^{-2}\ \text{s}^{-1}) = 10^{-8.19}\ (O_2)^{\ 0.5} / \{H^+\}^{0.11} \qquad (4.1)$$

where (O_2) is the concentration of dissolved oxygen and $\{H^+\}$is the activity of H^+. Oxygen concentration in the oxygen minimum zone was approximately 70 µM, and the pH = 8.1, so that substituting into Equation (4.1) produces an oxidation rate of ~4.2×10^{-10} mols m^{-2} s^{-1}. The transit time to the furthest offshore sampling site (~900 km at 10 cm s^{-1}) was estimated as 104 days, and hence 86% of a ~4 µm diameter pyrite (the maximum size observed) would survive oxidation (and about 46% of a 1 µm diameter grain survives). However lateral velocities are commonly slower than 10 cm s^{-1} and more oxidation of pyrite would create a viable source of iron (oxyhydr)oxides for an oxic shuttle (see Section 4.3 and Fig. 4.2). Eroded shelf sediments, it seems, are potential sources of pyrite Fe (see also Yucel *et al.*, 2011) and reactive Fe (as Fe (oxyhydr)oxides and as Fe-Organic Matter aggregates) to an oxic shuttle.

4.5 Reactive Iron Sourced from Shelf Sediment Porewaters

Diffusion of Porewater Fe into Oxic Seawater. Shelf sediments that contain organic C can produce Fe-rich porewaters through the microbial reduction and dissolution of iron (oxyhydr)oxides during anoxic diagenesis (Lovely and Phillips, 1988; Canfield, 1989; Canfield *et al.*, 1993; Thamdrup and Canfield, 1996; Taylor and Macquaker, 2011). The microbial reduction of iron (oxyhydr)oxides is widespread in near-surface organic C-bearing shelf sediments but in most cases iron reduction is closely followed by sulphate reduction and Don has shown (Canfield, 1988) that porewater dissolved Fe can be almost quantitatively precipitated by dissolved sulphide as iron sulphides in near-surface sediments (Fig. 4.4). However in circumstances where sulphate reduction is limited, porewaters may retain high dissolved Fe concentrations over depths of a metre or more. These diagenetic conditions are favoured by low concentrations of metabolisable organic matter and high sedimentation rates (also high rates of re-working, see below), which produce sediments that have significant potential to recycle porewater dissolved Fe back to the water column.

This recycled dissolved iron does not remain in solution in oxic seawater because oxidation to Fe(III) is rapid and seawater is close to saturation with iron (oxyhydr)oxides. Aqueous Fe(III) can only be maintained in solution at nanomolar levels by complexing with organic ligands; otherwise the precipitation of ferrihydrite occurs (see Section 2.1). Once the complexing capacity for Fe(III) is locally exhausted, any remaining aqueous Fe(II) is rapidly oxidised and precipitated as nanoparticulate ferrihydrite (Raiswell and Anderson, 2005). Some nanoparticulate

ferrihydrite will aggregate or be scavenged by suspended sediments over the continental shelf and thus be re-deposited to surface shelf sediments, but some may remain in suspension and be transported across the shelf into deeper water (Fig. 4.1). Freshly precipitated ferrihydrite is extremely reactive and the re-deposited material is rapidly reduced and these repeated oxidation-reduction cycles may enhance export from shelf sediments (Lyons and Severmann, 2006). Transport from shelf to deeper water may occur as aqueous, complexed Fe(III) or nanoparticulate ferrihydrite aggregates with or without organic matter (see Supplementary Information SI-2).

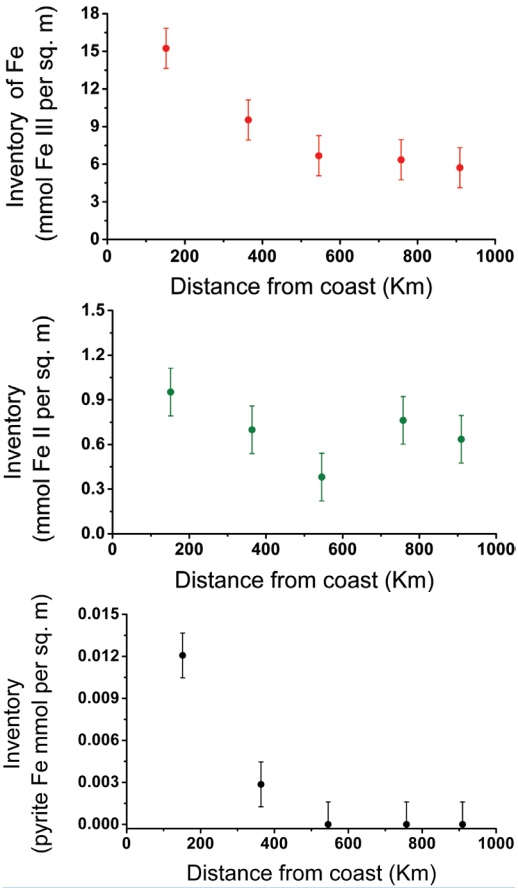

Figure 4.3 Inventory of particulate Fe in suspended sediments from the eastern tropical North Atlantic (after Lam *et al.*, 2012).

Diffusion from shelf sediment porewaters supplies Fe(II) which is rapidly oxidised to supply Fe(III) (oxyhydr)oxides for an oxic shuttle. These Fe (oxyhydr)oxides can cross the chemocline by sinking, scavenging or mixing into underlying anoxic waters, where reduction to Fe(II) will occur. An anoxic shuttle would also acquire aqueous Fe by diffusion of Fe(II) directly into the chemocline from shelf sediments. Fe transported in either shuttle as aqueous, complexed species, or Fe oxyhydroxides, is readily precipitated in a sulphidic water column, and is thus potentially capable of producing the observed enrichment of Fe_{HR}/FeT in deep basin euxinic sediments in the Phanerozoic.

Measurements of Diffusive Fluxes of Fe into Oxic Seawater. Shelf sediment porewaters supply dissolved iron into overlying seawater by diffusion across the sediment-water interface (McManus *et al.*, 1997; Berelson *et al.*, 2003; Elrod *et al.*, 2004). The contribution of this mechanism to shuttle transport is supported by

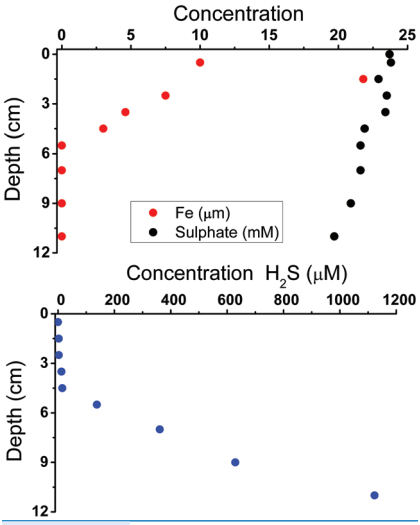

Figure 4.4 Porewater profiles of dissolved Fe, sulphate and sulphide at FOAM (after Canfield, 1988).

iron isotope measurements showing that isotopically light iron derived from the continental shelf may make a significant contribution to deep sea sediments (Severmann *et al.*, 2009; Homoky *et al.*, 2009). Benthic chamber measurements of diffusive fluxes for *filterable* Fe (<0.45 μm) from California shelf sediments by McManus *et al.* (1997) and Elrod *et al.* (2004) ranged up to 37 μg cm^{-2} $year^{-1}$ with a mean of 8.8 μg cm^{-2} yr^{-1}. These values of *filterable* Fe were an average of 75 times higher than estimated from diffusive flux calculations and were believed to be elevated by biological reworking. Fluxes from diffusion alone have been estimated from simple models by Johnson *et al.* (1999) in the coastal upwelling system off California (10 μg cm^{-2} $year^{-1}$) and Blain *et al.* (2007) for the Kergelen plateau (0.2 μg cm^{-2} yr^{-1}). These data seem to suggest that fluxes lie in a narrow range that rarely exceeds 30 μg cm^{-2} $year^{-1}$ that scarcely seems enough to provide the iron enrichment in euxinic sediments. In fact diffusive fluxes of this magnitude could only produce the enrichments found in the Black Sea (16 to 35 μg cm^{-2} yr^{-1}; see Section 4.7) if transportation occurred without loss.

Mixing of Porewater Fe into Oxic Seawater. Diffusive fluxes are enhanced by the physical and/or biological resuspension and mixing of porewater and bottom sediments into overlying oxic seawater. These processes occur in a particularly efficient form (see Section 3.4) in the sediments of the Amazon Inner Shelf (Aller *et al.*, 1986). Rapid rates of physical reworking produce sediments where sulphate reduction is suppressed (and pyrite re-oxidised), and high concentrations of dissolved Fe (up to 4 mM) occur over depths of a metre or more beneath the sediment surface (Fig. 4.5). These diagenetic conditions occur in the extensive mobile mud belts along the Amazon-Guianas shelf and the Papua shelf (Aller *et al.*, 2004; Aller and Blair, 2006). Physical re-working mixes porewater dissolved Fe into the water column where colloidal/nanoparticulate iron (oxyhydr)oxides are formed that can be exported from the shelf.

The potential for re-working modern shelf sediments as a source of reactive iron has also been identified by Johnson *et al.* (1999) in an upwelling region off the coast of California. Here the highest concentrations of leachable iron (particulate iron soluble in hydroxylamine hydrochloride plus aqueous iron) were found during upwelling events, with lower concentrations occurring during times of high river flow and when offshore winds supplying atmospheric dust were less

frequent. A sediment source of iron was clearly implicated, and resuspension of shelf sediments was the favoured explanation because diffusive fluxes of iron from reducing sediments (see above) were thought to be too low. Nishioka *et al.* (2007) also proposed that the enrichment of iron in filtered (<0.22µm) and acidified seawater samples collected in the Western Subarctic Pacific were due to resuspension of shelf sediments from the Sea of Okhotsk.

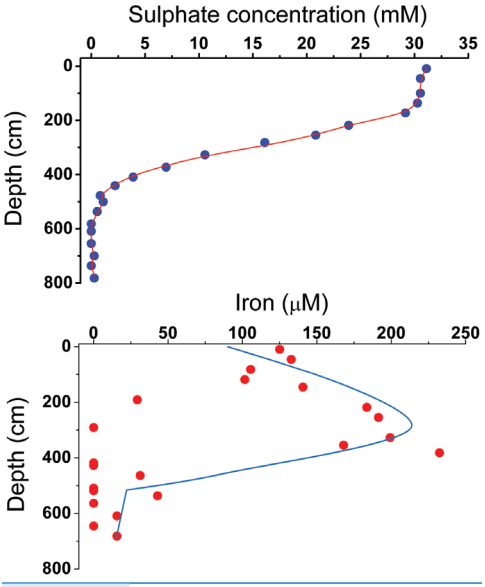

Figure 4.5 Porewater profiles of sulphate and iron in Amazon shelf deposits (after Aller *et al.*, 1996).

Physical reworking is clearly able to produce suspensions of Fe (oxyhydr)oxides that can potentially be exported from shelf sediments, but flux measurements are extremely difficult to obtain from sediments that are continually re-worked. In these circumstances diagenetic modelling represents the only practical approach for estimating the rates at which reworking can supply iron for Fe_{HR}/FeT enrichment.

Estimates of Porewater Fluxes from Diagenetic Models. Steady state diagenetic models (e.g. Wang and Van Cappellen, 1996; Wijsman *et al.*, 2001; Berg *et al.*, 2003) are capable of identifying the release of dissolved Fe from sediment porewaters. These studies demonstrate that the combined diffusive and bioirrigative flux of dissolved Fe to the overlying seawater may be significant with estimates ranging from 3-150 µg cm^{-2} $year^{-1}$ (Wang and Van Cappellen, 1996; Wijsman *et al.*, 2001). These models indicate that the combined effects of diffusion plus bioirrigation may significantly extend the range of fluxes determined by benthic chamber measurements.

In collaboration with Caroline Slomp, I have sought to use a coupled reactive-transport model (modified from that of Reed *et al.*, 2011) to further understand the factors determining the release of dissolved Fe from shelf porewaters, and to study the impact of short-term biological or physical reworking. Transport of solutes to overlying seawater is envisaged to occur by molecular diffusion, bioturbation and advection (burial). Bioirrigation is represented as a non-local exchange with the surface water using a mixing coefficient (D_b) that varies with depth (Boudreau, 1984). The model is parameterised using a reference case, which is a shelf sediment with a generic composition representing offshore

sandy shelves, where an active cycling of Fe and Mn is observed (Slomp *et al.*, 1997), and where episodic reworking of particles is known to be important (Van der Zee *et al.*, 2003).

Preliminary results (Slomp, pers. comm.) for the steady state reference case (Fig. 4.6) show the exchange of Fe between aqueous Fe^{2+} and three solid phase pools ($Fe(OH)_3$, FeS and FeS_2) for an $Fe(OH)_3$ depositional rate of 140 μg cm^{-2} yr^{-1} and a total organic C flux of 960 μg cm^{-2} yr^{-1}. This reference case produces a bioirrigation recycling flux of Fe^{2+} of 39 μg cm^{-2} yr^{-1} to the overlying seawater. As a next step Caroline has examined the sensitivity of the benthic fluxes of Fe^{2+} to changes in bioirrigation, sediment mixing, the incoming Fe (oxyhydr)oxide flux and organic C loading (Table 4.2).

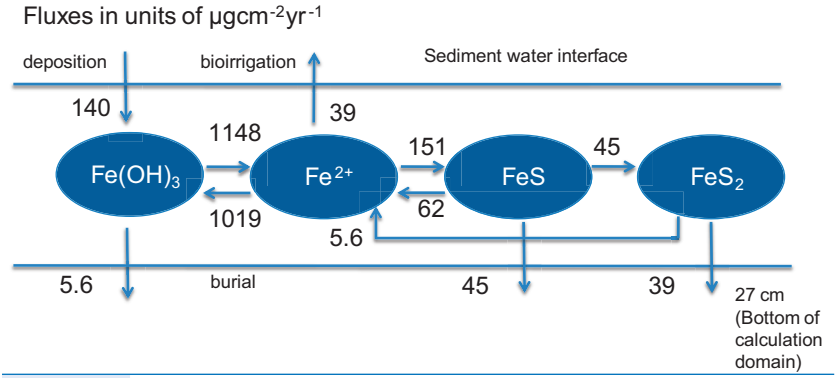

Figure 4.6 The annual Fe-cycle in the shelf sediment as simulated by the multi-component model in the reference case. All rate and flux values are presented in μg cm^{-2} yr^{-1} and are rounded to the nearest number. Rate values are integrated over the upper 27 cm of the sediment. Note that only the easily reducible $Fe(OH)_3$ is included in this diagram (Slomp, pers. comm.).

Table 4.2 shows that diffusive fluxes from the generic shelf sediment deposited in oxygenated bottom water conditions are in the range 0.6 to 5 μg cm^{-2} yr^{-1}). The diffusive fluxes are little affected by doubling Fe (oxyhydr)oxide deposition rates but they are sensitive to the incoming organic C flux. The overall values are comparable to diffusion only measurements, which we have seen rarely exceed 30 μg cm^{-2} yr^{-1}. Significant increases (Table 4.2) in the diffusive flux (up to 63 μg cm^{-2} yr^{-1}) are found where deposition occurs from anoxic bottom waters. However Table 4.2 shows that bioirrigation fluxes are generally much more important that diffusive fluxes and can reach 104 μg cm^{-2} yr^{-1} with increased deposition of Fe (oxyhydr)oxides. The model does not account for any precipitation of Fe^{2+} in irrigated burrows, i.e. the bioirrigative fluxes are maximum estimates.

Table 4.2 Benthic recycling fluxes (μg Fe cm^{-2} yr^{-1}) for different modifications of a generic shelf sediment (Slomp, pers. comm.).

Steady State Modifications	Total Benthic Flux	Diffusion	Bioirrigation	Contribution of bioirrigation
Reference case (R)	40.3	0.6	39.7	99%
R with 2x Organic C flux	13.5	4.5	9.0	68%
R with 2x $Fe(OH)_3$ flux	104	0.6	104	99%
R with 2x D_b	37.5	1.1	36.4	97%
R with 2x bioirrigation of all solutes	48.7	0.6	48.1	99%
R with no bioirrigation of Fe^{2+}	0.6	0.6	0.00	0%
R with no bottom water O_2, no bioirrigation, no mixing	62.7	62.7	0.00	0%

These results suggest that shelf sediments can generate significant sources of Fe through bioirrigation, sediment re-working and direct diffusive release to the water column. The latter process is most important if bottom waters are low in oxygen or anoxic. Organic C and $Fe(OH)_3$ deposition play a key role on the total production of Fe^{2+} in the sediment and its benthic release which increases in a complex fashion as both inputs increase (Fig. 4.7). These preliminary results suggest that relatively high fluxes can be generated, especially in iron-rich sediments (up to 104 μg cm^{-2} yr^{-1}). Shelf sediment diagenesis and reworking are also able to produce the larger fluxes than diffusion alone.

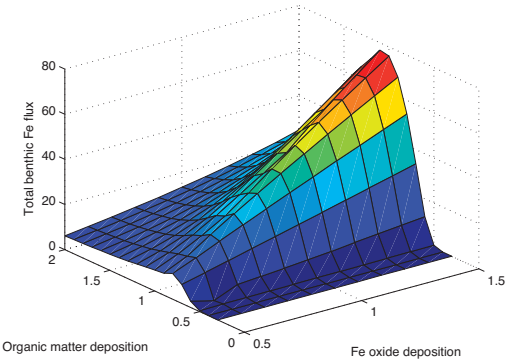

Figure 4.7 Steady state response of total benthic Fe(II) fluxes (in μg cm^{-2} yr^{-1}) to changes in incoming Fe-oxide flux and organic matter loading. Both axes are scaled relative to the reference run where 1 represents a value of 140 μg Fe cm^{-2} yr^{-1} for the $Fe(OH)_3$ flux and 960 μg C cm^{-2} yr^{-1} for the organic C flux (Slomp, pers. comm.).

4.6 Shuttle Transport

Decreases in *filterable* Fe (recall that this measurement combines aqueous, nanoparticulate and colloidal species; Section 1.2) have been observed over considerable distances (hundreds to thousands of km) away from the shelf in surface waters in the northwestern Atlantic Ocean (Wu and Luther, 1996) and in waters at the oxygen minimum in the northeast Pacific (Martin and Gordon, 1988). The Equatorial and the New Guinea Coastal Undercurrents (Mackey *et al.*, 2002) are also enriched in particulate plus aqueous iron (measured on filtered and acidified samples). These studies appear to capture the operation of a shelf-derived transport flux but how quickly does transport occur?

In general, the lateral velocities of mid-depth currents in oxic seawater rarely exceed 10 cm s^{-1} in the ocean basins, and are more typically ~1 cm s^{-1} (e.g. in the Ross Sea and in the sub-polar North Atlantic; Sedwick and DiTullio, 1997; Lavender *et al.*, 2005). However velocities are much faster (up to 100 cm s^{-1}) in the undercurrents studied by Mackey *et al.* (2002). During transport in an oxic shuttle nanoparticulate ferrihydrite may dissolve to form aqueous Fe(III), or sink by becoming attached to sediment grains or scavenged by large aggregates. Transformation of ferrihydrite to goethite/haematite is unimportant in a euxinic basin because all the (oxyhydr)oxides are highly reactive towards sulphidation and reductive dissolution (Table 4.1).

These processes affect the potential for an oxic shuttle to deliver highly reactive Fe to remote basin or open ocean sites, and to transfer highly reactive Fe into the chemocline to enhance an anoxic shuttle. These processes are roughly quantified in the following model. Assume that a package of water moving off the shelf contains a mass M_t of nanoparticulate ferrihydrite at any time t and that the removal processes follow first order kinetics that can be described by a rate constant k (see Supplementary Information SI-7) that combines the individual rate constants for dissolution (modified by aging) and sinking (plus scavenging). The rate of change of M_t is given by:

$$dM_t/dt = -kM_t \tag{4.2}$$

$$\int dM_t/M_t = -k \int dt \tag{4.3}$$

Integrating produces

$$\ln (M_t) = -kt + \text{constant} \tag{4.4}$$

Assuming that the initial mass of nanoparticulate ferrihydrite is M_o when t = 0 produces

$$\ln (M_t/M_o) = -kt$$

or

$$M_t/ M_o = e^{-kt} \tag{4.5}$$

Equation (4.5) describes how the mass of nanoparticulate Fe decreases with time due to loss by dissolution, sinking and scavenging. Rate constant values for dissolution, (modified by aging/aggregation), sinking and scavenging were derived for temperatures of 10-12°C (see Table SI-7 in Supplementary Information SI-7) and can be used to solve equation (4.5) to find the proportion of the original mass of nanoparticulate Fe (M_t/ M_o) that is left as a function of the transport time. The rate constant for dissolution (0.0015 day^{-1}; Table SI-7) is a minimum value that is appropriate for time periods in excess of 100 days and loss by sinking through attachment to fine particles has a rate constant of 0.001 day^{-1} (Table SI-7). Solving equation (4.5) with k = 0.0025 day^{-1} for a time of 100 days shows that M_t declines to 77% of M_o. The loss of 23% is divided between sinking (10%) and dissolution (13%). For a time of 1000 days the comparable figures show M_t declining to 8% of M_o (divided between a 55% loss by dissolution and a 37% loss by sinking). In an oxic shuttle the aqueous Fe derived from the dissolution of ferrihydrite is likely to be used to support productivity in the open ocean (see Supplementary Information S1), but the losses by sinking would transfer highly reactive Fe into the underlying chemocline to enhance anoxic shuttle transport.

4.7 Insights from the Black Sea

The Black Sea is our best natural laboratory for studying shuttle enrichment in a euxinic basin. The basin-wide continuity of millimeter-scale laminae in the deep water sediments of the Black Sea (Fig. 4.8) testify to the sustained efficiency of long range oxic and/or anoxic shuttle transport. This, in turn, suggests that the shuttle operates in a particularly efficient form in the Black Sea. Working with Tom Anderson (Raiswell and Anderson, 2005) I have attempted to understand the factors which relate shelf generation rates to rates of deep basin enrichment. We have shown that fluxes from sediments do not represent the delivery fluxes to the deep basin for two reasons. First, not all the iron released from the sediment is exported from the shelf and we defined an export efficiency term (ε) to account for the loss of iron by re-deposition to the shelf. The ε term has proved difficult to quantify (Raiswell and Anderson, 2005) but Tom and I (Anderson and Raiswell, 2004) were able to estimate that the deep basinal sediments in the Black Sea received ~5% of the siliciclastic sediments deposited on the shelf. Second, the ratio of the shelf generating area (S) to the basin sink area (B) may act to dilute or concentrate the delivery flux. In the Black Sea the S/B ratio is 0.42, assuming that all the shelf area with <200m water depth generates a shelf flux which is equally dispersed over the remaining area. By comparison, the S/B ratio for the world oceans is ~0.075 and thus shelf fluxes are dispersed over a much wider area and produce lower enrichments in deep sea sediments (Raiswell and Anderson, 2005). However Fe enrichments are observed in sediments deposited during Oceanic Anoxic Events (such as the Jurassic; see Poulton and Raiswell, 2002) when widespread euxinicity must also have been associated with low S/B ratios. Explanations of enrichment/dilution based on S/B ratios are clearly very tentative given the uncertainty over how much of the shelf actually recycles iron

and how much iron is exported (see Section 7.4). Second, we suggested that euxinic water columns may provide a particularly efficient chemical (sulphidic) trap for Fe (oxyhydr)oxide nanoparticulates compared to removal by settling into oxic deep sea sediments (but see Lyons and Severmann, 2006). Neither explanation seems convincing.

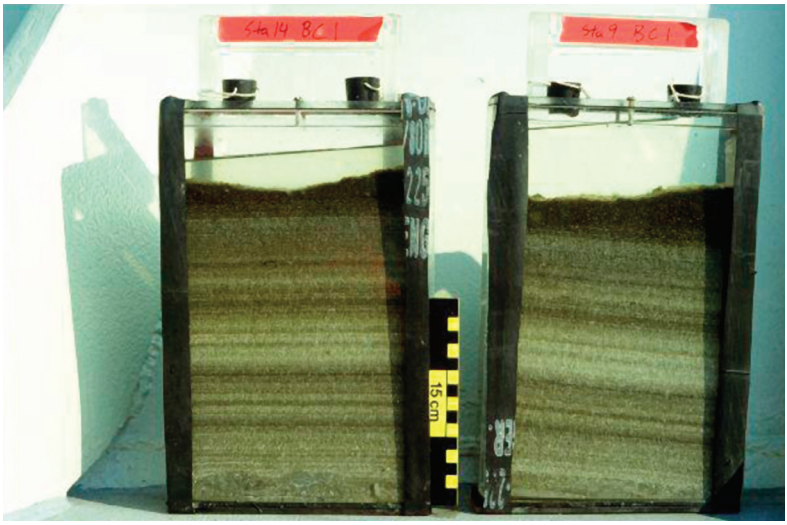

Photo from Tim Lyons.

Figure 4.8 Microlaminated sediments from the upper portion of Unit I in the Black Sea. Light and dark bands represent carbonate and siliciclastic sediment in cores at sites 210 km apart (from Lyons and Berner, 1992, with permission from Elsevier).

However, it seems that relatively high shelf fluxes are required to generate the observed Fe enrichments in the Black Sea. Wijsman *et al.* (2001) estimate that a deep basin delivery rate of 16 to 35 μg cm^{-2} yr^{-1} of Fe in the Black Sea requires a shelf flux of 140 μg cm^{-2} yr^{-1}. This flux is certainly higher than diffusion only data, but is consistent with fluxes estimated by computer modelling of iron released from physically and/or biologically reworked shelf sediments. In the Black Sea lateral velocities are ~0.5 cm s^{-1} (Buessler *et al.*, 1991) at the interface between the suboxic and sulphidic zones (typically around 150-200 depth). Travel distances from the shelf to the central deep basin are at most around 600 km, which indicates travel times of <4 years (~1500 days). Over this timescale significant proportions (see Section 4.6) of oxic shuttle Fe would pass into the chemocline to enhance anoxic shuttle delivery to the deep basin. Perhaps the Black Sea is unique in having a high shelf generating capacity, which can be relatively efficiently transported by the combined effects of an oxic and anoxic shuttle.

Final Thoughts. We have identified two potential sources for iron enrichment; eroded shelf sediments and porewater dissolved iron that is added into the overlying water to produce a variety of highly reactive Fe species. Iron isotopes offer the possibility that porewater Fe derived from the shelf can be identified in deep basin sediments. Distinctively low $\delta^{56}Fe$ values have been found in continental shelf source sediment (Severmann *et al.*, 2009) that can be recorded in euxinic sediments (Lyons and Severmann, 2006; Duan *et al.*, 2010). Further isotope studies should clarify the relative importance of eroded shelf sediments and porewater dissolved Fe in producing the distinctive enrichment signal in euxinic sediments. It is reassuring that we can identify modern shelf sources and shuttle transport processes that could produce the distinctive and robust enrichment signals that we find in modern and ancient euxinic sediments. More quantitative mass balance data are the key to improving our understanding of shuttle enrichments, and the roles of oxic and anoxic transport, but the paucity of mass balance data does not detract from the use of Fe_{HR}/FeT (or FeT/Al) to recognise enrichment signals.

5. IRON TRANSPORT BY AEOLIAN DUST

5.1 Perspective: The Iron Hypothesis

In the 1990's, two concepts were linked to provide a new focus on iron biogeochemistry within the ocean-atmosphere system. The first recognised that iron could limit phytoplankton productivity in the ocean. Photosynthesis is usually controlled by the delivery of nutrients by upwelling from the deep waters to the photic zone. However in some regions of the oceans the delivery of nutrients exceeds demand and planktonic photosynthesis is limited by some other factor (Fig. 5.1). We now know that iron is the limiting factor in these regions, which are termed High Nutrient Low Chlorophyll (HNLC). One such area of much interest is the Southern Ocean.

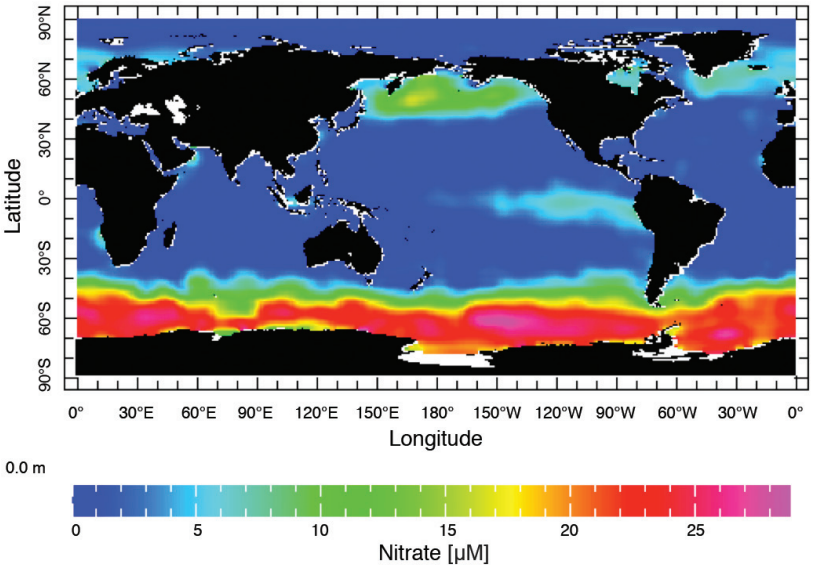

Figure 5.1 HNLC areas in the oceans (shown in red) where iron deficiency limits photosynthesis (data from Levitus *et al.*, 1994).

The second concept recognised the atmosphere as an important source of bioavailable Fe to the oceans from the dissolution of wind-blown (also termed aeolian) dust derived from the continents. The rates at which continentally-derived mineral dust is delivered by winds into the ocean are relatively low

compared to sediment delivery by rivers, yet winds are considerably more efficient at long range transport and are able to reach parts of the ocean that are inaccessible to rivers (e.g. Jickells *et al.*, 2005 and references therein). The bioavailable iron added by aeolian dust supports photosynthesis in the HNLC areas in turn removing CO_2 from the atmosphere and influencing atmospheric CO_2 concentrations and climate. This 'Iron Hypothesis' as expressed by Martin (1990), linked these two concepts over modern and glacial-interglacial timescales and Martin is famously quoted (Fig. 5.2) as saying 'Give me half a tanker full of iron and I will give you an ice-age'.

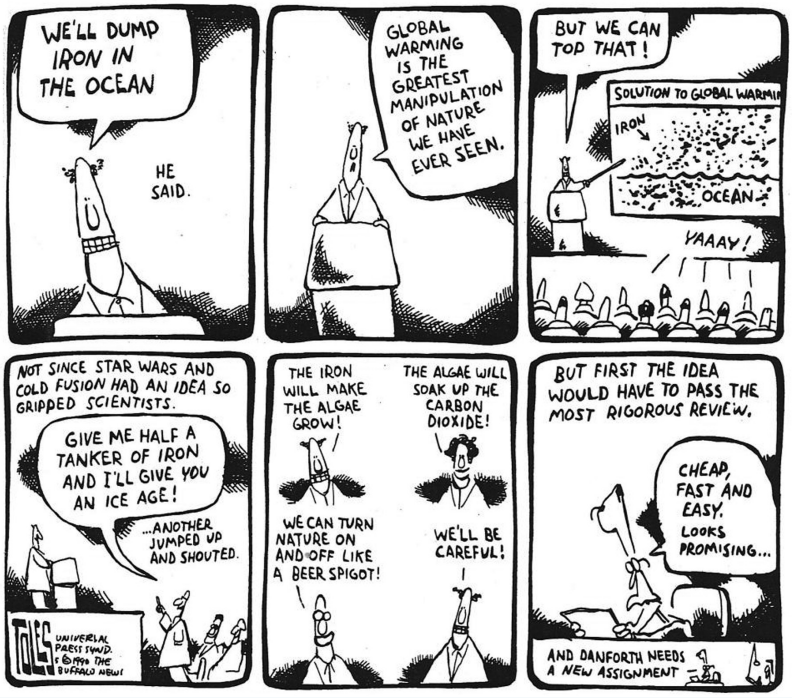

Figure 5.2 Ocean fertilisation: fact or fantasy (from Chisholm and Morel, 1991, with permission from Universal Press Syndicate).

5.2 Aeolian Dust: Something in the Wind?

The 'Iron Hypothesis' has been most intensively studied in the Southern Ocean and most hotly debated (Fig. 5.2) in relation to proposals to fertilise HNLC waters to diminish the effects of anthropogenic CO_2 emissions (Chisholm *et al.*, 2001; Boyd, 2008). For many years it has been assumed that there was only one source

of iron to the Southern Ocean – aeolian dust – which came from outside the marine environment. Now a variety of sources have been recognised that include, shelf sediments, hydrothermal activity and icebergs (Cassar *et al.*, 2007; Boyd and Elwood, 2010; Tagliabue *et al.*, 2010) but aeolian dust is still considered to be a significant source of bioavailable Fe (Fig. 5.3). However there are important uncertainties (Boyd and Elwood, 2010; Breitbarth *et al.*, 2010) in assessing the impact of aeolian dust. These relate to the roles of, and interactions between, aqueous, colloidal/nanoparticulate and particulate Fe phases both in the source regions and following deposition into seawater (Fig. 2.1). Mineralogy needs to be a major player in these discussions.

Many different types of anthropogenically derived materials are found in the atmosphere but mineral dust is the only significant source in the pre-anthropogenic Fe cycle. Dust particles generated by continental erosion have a size range of 1 nm to 100 µm diameter and are removed from the atmosphere by gravitational settling, dry deposition or wet deposition (washed out by rain). Very large particles are quickly lost by gravitational settling but particles <10 µm diameter can be transported large distances (thousands of kilometres) and the average size of dust several hundred kilometres from source is 3µm diameter. The numbers of particles increases by many orders of magnitude as the grain-size decreases but most surface area occurs in the size range 10 nm-1µm which contains the smallest grains, whereas most mass is associated with larger grains in the 100 nm-50 µm range (e.g. Buseck and Adachi, 2008; Engelbrecht and Derbyshire, 2010).

Figure 5.3 But you told me this stuff was bio-available...

Present-day atmospheric dust is derived mainly from arid and semi-arid desert regions, mostly from North Africa, the Arabian Peninsula, Central Asia, China and North America in the Northern Hemisphere, and from Australia, South Africa and South America in the Southern Hemisphere (Fig. 5.4). An additional source of aeolian dust is rock flour produced beneath glaciers and deposited on glacial outwash plains (Schroth *et al.*, 2009; Crusius *et al.*, 2011) which may have been more important in the last glacial period when large ice sheets were common (Mahowald *et al.*, 2006).

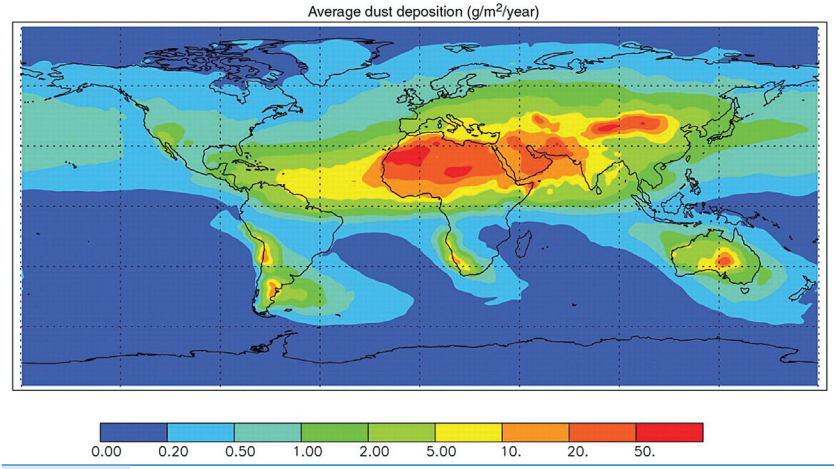

Figure 5.4 Rates of aeolian dust deposition (from Jickells *et al.*, 2005, with permission from the American Association for the Advancement of Science).

Dust Mineralogy. Whatever the provenance, the Fe in aeolian dust may be present in a wide range of minerals that reflect the geology of the source area, the weathering processes taking place and alteration during transport. As a starting point I have compiled (Table 5.1) some representative mineralogical data for dusts collected in several different source and depositional areas. Patagonia dust sources are represented by 10 samples of topsoils from northern to southern Patagonia (Gaiero *et al.*, 2004). These topsoils are the source of, and are thus similar to, aeolian dusts sampled over the same areas in that quartz and feldspars are the main constituents and are accompanied by calcite and smectite with minor illite, kaolinite and chlorite. In effect these are dust precursors. Shen *et al.* (2009) present mineralogical data for 110 dust samples collected over a two year period from 4 source areas across northern China from east to west. The Saharan samples (Glaccum and Prospero, 1980) were collected from three dust events that were sampled as they crossed the North Atlantic. These sources are compared (Table 5.1) to 13 samples of dust deposited in Spain and sourced from the Western Sahara, Moroccan Atlas and Central Algeria (Avila *et al.* (1997) and one sample deposited in an area receiving dust from the Chinese Loess Plateau (Shen *et al.*, 2009).

We note that the samples in these studies have been collected and treated in different ways. However they provide a reasonable indication of the variability arising from different source areas and alteration during transport. Dusts from these widely-separated geographical regions contain essentially the same major minerals but the within-source and between-source variations are large (Table 5.1). Dusts received at the depositional sites are similar in mineralogy to the source dusts except where long range transport is associated with gravitational

settling of the larger and heavier quartz and feldspar particles, thus enriching the finer clay fraction (Glaccum and Prospero, 1980; Baker and Jickells, 2006). Carbonate contents may be variable and individual dust samples commonly contain minor amounts of other minerals; e.g. palygorskite, halite and gypsum, yet, irrespective of source and transport effects, the only major minerals that contain significant concentrations of Fe are clay minerals (illite, smectite, chlorite

Table 5.1 Major minerals in aeolian dust source areas and deposition sites.

Mineral	Source Areas			Deposition Sites	
	Patagonia[1]	China[2]	Sahara[3]	China	Spain[4]
Quartz	10-40%	19-26%	13-21%	15%	14-17%
Potassium Feldspar		1-6%	0.4-2.4%	1%	
Plagioclase Feldspar	7-54%	6-15%	3-6%	4%	2-4%
Calcite	0-46%	1-11%	3-10%	5%	1-12%
Dolomite		0-4%		2%	1-5%
Smectite	20-46				6-27%
Illite	0-7%	37-43%	52-65%	50%	34-41%
Kaolinite + Chlorite	0-11%	13-20%	10-14%	23%	10-40%

1. Range of compositions for samples collected at ten different localities (Gaiero *et al.*, 2004). 2. Range of mean compositions for samples collected at four different localities (Shen *et al.*, 2009). 3. Range of compositions for samples collected at three different localities (Glaccum and Prospero, 1980). 4. Range of mean compositions at three sites (Avila *et al.*, 1997).

and mixed-layer minerals) and iron (oxyhydr)oxides, most commonly goethite and haematite and occasionally magnetite (e.g. Arimoto *et al.*, 2002; Lafon *et al.*, 2004; 2006; Lazaro *et al.*, 2008; Engelbrecht and Derbyshire, 2010). Both clays and Fe (oxyhydr)oxides may be eroded directly from bedrock and transported essentially unaltered, or may be weathered before transport. Even intermittent exposure to moisture weathers Fe^{2+}-bearing minerals producing nanoparticulate iron (oxyhydr)oxides and these, along with clay minerals, seem the most likely sources of bioavailable iron to the oceans.

5.3 Iron Minerals in Aeolian Dust as Sources of Bioavailable Fe

Clay and Fe Silicate Minerals. Clays have been identified as a potential source of iron based on dissolution experiments (Journet *et al.*, 2008) which showed that leaching at pH 2 with nitric acid (in order to simulate atmospheric processing; see Section 5.4) released more iron from clays than from goethite, magnetite and haematite. However the commercial goethite and haematite used in these experiments were sourced from metamorphic rocks and their solubility is likely

to be much lower than those of iron (oxyhydr)oxides present in the soil system. Nevertheless clays do contain small concentrations of potentially bioavailable Fe that can be extracted by ascorbic acid (typically ~1% of the total Fe; Raiswell, 2011b) and which may also dissolve in seawater. Note that Simon Poulton and I have found that clay minerals in natural systems are closely associated with nanoparticles of iron (oxyhydr)oxides (Poulton and Raiswell, 2005) and disentangling these two sources will be extremely difficult.

A more powerful argument for the supply of bioavailable Fe from Fe^{2+}-bearing clays and silicates has been offered by Schroth *et al.* (2009) who have carefully characterised the mineralogy of dust from arid and glacial regions sourcing aeolian dust. Dusts from the arid regions contained >70% of the total Fe as ferrihydrite plus small amounts of goethite, haematite or hornblende. By contrast the glacial samples contained smaller proportions of Fe as ferrihydrite (10-20%) plus large concentrations of biotite and hornblende or Fe^{2+}-bearing smectite. The dusts were subjected to distilled water leaches that, unexpectedly, produced sequential soluble Fe values that accumulated to ~2-3% of the total Fe for the glacial samples (much larger than for the arid samples for which <0.5% of the total Fe was leachable). Schroth *et al.* (2009) point out that Fe^{2+}-bearing silicates are more soluble than iron (oxyhydr)oxides and thus interpret the leached Fe as being derived mainly from silicates. A hugely important potential source of bioavailable Fe from Fe^{2+}-bearing silicates is indicated.

However, the distilled water leaches were filtered (<0.4 μm) and then acidified to pH 2 before analysis and the data therefore represent *filterable* Fe values, which might include nanoparticulate Fe released from the disaggregation and/or dissolution of ferrihydrite during leaching. Schroth *et al.* (2009) believe that these effects were unimportant but it would be valuable to repeat these experiments using filtration techniques that discriminate between aqueous and nanoparticulate Fe species. It is worth pointing out the leaching was carried out under nitrogen gas which would also minimise oxidation of any Fe(II) released from silicates whereas in natural systems the Fe(II) may be released only slowly, allowing in situ oxidation which might inhibit further reaction (see Supplementary Information SI-5). Further studies of Fe dissolution from Fe^{2+}-bearing silicates in aeolian dusts are needed but the emphasis on mineralogy is welcome and timely.

Iron (Oxyhydr)oxides. Few studies of aeolian dust contain any detailed characterisation of the iron mineralogy. Goethite and haematite are commonly reported (see above), but these minerals are, at best, only weakly bioavailable in seawater unless altered by photochemical reduction or grazing (see Supplementary Information SI-5 and SI-7). Ferrihydrite has very rarely been reported in air-borne samples. This is unsurprising in view of its rapid transformation to goethite/haematite in source areas where water is at least transiently present (Fig. 2.4). Note that the occurrences of ferrihydrite reported by Schroth *et al.* (2009) and Crusius *et al.* (2011) refer to dusts collected from source areas rather than actual air-borne material. This distinction raises an important question – could ferrihydrite formed in the weathering environment represent a potential source of bioavailable Fe in aeolian dust? Probably not, because ferrihydrite ages

rapidly to form goethite/haematite mixtures and repeated cycles of wetting and drying occur even in arid and glacial environments, decreasing the solubility of nanoparticulates through aggregation and transformation (see Supplementary Information SI-4). It is very doubtful whether the time prior to becoming airborne would ever be short enough for fresh ferrihydrite to constitute a significant component of aeolian dust prior to transport in the atmosphere, unless aggregation and transformation are somehow inhibited. Given that aeolian dusts contain only small concentrations of Fe in minerals that are leachable in seawater it seems logical to focus our attention on alteration during transport through the atmosphere.

5.4 Atmospheric Processing of Aeolian Dust

Reaction Pathways. There is a powerful case to be made for the alteration and solubilisation of Fe from poorly-reactive minerals, such as goethite, haematite and Fe-bearing clays, during aeolian transport but unravelling the details of dust-cloud interactions (Fig. 5.5) has proved a substantial hurdle. Usher *et al*. (2003) have reviewed the literature on the interactions of trace atmospheric gases with moisture and dust particles. Two main acidic gases are produced in clouds (nitric and sulphuric acids) along with an alkali (ammonia) and an oxidant (ozone) – together constituting a potent reactant mixture. The pH of moisture in clouds can range from 4 to 8 (but lower pH values occur in the aerosols produced by evaporation; see below), so simple acid dissolution of dust must be important. Sulphuric acid is usually considered as the principal acidic reagent because it is mainly associated with the finer, far-travelled particles (<0.1 μm) whereas nitric acid is mainly associated with coarser particles (>0.1 μm) which tend to settle out during long range transport (Andreae and Crutzen, 1997). However even a simple system involving nitric and sulphuric acids, with and without ammonia, can follow many possible alteration pathways for dusts containing a range of different iron minerals accompanied by varying amounts of carbonate (that can neutralise acids) and seasalts.

Further complications arise because most clouds do not produce precipitation and thus dust particles may experience many cycles of exposure to moisture (plus gaseous reactants) interspersed with longer periods of drying and evaporation over transport times that typically range from days to weeks (Jickells and Spokes, 2001). Evaporation increases the concentrations of acid reactants and the resulting aerosol water film may reach pH values of 2 or less (Zhu *et al*., 1992; Meskhidze *et al*., 2003). This initially enhances dissolution, but ultimately evaporation also causes the precipitation of new phases. Ammonia in the aqueous phase reacts with nitric and sulphuric acids to produce ammonium nitrate and sulphate salts that precipitate by evaporation on to dust particles, inhibiting further acidic reaction (Usher *et al*., 2003). In a similar fashion, iron leached by nitric and sulphuric acids from dust minerals may also be precipitated by evaporation to form new iron (oxyhydr)oxides.

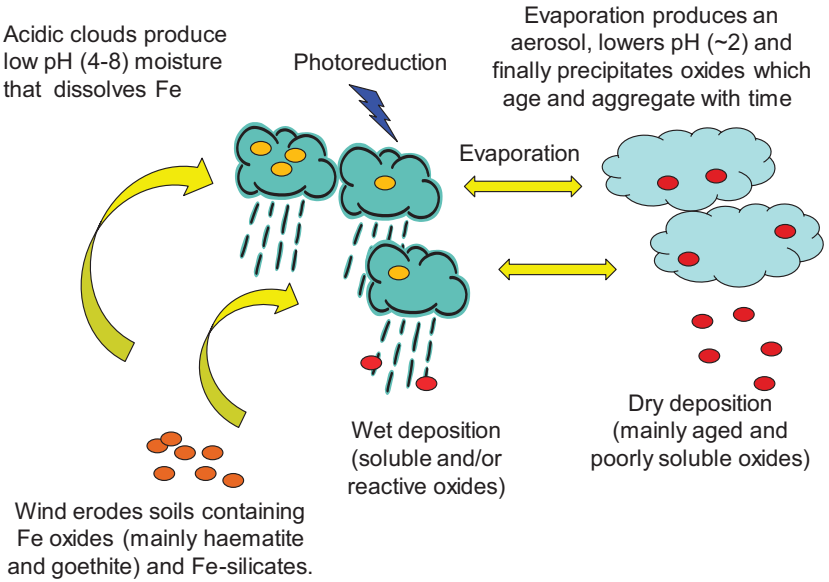

Figure 5.5 Atmospheric processing of aeolian dust.

The interactions between aeolian dust and the acidic species found in clouds also take place in sea ice in the Arctic (Measures, 1999) and Antarctic (Sedwick and DiTullio, 1997; Meguro *et al.*, 2004; Lannuzel *et al.*, 2007, 2008). Sea ice acts as an aeolian dust collector and the dust concentrates on the ice surface as melting occurs. Snow deposition also scavenges acidic species from the atmosphere and a slightly acidic melt results (pH 5.5-6.0; Meguro *et al.*, 2004) in which iron (oxyhydr)oxides are dissolved. Lannuzel *et al.* (2007) found that the concentration of Fe released by acidifying melted sea ice from East Antarctica (to pH 1.8) was typically 3-5 times higher than in seawater at the same location. The production of bioavailable Fe from dust processed by sea ice melt produces phytoplankton blooms and chlorophyll enriched waters associated with the receding edge of the sea ice around the coast of Antarctica (Meguro *et al.*, 2004).

There is also the potential for photochemical reduction in the atmosphere to alter Fe(III) to the more soluble, and more bioavailable, Fe(II) state (see Supplementary Information SI-6 and Fig. 2.6). Complexation of Fe(III) by organic ligands such as formate, acetate and oxalate found in clouds also promotes the photoreduction of Fe(III) causing Fe(II) to be released into the aqueous phase (Erel *et al.*, 1993; Zhu *et al.*, 1993; Siefert *et al.*, 1994). However when solar radiation is absent Fe(II) would be rapidly oxidised back to Fe(III) and stabilisation of Fe(II) would seem to require that organic complexes are formed. Laboratory simulations

of photochemical reduction also suggest that photochemical reduction, acting alone, produces only small increases in iron dissolution (Zhu *et al*., 1993; Spokes and Jickells, 1996).These difficulties have led some workers (e.g. Zhu *et al*., 1997) to conclude that photochemical processes are unlikely to have a substantial effect on the dissolution of Fe from dust.

Dissolution Experiments. Faced with this complexity most studies have adopted an empirical approach to quantify the production of soluble Fe (assumed to be bioavailable) using dust-acid dissolution studies. Treatment of atmospheric dust with acidified distilled water is an obvious approach to quantify how much Fe could be solubilised as a result of atmospheric processing but it has yielded very variable results (from <1% to 21% of total Fe solubilised; Boyd *et al*., 2010a). Does this variability result from different experimental protocols or different dust mineralogies? Certainly a variety of different protocols have been chosen most of which attempt to combine the effects of all the different possible reaction pathways into three variables: pH, dissolution medium and extraction time (Boyd *et al*., 2010a; see also literature reviewed by Jickells and Spokes, 2001). A common, agreed protocol would be an important step forward but the perspective I offer below is that more attention needs to be devoted to dust mineralogy and to the role of colloids/nanoparticles in the interpretation of the dissolution experiments.

More complex experimental simulations of atmospheric processing have shown that reversing low-to-high pH cycling of dust does not affect the final amount remobilised (Spokes and Jickell, 1996; Mackie *et al*., 2005). This reversibility only makes mineralogical sense to me if the Fe is released from, and returned to, similar minerals – suggesting either adsorption or the involvement of iron (oxyhydr)oxides that were either present in the original dust or were formed during the sample pre-treatment with distilled water. Another surprising result was that the rate of Fe release into solution was inversely proportional to dust concentrations (Spokes and Jickells, 1996; Mackie *et al*., 2005). Jickells and Spokes (1996) suggest that higher dust concentrations may have reached a level at which particle adsorption sites were effective at removing Fe from solution, or that the Fe released may have formed colloids. A mineralogical influence has also been detected in long-term dissolution experiments. Most dust dissolution experiments are carried out over relatively short periods of time (days to weeks) but year-long in situ dissolution experiments in the Mediterranean seawater (Wagener *et al*., 2008) identified two pools of iron; a fast released pool which was dissolved an order of magnitude more quickly than a slow released pool (from which the rate of dissolution appeared to be controlled by organic ligands). These data convince me that there is a mineralogical control on dust dissolution and dissolution kinetics.

The role of mineralogy has emerged most clearly from the high resolution microscopy studies of Shi *et al*. (2009) who found nanoparticulate iron (oxyhydr) oxides (including ferrihydrite, Fig. 5.6) and goethite in wet-deposited Saharan dust (Fig. 5.7). The ferrihydrite-bearing material contained trace concentrations of Al, Cr, Si and Ca, possibly indicating formation by atmospheric processing of

clay minerals. Experimental simulation of repetitive atmospheric processing also produced similar goethite nanoparticulates, establishing a valuable connection between process and mineral product. This work did not attempt to determine whether these newly-formed iron nanoparticulates were soluble in seawater, that work remains to be done. A kinetic study by Shi *et al.* (2011a) has found that the dissolution of Saharan and Asian dusts at pH 1-2 could be explained by a first order model using three pools of Fe. A fast release pool had a first order rate constant of 25 hr^{-1}, similar to aged ferrihydrite or poorly crystalline Fe (oxyhydr) oxides. An intermediate pool had a rate constants that mostly ranged from 0.1-0.5 hr^{-1} and was inferred to be poorly reactive iron (oxyhydr)oxides, whilst the slow pool had rate constants ranging from 0.0008-0.006 hr^{-1}, comparable to those of illitic clays.

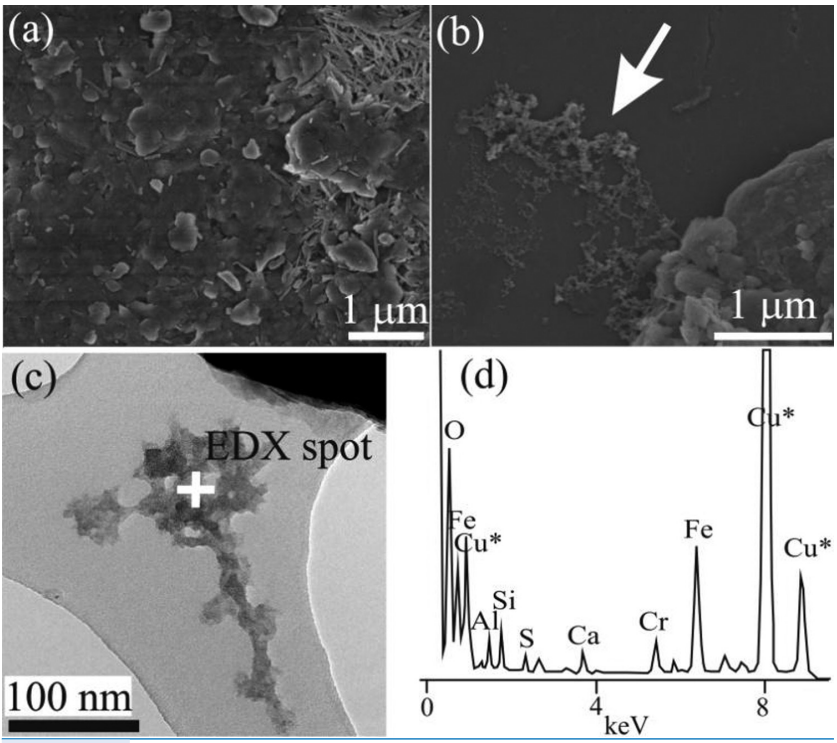

Figure 5.6 SEM images of (a) Eastern Mediterranean dry deposited dust consisting of large mineral dust particles, (b) Western Mediterranean wet deposited dust with arrow showing nanoparticle aggregates, (c) TEM image of nanoparticle aggregate of ferrihydrite in Western Mediterranean dust, (d) EDX spectrum of area (c) showing Fe as the dominant element, Cu from specimen holder (from Shi *et al.*, 2009, with permission from the American Chemical Society).

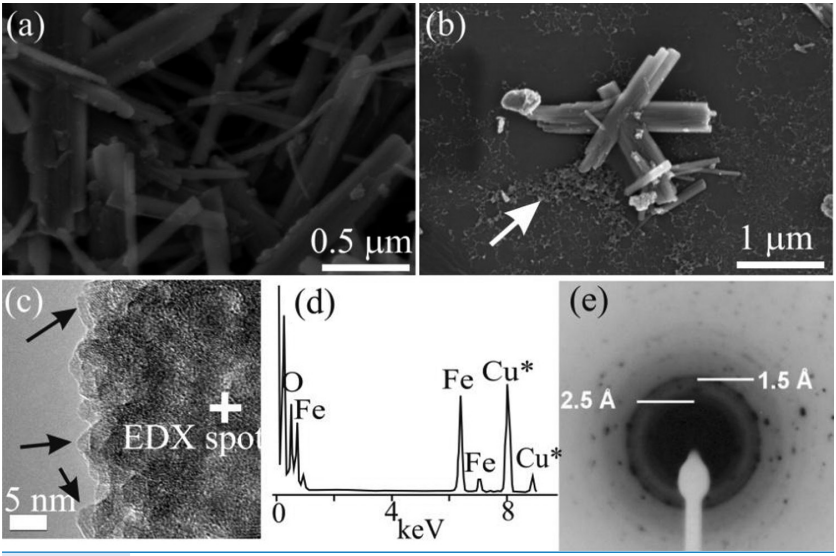

Figure 5.7 SEM images of goethite particles (a) Before simulated cloud processing, (b) After simulated cloud processing with arrow pointing to neo-formed Fe nanoparticle aggregates, (c) TEM image of the nanoparticle aggregate with arrows showing pseudohexagonal shape indicative of ferrihydrite, (d) EDX spectrum of area (c) showing Fe and O as the only elements present (Cu from specimen holder), (e) SAED pattern of area (c) with indexed Bragg distances corresponding to 2-line ferrihydrite (from Shi *et al.*, 2009, with permission from the American Chemical Society).

Atmospheric processing, it seems, can produce fresh ferrihydrite which is the iron (oxyhydr)oxide that is most readily bioavailable (see Supplementary Information SI-1), but fresh ferrihydrite produced in dust source areas may also survive until deposition in seawater, where transformation is inhibited by cementation as demonstrated by Shi *et al.* (2011b). These authors showed that dust derived from palaeo-lake deposits preserved readily soluble ferrihydrite enveloped in a carbonate coating. Carbonate dissolution during atmospheric processing might thus rejuvenate fresh ferrihydrite which is potentially bioavailable (Fig. SI-1). Cementation by other minerals may also play a similar role. Collectively these results place iron (oxyhydr)oxide mineralogy at the heart of the debate over aeolian dust as a source of bioavailable iron.

Final Thoughts. Simple acid dissolution experiments on dust have provided very variable results and demonstrated a need for detailed characterisation of the mineralogy and morphology of potentially-soluble Fe phases (such as clays and nanoparticulate iron (oxyhydr)oxides), both before and after acid dissolution. Similar dissolution experiments with synthetic or natural Fe minerals instead of dust requires that these minerals also replicate the mineralogy and morphology of

the phases found in atmospheric dust. The experimental dissolution of nanoparticulate Fe minerals in seawater must also discriminate between the Fe physically released as nanoparticles and the Fe chemically dissolved as aqueous species. Nearly all of the experimental studies are based on measurements made on solutions filtered through 0.2 or 0.45 µm membrane filters. The assumption that these measurements represent aqueous Fe is invalid at near-neutral pH and in seawater where the iron (oxyhydr)oxides have solubility minima (Cornell and Schwertmann, 2003). Instead these data represent *filterable* Fe measurements and it is probable that some of the variability in reported data for *filterable* Fe results from the inclusion of varying amounts of colloidal/nanoparticulate Fe (oxyhydr) oxides, depending on the experimental protocol.

In fact, dust leaching experiments by Aguilar-Islas *et al*., 2010) using seawater have shown that aqueous Fe (<0.02 µm) was negligible in most dust extractions compared to *filterable* Fe (<0.4 µm). This study also showed that more variability in leach data arises from different aerosols, rather than the extraction protocol, which clearly points to a mineralogical influence. Dissolution was also enhanced by the presence of the siderophore DFOB (considered to represent the effects of ligands forming strong complexes with iron) in a result which echoes the findings of Wagener *et al*. (2010). Dissolution experiments should also attempt to determine the mechanisms of dissolution and quantify their kinetics for different types of dust (or types of Fe minerals found in dust) and derive rate constant data that are specific to the minerals found in dust.

The dissolution experiments of Aguilar-Islas *et al*. (2010) and Wagener *et al*. (2010) also show the importance of addressing the fate of atmospherically-processed dust on entering seawater. Dust is removed from the atmosphere by dry or wet deposition with the former generally predominating by approximately 2:1, although proportions vary in time and space (Jickells and Spokes, 2001). Dry deposition delivers the original dust minerals plus any new or altered phases produced by cloud processing. Wet deposition delivers the same components accompanied by a solution that may vary in pH from 4-8 and that may contain aqueous Fe. These dust-iron mineral-solution mixtures are initially deposited into a microlayer at the sea surface where dissolved and colloidal organic matter is abundant. Residence times of aeolian dust in the microlayer are short (1-15 hr; Chester, 2003) but may still exert a critical influence by forming aqueous Fe-Organic Matter complexes or nanoparticulate-Organic Matter aggregates (see Section 2.2). The dissolution of mineral material in wet and dry deposition appears to be aided by the presence of siderophores, but what will be the fate of the aqueous Fe following wet deposition into seawater? Does complexing prevent precipitation as nanoparticulate Fe (oxyhydr)oxides and thus maintain bioavailability (see Supplementary Information SI-1) or is aqueous Fe precipitated as iron (oxyhydr)oxides which then need to undergo ligand-aided dissolution? Carefully planned and rigorous experimentation will be needed to unravel these complexities.

5.5 Modelling Iron Dissolution from Ferrihydrite-bearing Aeolian Dusts in Seawater

Model Input. The model developed in Supplementary Information SI-7 is used below to quantify the potential delivery rate of bioavailable Fe solely from the iron extractable by ascorbic acid. This Fe (see Raiswell *et al*., 2010) is assumed to be present in dust that has been atmospherically processed as nanoparticulate ferrihydrite (in dry deposition) accompanied by an aqueous/instantaneously soluble form (in wet deposition). Fe delivered as other minerals is assumed to be non-bioavailable in comparison to ferrihydrite. The model utilised here is intended to compare the role of different processes in supplying and removing bioavailable iron from dust minerals in the photic zone of the Southern Ocean following the approach I developed in Raiswell (2011b). The model differs from my earlier model in the following respects. First, the present model is applied to the whole Southern Ocean rather than just the Weddell Sea. Second, modified values of the rate constants are used as summarised in Table SI-7 (see also Supplementary Information SI-7). These data can be used in equations 5.1 and 5.2 (originally derived from SI-7.9 and SI-7.10) to estimate the annual flux of bioavailable Fe to the Southern Ocean derived by both wet and dry deposition:

$$B_i = k_{B.} \times F_A \times t /K - k_B \times F_A (1 - e^{-Kt})/K^2 \quad (5.1)$$

$$M_B = B_i + c \times S \times t \quad (5.2)$$

The model assumes that the dust flux to the Southern Ocean occurs uniformly over space and time, although in fact deposition is highly episodic. The Southern Ocean receives 6% of the global dust flux (Jickells *et al*., 2005) or 960 Gg yr^{-1} of total Fe and ~1% of the total Fe is assumed to be present as ascorbic acid-extractable iron that can produce bioavailable Fe in seawater. Raiswell (2011b) and Shi *et al*. (2011a) showed that ascorbic acid-extractable Fe in air-borne dust ranged from 0.8 to 2.5% (average ~1%) of total Fe. Hence ascorbic acid-extractable Fe is added at a rate of 9.6 Gg yr^{-1} which is assumed to comprise dry and wet deposition in the ratio 2:1 (dry 1.7×10^4 kg day^{-1} and wet 0.9×10^4 kg day^{-1}). Wet deposition is initially assumed to be instantaneously soluble in seawater (see below) although estimates of solubility vary from 4-30% (Gao *et al*., 2003). Thus equation (5.2) becomes:

$$M_B = 1.7 \times 10^4 (k_B \times t/K) - 1.7 \times 10^4 \times k_B (1 - e^{-Kt})/K^2 + 0.9 \times 10^4 \times t \quad (5.3)$$

Equation (5.3) is now used to estimate the rate of bioavailable Fe delivery in a series of different scenarios that examine the effects of different combinations of the processes listed in Table SI-7.

Model Output. A basic model (Model 1) is first constructed that examines the input of bioavailable Fe from the dissolution of ferrihydrite (with the first order rate constant k_B corrected for temperature and varying with time from 0.003 initially to 0.0007 day^{-1} after 100 days; see Supplementary Information SI-7). The loss of nanoparticulate Fe is considered to occur by sinking (maximum

k_L = 0.001 day^{-1}), scavenging (k_L = 0.25 day^{-1}) and transformation (k_L = 0.003 day^{-1}) and thus K = k_B + 0.254 day^{-1} (see Supplementary Information SI-7 and Table SI-7). Model outputs show that the net result of the processes that deliver, and remove nanoparticulate Fe, produce dissolved and bioavailable Fe at a rate that climbs quickly over approximately 5 days to reach a value of ~10^5 kg and then climbs slowly to a maximum ~3 × 10^6 kg after a year (Fig. 5.8a). This addition is substantially by wet deposition which always exceeds that from dry deposition by at least two orders of magnitude (Fig. 5.8a); thus dissolved Fe addition from wet deposition is 3.2 × 10^6 kg yr^{-1} compared to 1.6 × 10^4 kg yr^{-1} by dry deposition in this model. The model delivery rate of bioavailable Fe of ~3 × 10^6 kg yr^{-1} is higher than the 8 × 10^5 kg yr^{-1} estimated by Lancelot *et al.* (2009) but an order of magnitude lower than the estimate of 2 × 10^7 kg yr^{-1} (see Section 7.3) based on Tagliabue *et al.* (2009).

This basic model is amended (Model 2) by incorporating the effects of siderophore-aided dissolution with the first order rate constant k_B corrected for temperature and varying with time from 0.1 initially to 0.045 day^{-1} after 100 days (see Supplementary Information SI-7). Loss processes are the same as in Model 1 and thus K = k_B + 0.254 day^{-1}. The delivery of bioavailable Fe (Fig. 5.8b) is essentially the same as Model 1, simply because the supply by wet deposition dominates that by dry deposition, although only by an order of magnitude because of the faster rates of release from dry deposition by siderophore-aided dissolution. The same is also true for Model 3 (Fig. 5.8b) which adds the effects of photochemical reduction (or grazing) on the formation of bioavailable Fe to the basic model. Model 3 only produces slightly larger outputs of bioavailable Fe than Model 2. Both siderophore-aided dissolution and photochemical reduction (or grazing) increase the delivery of bioavailable Fe from dry deposition by about an order of magnitude but this is still insufficient to produce any significant overall increase in bioavailable Fe supply which is still dominated by the wet flux.

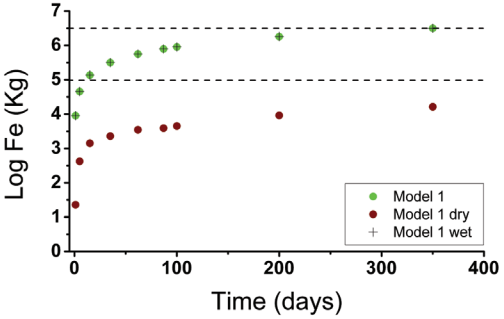

Figure 5.8a Rates of delivery of bioavailable Fe by aeolian dust to the photic zone in the Southern Ocean from a basic model incorporating ferrihydrite dissolution and transformation, and loss of nanoparticulates by sinking and scavenging. Contributions from wet and dry deposition are combined for the total delivery. Upper and lower horizontal dashed lines indicate estimates of bioavailable Fe in Table 7.1, based on Tagliabue *et al.* (2009) and Lancelot *et al.* (2009) and this applies also to Figures 5.8b and 5.8c below.

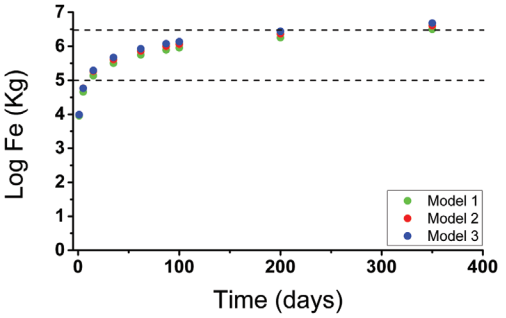

Figure 5.8b Rates of delivery of bioavailable Fe to the photic zone in the Southern Ocean from the basic model (Model 1) amended by enhanced addition from siderophore-aided dissolution (Model 2), and photochemical reactions (Model 3). Lines as in Figure 5.8a.

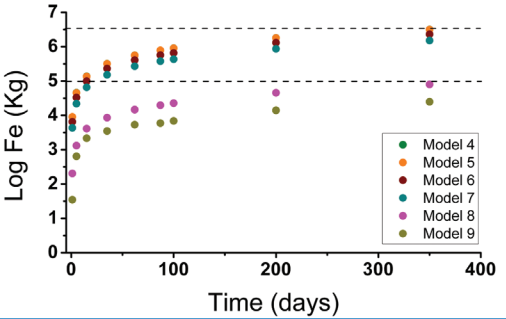

Figure 5.8c Rates of delivery of bioavailable Fe to the photic zone in the Southern Ocean from the basic model amended for increasing losses of grazing (Model 4), more rapid scavenging (Model 5), changing the ratio of dry: wet deposition from 2:1 to 3:1 (Model 6), decreasing the solubility of wet deposition to 50% (Model 7) and 2% (Model 8) and using all dry deposition (Model 9). Lines as in Figure 5.8a.

Models 4 and 5 (Fig. 5.8c) examine the influence of faster losses by scavenging that produce losses of the nanoparticulate Fe added by dust through ingestion and incorporation into faecal pellets (see Supplementary information SI-7). Model 4 adds a scavenging loss with a relatively low rate constant (k_B = 0.1 day^{-1}) and model 5 shows the effects of faecal pellet scavenging using a rate constant of k_B = 12 day^{-1} (which is the maximum literature value; Table SI-7). These models still continue to show essentially the same outputs of bioavailable Fe as Model 1, again because wet supply is dominant and represents an instantaneous source of bioavailable Fe comparatively unaffected by scavenging. Model 6 examines the influence of changing rates of wet deposition delivery by altering the ratio of dry:wet deposition from 2:1 to 3:1, which does produce a slight decrease in the delivery of bioavailable Fe although this is still insufficient to distinguish this output from models 4 and 5 in Figure 5.8c.

Finally Models 7 and 8 explore the effects of decreasing the solubility of wet deposition from 100% to 50% and then 2% (from Gao *et al.,* 2003) assuming that the remaining part of wet deposition is insoluble in seawater (Fig. 5.8c). Model 7 (50% solubility) produces a slight decrease in the delivery of bioavailable Fe (as compared to Model 1) but Model 8 (2% solubility) produces a decrease of around two orders of magnitude in bioavailable Fe delivery to ~7.9 × 10^4 kg yr^{-1} as compared to the basic model. Model 8 (Fig. 5.8c) delivers

an order of magnitude less bioavailable Fe than the estimate by Lancelot *et al.* (2009). Model 9 assumes that all the dust flux to the Southern Ocean is by dry deposition alone and produces a supply of bioavailable Fe (2.5×10^4 kg yr^{-1}) somewhat lower than Model 8 and more than an order of magnitude lower than estimate of bioavilable Fe delivery from Lancelot *et al.* (2009).

Final Thoughts. The model outputs show that the processes which remove nanoparticulate Fe associated with dust from the photic zone (sinking, scavenging and incorporation into faecal material) exert relatively little influence on rates of bioavailable Fe delivery in any of the model outputs. Furthermore, wet deposition alone supplies sufficient aqueous bioavailable Fe to match other estimates of aqueous supply to the Southern Ocean (see Table 7.1) and this delivery is not significantly enhanced by siderophore-aided dissolution and photochemical (or grazing) additions. This suggests to me that the really important questions relate to the nature of wet and dry deposition (see also Breitbarth *et al.*, 2010). There are, at present, no clear answers to the questions raised below.

Wet deposition of a Fe in a form that is instantaneously soluble in seawater is potentially an extremely important source of bioavailable Fe. What is the nature of wet deposition? Is it accompanied by the delivery of aqueous iron or iron in a form that is instantaneously soluble in seawater (as these models assume) and, if so, how large is this flux? Do these forms of iron become complexed in seawater or is the iron precipitated as iron (oxyhydr)oxides accompanied by organic matter? What are the mineral forms of iron in wet deposition that can be atmospherically processed to form bioavailable Fe? Ferrihydrite and goethite, along with Fe-bearing silicates, seem the most likely minerals but is atmospheric processing capable of producing these minerals in forms that can dissolve in seawater, and how quickly does dissolution occur?

Dry deposition of all the Southern Ocean dust flux as ferrihydrite appears incapable of producing dissolved Fe at significant rates by dissolution unless rates are enhanced by the involvement of siderophores and/or photochemical reduction. However, what actually is the mineralogy of iron in dry deposition? Is the main mineralogy ferrihydrite or goethite and are these minerals present in forms that can supply bioavailable Fe by dissolution, siderophore-aided dissolution and photochemical reduction in seawater? The basis of all the models is the dissolution data used for ferrihydrites. Are the data used, and the changes in solubility with time, representative of the phases found in wet and dry deposition? These questions provide a challenging agenda.

6. IRON EXPORT BY ICEBERGS AND SUBGLACIAL RUNOFF

6.1 Retrospective: Starting on Glaciers

I am just starting a graduate student on the geochemistry of meltwaters. I have never taken any glaciology courses but there is good glaciological expertise in the School of Environmental Sciences, at the University of East Anglia. These colleagues and myself are about to carry out dye-tracing experiments on glaciers in the Swiss Alps. The graduate students are diluting the rhodamine dye and getting ready to inject the dye into a crevasse. We intend to collect meltwater samples downstream beyond the glacier snout, where we have established a monitoring station (Fig. 6.1a). There is uncertainty of the degree of dye dilution which seems to be excessively large. Eventually we settle on a lesser dilution, tip the dye down a crevasse and make our way back to the monitoring station (Fig. 6.1b). About 2 hours later the dye starts to reach the station and there is much cheering and back slapping as the water gets redder and redder. The fluorimeter readings rise steadily and the water continues to get redder and redder. The water now becomes a deep, dirty scarlet and the fluorimeter readings go off scale. Nearby tourists notice the phenomena but I affect nonchalant disinterest. A large stretch of the meltwater stream is now stained and the red stretch of water continues to extend further and further downstream. The tourists enquire whether members of the party

Photo from Martyn Tranter.

Figure 6.1a Thinking about dye-tracing meltwater streams.

Photo from Martyn Tranter.

Figure 6.1b Analysing meltwater samples.

have been crushed beneath the glacier. I pretend not to hear and lead the group off down the valley. I am glad we had the foresight to collect a supply of drinking water from the stream earlier that day.

6.2 Perspective: Biogeochemistry in the Cryosphere

Glaciers and icesheets are microbially active. Approximately 10% of the earth's surface is covered by ice and, in my early days, I and most other geochemists, thought that the ice-rock interface was abiotic and that geochemical reactions were mainly inorganic (Raiswell, 1984). This premise was based on the belief that little metabolisable organic matter was present, and seemed to be supported by observations of meltwater composition that I and others had made which could be explained in terms of simple inorganic reactions; mainly CO_2 dissolution, calcite dissolution and sulphide oxidation (Raiswell, 1984; Raiswell and Thomas, 1984; Tranter *et al.*, 1993; Brown, 2002; Tranter, 2005). This view has been displaced only slowly as it was realised that microbially-driven redox reactions such as denitrification and organic matter oxidation along with the microbial oxidation of sulphide minerals (Fairchild *et al.*, 1993; Tranter *et al.*, 1994; Tranter *et al.*, 2002) were required to explain the composition of glacial meltwaters. Wind-blown organic matter, it seems, can be washed into the subglacial environment from the glacier surface (Stibal *et al*, 2008), and organic matter-bearing soils can be over-ridden as glaciers advance (Brown, 2002). There is now also evidence that the kerogen in ancient bedrocks may be metabolisable in the subglacial environment (Wadham *et al.*, 2004). The emerging realisation that kinetic and thermodynamic constraints do not solely control meltwater geochemistry has been accompanied by microbial studies of meltwaters and subglacial environments (Sharp *et al.*, 1999; Skidmore *et al.*, 2000; Bottrell and Tranter, 2002). These studies have shown that populations are diverse and widespread, and are able to influence the nature and extent of subglacial weathering reactions. Microbial life in the subglacial environment, as elsewhere, requires no more than water, organic matter and nutrients, but greatly speeds up weathering processes especially those reactions which provide a source of energy, such as the oxidation of Fe^{2+}-bearing rock minerals.

The presence of water and nutrients is clearly possible for temperate glaciers which are composed of warm ice at the pressure melting point, and where meltwater is present at the ice-rock interface. However the properties of warm-based glaciers are in stark contrast with those of polar (cold-based) glaciers and ice sheets where there is cold ice below the melting point, frozen to the glacier bed, and which have no meltwater at the ice-rock interface. Intermediate between these two are polythermal glaciers, where an inner temperate region is surrounded by a cold-based margin (Brown, 2002). Temperate and polythermal glaciers both clearly contain the necessary ingredients for microbially-fuelled weathering reactions; water is present, organic matter can be available and the rock flour produced by glacial grinding can also supply nutrients. Not surprisingly

microbial populations have been identified in temperate glaciers (Sharp *et al.*, 1999; Skidmore *et al.*, 2000), polythermal glaciers (Wadham *et al.*, 2004) and the margins of icesheets (Yde *et al.*, 2010).

Can microbial weathering also occur in the colder Antarctic glaciers and icesheets? Antarctic glaciers and icesheets clearly contain sediment-rich layers (Fig. 6.2a and cover) that may contain organic matter so the question comes down to whether there is evidence that water can exist. In fact the major icesheets in Antarctica (and Greenland) contain ice streams that stretch for hundreds of kms and are up to 50 km wide and 2 km thick. Here ice moves relatively rapidly due to basal melting arising from geothermal and frictional heating which produces a bed of sediment saturated with liquid water that is thought to cover more than 50% of the area of the Antarctic ice sheet (Rignot *et al.*, 2008; Pattyn, 2010). However only basal meltwater produced beneath ice streams around the Antarctic periphery (~20%) of the ice area is likely to have a hydraulic pathway to the Southern Ocean and the potential discharge from ice sheets to the Southern Ocean is estimated to be 18-31 km^3 (Wadham *et al.*, 2010a).

Figure 6.2a Sediment-bearing iceberg in the Southern Ocean (from Raiswell, 2011a, with permission from Elements).

Even in cold-based Antarctic glaciers where basal temperatures may be –15 to –20°C, zones of temperate ice may exist (Hubbard *et al.*, 2004) and there may also be thin films of water (20-40 nm) at the ice-rock interface (Cuffey *et al.*, 1999). Evidence for the existence of water also comes from high resolution microscopy studies of sediments in Antarctic icebergs and glaciers that contain the Fe mineral schwertmannite (Raiswell *et al.*, 2009). Schwertmannite (see Supplementary Information SI-6) mainly forms by the oxidative, aqueous weathering of pyrite at low pH (Bigham *et al.*, 1996) and it probably transforms to goethite/haematite mixtures in contact with water (Schwertmann and Carlson, 2005) in <100 years (Raiswell *et al.*, 2009). Schwertmannite entombed in ice demonstrates the existence of transient aqueous microenvironments where microbial weathering may occur even in cold-based glaciers. The presence of water in cryogenic environments enables Fe cycling to occur, which in turn is able to influence ocean chemistry.

6.3 Export of Fe to the Southern Ocean by Subglacial Runoff and Icebergs

Subglacial Runoff. I and others now believe that the iron in subglacial runoff from Antarctic glaciers and icesheets is largely derived from sulphide oxidation, which appears to be the dominant biogeochemical reaction in the shallow sediments beneath the Antarctic Ice sheet (Raiswell *et al.*, 2009; Skidmore *et al.*, 2010; Wadham *et al.*, 2010b). In Antarctica, as in other glacial environments, pyrite oxidation consumes oxygen and ultimately drives oxygen down to low, or zero, concentration levels producing anoxic conditions at the ice-rock interface (Brown *et al.*, 1994; Raiswell *et al.*, 2009; Wadham *et al.*, 2012). In turn, anoxic conditions in organic C-bearing subglacial sediments produce suitable environments for microbial Fe reduction, sulphate reduction and methanogenesis (Wadham *et al.*, 2004; Wadham *et al.*, 2010b; Boyd *et al.*, 2011). There are few data on the composition of subglacial waters from Antarctica but concentrations of Fe(II) appear to range from 40-4000 μM (Wadham *et al.*, 2012), many orders of magnitude in excess of the *filterable* Fe concentrations in surface seawater in Antarctica (1-2 nM; see above). It is an intriguing possibility that the discharge of sub-glacial iron-rich waters (Fig. 6.2b) from the Polar regions may have contributed to the ferruginous deep-ocean conditions (Mikucki *et al.*, 2009; Poulton and Canfield, 2011) that formed the BIFs associated with the Neoproterozoic glaciations (see Section 9.6).

Photo from Tim Lyons.

Figure 6.2b Discharge of Fe (oxyhydr)oxides from the glacier Austre Brøggerbreen, Svalbard.

However the discharge of anoxic subglacial waters into oxic seawater will mostly result in the rapid oxidation of aqueous Fe(II) to ferrihydrite nanoparticles (Raiswell *et al.*, 2006; 2008a). The critical, as yet unanswered question, is whether this potentially bioavailable iron is used to fuel productivity on the shelf, thus producing an 'Island Effect' where enhanced productivity occurs adjacent to land masses (Blain *et al.*, 2007; Ardelan *et al.*, 2010), or whether the iron is exported to the remote HNLC areas of the Southern Ocean.

Icebergs. Iceberg-hosted sediments also constitute another potential source of bioavailable Fe present as ferrihydrite nanoparticles with a high export potential. In the past it was often assumed that subglacial sediments were inert

but, although rates of weathering are generally restricted by low temperatures and limited access to water, these restrictions are offset by the occurrence of freshly ground rock debris and by microbial activity (see above and Brown, 2002). Thus chemical weathering oxidises Fe^{2+}-bearing rock minerals to produce Fe^{3+} (oxyhydr)oxides and nanoparticulate ferrihydrite, goethite, lepidocrocite, haematite and schwertmannite have all been recognised in iceberg-hosted and subglacial sediments from the Arctic and Antarctic (Raiswell *et al.*, 2006; 2008a; 2009; Shaw *et al.*, 2011a). The Antarctic ice streams terminate in huge ice shelves where most ice is lost by calving into icebergs. A critical feature of iceberg delivery to the oceans is that freezing preserves the most reactive nanoparticles by limiting access to water and slowing down the rates at which transformation to less reactive iron (oxyhydr)oxides occurs (see Fig. 2.4 and Supplementary Information SI-3). The preservation of nanoparticulate iron (oxyhydr)oxides in ice, and their delivery by the iceberg conveyor belt away from the continental shelf, exerts a significant impact on the productivity of the Southern Ocean (Raiswell *et al.*, 2008a).

Ever since John Martin proposed that iron is the limiting nutrient in the Southern Ocean (Martin, 1990), it has been widely assumed that wind-blown dust is the main mineral source of bioavailable iron to this region (see Sections 5.1 and 5.2). However the sediments in free-floating icebergs (Fig. 6.2b and cover) contain nanoparticulate iron (oxyhydr)oxides. This Fe is potentially bioavailable and can contribute at least as much-or perhaps even more-bioavailable iron as wind-blown dust (Raiswell *et al.*, 2008a). Icebergs in the Southern Ocean, particularly in the Weddell Sea (where their frequency is increasing) are thus likely to boost ocean productivity significantly as they melt (Smith *et al.*, 2011). Indeed melting icebergs that release bioavailable Fe to HNLC ocean areas can enhance photosynthesis and may serve as a significant carbon dioxide sink.

Observations of floating icebergs reinforce a role for the delivery of bioavailable Fe from sediment released by melting. Smith *et al.* (2007) demonstrated that melting icebergs in the Weddell Sea are associated with hot spots of biological activity (Fig. 6.3). In addition to significant enrichments of glacial sediment around two icebergs they also found high concentrations of chlorophyll, krill and seabirds. Extrapolating their results to the Weddell Sea as a whole, Smith *et al.* (2007) estimated that similar-sized icebergs already influence 39% of the surface ocean in this area. They expect that area of influence to increase as atmospheric warming continues the trend of ice sheet disintegration and iceberg production throughout the Southern Ocean. Iceberg enhancement of photosynthesis may thus help to mitigate global warming (Raiswell *et al.*, 2008a).

6.4 Modelling Iron Dissolution from Iceberg-hosted Sediments and Subglacial Runoff

Model Input. The model developed in the Supplementary Information SI-7 is now used to quantify the potential delivery of bioavailable Fe solely from the iron extractable by ascorbic acid (assumed to be present as nanoparticulate

ferrihydrite) present in iceberg-hosted sediments. The model utilised here is only intended to compare the role of different processes in supplying and removing bioavailable iron from icebergs in the photic zone of the Southern Ocean. The model follows the approach I adopted in Raiswell (2011b), from which it differs in the following respects. First, the present model is applied to the whole Southern Ocean rather than solely to the Weddell Sea. Second, different values of the rate constants are used as are given in Table SI-7.

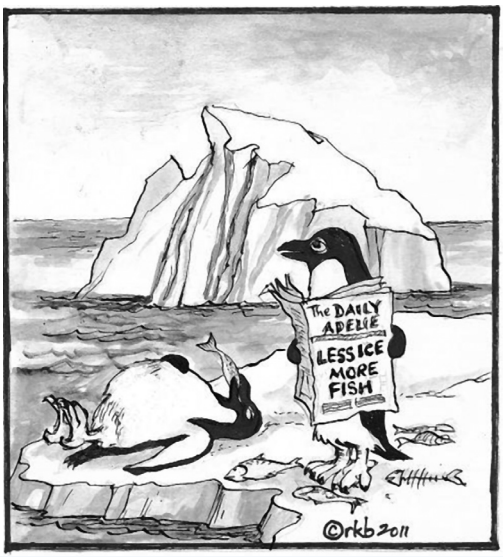

Figure 6.3 You know, this global warming is turning out a lot better than I expected!

These constants can be used in equations 6.1 and 6.2 (originally derived from SI-7.9 and SI-7.10) to estimate the annual flux of bioavailable Fe to the Southern Ocean derived by both ferrihydrite dissolution and aqueous Fe:

$$B_i = k_B \times F_A \times t / K - k_{B.} \times F_A (1 - e^{-Kt}) / K^2 \quad (6.1)$$

$$M_B = B_i + \boldsymbol{c} \times \boldsymbol{S} \times t \quad (6.2)$$

In Raiswell (2011b) I used a value of 150 $km^3\ yr^{-1}$ as a minimum estimate for the volume of ice melting annually from Antarctica. This estimate was derived from measurements of time-variable gravity (Velicogna and Wahr; 2006) which do not account for the erosive loss of ice and is therefore much too low. Earlier I (Raiswell *et al.*, 2006) had used a larger estimate of 2000 km^3yr^{-1} but the models in this section are based on a conservative value of 1000 km^3yr^{-1} which gives a daily melting rate of 10 km^3day^{-1} for a melt season of 100 days. Assuming a sediment content of 0.5 kg m^{-3} with an ascorbic acid-extractable iron (present as nanoparticulate ferrihydrite) content of 1.5×10^{-3} kg per kg (as in Raiswell *et al.*, 2006; Raiswell, 2011b; Shaw *et al.*, 2011b) enables the delivery rate of ascorbic acid-extractable iron to be estimated as 7.5×10^6 kg day^{-1}. Equation (6.1) then becomes:

$$B_i = 7.5 \times 10^6 \times k_B \times t / K - 7.5 \times 10^6 \times k_B (1 - e^{-Kt}) / K^2 \quad (6.3)$$

Equation 6.3 requires an estimate for the concentration of aqueous Fe added by melting which is difficult to make. Measurements of Fe concentrations in icemelt from unfiltered, acidified samples of snow and ice in Antarctica are

given by Martin *et al.* (1990) for ice (26 nM), Loscher *et al.* (1997) for ice (26-99 nM) and surface snow (31-53 nM), Edwards *et al.* (1998) for surface ice (0.7-2.5 nM) and Edwards and Sedgewick (2001) for surface snow (0.8-21 nM). However, these data include an unknown contribution from acidified particulates. With colleagues I (Raiswell *et al.*, 2008) have measured relatively low Fe concentrations in Antarctic glaciers and icebergs (1.0±1.3 nM). These measurements were made on melt samples filtered through <0.2 µm which represent nanoparticulate plus aqueous Fe. Our mean concentration, with a melting rate of 1000 $km^3\ yr^{-1}$, produces a maximum of only 1.3×10^5 kg yr^{-1} of aqueous plus nanoparticulate Fe. We will see that this is small in relation model outputs of potentially bioavailable Fe delivered by iceberg nanoparticulates, except where these assume very rapid losses by faecal pellet scavenging.

There is, however, a significant additional flux of subglacial water from the margins of the ice streams. This flow averages 24 $km^3\ yr^{-1}$ (Wadham *et al.*, 2010a) and may be oxic or anoxic (Section 6.3). Concentrations of *filterable* Fe (filtered through 0.45 µm) in oxic subglacial waters have been estimated to range from 0.002 to 0.2 µM (Wadham *et al.*, 2012), providing an annual delivery flux of 2.7×10^3 to 2.7×10^5 kg yr^{-1}. At the upper end of this range the flux is comparable to the flux of potentially bioavailable Fe from iceberg-hosted nanoparticulate ferrihydrite (where faecal losses are high, see below), but *filterable* Fe comprises colloidal, nanoparticulate and aqueous Fe. Since equation 6.1 is based on the delivery of nanoparticulate Fe as ferrihydrite, data that include aqueous, nanoparticulate and colloidal species would in effect count the nanoparticulate/colloidal flux twice. Much higher concentrations of *filterable* Fe could occur in anoxic waters (40 to 4000 µm; Wadham *et al.*, 2012) but rapid oxidation and mixing with seawater would precipitate a substantial proportion of ferrihydrite (Raiswell, *et al.*, 2008a). Furthermore aggregation, sinking and scavenging produce efficient deposition of ferrihydrite to shelf sediments and an unknown (but probably small) proportion of nanoparticulate ferrihydrite would be exported from the shelf (see Section 4.7). The models used here will therefore ignore aqueous Fe sources from both ice melt and subglacial melt.

Model Output. Using the data above, I have constructed a basic model (Model 1; Fig. 6.4a) to examine the input of bioavailable Fe from the dissolution of nanoparticulate ferrihydrite delivered by icebergs. This model is based on a first order dissolution rate constant k_B corrected for temperature and varying with time from 0.003 initially to 0.0007 day^{-1} after 100 days; see Supplementary Information SI-7). The loss of nanoparticulate Fe occurs by sinking (maximum k_L = 0.001 day^{-1}), scavenging (k_L = 0.25 day^{-1}) and transformation (k_L = 0.003 day^{-1}) producing a combined k_L = 0.254 and $K = k_B + k_L$) which gives $K = k_B + 0.254$ day^{-1}. Model outputs show that the delivery of iron climbs quickly over approximately 40 days to reach a value of ~3×10^6 kg yr^{-1} with relatively little change then to 100 days (Fig. 6.4a). This mass of bioavailable Fe is rather larger than that estimated to occur from aeolian dust (8×10^5 kg yr^{-1}) by Lancelot *et al.* (2009) but is about a factor of 5 lower than the estimates by Tagliabue *et al.* (2009, 2010).

The basic model is next amended (Model 2) by incorporating the effects of siderophore-aided dissolution with the first order rate constant k_B corrected for temperature and varying with time from 0.1 day^{-1} initially to 0.04 day^{-1} after 100 days (see Supplementary Information SI-7). Loss processes are the same as Model 1 and thus $K = k_B + 0.254\ day^{-1}$. The delivery of bioavailable Fe exceeds 10^7 kg after 5 days and reaches a maximum of 2×10^8 kg (Fig. 6.4a), significantly larger than Model 1 and also larger than the highest estimates of production from aeolian dust, by Tagliabue *et al.* (2010). Model 3 adds the effects of photochemical reduction (or grazing) on the basic model and produces essentially the same outputs of bioavailable Fe (>10^8 kg) as Model 2. Both siderophore-aided dissolution and photochemical reduction (or grazing) have the capacity to increase the delivery of bioavailable Fe over simple dissolution by approximately 2 orders of magnitude. The influence of siderophores and photochemical reduction is much larger than with aeolian dust, for which wet deposition is more significant than the dissolution of nanoparticulate Fe (which is the only iceberg source).

The remaining models (Fig. 6.4b) examine the influence of increasing losses by faecal pellet scavenging and by decreasing F_A. Model 4 adds a relatively low rate constant for faecal pellet scavenging (k_L =0.1 day^{-1}) and model 5 shows the effects of a higher rate constant (k_L = 12 day^{-1}; Table 7.1 and see Supplementary Information SI-7). Despite the increased losses, both these models still reach the range of bioavailable Fe delivery of 10^5 to 3×10^6 kg yr^{-1} estimated to occur from aeolian dust (given by the horizontal lines in Fig. 6.4b). Finally, Model 6 explores the effects of decreasing F_A from 0.75×10^7 kg day^{-1} to 0.75×10^6 kg day^{-1}, and this change produces a corresponding one order of magnitude decrease in bioavailable Fe delivery compared to the basic model and reaches a maximum delivery rate of almost 10^5 kg in 100 days.

Final Thoughts. The models clearly require improved data for the rate constants for siderophore-aided dissolution, photochemical reduction, scavenging and grazing (see also Section 5.5), but it is difficult to avoid the conclusion that simple dissolution of ferrihydrite from iceberg-hosted sediment is at least as effective at supplying bioavailable Fe as aeolian dust.

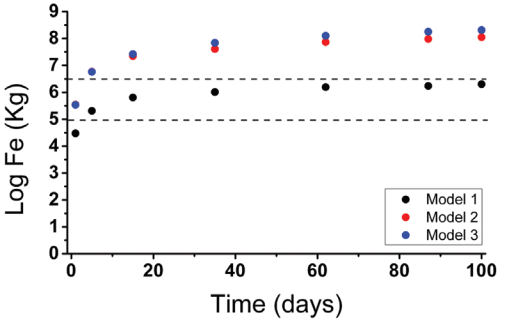

Figure 6.4a Rates of delivery of bioavailable Fe from icebergs to the photic zone in the Southern Ocean. The basic model (Model 1) is amended by enhanced addition from siderophore-aided dissolution (Model 2) and photochemical reactions (or grazing) (Model 3). Upper and lower horizontal dashed lines indicate estimates of bioavailable Fe in Table 7.1, based on Tagliabue *et al.* (2009) and Lancelot *et al.* (2009) and this applies also to Figure 6.4b below.

Aside from the rate constant data, the principle sources of uncertainty relate to glaciological variables; specifically the rate of melting from Antarctica, the sediment content of icebergs and the fate of Fe delivered by anoxic subglacial waters. However the significance of iceberg supply in relation to aeolian dust seems robust assuming that the value of F_A (the delivery rate of nanoparticulate ferrihydrite which combines rate of melting and sediment content) is no more than an order of magnitude too large.

The estimates produced here further emphasise the potential influence of icebergs through the glacial supply of labile Fe as nanoparticulate (oxyhydr) oxides to the Southern Oceans. Our findings indicate that a more comprehensive study of iceberg-hosted sediment is now required to ascertain the extent to which iron (oxyhydr)oxide nanoparticulates are present in icebergs, their geographical distribution and their bioavailability. Identifying icebergs as a significant – but previously overlooked – source of bioavailable Fe sheds new light on how the oceans respond to periods of atmospheric warming. It is possible, for example, that the iceberg delivery of sediment containing iron as (oxyhydr)oxides during the Last Glacial Maximum (18000-21000 years ago) could have been sufficient to fertilize the increase in ocean productivity required to drawdown CO_2 to the levels observed in ice cores. And if icebergs mitigated against climate warming in the past, they may have the capacity to do so in the near future.

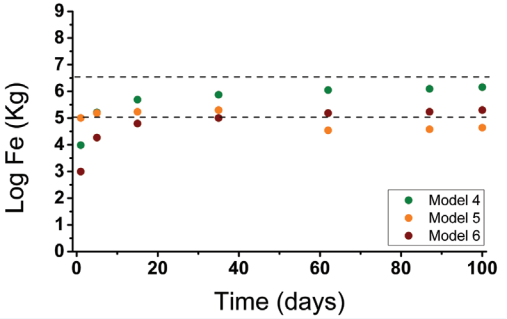

Figure 6.4b Rates of delivery of bioavailable Fe by icebergs to the photic zone in the Southern Ocean. The basic model is amended for increasing losses by faecal pellet scavenging at minimum and maximum rates (Model 4 and Model 5 respectively) and lower FA (Model 6). Lines as in Figure 6.4a.

7. IRON SOURCES TO THE OCEANS

7.1 Perspective: Constructing the Input Budget

Surprisingly, in view of the widespread interest in the behavior of iron in the ocean, there have been few attempts to construct a comprehensive set of estimates for the inputs of soluble iron to the global ocean (de Baar and de Jong, 2001; Tagliabue *et al.*, 2010). At the start of the new millennium the most important external source to the Southern Ocean was thought to be aeolian dust but multiple sources are now known to occur (Cassar *et al.*, 2007; Tagliabue *et al.*, 2010) and a much more complex picture is emerging. This section utilises the data discussed throughout this paper to produce new estimates for the sources of Fe to both the global ocean and the Southern Ocean (here defined as the area >60°S). The main focus in these budgets is on iron delivered to the surface waters of the open ocean (away from the continental shelf). Hydrothermal inputs to deep waters are included for comparison although it is unclear how much influence these exert on surface waters (Tagliabue *et al.*, 2010; Wu *et al.*, 2011). Where possible, the budget distinguishes between aqueous (A), nanoparticulate (N) and colloidal (C) inputs based on the arbitrary size separations discussed in Section 1.2 and it is assumed, as a rough approximation, that *filterable* iron (F) = A + N + C for the individual fluxes

7.2 Riverine Inputs

Estimates of riverine input are derived from the product of global river discharge and the mean concentration of aqueous Fe. Discharge measurements reviewed by Chester (2003) indicate a riverine flux of 37×10^{12} m^3 yr^{-1} which falls within the range of a more recent analysis by Dai *et al.* (2009) covering global discharge over the period 1950-2005. Concentrations of iron vary greatly, partly because of contamination effects that were prevalent in the early literature before ultra-clean techniques were adopted, and partly because of methodological problems arising from filtration techniques that did not separate aqueous, nanoparticulate and colloidal iron species and therefore measured only *filterable* Fe (Section 1.2).

Filterable iron (<0.45μm) is known to behave non-conservatively during passage through an estuarine salinity gradient, such that plots of *filterable* iron against salinity lie on a curve below the linear mixing line (see Chester, 2003). *Filterable* iron is present mainly as iron (oxyhydr)oxides that are stabilised in a colloidal suspension by organic matter but are substantially removed (typically 90%) by aggregation during passage through estuaries (Chester 2003; and Supplementary Information SI-4). This basic pattern of iron colloid/nanoparticle

aggregation has been established for many of the world's major rivers but more detail has emerged from separation of *filterable* Fe into colloids/nanoparticles and aqueous species (Dai and Martin, 1995). Aqueous iron (which they defined as <3 nm diameter) then shows a linear, conservative trend with increasing salinity but the 3 nm to 0.4 µm diameter fraction (mainly nanoparticulate plus colloidal Fe; Section 1.2) shows concave trends with increasing salinity, similar to those described above for the *filterable* iron fraction (to which it is the main contributor).

Table 7.1 Summary of estimates of Fe fluxes to the Global Ocean and the Southern Ocean. Individual inputs are discussed below.

Source	Global Ocean Gg yr^{-1}	Southern Ocean Gg yr^{-1}
Riverine (A) Riverine (C+N) Riverine (F)	80 60 140	0 0 0
Aeolian (A) Aeolian (C+N) Aeolian (F)	560-1870 970-1160 1530-3030	0.1-3.0 4-17 4-20
Recycled from Sediments (F)	50-250	13-32
Oxic Subglacial Meltwater (A) Oxic Subglacial Meltwater (C+N) Oxic Subglacial Meltwater (F)	0.5 0.7 1.2	– – 0.003-0.3
Icebergs (N+A) Iceberg Sediment (C+N) Iceberg Sediment (F)	0.11-0.16 900-1380 900-1380	0.06-0.12 750-1250 750-1250
Hydrothermal (F)*	50	21
Total (A) Total (C+N) Total (F)	640-1950 1930-2600 2620-4800	0.16-3.1 750-1250 770-1300

A = Aqueous Fe (<0.02 or 0.03 µm), C = Colloidal Fe (1µm to 0.1 or 0.2µm), N = Nanoparticulate Fe (0.1 or 0.2 µm to 0.02 or 0.03µm) and F = *Filterable* Fe (<0.45µm) ~A + N + C for each individual flux. Totals to 2 or 3 significant figures as appropriate.*Hydrothermal contribution to surface waters is uncertain and is omitted from totals.

Size fractions collected from river water by Stolp and Hassellov (2007) comprise two distinct components. One component is organic and averages 0.5 to 3 nm in diameter. This component has a strong UV absorbance typical of natural organic matter, and fluoresces like humic and fulvic materials. The other component is Fe-rich, >3nm in diameter, and has a chemical composition and morphology consistent with ferrihydrite nanoparticles (see also Breitbarth *et al.*, 2010). Riverine inputs to the ocean clearly need to distinguish between aqueous Fe and colloidal/nanoparticulate Fe. De Baar and de Jong (2001) and Krachler *et al.* (2005) consider the best estimate of the concentration of aqueous iron to be

40 nM (<3 nm diameter; see above and Dai and Martin, 1995), which gives an aqueous global input of 80 Gg yr^{-1}. De Baar and de Jong (2001) also estimate the riverine discharge of *filterable* Fe across the shelf into the oceans to be 140 Gg yr^{-1}, and thus the colloidal/nanoparticulate input is at least 140 minus 80 or 60 Gg yr^{-1} (Table 7.1). We consider inputs of subglacial melt to the Southern Ocean separately and thus assume no riverine inputs to the Southern Ocean.

7.3 Aeolian Inputs

There have been many attempts to estimate the global supply of iron that can be transferred into the ocean by the dissolution of atmospheric dust. There is reasonably close agreement (Breitbarth *et al.*, 2010) between approaches based on observations and modelling (or a combination of the two) and both produce a range of 1000-2000 Tg yr^{-1} for the total mass of dust deposited to the land and ocean (see Mahowald *et al.*, 2006). Based on these sources the average mass of dust deposited to the global ocean is approximately 450 Tg yr^{-1}. Assuming a total iron content of 3.5%, the average dust input of total Fe to the ocean is 16000 Gg yr^{-1} of which 6% (or 960 Gg yr^{-1}) is delivered to the Southern Ocean (Jickells *et al.*, 2005). Most subsequent studies utilise these data sources (e.g. Tagliabue *et al.*, 2010; Fan *et al.*, 2006). Table 7.2 summarises a selection of recent estimates and is not intended to be comprehensive.

However the fraction of the total Fe that can dissolved from atmospheric dust is usually determined operationally as 'fractional solubility.' Fractional solubility is defined as the percentage of the total Fe that can be dissolved from atmospheric dust, but estimates of fractional solubility vary widely depending on the dissolution conditions (see Section 5.4). Most recent models either partition the dust flux into wet and dry deposition (and use different fractional solubilities for each) or different fractional solubilities are assumed for rapidly and slowly-dissolved Fe fractions.

Table 7.2. Various estimates for the delivery of aqueous and soluble Fe to the global ocean by wet and dry deposition.

Source	Dry Deposition of Total Fe (Gg yr^{-1})	Dry Deposition of Soluble Fe (Gg yr^{-1})	Wet Deposition of Total Fe (Gg yr^{-1})	Wet Deposition of Aqueous Fe (Gg yr^{-1})
De Baar and de Jong (2001)	9780-24500	0	4190-10600	560-1450
Fan *et al.* (2006)	21000	966	11000	1870
Moore *et al.* (2004)	–	1740	–	1160

De Baar and de Jong (2001) separate dust inputs into dry deposition (9780-24500 Gg yr^{-1}; fractional solubility 0%) and wet deposition (4190-10600 Gg yr^{-1}; assumed to comprise of 86% particulates and 14% aqueous Fe; Table 7.2). It is not clear how this wet particulate component relates to colloidal/nanoparticulate Fe and this data is therefore ignored. Fan *et al*. (2006) assume that wet deposition (11000 Gg yr^{-1}) has a fractional solubility of 17% (giving 1870 Gg yr^{-1} of aqueous Fe) and that dry deposition (21000 Gg yr^{-1}) has a fractional solubility of 4.6% (giving 966 Gg yr^{-1} of soluble Fe; see Table 7.2). Finally, Moore *et al*. (2004) use a total Fe dust flux of 58000 Gg yr^{-1} which is assumed to have a fractional solubility of 2% Fe (1160 Gg yr^{-1}). This fraction is assumed to dissolve instantaneously in the surface ocean (thus behaving as wet deposition) with a further 3% (1740 Gg yr^{-1}) dissolving slowly with depth (as would dry deposition; Table 7.2). Collectively the instantaneously soluble Fe is here considered to be aqueous Fe (but see Section 5.5) and thus the aqueous Fe delivery rates discussed above fall in the range 560-1870 Gg yr^{-1}. The Fe that can be dissolved from dry deposition (here assumed to be colloidal/nanoparticulate Fe (oxyhydr)oxides) falls in the range 970-1740 Gg yr^{-1}, rather similar to the aqueous Fe from wet deposition.

Estimates of the dust iron inputs to the Southern Ocean are much smaller (4.5-30 Gg yr^{-1}; Tagliabue *et al*., 2010) and are based on data from Mahowald *et al*. (2006), Raiswell *et al*. (2008a) and Tagliabue *et al*. (2009) which represent Fe supplied by wet and dry deposition, here attributed to *filterable* Fe. However, the 30 Gg yr^{-1} estimate from Tagliabue *et al*. (2009; 2010) is based on a Southern Ocean area >35°S, which is approximately 50% larger than the area of the Southern Ocean used here (>60°S) and thus a range of 4-20 Gg yr^{-1} for *filterable* Fe is preferred in Table 7.1. Lancelot *et al*. (2009) produce an estimate of aqueous, bioavailable Fe of 0.8 Gg yr^{-1} to the Southern Ocean based on Fe supplied from an instantaneously soluble, and a slowly-dissolving, mineral fraction.

It is instructive to compare these inputs to the Southern Ocean with the model estimates (Section 5.5) for the supply of aqueous, bioavailable Fe derived from wet deposition plus the dissolution of Fe from nanoparticulate Fe (oxyhydr) oxides. The model estimates mostly fall in the range 0.1-3.0 Gg yr^{-1}, depending on the assumptions of solubility of wet deposition, and the relative proportions of wet and dry deposition. Nevertheless a range of aqueous, bioavailable Fe of 0.1-3.0 Gg yr^{-1} encompasses both the Lancelot *et al*. (2009) data and the model data from Section 5.5. This range is therefore used in Table 7.1 as a tentative estimate for the aqueous iron input to the Southern Ocean from atmospheric dust. The difference between the ranges for aqueous Fe and *filterable* Fe is assumed to represent colloidal/nanoparticulate Fe, giving the range of 4-17 Gg yr^{-1} in Table 7.1.

7.4 Sediments

Most estimates of iron produced by benthic recycling are based on the data of Elrod *et al.* (2004) who measured a mean flux of 8.8 μg cm^{-2} yr^{-1} for shallow water, bioirrigated sites and deeper water sites with oxygen-depleted bottom waters on the California shelf. These fluxes represent *filterable* Fe and therefore include colloidal, nanoparticulate and aqueous Fe. It is uncertain whether this benthic flux estimate is representative bearing in mind that data are few and that episodic re-working can produce substantial short-term fluxes (see Section 4.5). Nevertheless Elrod *et al.* (2004) use this data to derive an estimate of 2600 Gg yr^{-1} of *filterable* Fe to the open ocean assuming all the global shelf area produces iron at the same rate. A further complication arises in determining how much of this flux can be exported from the shelf (see Sections 4.6 and 4.7). Elrod *et al.* (2004) argue that the recycling flux will be most efficiently delivered to surface waters (where it can enhance productivity) where upwelling occurs at the shelf margin. Upwelling mainly (but not exclusively) occurs on eastern boundary shelves that constitute about 5% of the global shelf area. Assuming that 5% of the shelf flux can be exported to surface waters in the open ocean produces a substantially lower flux of 120 Gg yr^{-1} of *filterable* Fe delivery (see below).

The model-derived estimates of Moore *et al.* (2004), Aumont and Bopp (2006) and Moore and Braucher (2008) are also based on benthic flux measurements in the range 2-4 μg cm^{-2} yr^{-1} and produce global estimates of 260-5600 Gg yr^{-1}. De Baar and de Jong (2001) derive a comparable estimate of 2000-3000 Gg yr^{-1} based on the difference between shelf inputs and outputs. Collectively these data mainly lie within a range of 1000-5000 Gg yr^{-1} which assumes that the total flux can be exported and that all shelves have a similar generating capacity. Anderson and Raiswell (2004) estimate that ~5% of the shelf siliciclastics in the Black Sea are exported to the deep basin and, in the absence of more definitive data, this is assumed to represent the export efficiency (but see Raiswell and Anderson, 2005). The data in Table 7.1 assume on this basis that 5% of the flux can be exported (see above also) which produces a range of 50-250 Gg yr^{-1} for global delivery of *filterable* Fe. The benthic iron recycling flux measurements of Elrod *et al.* (2004) also form the basis for the Southern Ocean *filterable* Fe input estimates of 21 Gg yr^{-1} by Lancelot *et al.* (2009) and the range of 260-640 Gg yr^{-1} chosen from the literature by Tagliabue *et al.* (2010). Here we prefer this range of 260-640 Gg yr^{-1}, which, with an assumed export efficiency of 5%, produces the range of 13-32 Gg yr^{-1} shown in Table 7.1.

7.5 Subglacial Meltwater Inputs

This section deals with subglacial meltwater inputs to the ocean as distinct from inputs derived from the melting of icebergs in the oceans (Section 7.6). Wadham *et al.* (2012) estimate subglacial runoff from Greenland as 400 km^3 yr^{-1} and from

Antarctica as 18-31 $km^3\ yr^{-1}$ (mean 24 $km^3\ yr^{-1}$). Statham *et al.* (2007) have analysed meltwater from two Greenland glaciers using rigorous trace metal clean procedures and sequential filtration. The weighted means of the iron concentrations in the <0.03 µm (assumed to be aqueous) and 0.03-0.4 µm (assumed to be colloidal/nanoparticulate) filtered size fractions were 22.4 and 30.8 nM respectively. These data provide an estimate for the aqueous Fe input of 0.5 Gg yr^{-1} and a colloidal/nanoparticulate Fe input of 0.7 Gg yr^{-1} for oxic meltwaters from Greenland. Meltwater inputs to the Southern Ocean are much smaller but Wadham *et al.* (2012) estimate *filterable* iron concentrations from Antarctica to be 2 to 200 nM which give fluxes of 0.003 to 0.3 Gg yr^{-1} of *filterable* Fe from oxic meltwaters. Table 7.1 uses the Greenland data as the global estimate as this flux is substantially larger than that from Antarctica (see above).

However it has recently emerged (Wadham *et al.*, 2012) that anoxic subglacial inputs from both Antarctica and Greenland may have much higher concentrations of *filterable* Fe (40 to 4000 µM). Wadham *et al.* (2012) assert that the anoxic estimates are more realistic than the oxic fluxes but acknowledge that much of this flux may not escape precipitation as iron (oxyhydr)oxides beneath the iceshelf margins or on the shelf, prior to delivery to the open ocean. The uncertainties in estimates of anoxic delivery are extremely large but a concentration of 40 µM *filterable* Fe with 1% exported to the open ocean would correspond to a subglacial *filterable* iron flux of 9 Gg yr^{-1} from Greenland and 0.5 Gg yr^{-1} from Antarctica. However the anoxic delivery could be both substantially higher or lower than these preliminary estimates and, for this reason, anoxic delivery values are not reproduced in Table 7.1. We note however that anoxic delivery of aqueous Fe has the potential to overwhelm oxic meltwater delivery and this is a major issue that needs to be addressed in the coming years.

7.6 Iceberg Inputs

Icebergs contain a supply of iron derived from terrestrial sources (glacial debris and atmospheric dust) in addition to aqueous Fe present in precipitation. These sources may be accompanied by sediments and porewater Fe that becomes frozen into the iceberg as the continental shelf is crossed. Estimates of iceberg Fe delivery are often based on Fe concentrations in unfiltered icemelt after acidification which include variable concentrations of aqueous, colloidal/nanoparticulate and particulate Fe, as is discussed in Section 6.4. These concentration data form the basis of the estimates by Lancelot *et al.* (2009) and Tagliabue *et al.* (2010) but they include an unknown contribution from acidified particulates. In a recent study of Antarctic glaciers and icebergs, we have found (Raiswell *et al.*, 2008a) relatively low Fe measurements (mean 1.0 nM) for samples filtered through <0.2 µm and not acidified. The estimates for the global and Southern Ocean fluxes of aqueous plus nanoparticulate Fe from icebergs shown in Table 7.1 are based on this concentration which leads to fluxes of aqueous plus nanoparticulate Fe of 0.11 to 0.16 and 0.06 to 0.12 Gg yr^{-1} respectively (as shown below).

Different workers have used different values for the global iceberg supply. Raiswell *et al.* (2006) combined data from Church *et al.* (2001) for iceberg calving from Antarctica (2000 km^3 yr^{-1}) with that from Greenland (200 km^3 yr^{-1}) along with data from Lisitzin (2002) for smaller ice masses (700 km^3 yr^{-1}) to get a combined total of 2900 km^3 yr^{-1}. The product of this volume and a concentration of 1 nM (Raiswell *et al.*, 2008a) gives a global input of nanoparticulate plus aqueous Fe from icebergs as 0.16 Gg yr^{-1}. The lower rate of ice loss of 1000 km^3 yr^{-1} from Antarctica) used in Section 6.4 (together with the losses from Greenland and smaller ice masses) forms the basis of a more conservative estimate of 0.11 Gg yr^{-1} and the range 0.11-0.16 Gg yr^{-1} is used for the global estimate in Table 7.1. The above mentioned range of ice loss rates of 1000 to 2000 km^3 yr^{-1} (see above) together with a concentration of 1 nM provide a nanoparticulate plus aqueous Fe input from icebergs of 0.06 to 0.12 Gg yr^{-1} for the Southern Ocean.

We (Raiswell *et al.*, 2008a) have estimated the iceberg input of nanoparticulate Fe to the Southern Ocean derived from sediments to be 1250 Gg yr^{-1}. This was based on melting 2500 km^3 yr^{-1} of ice containing 0.5 kg m^{-3} of sediment with an ascorbic acid-extractable Fe content of 0.1%. The models in Section 6.4 use a lower (more conservative) total ice volume (1000 km^3 yr^{-1}), the same sediment content but a higher ascorbic acid-extractable Fe content (0.15%). This produces an input of ascorbic acid-extractable Fe of 750 Gg yr^{-1}. These data are used in Table 7.1 to provide a range of 750-1250 Gg yr^{-1} for the input of colloidal plus nanoparticulate Fe into the Southern Ocean. The models in Section 6.4 estimate how much of this Fe could be dissolved to produce bioavailable Fe. Model 1 in Figure 6.4a produced a bioavailable flux of Fe of 3 Gg yr^{-1} but fluxes up to 100 Gg yr^{-1} were reached for dissolution enhanced by siderophores and photochemical reduction or grazing. These bioavailable Fe fluxes represent 0.5% to 13% of the total input of colloidal plus nanoparticulate Fe (which is 750 Gg yr^{-1} as measured by ascorbic acid extraction).

The same approach is used to determine the delivery of ascorbic acid-extractable Fe by icebergs from Greenland melting at a rate of 200 km^3 yr^{-1} (Raiswell *et al.*, 2006) This delivery rate, assuming the same sediment contents and ascorbic acid-extractable Fe contents as the Southern Ocean icebergs, increases the Southern Ocean input by approximately 10-20% and provide a nanoparticulate plus colloidal Fe delivery to the global ocean of 900-1380 Gg yr^{-1} (Table 7.1).

The budget excludes sea ice which contains atmospheric dust that can be dissolved in the slightly acidic conditions produced by melting (Meguro *et al.*, 2004). However sea ice has a life time of several weeks to 1-2 years (de Baar and de Jong, 2001) and acts mainly to delay the delivery of Fe from dust to the oceans until melting occurs. Sea ice is therefore considered to be an atmospheric source which is processed to produce aqueous Fe and hence the contribution of Fe from melting sea ice is accommodated in the estimates of atmospherically processed aeolian dust supplied to the Southern Ocean (see Section 5.4).

7.7 Hydrothermal Inputs

A relatively large hydrothermal flux estimate of 1700-5000 Gg yr^{-1} of colloidal Fe (Table 7.1) is provided by de Baar and de Jong (2001). Elderfield and Schultz (1996) estimated a flux of 1000-10000 Gg yr^{-1} for the dissolved iron from axial high temperature vents and diffuse low-temperature flow but much of this is precipitated as iron (oxyhydr)oxides and it was believed to produce a negligible net input to the global ocean (see also Poulton and Raiswell, 2002). However complete removal by precipitation may be prevented by complexing with organic ligands and on this basis Bennett *et al*. (2008) estimated a hydrothermal dissolved iron flux of >17 Gg yr^{-1}. Tagliabue *et al*. (2010) found that a global hydrothermal flux of 50 Gg yr^{-1} of dissolved Fe (21 Gg yr^{-1} to the Southern Ocean) was best able to reproduce the global distribution of dissolved iron in the deep ocean (>2 km) but this Fe had relatively little impact on surface waters in both the global ocean and the Southern Ocean. The estimates of both Bennett *et al*. (2008) and Tagliabue *et al*. (2010) are based on measurements after filtration through 0.4 µm and are thus *filterable* Fe fluxes (which contain colloidal and nanoparticulate Fe). Collectively these data suggest that the best estimates for the *filterable* Fe hydrothermal fluxes are 50 Gg yr^{-1} to the global ocean and 21 Gg yr^{-1} to the Southern Ocean. These data are not included in the totals in Table 7.1 as their influence on surface waters is uncertain.

7.8 Budget Overview

Table 7.1 breaks new ground in attempting to distinguish between different forms of Fe (aqueous, colloidal/nanoparticulate and *filterable*) which vary in their reactivity and bioavailability. There are clearly considerable errors on many of the estimates in Table 7.1 but the dominant aqueous supply to the global ocean appears to be aeolian (with the important proviso that the estimates of fractional solubility for wet deposition actually represent instantaneously soluble Fe) and this source urgently needs more research (see Section 5.5). The colloidal/nanoparticulate Fe fluxes approximate to the *filterable* Fe fluxes and the dominant *filterable* Fe fluxes to the global ocean appear to be from aeolian dust and iceberg-hosted sediments, which are almost an order of magnitude larger than the next most important flux from shelf sediment recycling (subject to the assumptions on generation and export discussed above). The scientific effort on aeolian fluxes needs also to be matched by more measurements of iceberg delivery, for which there are few data. In the Southern Ocean the aqueous flux from aeolian wet deposition may be overwhelmed from subglacial inputs (see Section 7.5) but it seems clear that the most important *filterable* Fe flux is from iceberg-hosted sediments, compared to which aeolian deposition and sediment recycling are much less important. All these fluxes (and their bioavailability) are poorly constrained and need to be the focus of new scientific effort. Note that only the aqueous fluxes

listed in Table 7.1 can be assumed to be completely bioavailable and fluxes that deliver colloidal/nanoparticulate Fe may be only 1-10% bioavailable (see above and Raiswell *et al.*, 2008a). Besides the urgent need for more analytical data to better constrain these fluxes, computer models of both the global ocean and Southern Ocean chemistry need to be carefully re-evaluated to account for the differences in bioavailability between aqueous Fe and Fe present as colloids and nanoparticles in the different inputs shown in Table 7.1.

7.9 Final Thoughts

The last fifty years have brought huge changes in the way Earth surface systems are studied by geoscientists. At the start of this period geochemical studies of surface systems were commonly published in the *Journal of Sedimentary Petrology*; a title which carried the clear implication that mineralogy was an essential perspective. Now, however, a whole variety of sub-disciplines contribute to geochemical studies of surface systems but mineralogy has slipped from centre stage. It is now more important than ever that a more mineralogical view is adopted in future studies of the iron biogeochemical cycle in order to characterise colloids and nanoparticles, and define their role in aquatic environments. Wells and Goldberg (1994) observe, with some prescience, that *'the chemical behaviour of colloidal constituents will not be predicated on bulk solution chemistry considerations alone'* and that *'distinguishing between soluble, colloidal and particulate phases will be essential if we are to understand the cycling of matter in the ocean.'*

This is a message that has been forgotten until recently (see Breitbarth *et al.*, 2010).

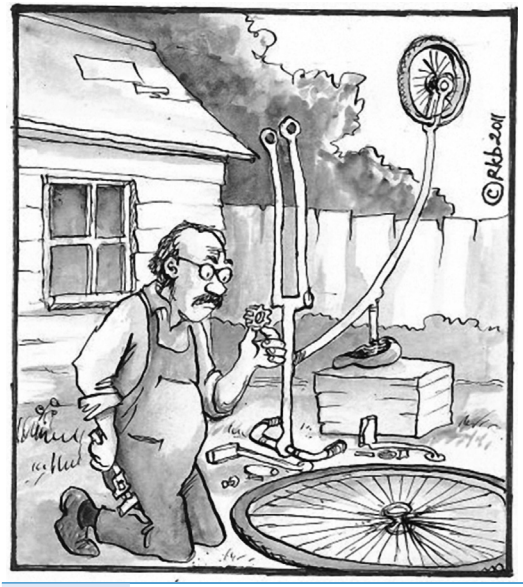

Figure 7.1 Even the early iron cycles were much more complicated than expected.

Grasping the big picture of the iron biogeochemical cycle has never been easy; certainty always seems to be tantalisingly out of reach as each layer of complexity is stripped away only to reveal another (Fig. 7.1). By contrast, in the next two sections, we will embark on our view of

the iron biogeochemical cycle in ancient rocks in the hope that the passage of time will blur the complexities, like viewing an Impressionist painting from a distance. A key target in the following sections is to track the evolution of the oceans and atmospheres through time. The continued stream of exciting papers (Section 9) bear witness to the success geoscientists have had in unraveling the redox history of the early Earth through the Archean and Palaeoproterozic when oxygen first began to increase. The platform for this success has required first, a detailed understanding of sedimentary Fe diagenesis, and second, investment in drilling that has provided pristine samples from critical time periods. It will also prove to be important through these time periods, as well as in the Phanerozoic, that careful attention is also given to sedimentological and depositional characteristics.

The redox records have been based primarily around use of the C-S-Fe indicators (the evolution of which was the subject of Section 3), using the improved definition of highly reactive iron that includes carbonate minerals and magnetite as well as (oxyhydr)oxides and pyrite. Analytical techniques that have sufficient selectivity to separate these different minerals have been a key development. Nevertheless the continued progress in this area, and in a wider geological context, requires that selectivity is justified on a case-by-case basis. Quantitative X-ray Diffraction, combined with other modern mineralogical techniques, can provide valuable independent evidence that selectivity has been achieved. Here, as in the Phanerozic iron cycle, we will see that solid phase analytical techniques providing mineralogical data need to be routinely integrated with chemical speciation studies and sedimentological characteristics.

8. THE INTERACTION OF IRON WITH OTHER BIOGEOCHEMICAL CYCLES

8.1 Retrospective (or how I jumped on the "iron train": Don Canfield)

In the summer of 1982, I arrived safely in New Haven from Ohio, with all my worldly possessions packed into the back of my 1969 International Harvester pickup truck. After unloading my things at the graduate student dorm, Helen Hadley Hall, a boxy 1950's Eastern-block-inspired construction, I parked my truck in the student garage[1]. My project was to study the rate of pyrite formation in marine sediments, and eager to get started, I walked briskly across the parking lot to Kline Geology labs. Here I met my advisor, Bob Berner, who, after showing me around, introduced me to the fast-talking Rob Raiswell (on sabbatical at the time), who, with exaggerated arm movements, enthusiastically related the mysteries of concretion formation, and was convinced that we would find them in Long Island Sound sediments, if only we looked hard enough. I didn't understand everything that Rob said, but it sounded important, and the next day I sailed with Bob Berner's soon-to-finish student Joe Westrich onto Long Island to collect sediment cores at three different sites. Back in the lab, and for the next week, I carefully sieved these sediments and poked through the debris anticipating a big find. No concretions emerged, but I got my first look at pyrite framboids, and observed all kinds of different pyrite associations with plant material, diatoms and foraminifera. My interest in pyrite formation was aroused, especially the details of how sedimentary Fe species and sulphide interact. This led to one of my main PhD thesis topics and is explored in more detail below.

I never did return to explore rates of pyrite formation, but I did continue, together with Rob in many cases, to explore the geochemistry of Fe as well as the cycling of Fe through Earth history. As it turns out, Fe interacts with many other elements, and in ways that act to control the chemistry of the environment. In this section, I will look at how Fe interacts with the cycles of many other elements of biogeochemical interest. Many of these interactions are promoted by microbes, the real workhorses in driving biogeochemical cycles. These interactions help to inform us on the history of Fe cycling through time, which is the subject of Section 9.

1. As I recall, the garage fee was about 1/3 of my take-home Yale stipend of 450 dollars a month. It was either beer or garage, and the obvious choice forced me park my truck back in Ohio for the next 2 years. When my salary rose to the point where I could afford the truck, I chased the mice out, started her up, and enjoyed a very memorable ride back to New Haven.

8.2 Oxygen

As described in previous sections, the geochemistries of Fe and oxygen are intimately linked. In oxygenated environments, Fe(III) is the thermodynamically stable oxidation state. Aqueous Fe(III) (and some Fe(II) as well; see Section 2.2) in seawater is present as organic complexes, but, at circum-neutral pH, most Fe(III) is found hydrolysed into a variety of (oxyhydr)oxide phases. In the absence of oxygen, Fe(II) is much more stable and dissolved Fe(II) will often accumulate (although not in the presence of nitrate as we will explore below) until saturation with some mineral phase is reached.

At the interface between oxic and anoxic environments, reaction fronts are frequently established between Fe(II), in its aqueous and solid forms, and oxygen. We can envisage various types of reaction fronts. Perhaps the most obvious is the type established when strong gradients of oxygen meet opposing gradients in aqueous Fe(II) such as found, for example, in aquatic sediments, anoxic lakes, ground water springs, and hydrothermal fluids. Other reaction fronts are established between oxygen and solid Fe(II) phases in, for example, weathering environments where pyrite-rich shale is exposed to the atmosphere. We will consider each of these different types of reaction interfaces starting with the oxidation of aqueous Fe(II) with oxygen.

Reaction Between Fe(II) and Oxygen. Mix an Fe(II) solution into oxygenated seawater, and Fe (oxyhydr)oxides are very rapidly formed. Indeed, if the water remains well aerated, within 10 minutes, or less, the Fe(II) will be completely removed. These kinetics are well described by the following rate law (Millero *et al*., 1987; Singer and Stumm, 1970; Stumm and Lee, 1961):

$$-d[Fe^{2+}]/dt = k[Fe^{2+}][O_2]\ [OH^-]^2 \qquad (8.1)$$

For a range of temperatures and ionic strengths, the rate constant $k = \log k_o - 3.29I^{0.5} + 1.52I$, where $\log k_o = 21.56\text{-}1545/T$, I is ionic strength and T is temperature in degrees Kelvin (Millero *et al*., 1987). From this rate law, we can see that the oxidation rate accelerates with higher concentrations of Fe^{2+}, higher concentrations of O_2 and at higher pH.

We also know from practical experience that in nature microbes are typically associated with environments supporting aqueous Fe(II) oxidation. For example, iron (oxyhyr)oxide-encrusted sheaths of the Fe(II)-oxidiser *Leptothrix* spp. or the helical (oxyhyr)oxide-encrusted stalks of *Gallionella* spp. are typically found populating areas where Fe(II) seeps into the oxygenated surface environment (Emerson *et al*., 2010). The oxidation of Fe(II) with oxygen by microbes is clearly a thermodynamically favorable process; however, microbes in nature must compete with rapid inorganic oxidation. This is perhaps their biggest challenge, and experiments suggest that at circum-neutral pH, such as typically found in natural environments, they are only marginally successful at doing so. For example, the Fe(II)-oxidising groundwater organism *Sideroxydans lithotrophicus* did

not accelerate Fe(II) oxidation over inorganic rates in experiments at full oxygen saturation of 275 μM and a pH = 6.2 (Druschel *et al.*, 2008). However, a microbial effect was observed at reduced oxygen concentrations of between 9 and 50 μM. The size of the effect seemed to scale inversely with oxygen concentration (see Fig. 8.1) (Druschel *et al.*, 2008), where, with the exception of one apparently aberrant experiment (Fig. 8.1), microbes accelerated Fe(II) oxidation rates from 17 to 75%. Similar extents of microbial contribution to Fe(II) oxidation were found in experiments with iron-oxidisers isolated from the rhizosphere of wetland soils (Neubauer *et al.*, 2002), where a mixed population of microbial mat Fe oxidisers accelerated rates of Fe oxidation by from 40% to 300% (Rentz *et al.*, 2007).

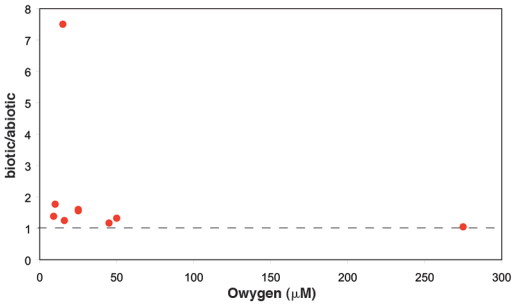

Figure 8.1 Ratio of the oxidation kinetics of Fe(II) in a strictly abiotic reaction and in the presence of Fe(II) oxidising-microbe *Sideroxydans lithotrophicus* at a pH of 6.2. Microbes accelerate the oxidation kinetics over abiotic rates at reduced oxygen concentrations (data from Druschel *et al.*, 2008).

It makes sense that microbes contribute more to Fe(II) oxidation at lower oxygen concentrations. This is because the rates of the inorganic oxidation process decrease as oxygen concentrations fall (equation 8.1), whereas the enzymes conducting Fe(II) oxidation by microbes are apparently saturated with oxygen even at very low concentrations. To my knowledge, this has not been explored explicitly for Fe oxidisers, but it is true for other aerobic microbes where half-saturation values with respect to oxygen utilisation are in the micromolar to sub-micromolar range (e.g. (Longmuir, 1954; Stolper *et al.*, 2010)). In any event, Fe oxidisers seem to preferentially populate the low-oxygen regions of gradient systems where they are active, presumably providing them with a strong kinetic advantage over inorganic Fe(II) oxidation (Druschel *et al.*, 2008; Emerson *et al.*, 2010; Emerson and Revsbech, 1994a,b). By contrast, at pH <5, the rates of inorganic oxidation are sluggish, and Fe-oxidisers can accelerate rates of Fe(II) oxidation by orders of magnitude over inorganic rates (Ferris, 2005; Singer and Stumm, 1970).

The products of microbial Fe oxidation depend very much on pH. At circum-neutral pH, ferrihydrite predominates initially (Supplementary Information SI-3 and Cornell and Schwertmann, 2003). At low pH, oxidation products include ferrihydrite, goethite, and, if pyrite oxidation provides abundant sulphate, jarosite ($[(H, Na, K)Fe_3(OH)_6(SO_4)_2]$ and schwertmannite predominate (see Supplementary Information SI-6 and Ferris, 2005; Kupka *et al.*, 2007). With time, schwertmannite converts to goethite/haematite (Cornell and Schwertmann, 2003; Davidson *et al.*, 2008) or jarosite (Wang *et al.*, 2006).

Pyrite Oxidation with Oxygen. Oxygen also interfaces with Fe through the weathering and oxidation of solid phases, of which iron sulphides, and in particular pyrite, are the most abundant and the best studied. This process was briefly discussed in Section 4.4, and it will be explored in more detail here. In considering the pathways of pyrite oxidation, pH is an important consideration. At low pH, the most efficient pathway of pyrite oxidation is only indirectly linked to oxygen. It seems, rather, that in natural settings, the main oxidation pathway for pyrite is by reaction with aqueous Fe(III) (e.g. Nordstrom and Southam, 1997):

$$FeS_2 + 14Fe^{3+} + 8H_2O \rightarrow 15Fe^{2+} + 2SO_4^{2-} + 16H^+ \quad (8.2)$$

In principle, reaction 8.2 is an anoxic oxidation pathway. However, the Fe^{3+} must be made available, and this happens through oxidation with O_2 as follows:

$$14Fe^{2+} + 3.5O_2 + 14H^+ \rightarrow 14Fe^{3+} + 7H_2O \quad (8.3)$$

The overall reaction then becomes:

$$FeS_2 + 3.5O_2 + H_2O \rightarrow Fe^{2+} + 2SO_4^{2-} + 2H^+ \quad (8.4)$$

Each of these reactions has possible abiotic and biotic pathways, and after a careful review of the available literature, Nordstrom and Southam (1997) came to the following conclusions:

(a) Reaction 8.4 may represent the sum of two separate pathways (reactions 8.2 and 8.3) or a direct oxidation pathway with oxygen. Available experiments suggest, however, that the direct pathway is at least one order of magnitude slower at acid pHs.

(b) Microbes often sit directly on the pyrite surface during oxidation. Whether they employ reaction 8.4 or the sum of reactions 8.2 and 8.3 is unclear. However, the overall reaction rate is faster if microbes are separated from the surface and oxidation proceeds through reaction 8.2. This relationship could imply that the microbes hinder access of Fe^{3+} to the pyrite surface, but it is more likely that microbes conduct reaction 8.3 faster than they can oxidise pyrite through direct contact.

(c) In the presence of microbes, reaction 8.2, an inorganic reaction, seems to be the rate-limiting step. However, since reaction 8.3 is so dramatically enhanced through microbial oxidation, the overall process of pyrite oxidation under acidic conditions is considerably enhanced through microbial intervention.

At high pH, ferric iron is nearly insoluble (forming Fe(oxyhydr)oxide phases; see Section 2.2 and Cornell and Schwertmann, 2003), and the pathway of pyrite oxidation represented by equations 8.2 and 8.3 is of less importance. Indeed, the role of microbes in promoting pyrite oxidation at circum-neutral pH in nature is not clear.

Pyrite, however, does oxidise with oxygen in the absence of microbes, and the inorganic kinetics of pyrite oxidation have been well explored through a range of pH (e.g. (McKibben and Barnes, 1986; Nicholson *et al*., 1988; Smith and

Shumate, 1970; Williamson and Rimstidt, 1994). After compiling the available data, and in light of their own experiments, Williamson and Rimstidt (1994) derived a rate law that applies to the kinetics of oxidation over a broad range of pH (2-10) and dissolved oxygen concentrations (approximately 1 μM to 19 mM; where the high levels are well beyond air-saturation values and represent experiments conducted at high pressures of up to 25 bars; Smith and Shumate, 1970). The rate of pyrite oxidation is given in equation 8.5. We saw this rate law previously in Section 4.4 (equation 4.1) in relationship to understanding the survival time of fine-grained pyrite, apparently derived from continental shelf sediments, during transport in oxygenated marine waters.

$$\text{Rate of pyrite oxidation (mol m}^{-2}\text{ s}^{-1}) = 10^{-8.19}\,(O_2)^{\,0.5}/\,\{H^+\}^{0.11} \qquad (8.5)$$

The data from Williamson and Rimstidt (1994) have been recalculated to a common pH of 6 [$Rate_{pH6} = Rate_{measured}*(M_{H+measured})^{0.11}/(10^{-6})^{0.11}$] and compared to oxygen concentration in Figure 8.2. The rate predicted from equation 8.5 at this same pH is also shown.

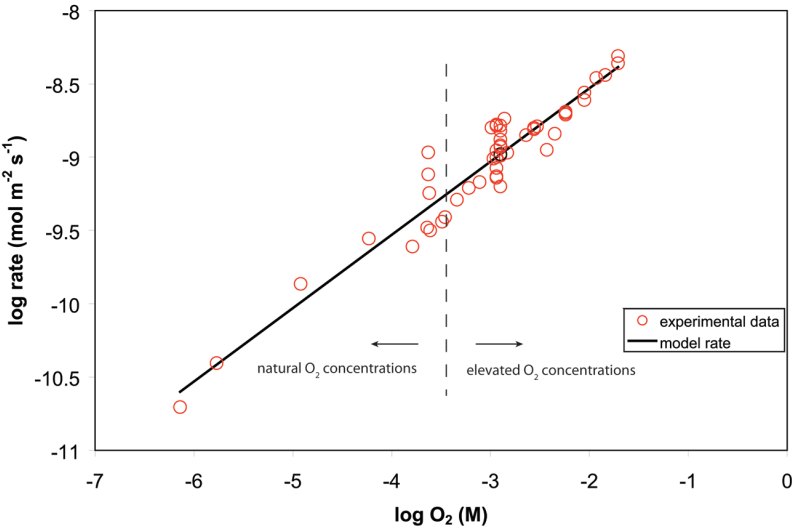

Figure 8.2 Rates of pyrite oxidation as a function of oxygen with rates normalised to pH = 6. Also shown is the predicted oxidation rates from equation 8.5 (data from compilation in Williamson and Rimstidt, 1994).

A few key points are obvious from this comparison. First, as discussed by Williamson and Rimstidt, (1994), the rate law provides a reasonably good prediction of inorganic pyrite oxidation rate over a range of several orders of magnitude in oxygen concentration. Second, most of the available oxidation rate data is from experiments with oxygen concentrations elevated over those found in nature. Finally, this rate law has been applied to calculating pyrite oxidation

rates under nM (or lower) oxygen levels (Anbar *et al.*, 2007; Canfield *et al.*, 2000), as was believed the case in surface waters before the general oxidation of the Earth's atmosphere around 2.3 to 2.4 billion years ago (Farquhar *et al.*, 2000; Pavlov and Kasting, 2002; Stolper *et al.*, 2010). Such oxygen levels are orders of magnitude lower than the lowest used in experiments to date. So, the question becomes, does the rate law in equation 8.5 still apply at such low levels of O_2? It will be a high priority to explore these kinetics at much lower oxygen levels as relevant for assessing pyrite oxidation on the early Earth and sulphate fluxes to the early Earth ocean.

8.3 Phosphorus

The cycles of Fe and phosphorus are intimately linked in aquatic systems through the strong adsorption of phosphate onto Fe (oxyhydr)oxide phases and its release as these phases are reduced. This association was recognised long ago in lakes where a number of early limnological pioneers noted the liberation of phosphate from sediments after the reduction of Fe (oxyhdr)oxides to Fe(II) and the efficient experimental removal of phosphate onto Fe oxide "gels" (Einsele, 1938; Mortimer, 1941; Ohle, 1937). Perhaps not surprisingly, this association has gained huge importance in understanding the regulation of phosphorus availability in both terrestrial and aquatic systems. The literature on this subject is vast, and it will not be my intention here to provide an exhaustive review. Rather, I will focus on the Fe-P association and the specific aspects of this association that will allow us to discuss how changes in this association through time may have influenced P availability in the past.

Present-Day Interactions between P and Fe (Oxyhydr)oxides. The development of sequential extraction techniques has been a key to understanding the role of Fe (oxyhydr)oxides in influencing P sequestration in sediments (Ruttenberg, 1992). Probably the best known scheme was developed by my fellow Berner student and contemporary Kathleen Ruttenburg. Kathleen laboured long and hard to test and calibrate an extraction scheme that could be applied to separating P into its constituent associations in sediments. Basically, a number of different chemical extractants are applied (either in sequence or in parallel) to target specific phosphorus associations within sediments. These extractions have been applied to a variety of different sediments ranging from sulphidic continental margin sediments to deep sea sediments (Ruttenberg, 1993). Results show that Fe-associated P is enriched in the upper Fe (oxyhydr)oxide-containing region of the sediment (Jensen *et al.*, 1995) and that Fe (oxyhydr)oxide-poor, sulphidic sediments retain no measurable Fe-bound phosphorus. In contrast, sediments from both the continental margin and the deep sea that preserve Fe (oxyhydr)oxides to depth contain appreciable amounts of Fe (oxyhydr)oxide-bound P, accounting for up to 30% of the total phosphorus within the sediments (Ruttenberg, 1993). Although the data set is small, results indicate that globally,

Fe-bound P may account for about 20% of the total P removed in sediments (not including detrital P), a value comparable to the removal flux of organic phosphorus (Ruttenberg, 1993, 2003).

As demonstrated in the early limnological work, the strong association between phosphate and sedimentary Fe (oxyhydr)oxides generates an "Fe-cap" that hinders phosphate from escaping the sediment as long as Fe (oxyhydr)oxides persist in the upper sediment surface layers. Indeed, from a combination of his own observations and a survey of the literature, another of Bob Berner's PhD students, Ellery Ingall (Ingall and Jahnke, 1997), found that much less phosphorus was released from sediments overlain with oxygenated water than would be expected assuming that the sedimentary organic matter decomposed with a ratio of C/P of 106, the nominal "Redfield ratio" of organic matter. In contrast, for sediments underlying low-oxygen water columns, the release of P was much greater, equalling or even in some cases exceeding that expected for "Redfield Ratio" organic matter stoichiometry. In other work, a seasonal sediment study of P cycling from a coastal site in Denmark (Jensen *et al*., 1995) revealed, as expected, a strong association between P and Fe (oxyhydr)oxides in the surface sediments. The sediment flux of phosphate from the sediment was relatively low during the winter and spring when the Fe-(oxyhydr)oxide pool was accumulating, but high in the summer and fall due to high temperatures and the rapid microbial and chemical reduction of the Fe (oxyhydr)oxide pool (Jensen *et al*., 1995). All in all, Fe (oxyhydr)oxides bind phosphate strongly and act as an important phosphate sink where they accumulate.

The differential retention of phosphate under oxic sediment deposition conditions and its loss under anoxic conditions has prompted the development of an interesting feedback mechanism potentially stabilising concentrations of atmospheric oxygen. This idea was forwarded by Philippe Van Cappellen, yet another Berner PhD student, and Ellery Ingall, during numerous late night library discussions, and if I remember right, many rounds of beer at the local pub Archie Moores (Van Cappellen and Ingall, 1997). The model proposes that as atmospheric oxygen levels fall, ocean anoxia expands, reducing the Fe (oxyhydr)oxide phosphate removal pathway and enhancing the availability of phosphate to fuel primary production in the oceans. Enhanced primary production delivers more organic carbon to sediments, enhancing carbon burial which acts as an oxygen source to the atmosphere (e.g. Berner, 2004; Garrels and Perry, 1974). In essence, the P that is buried with Fe oxides under oxic water column conditions is instead buried with organic matter under anoxic conditions, enhancing the burial of organic carbon. This feedback is further enhanced because, for reasons still uncertain, the organic C/P ratio is much higher when organic matter is buried under anoxic water column conditions compared to when it is buried under an oxic water column (Ingall *et al*., 1993). This means that more organic matter can be buried under anoxic conditions compared to oxic conditions for an equal amount of phosphorus.

Early Earth Interactions between P and Fe (Oxyhydr)oxides. The iron (oxyhydr)oxide control on phosphorus availability may have influenced phosphate availability and primary production well into the distant geological past. We will discuss the evolution of ocean chemistry in more detail in Section 9, but before about 1.9 billion years ago, banded iron formations (BIFs) were relatively common (Holland, 1984a; Isley and Abbott, 1999; James, 1966). Many of these are rich in oxide phases and probably accumulated originally from Fe (oxyhydr)oxide deposition, although subsequent diagenesis has changed this original Fe mineralogy (Beukes and Klein, 1992; Fischer and Knoll, 2009; Holland, 1984a). These early BIFs also contain some phosphorus prompting my colleague Christian Bjerrum and myself (Bjerrum and Canfield, 2002) to propose that the association of P with Fe oxides in BIFs generated a huge P sink, limiting the concentration of phosphorus in the oceans and reducing marine primary production. In developing this idea, we used the affinity of phosphorus for modern hydrothermally derived Fe (oxydr)oxides as a guide (Feely *et al*., 1998). Indeed, the P/Fe ratios in the hydrothermal particles correlated with the phosphate concentration of the water where the particles were formed (Fig. 8.3). From this, a partition coefficient could be defined, which, when combined with the P/Fe ratios measured in <1.9 Ga BIFs, pointed to low marine phosphorus concentrations of 0.15 to 0.6 μM. These values can be compared to the much higher present-day ocean average of 2.3 μM, and if true, such low early Earth marine phosphate levels may have limited rates of primary production.

Subsequently, Kurt Konhauser and colleagues (Konhauser *et al*., 2007) demonstrated that Fe (oxyhydr)oxides precipitated in the presence of dissolved silica adsorb less phosphate than iron (oxyhydr)oxides precipitated in the absence of silica, and the more silica, the less P adsorption. A variety of experiments were performed with silica concentrations of 0 mM, 0.67 mM (representing saturation with the silicon dioxide crystobalite), and 2.2 mM (representing saturation with amorphous silica). These results are presented in Figure 8.3 together with the natural hydrothermal particles. Konhauser *et al*. (2007) echoed earlier discussions arguing that early in Earth history, long before the evolution of silica-precipitating diatoms and sponges, the oceans likely reached saturation with some silicon oxide phase (Siever, 1992).

This seems reasonable, but other inorganic silica removal mechanisms may have existed on the Earth before the evolution of biological removal pathways. Indeed, Fischer and Knoll (2009) have argued that, due to the strong affinity of silica for freshly precipitated Fe (oxyhydr)oxides, the precipitation of Fe (oxyhydr) oxides during BIF formation could have represented a substantial silica removal pathway. The present-day fluxes of silica and reactive Fe to the oceans are comparable at about 7-9 $\times$ 10^{12} moles yr^{-1} (Laruelle *et al*., 2009; Poulton and Canfield, 2011), and the affinity of silica for "amorphous" Fe (oxyhydr)oxides scales with silica concentration, but is equimolar with Fe at silica levels of about 1 mM (Davis *et al*., 2002). This means that if the relative fluxes of reactive Fe and Si did not change dramatically in the past, then the removal of silica with Fe (oxyhydr) oxide could have buffered silica concentrations to well below saturation with

amorphous silica early in Earth history. Therefore, more phosphorus may have adsorbed onto Fe (oxyhydr)oxides than expected from water saturated with silicon dioxide phases.

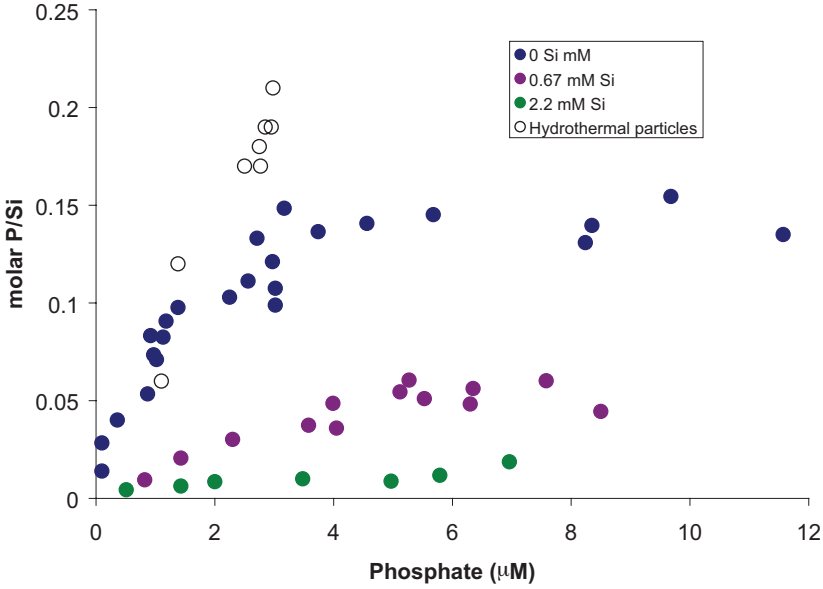

Figure 8.3 Results from phosphorus absorption experiments onto ferrihydrite in the presence of various concentrations of dissolved silica. Also shown is the composition of natural hydrothermally derived Fe (oxyhdr)oxide particles. See text for details.

We return now to the natural Fe (oxyhydr)oxide particles collected in proximity to various hydrothermal vents throughout the global ocean (Feely *et al.*, 1998) (Fig. 8.3). These particles formed in waters with ambient silica concentrations ranging from about 30 μM (particles with the lowest P/Fe) to around 170 μM (particles with highest P/Fe). There is no obvious relationship between phosphate adsorption onto Fe (oxyhydr)oxides and Si levels for the natural particles, but these particles may have formed at Si concentrations where such effects do not occur. Also, these particles do not seem to saturate at phosphate levels where the synthentic particles (0 mM) begin to show saturation behaviour suggesting some differences between these and the synthetic particles. It will be important to explore the differences between the adsorption behaviour of the natural and synthetic particles, but the results of Konhauser *et al.* (2007) suggest that our phosphate concentration estimates (Bjerrum and Canfield, 2002) may be too low by amounts depending on the silica content of the ancient oceans.

8.4 Carbon

Thus far, we have mostly considered how Fe interfaces with other biogeochemical cycles through inorganic reactions. Biology, however, also interfaces directly with the Fe cycle in many ways, and the cycles of carbon and Fe are one such example. As we will introduce here, and explore in more detail in Section 9, the biological regulation of the coupled Fe and carbon cycles has been prominent, in different ways, through most of Earth history.

The most important couplings between iron and carbon are through photosynthetic production of organic matter and through the decomposition of organic matter by dissimilatory iron reduction. The reactions representing these processes are shown below, and each will be considered in turn.

Anoxygenic Fe^{2+} oxidation:

$$4Fe^{2+} + 11H_2O + CO_2 \rightarrow 4Fe(OH)_3 + CH_2O + 8H^+ \quad (8.6)$$

Dissimilatory Fe reduction:

$$4Fe(OH)_3 + CH_2O + 8H^+ \rightarrow 4Fe^{2+} + 11H_2O + CO_2 \quad (8.7)$$

Anoxygenic Fe(II) Oxidation.When we think of photosynthesis, we normally think of oxygen-producing photosynthetic organisms like plants, algae and cyanobacteria. These certainly dominate photosynthesis today. However, oxygen producers were not the first photosynthetic organisms on Earth. The earliest were instead the so-called anoxygenic phototrophs, which use solar energy to promote the oxidation of reduced compounds like H_2, H_2S and Fe^{2+} (e.g. Blankenship, 2001; Hartman, 1984; Hohmann-Marriott and Blankenship, 2011; Olson, 1978). While sulphide-oxidising anoxygenic phototrophs have been known for 80 years (Van Niel, 1931), the earliest speculations of Fe^{2+}-oxidising anoxygenic phototrophs of which I am aware was from the pioneering geochemist Bob Garrels (Garrels *et al*., 1973) who stated, with relevance to Fe (oxyhydr)oxide precipitation in BIF formation:

> *"…that Archean and Animikie times were dominated by prokaryotic microorganisms that reduced CO_2 to CH_2O in the hydrosphere by accepting electrons from suitable donors, such as ferrous iron"*

They continue:

> *"In the photic zone of the iron basins, the iron would be oxidized by prokaryotic photosynthesizing organisms and deposited as ferric oxide…"*

Others added to these speculations, with Hartman (1984) echoing the earlier sentiments of Garrels *et al*. (1973) that Fe-oxidising anoxygenic phototrophs may have contributed to BIF deposition.

The first actual demonstration of anoxygenic phototrophic Fe^{2+} oxidation was by Fritz Widdel, (Widdel *et al*., 1993), who was able to isolate Fe-oxidising organisms from a drainage ditch near the Max Planck Institute in Bremen, Germany. Two different strains were isolated (Ehrenreich and Widdel, 1994),

both of which were members of the so-called "purple bacteria". Other purple bacterial phototrophic Fe-oxidisers have also been isolated (e.g. Croal *et al*., 2004; Straub *et al*., 1999), as well as a single *Chlorobium*-associated phototroph (*Chlorobium ferrooxidans*) (Heising and Schink, 1998). *Chlorobium* species are normally known as sulphide oxidisers and are quite distinct phylogenetically from the purple bacteria.

Experiments reveal that all known Fe^{2+}-oxidising phototrophs induce the precipitation of ferrihydrite as their initial mineral product (Kappler and Newman, 2004), and over time (on the order of weeks), a portion of these precipitates age to a combination of goethite and lepidocrocite (see Supplementary Information SI-3 and SI-6). The Fe-oxidising organisms could oxidise aqueous ferrous Fe^{2+} as well as the Fe(II) in siderite and FeS, but not pyrite (FeS_2), magnetite (Fe_3O_4) or vivianite ($Fe_3(PO_4)_2$). Observations under scanning electron microscopy revealed that the cell surfaces were typically covered with patches of Fe (oxyhydr)oxides. Complete cell coverage was rare, and some cells were free of Fe (oxyhydr)oxides. In reviewing the evidence, Kappler and Newman (2004) proposed a precipitation mechanism where either aqueous Fe(III) (possibly complexed) or colloidal/nanoparticulate Fe(III) aggregates are liberated from the surface of the cell after formation. After leaving the cell, Fe^{3+} ions are hydrated and joined with other Fe colloids/nanoparticles in their aggregation into larger particles. While some of Fe (oxyhydr)oxide aggregates settle from solution, others, along with some Fe^{3+} ions, are attracted to the negatively charged cell surface, nucleating into larger aggregates on the cells. Overall, however, the mineralogical products of anoxygenic phototrophic Fe oxidation have not yet been explored with the same rigour as those formed in and collected from the ocean and discussed in Section 2.2 and in the Supplementary Information SI-6.

Coming back to original proposition of Bob Garrels, is it likely that anoxygenic phototrophic Fe-oxidisers could have contributed to the formation of BIF early in Earth history? To help answer this, the physiology of phototrophic Fe-oxidisers has been studied under a range of different light conditions, temperatures and pHs (Hegler *et al*., 2008). Given assumptions about ancient ocean Fe(II) levels and mixing rates, these physiological data were utilised in a simple mass-balance model to show that Fe(II) oxidising phototrophs could indeed have oxidised all the Fe(II) mixing to the surface from a deep ocean source, and thus, they could have contributed substantially to BIF formation (Kappler *et al*., 2005) in the absence of atmospheric O_2.

There is, however, more to the story. Nearly all strains of phototrophic Fe(II) oxidisers thus far cultured have been isolated from surface environments like shallow ditches, which have little direct relevance to the marine pelagic environments where Fe^{2+}-oxidising phototrophs may have contributed to BIF formation on the ancient Earth. Indeed, it is not easy to imagine where such analogue environments may be found as, when modern marine waters turn anoxic, they typically become sulphidic. However, a few modern meromictic lakes provide what would seem to be reasonable analogues of ancient marine

ferruginous conditions. One of these is Lake Matano, Indonesia. This lake has been intensively studied by Sean Crowe, a postdoc in my lab, and my former PhD student CarriAyne Jones. Lake Matano is a deep water oligotrophic lake with a permanent chemocline located at about 110 to 120 m water depth. Here, oxygen disappears, Fe(II) accumulates, light is low and what little sulphate is present in the lake (only 20 μM) is rapidly removed from the water column with minimal sulphide accumulation (Crowe *et al.*, 2008). These aspects of lake chemistry are shown in Figure 8.4. Also found in Lake Matano is the accumulation of Bchl *e*, a diagnostic light-harvesting pigment for low-light-adapted "brown" strains of the anoxygenic phototroph *Chlorobium*. Thus, anoxygenic phototrophs are important members of the chemocline ecosystem in Lake Matano. As sulphide is only available in low concentrations, and since Fe(II) is abundant, Crowe *et al.* (2008) argued that the *Chlorobium* population in Matano is conducting anoxygenic Fe(II) oxidation. Unfortunately, cultures of anoxygenic phototrophic bacteria have not yet been isolated from the lake, so their role in Fe(II) oxidation has yet to be proven. Nevertheless, Lake Matano provides strong indications that anoxygenic phototrophic Fe(II)-oxidising bacteria were present in ancient ocean-analogue environments, lending more support to the idea that such populations could have contributed significantly to BIF formation.

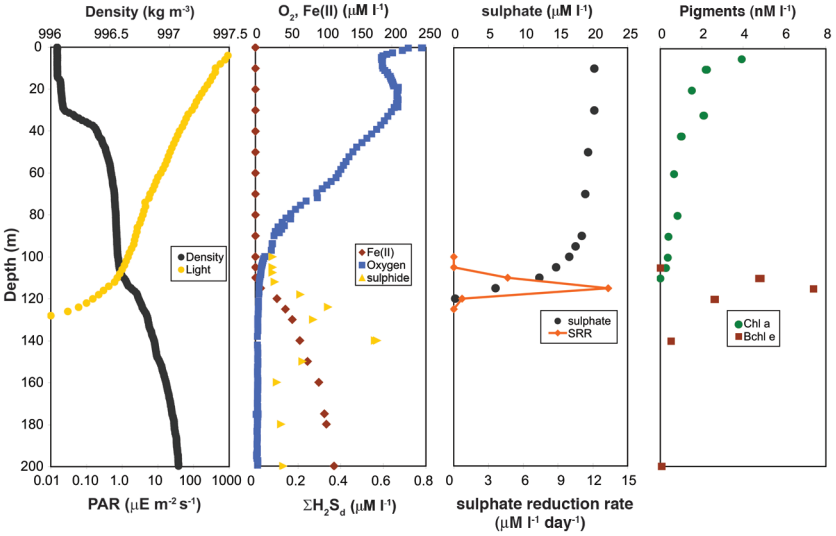

Figure 8.4 Distribution of various chemical, biological and physical parameters with depth in Lake Matano, Indonesia.

Microbial Dissimilatory Iron Reduction. Iron and organic carbon are also intimately coupled through the process of dissimilatory iron (oxyhydr) oxide reduction. This pathway may be viewed as the reverse of the phototrophic

production of organic carbon described above (compare reactions 8.6 and 8.7). One of the earliest experimental demonstrations of microbially mediated Fe reduction was provided by Starkey and Halvorson (1927) who observed microbial growth during the reduction of freshly precipitated ferric (oxyhydr)oxides to Fe(II) by both mixed and pure cultures of bacteria, although they did not directly link microbial growth to the Fe reduction process or view it as an energy metabolism. The wording is vague, but Bromfield (1954) does link microbial activity to Fe reduction and hints that this may involve metabolic enzymes. He argues, furthermore, that the process may be accelerated when organic substances can mobilise the ferric iron bound in the (oxyhydr)oxides. Later, bacteria capable of reducing iron (oxyhydr)oxides were isolated from the environment (e.g. Decastro and Ehrlich, 1970; Jones, 1983; Ottow, 1968; Takai and Kamura, 1966), and microbes were clearly linked to iron reduction in both lake and marine sediments (Jones *et al*., 1983; Sørensen, 1982). The field gained a tremendous boost when the iron reducers *Geobacter metallireducens* (Lovley and Phillips, 1986) and *Shewanalla putrefacians* (Obuekwe and Westlake, 1982) were isolated from the environment and were demonstrated to respire well-defined organic substrates and to link respiration to growth.

Since then, there has been amazing progress in our understanding of the iron reduction process, the organisms doing it, and its environmental significance. Since the early identification of *Geobacter metallireducens* and *Shewanalla putrefacians* as dissimilatory iron reducers, the number of known Fe-reducing species has exploded. Iron reducers are represented in both the bacterial and archaeal domains (Lovley *et al*., 2004) and they reflect the limits of temperature adaptations in nature, including hyperthermophilic members with growth temperatures up to 121°C, the highest known for any organism on Earth (Kashefi and Lovley, 2003).

How Dissimilatory Iron Reducers Access Iron: How do the organisms accomplishing Fe reduction access the ferric Fe they use? There is not a simple answer as several processes seem to be involved. First, many Fe-reducing organisms require direct contact with the Fe (oxyhydr)oxide in order to conduct Fe reduction (e.g. Munch and Ottow, 1982; Nevin and Lovley, 2000). This contact is required because Fe (oxyhydr)oxides are quite insoluble (Section 2.2 and Cornell and Schwertmann, 2003), and redox-active proteins involved in electron transfer during Fe reduction are often located at the outer cell membrane (Gralnick and Newman, 2007; Myers and Myers, 1992). Not all electron transfer, however, proceeds through surface-bound proteins. In a spectacular recent finding, *Geobacter sulfurreducens* can transfer electrons to Fe (oxyhydr)oxide surfaces with electron-conductive pili, so-called nanowires (Reguera *et al*., 2005). Indeed, extensive microbial nanowire networks are quickly established in artificial soil systems, leading to speculation that the subsurface may be "hardwired" (Ntarlagiannis *et al*., 2007; Nielsen *et al*., 2010). Thus, electrons may be transported between organisms through nanowires. This means that the oxidants and reductants driving microbial processes may be well separated in space. Such a new

view of microbial metabolism represents a paradigm shift akin to realising that you can call from Dallas to your aunt Agnes in Chicago by telephone, when before you thought you needed to speak to her in person in her own living room.

Other strategies are also used by Fe reducers to access Fe which require no direct contact with the Fe (oxyhydr)oxides. Harking back to the discussion of Bromfield (1954) as mentioned above, some Fe reducers secrete chelators, so-called siderophores, which can liberate the Fe(III) from Fe (oxyhydr)oxides and bring it into solution for utilisation by Fe-reducing organisms (see Section 2.2, Supplementary Information SI-1 and Gralnick and Newman, 2007; Kappler and Straub, 2005; Nevin and Lovley, 2002). A strategy of releasing chelators to access solid phase Fe(III) may make little sense for an individual bacterium, as the cost of generating chelators would outweigh the benefit of likely intercepting only a small proportion of the chelated Fe(III), but such a strategy could make sense for a dense population of Fe reducers where a higher proportion of the chelated Fe(III) would be intercepted and used.

Another strategy used by Fe reducers is the production of redox-sensitive compounds (quinones for example) that can accept electrons from the bacteria and deliver them extracellularly to the Fe (oxyhydr)oxide surface, reducing the Fe(III) to Fe(II) (Nevin and Lovley, 2002; Newman and Kolter, 2000). The idea that some iron reducers can take advantage of extracellular electron shuttles was first proposed by Lovley *et al.* (1996) who discovered that the Fe reducer *Geobacter metallireducens* could donate electrons to humic substances that, in turn, donated the electrons to Fe (oxyhyr)oxides, reducing Fe(III) to Fe(II) and liberating Fe(II) to solution. It was later revealed that quinone groups act as electron shuttles within the humics (Scott *et al.*, 1998). In an interesting twist on this theme, it appears that *Geobacter* cells can serve as capacitors, acting as a temporary electron sinks while awaiting contact with a suitable electron donor, like Fe (oxyhydr)oxides, where the electrons can be dumped (Esteve-Nunez *et al.*, 2008). Thus, *Geobacter sulfurreducens*, for example, contains an unusually large number of extracytoplasmic C-type cytochromes, which can act to temporarily store electrons. This strategy could allow the cells to produce ATP and conduct basic cell functions like maintenance and motility while charging the cytochrome capacitors in search of a suitable Fe (oxyhydr)oxide sink, later releasing this built-up charge when Fe (oxyhydr)oxides are encountered (Esteve-Nunez *et al.*, 2008).

All in all, a fascinating number of strategies are used by microbes to access Fe(III) for reduction. This demonstrates the extreme ingenuity of the microbial world in conducting their livelihoods and the ability of evolution to explore all corners for possible Fe acquisition strategies. In appears, also, that prokaryotes conducting dissimilatory Fe reduction have a wider arsenal of Fe acquisition techniques than aerobic prokaryotes and algae that take up Fe in surface seawater as explored in Supplementary Information SI-1.

How Fe Mineralogy Controls Fe Availability for Dissimilatory Reduction. Fe (oxyhydr)oxide minerals are found in a variety of forms and crystallinities in nature, and one would imagine that each of these factors would influence their

bioavailability for microbial reduction (Section 2.2 and Supplementary Information SI-6). Rather surprisingly, in a study of Fe-reduction by *Shewanella putrefaciens* on a variety of (oxyhydr)oxides including ferrihydrite, lepidocrocite, goethite and haematite, the main factors influencing rates of reduction were (oxyhydr) oxide surface area and cell density (Roden, 2003). When normalised to surface area, mineralogy had no obvious influence on reduction rate. This led the authors to conclude that the rate-limiting step for Fe reduction was the transfer rate of electrons to the mineral surface, which, they argued, would be controlled by both surface area and microbial density. In other studies, the microbial reduction of magnetite has also been demonstrated, but optimally in the pH range of 5 to 6, where the process is thermodynamically favorable for environmental concentrations of Fe(II) (Kostka and Nealson, 1995). Structural Fe in some clay minerals is also susceptible to microbial reduction, which could be of significance in many clay-rich sedimentary environments (Kostka *et al*., 1999).

In an interesting twist on the story, the accumulation of Fe(II) during the reduction of Fe (oxyhydr)oxides acts to hinder the reduction process through the adsorption of ferrous iron onto the (oxyhydr)oxide surface (Roden *et al*., 2000). The exact mechanism of the inhibition is not clear, but the adsorbed Fe(II) may lower the oxidation potential of the Fe (oxyhydr)oxide surface as discussed by Roden and Urrutia (2002). The Fe(II) inhibition on Fe (oxyhydr)oxide reduction can, however, be relieved when the Fe(II) is removed from the system. This has been demonstrated by Roden *et al*. (2000) who reported near complete reduction of synthetic goethite in a culture of *Shewanella putrefaciens* in a flow-through plug reactor, whereas only 13% of the goethite was reduced when Fe(II) accumulated in a closed system. The significance of this inhibition in nature, however, is uncertain as the diffusional loss of Fe(II) from porewaters could deplete Fe(II) to sufficiently low concentrations to remove the inhibitory effect. Indeed, in adsorption experiments, goethite surfaces were not saturated with Fe(II) until aqueous Fe(II) concentrations reached about 500 μM (Roden *et al*., 2000), a concentration much higher than typical of aquatic sediments.

The Significance of Fe Reduction in Nature. Running parallel with studies on the physiology, diversity and mechanisms of Fe reduction in pure microbial cultures, a number of studies have attempted to address the significance of Fe reduction in nature. Probably the first to demonstrate Fe reduction as a potentially significant sedimentary process was the study of Sørensen (1982). Here, the substantial accumulation of Fe(II) was observed in oxidised sediment slurries. The source of the Fe(II) was demonstrated to be microbial and rates of Fe reduction were greater than could be explained by the reaction of Fe (oxyhydr) oxides with the sulphide produced from sulphate reduction.

Even so, one can ask, how quantitatively important is Fe reduction in organic carbon mineralisation? How could this question even be approached? Robust tracer techniques exist for determining rates of sulphate reduction and rates of nitrogen transformations in the environment. Rates of oxygen uptake can

be measured in core incubations or using benthic landers[2], and oxygen profiles can be modelled to provide information on the depth distribution of oxygen utilisation. Iron (oxyhydr)oxides, however, are present in a variety of forms, which makes labelled tracer additions unreliable. Also, once reduced, Fe(II) can form a variety of mineral phases that are difficult to separate and extract quantitatively, and numerous processes, such as sulphate reduction, can also contribute to Fe reduction. This is a very complex problem, and to date, no reliable quantitative, direct methods of determining rates of iron reduction have been developed.

There were, however, early indications that Fe reduction may be important in organic carbon mineralisation. For example, after the development of oxygen microelectrodes, it became clear that in many sediments there existed 'dead zones' where little obvious organic matter mineralisation occurred. These zones existed between the depth to which oxygen and nitrate penetrated and the depth at which sulphate reduction rates peaked. Mark Hines (Hines *et al*., 1991), however, was able to measure active glucose turnover in this apparent "dead zone". Therefore, something was going on, and he suggested that this zone, in fact, housed active Fe and Mn reduction.

At about this time (1990), I had the pleasure of working in Aarhus in the group of Bo Barker Jørgensen. Jens Wügler Hansen was developing an air-tight "bag" strategy whereby sediments could be incubated free of oxygen but remain well mixed and easily subsampled. Using this technique, Jens, Bo Thamdrup and I developed an indirect method for measuring Fe (and Mn) reduction in sediments (Canfield *et al*., 1993). The method is time-consuming and involved, but the logic is quite simple. Sediment from a given site is homogenised into specific depth intervals and incubated in the absence of oxygen. Total rates of mineralisation are obtained from the accumulation rate of NH_4^+ and ΣCO_2, while rates of sulphate reduction are used to determine the portion of mineralisation contributed by sulphate reduction. These data are combined with the distributions of O_2, nitrate and solid phase Fe and Mn (oxyhydr)oxides to further define the zones of the different mineralisation processes. Rates of denitrification are measured separately.

In the end, one can define the zones where Fe and Mn reduction occur and use the mismatch between rates of sulphate reduction in total carbon mineralisation and rates of ΣCO_2 production[3] to determine rates. An example is shown in Figure 8.5 for station 6 from the Skagerrak, part of the belt seaway surrounding Denmark to the north. Here, Fe reduction is extremely important, dominating the anaerobic mineralisation of organic carbon. Rates of iron reduc-

2. A "lander" is a device, usually autonomous, that settles onto the sediment surface and from which experiments can be conducted. To measure oxygen uptake rates, a lander will contain a chamber which encloses a volume of sediment and monitors the rate of oxygen utilisation in the chamber.

3. In some cases rates of carbon mineralisation are determined, somewhat indirectly, by rates of ammonium liberation in the incubations. This is especially true if CO_2 is removed by carbonate precipitation during the incubations.

tion are 100 to 300 times higher than the rates of iron (oxyhydr) oxide input by sedimentation (Canfield *et al.*, 1993). Therefore, active iron reduction requires the active reoxidation of reduced iron phases within the sediment. This is promoted by any mixing process, but the activities of animals are likely the most important. Thus, active iron reduction requires active sediment mixing.

Probably due to the complexity of the approach, there are relatively few published data on the relative contributions of Fe (and Mn) reduction to total carbon mineralisation in sediments, at least compared to measurements of sulphate reduction, denitrification or sediment oxygen uptake. The data that do exist, however, suggest that Fe reduction can be a very important process of anaerobic carbon mineralisation in many cases, and the importance of the process scales with the concentration of poorly crystalline Fe (oxyhydr)oxides as determined from oxalate extraction (Jensen *et al.*, 2003; Thamdrup, 2000). Indeed, it appears that when the poorly crystalline Fe(III) concentrations exceed about 15 μmol cm^{-3}, dissimilatory Fe reduction accounts for more than 50% of the total amount of anaerobic organic carbon mineralisation (Fig. 8.6).

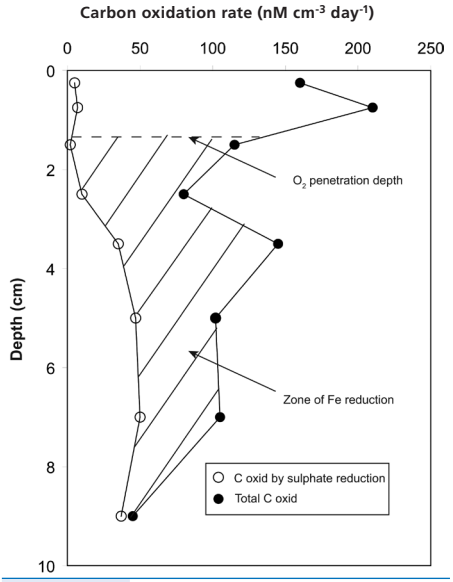

Figure 8.5 Plot marking rates of organic carbon mineralisation by sulphate reduction and total rates of organic carbon oxidation at Station S6 in the Skagerrak. Also shown is the depth of oxygen penetration and the hatched zone indicating rates of Fe reduction at this site. See text for details.

8.5 Manganese

In many ways, the biogeochemistries of Mn and Fe are very similar. Both of these elements form insoluble (oxyhydr)oxides under oxygenated conditions, they both are electron acceptors in organic matter mineralisation, and they each have a limited range of stable redox states in nature (Mn has a valance range of 2, Mn^{2+} to Mn^{4+}, and Fe has a range of 1, Fe^{2+} to Fe^{3+}). However, there are also important differences, and over five decades ago Krauskopf, (1957) described, with an early application of Eh/pH diagrams, how Fe^{2+} is more sensitive to oxidation than Mn^{2+}. He postulated that redox considerations alone could lead to the separation of

Fe and Mn (oxyhydr)oxide deposition if the environment was not too oxidising but was poised between MnO_2 and Fe (oxyhydr)oxide stability (Krauskopf, 1979). Such environments are found commonly in stratified lakes (Canfield *et al.*, 1995) and marine sediments (e.g. Froelich *et al.*, 1979) and must have contributed to the deposition of the massive Mn ore deposits occasionally found in the rock record (Calvert and Pedersen, 1993; Krauskopf, 1957; Maynard, 2010; Tsikos *et al.*, 2010).

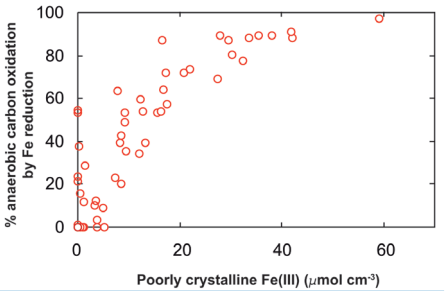

Figure 8.6 Percent of anaerobic carbon mineralisation channelled through Fe reduction in marine sediments as a function of poorly crystalline Fe(III) as defined by chemical extractions.

The cycles of Mn and Fe, however, interact in more direct ways. Postma (1985) determined that the reaction between Fe(II) and Mn (oxyhydr)oxides, producing dissolved Mn^{2+} and Fe (oxyhydr) oxides, should be thermodynamically favorable at the pH conditions normally found in nature. The reaction forming Fe (oxyhydr)oxides is:

$$MnO_2 + 2Fe^{2+} + 4H_2O \rightarrow Mn^{2+} + 2Fe(OH)_3 + 2H^+ \qquad (8.8)$$

In studying the kinetics of this reaction, Postma (1985) found that the reaction was extremely fast at a pH of 3, taking only a few minutes to reduce the added MnO_2. The reaction slowed dramatically at pH 4, indicating that a different reaction pathway was followed. At pH 3, dissolved Fe(III) was the reaction product, whereas solid phase $Fe(OH)_3$ was the product at pH 4. It was notable also that a green precipitate, presumably green rust, was observed at a pH > 6.3, which could provide one mechanism of green rust formation in nature at circum-neutral pH (Postma, 1985; Ahmed *et al.*, 2010).

However even at pH values >4 the reaction is still rather rapid, with MnO_2 persisting with a half life of hours (Postma, 1985). Rapid reaction is also indicated in nature. We have already discussed Lake Matano, Indonesia with reference to possible Fe(II) oxidation by anoxygenic photosynthesis, but the lake also contains active interactions between the Mn and Fe cycles (Jones *et al.*, 2011). My student CarriAyne Jones collected particles from various depths in the water column as part of her PhD thesis. Particles from the upper part of the chemocline are rich in Mn (oxyhydr)oxides, but these disappear within 5 to 10 meters depth as the settling particles are quickly reduced by aqueous Fe(II) which accumulates in the lower lake. This rapid reaction may place constraints on the circumstances surrounding the massive deposition of MnO_2 as has occurred in some ancient marine basins, and is the basis for massive sedimentary Mn accumulations (Maynard, 2010; Tsikos *et al.*, 2010). The results from Lake Matano suggest that the deposition of massive Mn deposits required either a very shallow water column or that the concentration of Mn^{2+} considerably exceeded aqueous Fe(II)

in the basin. The shallow water column helps allows Mn oxides to survive against persistent reduction by Fe(II) during the short transit to the sediments, while excess Mn^{2+} over Fe(II) allows an excess production of Mn oxides compared to the availability of Fe(II) to reduce the oxides.

8.6 Nitrogen

Broadly speaking, Fe interacts with nitrogen in two important ways: it is a central constituent of different metal cofactors regulating many aspects of the nitrogen cycle including those involved in nitrogen fixation (Glass *et al*., 2009; Morel and Price, 2003), and as Fe(II), iron also acts as an electron donor in nitrate reduction. We will look at each of these turn.

Influence of Iron on Nitrogen fixation. In various combinations with other trace metals like Mo, Ni, Cu and Mo, and sometimes by itself, Fe forms an essential constituent of various enzymes and metal cofactors used in a variety of nitrogen transformations. Excellent reviews are provided by Morel and Price (2003), Liu *et al*. (2009) and Klotz and Stein (2008). Of most interest here, however, is the nitrogenase enzyme promoting the fixation of atmospheric N_2 gas to ammonia by what are known as diazotrophic prokaryotic organisms. In the oceans, nitrogen is a limiting nutrient (Falkowski, 1997), and its limitation would be far more severe if the nitrogen losses—produced mainly through denitrification and anammox (the ANaerobic oxidation of AMMonium with nitrite) in the oxygen-depleted oxygen minimum zones (OMZs) and in marine sediments [e.g. (Dalsgaard *et al*., 2005; Lam and Kuypers, 2011)]—were not actively countered by nitrogen fixation. In the marine realm, most N_2 fixation is accomplished by cyanobacteria. The nitrogenase enzyme complex is composed of two subunits: (a) the dinitrogenase reductase subunit, (an Fe protein) that contributes reducing power to (b) the dinitrogenase subunit (an Fe-Mo protein), where the N_2 is reduced to ammonia. The Fe requirements for nitrogenase are huge, amounting to about 38 Fe atoms (and about 2 Mo atoms) per enzyme unit (e.g., (Miller and Orme-Johnson, (1992); Whittaker *et al*., 2011), making it among the most Fe-rich enzymes in nature.

In some diazatrophs, the Fe-Mo protein can be found in Fe only and V-Fe versions. These alternative dinitrogenase subunits are not known among marine cyanobacteria, but several strains of the freshwater cyanobacterium *Anabaena* can express each of the dinitrogenase varieties, with the specific expression depending on the particulars of trace metal availability (Eady, 1996; Joerger and Bishop, 1988). The Mo-Fe nitrogenase enzyme is more efficient at N_2 fixation than either of the alternative nitrogenases (Joerger and Bishop, 1988), and while estimates vary, Aubrey Zerkle, working in my lab, found that *Anabaena variabilis* fixed N_2 about 10 times as fast with abundant Mo (and Fe) in the growth medium, compared to when Mo was absent and presumably only the Fe nitrogenase was expressed (Zerkle *et al*., 2006). Consistent with many other studies

(e.g. (Berman-Frank *et al.*, 2001; Miller and Orme-Johnson, 1992), iron availability significantly influenced nitrogen fixation rate, and when Fe was completely absent, no nitrogen fixation could be detected.

Given the sensitivity of trace metal availability on the efficiency of nitrogenase activity, trace metal limitation has been argued to limit rates of nitrogen fixation in both the modern and the ancient oceans (Anbar and Knoll, 2002; Falkowski, 1997; Howarth *et al.*, 1988). Indeed, Fe limitation does, along with other factors such as light, temperature and surface water nitrate levels, exert an important global control on the distribution of nitrogen-fixing cyanobacteria in the modern ocean (Monteiro *et al.*, 2011). If Fe limitation becomes severe enough, global rates of marine primary production could be affected (Falkowski, 1997). As we shall explore in more detail in Section 9, Fe limitation may not have been severe earlier in Earth history when the oceans were dominantly anoxic, but Mo may have been limiting during periods of time when sulphidic conditions were considerably more expansive than today (Anbar and Knoll, 2002; Scott *et al.*, 2008). This idea has led to the fascinating hypothesis that during times of Mo limitation, nitrogen fixation may been limited by the inefficiency of the alternative nitrogenase enzymes, which may have been preferentially expressed (Anbar and Knoll, 2002). Therefore, in a cascade of effects, Mo limitation led to nitrogen limitation through inefficient N-fixation, leading in turn to reduced rates of global primary production (Anbar and Knoll, 2002).

Influence of Iron on Nitrate Reduction. Now we turn to our second example of microbially mediated interactions between the Fe and nitrogen cycles. One of the truly exciting aspects of contemporary microbial ecology is the rather frequent discovery of previously unknown microbial metabolisms. Microbial ecologists are keenly aware of the prospect that if a thermodynamically possible microbial metabolism can be identified (on paper that is), there is a good chance that Mother Nature has indeed evolved a metabolism to conduct it. During my time at the Max Planck for Marine Microbiology in Bremen, Germany, one such discovery of a "new" microbial metabolism was made by then PhD student Kristine Straub. She cleverly deduced that aqueous Fe(II) oxidation with nitrate, being thermodynamically possible, but kinetically inhibited, could be mediated by bacteria. She then generated a number of enrichment and pure microbial cultures that could do so (Straub *et al.*, 1996; Straub *et al.*, 2004), producing Fe (oxyhydr)oxides and N_2 gas as products. Due to this biological reaction, Fe^{2+} and nitrate are not expected to co-occur in natural environments at circum-neutral pH (Straub *et al.*, 2004). This conclusion is consistent with the depth distribution of redox sensitive species in marine sediments [e.g. (Froelich *et al.*, 1979)] and could explain why Fe(II) does not accumulate in nitrate-rich, oxygen-free oxygen minimum zones (OMZs) of the global ocean (Landing and Bruland, 1987). These points will become important in later discussions.

8.7 Sulphur

As mentioned in Section 8.1, my PhD project began as a study of the rate of pyrite formation in marine sediments. Before I could get to this, however, it was necessary to understand the first step, which was the reaction rate between sulphide and various Fe minerals in sediments. This turned out to be a bigger problem than I expected and kept me busy for the next few years.

In retrospect, it all seems desperately obvious, but I puzzled mightily over the observation that in marine sediments, the highest rates of sulphate reduction in sediments were often found in the complete absence of dissolved sulphide in the porewater. An example of this is shown in Figure 8.7 (compare with Fig. 4.4), from the so-called FOAM (Friends Of Anoxic Mud) site in Long Island Sound (Canfield, 1989). At this time, measurements of sulphate reduction rates in marine sediments were relatively few, as were studies where sulphate reduction rates were measured together with porewater sulphide and aqueous Fe(II) distributions. Despite this, and even before the first sulphate reduction rates were presented in the western[4] literature (e.g., (Jørgensen, 1977; Oremland and Taylor, 1978), Marty Goldhaber suggested that the reaction between iron minerals and sulphide could be rapid and control the sulphide concentration in sediments (Goldhaber and Kaplan, 1974). This seemed like a good idea, but how to test it?

In the end, I used a two-phase approach to tackle the problem. First, I adopted different chemical extractions to define the concentrations of different Fe minerals within marine sediments. These extractions were calibrated with pure, natural and synthetic Fe phases individually and in mixtures (Canfield, 1988, 1989; Raiswell *et al.*, 1994). The latest incarnation of this scheme with important modifications is presented in Poulton and Canfield (2005). These extractions showed that for the most part, different mineral phases could be rather cleanly separated with the different extractions. The next step was to determine the reaction rates between different Fe mineral phases and sulphide (Section 3.5). Some of these rates were experimentally determined by reacting pure Fe mineral phases with sulphide, and some were determined by exploring the kinetics of sulphide reaction with natural sediment Fe mineral phases. For detrital magnetite, which reacts slowly with sulphide, reaction kinetics were determined by monitoring the depth distribution of magnetite in a variety of sediments with different sulphide concentrations (Canfield and Berner, 1987). Rob and I also modelled the distributions of sulphide and Fe in slowly depositing sulphidic sediments off the Peru margin to shed light of the reaction kinetics of the more slowly reacting sheet silicate Fe pool (Raiswell and Canfield, 1996). In other cases, the extremely slow

4. The Russians were far ahead of western scientists in understanding the sulphur cycle. For example, Yu I. Sorokin had used the ^{35}S-SO_4 method to measure rates of sulphate reduction in the Black Sea in 1962 [Sorokin, Yu. I., 1962, Experimental investigation of the bacterial reduction of sulphates in the Black Sea with the help of S^{35}, *Mikrobiologiya*, 31, 402-410 (in Russian)].

reaction kinetics between sulphide and Fe in detrital sheet silicates were quantified by monitoring the isotopic composition and concentrations of pyrite with depth in sulphidic sediments from the FOAM site (Canfield *et al.*, 1992).

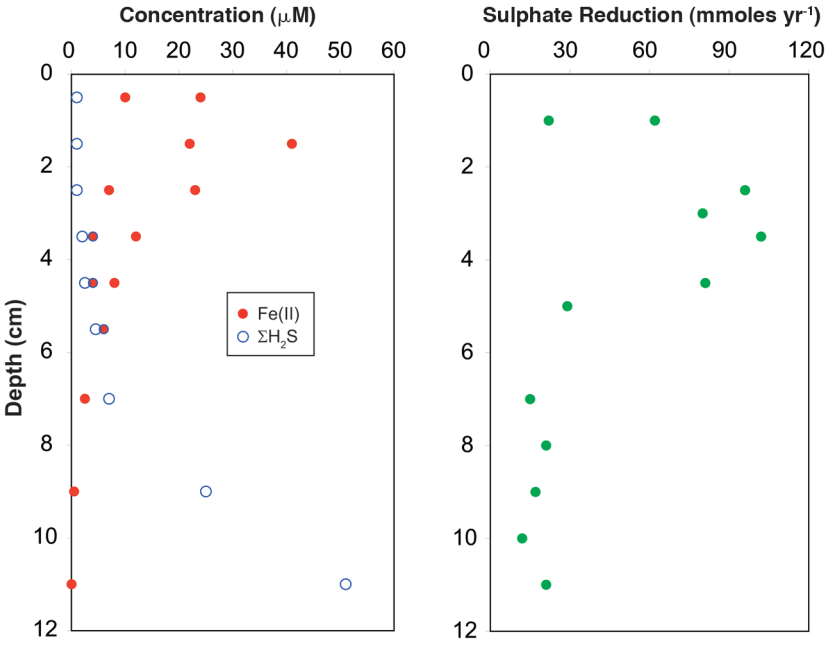

Figure 8.7 Depth distributions of Fe(II), ΣH_2S and rates of sulphate reduction at the FOAM site in Long Island Sound (data from Canfield, 1989).

Altogether, it was found that the reaction kinetics between Fe minerals and sulphide could be divided into two broad categories. The Fe (oxyhydr)oxides react rapidly with sulphide on time scales of less than a year compared to many thousands of years (or more) for the Fe bound in silicates. Magnetite seemed to fit somewhere in the middle, where I found reaction times of about 100 years for detrital grains in sediments of Long Island Sound. Simon Poulton has recently found much faster reaction times of 72 days for synthetic magnetite (Poulton, 2004). Part of the discrepancy is likely related to differences in the grain sizes and possibly also to differences in the purity of the different mineral grains (many of the natural minerals may exist in solid solution with other cations). Regardless, the picture remains the same, the (oxyhydr)oxides react quickly and the silicates slowly. Thus, the (oxyhydr)oxides will be expected to react with sulphide (if available) on early diagenetic time scales in coastal settings, whereas the silicates should not, and this observation forms part of the basis for using Fe speciation to determine ancient depositional environments. This discussion, and

the development of the ideas behind the use Fe speciation as an environmental indicator are presented in detail in Section 3, and a summary of the reaction kinetics between various Fe phases and sulphide have already been presented in Table 4.1.

Thus far, we have explored the kinetics of the interaction between sulphide and Fe minerals from the perspective that they are strict inorganic reactions. They are also thermodynamically favorable redox reactions in many cases and could potentially support a microbial metabolism. Thus far, there is no indication that any of the reactions between sulphide and the various iron (oxyhydr)oxides that form FeS support any type of microbial growth. However, the formation of pyrite from FeS is a further redox reaction, with two known possible pathways (see Section 3.2). One of these is the reaction between FeS and H_2S (Drobner *et al.*, 1990; Rickard, 1997), which produces H_2 as a product (equation 8.9). Günter Wächtershäuser has famously proposed that the electrons liberated during the oxidation of FeS with H_2S could have been used to reduce CO_2 to organic matter (equation 8.10), and that this coupled reaction may have formed the basis for early bio-molecule production in the origin of life (Wächtershäuser, 1988).

$$FeS + H_2S \rightarrow FeS_2 + H_2 \tag{8.9}$$

$$FeS + H_2S + 1/2CO_2 \rightarrow FeS_2 + 1/2H_2O + 1/2CH_2O \tag{8.10}$$

While organisms have not yet been proven to grow by this pathway, there are some tantalising indications that organisms may be involved in and accelerate the reaction leading to pyrite formation. The possible role of microbes was observed by Bo Thamdrup and myself while exploring the dynamics and isotopic fractionations associated with elemental sulphur disproportionation by pure microbial cultures (Canfield *et al.*, 1998). Pyrite was produced in our microbial system during this process at rates that were orders of magnitude faster than expected from inorganic reactions (Rickard, 1997). Were organisms involved and did they gain energy from the formation of pyrite? We were unable to tell for sure, but the possibility seems real.

Final Thoughts. As outlined above, Fe interfaces with the biogeochemical cycling of many different elements. Some of these interactions are strictly inorganic, such as phosphorus absorption onto Fe (oxyhydr)oxides, whereas others are strictly biological, such as the interface between iron and carbon cycles. Many of these interactions are critical in controlling aspects of the chemistry and the biology of the modern Earth surface environment. Harking back to Section 2.1, Fe plays a critical role in controlling primary production in the oceans, both as a limiting nutrient for algal production and as a limiting nutrient for nitrogen fixers who help regulate the concentration of nitrate in seawater. From another perspective, Fe (oxyhydr)oxides also bind phosphate, providing an important removal pathway of this nutrient from the oceans. Therefore, in different ways, the Fe cycle acts to both supply and remove nutrients from the oceans. Fe interfaces with the sulphur cycle, providing an important removal pathway of sulphur as pyrite from the oceans, and it interfaces with oxygen, as the pyrite is brought back into the weathering environment, ultimately supplying sulphate back to the oceans.

As explored in the next section, many of the interactions between iron and other biogeochemical cycles are at the core our understanding of the evolution of Earth surface chemistry through time. Still, in understanding the mineralogy and fate of Fe (oxyhydr)oxides formed through microbial processes, we lack the same rigor as applied to exploring this issue for Fe (oxyhydr)oxides formed through non-microbial processes in modern seawater as explored in Supplementary Information SI-3. Applying this rigor will fill an important gap between our understanding of how the Fe cycle works in modern oxic environments, defining most of the modern global ocean, and the interface between oxic and anoxic environments as defines the microbial world of Fe cycling both present and past.

9. THE HISTORY OF THE IRON BIOGEOCHEMICAL CYCLE

9.1 Historical Digression

In his classic book "The Biosphere" published first in 1926, but available in English in later translations (Vernadsky, 1998) Vladimir Vernadsky described the role of the biosphere in shaping and indeed controlling the chemistry of the planet. There are countless prescient insights in this book, but one that I would like to highlight was Vernadsky's assertion that, as far as he could see, the surface chemistry of the Earth had changed little through geologic time. This is apparent in the following remarkable statements which provide the earliest references of which I am aware to the long history of atmospheric oxygen and the nature of life on Earth through geologic time:

> *"In all geological periods, the chemical influence of living matter on the surrounding environment has not changed significantly; the same processes of superficial weathering have functioned on the Earth's surface during this whole time, and the average chemical composition of both living matter and the Earth's crust have been approximately the same as they are today."*

Somewhat later he states:

> *"The phenomena of superficial weathering clearly show that free oxygen played the same role in the Archean Era that it plays now in the biosphere. The composition of the products of superficial weathering, and the quantitative relationships that can be established between them, were the same in the Archean Era as they are today. The realm of photosynthesizers in those distant times was the source of the free oxygen, the mass of which was of the same order as it is now."*

We may or may not agree with the actual sentiments expressed here, but the logic and approach are impeccable. Vernadsky uses the same types of observation and the same types of reasoning that we use today to unravel the history of Earth surface chemical evolution and the significance of life in affecting this history. Our methods are better developed, but the main questions we seek to address, and the general approaches we use to address them, remain remarkably similar.

In what follows, we will explore the evolution of Earth surface chemistry through the lens of Fe biogeochemistry. This will give us clues as to how Fe has interacted with the biogeochemical cycles of other elements and ultimately, how these interactions may inform us as to aspects of the evolution of ocean and atmospheric chemistry through time. To explore this history, we must consider not only the interactions between Fe and elemental cycles as explored Section 8,

but we must also consider the dynamics of the Fe cycle and the regulation of Fe fluxes through Earth surface reservoirs, as discussed through the previous sections.

9.2 Fluxes of Fe and S

My earliest experience of doing science was during my senior year in college at Miami University, Oxford, Ohio. I was invited by my environmental chemistry teacher (and first scientific mentor), Bill Green, to work on the nearby Acton Lake. I was completely taken by the idea of actually doing research in the environment and jumped at the chance, leaving any ideas of pursuing a career in inorganic chemistry far behind.

Lake versus Marine Chemistry. Like many lakes in the Midwest of the United States, Acton Lake is diamictic, meaning that it mixes twice a year and that it is stratified during the summer. Also like many lakes in the Midwest and elsewhere, when summer stratified, the bottom waters go anoxic and accumulate dissolved Fe(II). Some of my very first geochemical measurements were of oxygen and Fe(II) concentrations in Acton Lake bottom waters, leading to my very first publication (Canfield *et al.*, 1984). This paper is no citation classic, but it started a 30 year on-and-off affair with stratified lakes, and it demonstrated an important difference between the anoxic waters of Acton Lake and anoxic basins of the ocean. Simply stated, in the modern realm, when lakes go anoxic, they tend to accumulate Fe(II), whereas when marine basins go anoxic, they tend to accumulate sulphide. The difference in the behaviour of these two systems, briefly mentioned in Section 8.4, forms the basis for understanding the evolution of different types of ocean chemistry through Earth history.

One obvious difference between Acton Lake and the oceans is sulphate concentration. In Acton Lake, sulphate concentration is low at about 300 μM (Green *et al.*, 1985). Low sulphate concentrations are a general feature of lakes (with some notable exceptions), compared to the high average modern marine sulphate concentration of 28 mM. Therefore, we could imagine that sulphate would be less available in lakes, compared to oceans, allowing the oceans a better chance to go sulphidic when anoxic. A beautiful example of the interplay between sulphate, sulphide and Fe(II) in a permanently anoxic ferruginous lake has already been shown for Lake Matano, Indonesia in Figure 8.4. Recall that in Lake Matano, sulphate, beginning at a very low concentration in the upper waters, is depleted in the upper reaches of the chemocline, and that the small amounts of sulphide produced are overwhelmed by the massive supply of Fe(II) in the lake, which is thus Fe(II), not sulphide, dominated.

Relative Fluxes of Fe and S to the Oceans. Therefore, sulphate concentration has something to do with determining whether an anoxic system will tend towards sulphidic or ferruginous conditions. However, sulphate concentration is

just a proxy for the real driver, which is the relative fluxes of highly reactive Fe[1] and sulphide (from sulphate reduction) to the anoxic system. If we have a system at circum-neutral pH[2], and if the sulphide flux exceeds the highly reactive Fe flux by a factor of two (the stoichiometric ratio of Fe to S in pyrite, FeS_2), then sulphide should accumulate. If sulphide production does not exceed the highly reactive Fe flux by a factor of 2, then Fe(II) should accumulate. This simple idea is expressed in cartoon form in Figure 9.1.

Returning now to Acton Lake and Lake Matano, the low sulphate concentrations in these lakes are a reflection of the low sulphate fluxes to them. The low sulphate fluxes are, furthermore, insufficient to drive enough sulphate reduction to remove the highly reactive Fe entering these lakes. The highly reactive Fe is dominantly composed of the iron (oxyhydr)oxides associated with detrital particles entering the lakes (see Section 3.5 for a more complete discussion of highly reactive Fe and footnote 1). The Fe(II) that accumulates is derived from the reductive dissolution of these highly reactive Fe phases. If there was no highly reactive iron flux to these lakes, sulphidic conditions would dominate despite the low sulphate fluxes and sulphate concentrations.

I had some idea of this simple control principle when I proposed a transition from ferruginous to sulphidic marine conditions during the Proterozoic Era in 1998 (Canfield, 1998). I will discuss this idea in more detail in a later part of this section, but to evaluate it, I estimated the flux of highly reactive Fe to the global ocean (based on dithionite extractable iron in river particulates; see also Section 3.5) and compared this to

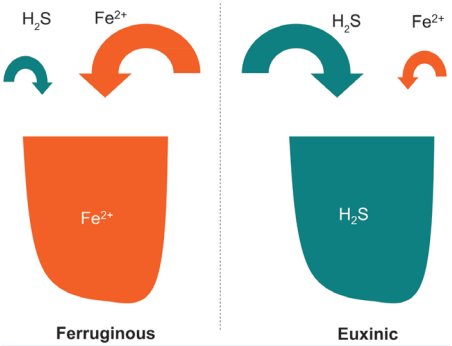

Figure 9.1 Cartoon showing how the relative fluxes of reactive Fe and sulphide production can determine the nature of anoxic water chemistry.

1. Highly reactive Fe includes the Fe phases which are viewed to be reactive on early diagenetic time scales. In oxic waters, highly reactive Fe is comprised mostly of particulate iron oxide and oxyhydoxide phases. In anoxic waters , some of these oxides and oxyhydroxides will be converted to other diagenetic products, and the highly reactive Fe pool consists of unconverted Fe oxides and oxyhydoxides together with Fe sulphides and Fe carbonate phases as well as dissolved Fe(II). See Sections 3.5 and 3.6 for further discussion.
2. The solubility product of FeS is given as $k_{sp} = a\mathrm{Fe}^{2+} a\mathrm{HS}^- / a\mathrm{H}^+$. As pH drops ($a\mathrm{H}^+$ increases), the concentration of HS^- increases to maintain FeS saturation at constant Fe^{2+}. Furthermore, the first dissociation constant for H_2S is about 10^{-7}. Therefore, as pH drops below 7, the concentration of HS^- begins to drop at any equal concentration of total H_2S ($H_2S + HS^- + S^{2-}$). This means that total H_2S concentrations must increase further to maintain saturation with FeS as pH drops below 7. Thus, below a pH of about 7, both ferruginous and sulphidic conditions can co-occur.

modern rates of sulphate reduction. The comparison revealed a clear excess of sulphate reduction over highly reactive Fe delivery, and I argued that because of this, if the oceans went anoxic with the same flux of sulphate to the oceans as today, they would become sulphidic. In fact, I made the wrong calculation, or rather, I mixed two different ideas. The RIGHT calculation would have been to compare the highly reactive Fe flux to the ocean to the sulphate flux, and not to worry about modern rates of sulphate reduction.

In fact, not all of the sulphate entering the oceans is necessarily available to end up as pyrite. Indeed, the sulphate entering the oceans can be removed by two major pathways; either as pyrite sulphur or as evaporitic $CaSO_4$. From simple S isotope mass balance considerations, a very high percentage of the sulphate entering the Proterozoic oceans, particularly early in the Proterozoic, was removed as pyrite (Canfield, 2004), so we don't need to worry so much about the $CaSO_4$ removal pathways. Therefore, the river flux of sulphate into the oceans provides the removal flux of pyrite from the oceans. How does this compare to the highly reactive Fe input flux?

Simon Poulton and I have discussed this at length. Our estimates rely heavily on previous Fe budget estimates generated by Rob and Simon (Poulton and Raiswell, 2002), along with best estimates for pre-anthropogenic sulphur delivery to the oceans (Poulton and Canfield, 2011). Our compilation is reproduced in Table 9.1. We find that, in contrast to my earlier approach, there is a great excess in highly reactive iron input to the oceans compared to sulphur input, with a S/Fe input ratio of 0.5, compared to the pyrite ratio of 2/1. Therefore, if the WHOLE ocean went anoxic, ferruginous conditions would be predicted. However, there is a great excess of highly reactive Fe deposition on inner shelf sediments, so the ratio of S/Fe left for removal onto the outer shelf, slope and deep sea is

Table 9.1 Global FeHR and S budgets for the modern ocean.

	FeHR	S†	S:FeHR
Fluxes ($\times 10^{12}$ mol y^{-1})			
Continental sources	6.5 ± 1.7	2.6 ± 0.6	
Hydrothermal	0.3 ± 0.1	0.5 ± 0.4	
Volcanic	-	0.2 ± 0.1	
Total	6.8 ± 1.7	3.3 ± 0.7	
Sinks ($\times 10^{12}$ mol y^{-1})			
Inner shore areas*	5.5 ± 0.6	1.0	0.2
Global ocean	1.3 ± 0.3	2.3	1.8

*Including the outer shelf, continental slope and the deep sea.
†Uncertainties on S sinks are not reasonably definable.

about 1.8/1, very close to the ratio in pyrite formation. Therefore, the system is apparently balanced near a switching point. This means that if anoxia develops below the ocean mixed layer of about 100 meters, small changes in either the S or Fe fluxes could drive the system to either sulphidic or ferruginous states. As we shall see below, the discussion is more subtle than this, and mixed chemical states during many times in Earth history were most likely the rule.

9.3 Life before Oxygen

In the following sections, I will provide a chronological view on the evolution of the Fe cycle and its interactions with many other biogeochemical cycles as outlined in Section 8. I will take as my starting point, somewhat counter to the views expressed above by Vernadsky (see Section 9.1), that oxygenic photosynthesis was not among the original microbial metabolisms on Earth (David and Alm, 2011; Raymond and Segre, 2006), and that there was a substantial oxidation of the Earth's surface environment, the so-called "Great Oxidation Event" around 2.3 to 2.4 billion years ago (Holland, 1984a,b; Farquhar *et al.*, 2000; Guo *et al.*, 2009). Further details on both these points will be elaborated on below as needed. This starting point, however, allows us to discuss a time in Earth history before oxygenic photosynthesis, when life existed in an essentially anoxic atmosphere. It is quite possible that this time in Earth's history is too far back to be represented in the geologic record. This would make the details of such a time unknowable from direct observations, and any discussions about it highly speculative. I accept this as a reasonable premise for the following discussion, but I believe we can start by recognising the following as likely:

(a) A time existed before the evolution of oxygenic phototrophs where anoxygenic photosynthetic organisms populated the surface environment. This is supported from arguments showing that the reaction centres used to convert light to energy during photosynthesis evolved first in anoxygenic phototrophs, and that these were later combined and used to form the coupled reaction centres (PSI and PSII) used in oxygenic photosynthesis. These views will not be further outlined here, but are elegantly expressed in work by Bob Blankenship and his colleagues (Blankenship, 1992; Blankenship and Hartman, 1998; Hohmann-Marriott and Blankenship, 2011).

(b) During this time, anoxygenic phototrophs conducted similar metabolisms as today. This is more of an assertion, but would not be unlikely as the reaction centers used by different anoxygenic phototrophs are similar (Hohmann-Marriott and Blankenship, 2011), and the enzymes used in the specific phototrophic transformations of Fe and S compounds, for example, are widely distributed and not terribly novel to the anoxygenic phototrophs.

(c) During this time, biogeochemical cycles were well established. Therefore, both autotrophic and heterotrophic metabolisms were present and complete cycles including the production and reduction of oxidised species could be identified for many elements including Fe and S. This is again an assertion, but it is not inconsistent with emerging views, based on whole genome analyses (David and Alm, 2011), on the antiquity of various enzyme families to bind specific redox-sensitive compounds. It appears, for example, that enzyme families binding Fe and S compounds were well established before the evolution of oxygenic photosynthesis (David and Alm, 2011).

(d) Fe(II) was in excess over sulphide as a solute in the global ocean. This assertion is consistent with the idea that sources of S to the global ocean before oxygen production were limited to volcanism and hydrothermal vents. These are minor sources of sulphur today compared to river runoff which delivers oxidised sources of S to the oceans; a river sulphur source would have been minimal in the absence of oxygen in the atmosphere. In contrast, Fe would have been supplied to the oceans by continental weathering and hydrothermal vents, and in these ancient vents, the Fe(II)/H_2S may have been considerably higher than today (Kump and Seyfried, 2005) and much higher than the ratio found in pyrite. This would produce a net source of Fe(II) to the oceans.

Iron Cycle before Oxygenic Photosynthesis. Given these premises, we can speculate on the existence of an early and dynamic Fe cycle. By analogy with Lake Matano, and the ability of anoxygenic phototrophs to oxidise iron, there would have been a population of in the surface waters, actively converting Fe(II) from the ocean depths into Fe (oxyhydr)oxides, and building biomass as a result. Both biomass and the Fe (oxyhydr)oxides would have settled back into the deep ocean, where Fe-reducing bacteria would have re-reduced the Fe (oxyhydr)oxides with the associated organic carbon. Any iron (oxyhydr)oxides escaping reduction would have accumulated into sediments and some of any excess organic carbon would have been decomposed by methanogens. A cartoon of this pre-oxygenic photosynthetic world is shown in Figure 9.2. A large host of other microbial metabolic processes would have also been in place, but they are outside the scope of the present discussion (see Canfield *et al.*, 2006).

How active might such an ancient Fe cycle been? This is a difficult problem bordering on the unknowable, but with certain assumptions, it is still possible to make a guess. Indeed, this issue has been approached both by myself (together with Minik Rosing and Christian Bjerrum) (Canfield, 2005; Canfield *et al.*, 2006) and by Jim Kasting and his group (Kharecha *et al.*, 2005). Our estimates differ, but it seems possible that such an "Fe-world" could have been quite active. In making our estimates, we took our clues from the modern ocean. Integrating all aspects of ocean circulation and organic matter recycling, the present 2.3 μM deep water phosphorus level supports a marine productivity of 4×10^{15} mol C yr^{-1} (Field *et al.*, 1998). We continued with a thought experiment, and asked how much deep water Fe(II) would be required to support this same amount

of productivity assuming that all the primary production was accomplished by anoxygenic photosynthetic Fe oxidation? Assuming a Redfield C/P ratio of 106/1 for organic biomass, and with the stoichiometry of Fe(II) oxidation to C-fixation during anoxygenic photosynthesis (4/1, equation 9.1), supporting today's production would take 2.3 μM P × 106 C/P × 4 Fe/C = 975 μM Fe(II) in the deep ocean.

$$7H_2O + 4Fe^{2+} + CO_2 \rightarrow 4FeOOH + CH_2O + 8H^+ \quad (9.1)$$

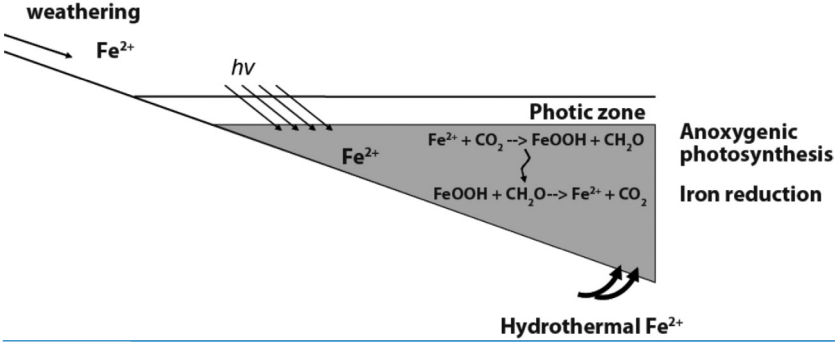

Figure 9.2 Cartoon of pre-oxygen Fe cycle; photons represented as hv (adapted from Canfield *et al.*, 2006).

Therefore, if this much Fe(II) was present in the pre-oxygenic photosynthetic deep ocean, then primary production rates in the ancient ocean could have matched those for the present ocean. This is a great deal of Fe(II), and a concentration rarely seen in natural aquatic environments of near neutral pH. Therefore, we viewed this value as likely too high, and we used Dick Holland's estimate of early deep-ocean Archean Fe(II) concentrations of 40 to 120 μM as our guide (Holland, 2004). With this much Fe(II), rates of primary production would have been at maximum 8 to 24 times less than present-day marine rates. After exploring other potential routes of primary production, we also concluded that an Fe(II)-driven carbon cycle would have produced far more primary production than any other cycle we could contemplate. Our overall conclusion was that even though Fe(II) cycling may have promoted the most active carbon cycle on the ancient Earth, rates of carbon cycling before oxygenic photosynthesis were low, and they accelerated dramatically with the evolution of oxygenic phototrophs. This conclusion supports a view expressed earlier by my postdoc mentor Dave Des Marais (Des Marais, 2000).

9.4 The Archean Eon

The Archean Eon spans from the earliest preserved rocks in the geologic record, about 4.0 Ga until the strictly defined border to the Proterozoic at 2.5 Ga. The Archean is subdivided into 4 Eras including the Eoarchean from about 4.0 Ga

until 3.6 Ga, the Palaeoarchean from 3.6 Ga to 3.2 Ga, the Mesoarchean from 3.2 Ga to 2.8 Ga, and the Neoarchean from 2.8 to 2.5 Ga. We discussed above in Section 9.2 and in Sections 3.3 / 3.4 and 8.2 / 8.7 how the Fe cycle is controlled by interactions with the cycles of sulphur and oxygen. This was certainly also the case through the Archean. To summarise the above discussion, oxygen availability has the dual role of:

(a) oxidatively weathering sulphide minerals on land, generating a sulphate flux to the oceans, and

(b) ventilating the deep ocean with oxygen and limiting the extent of marine anoxia if the concentrations of oxygen are high enough.

Sulphate availability depends on atmospheric oxygen concentration, but only at the low oxygen range. When oxygen reaches a certain level, probably somewhere in the 10^{-5} to 10^{-3} range of present atmospheric levels (PAL) (Anbar *et al.*, 2007; Canfield *et al.*, 2000) oxidative weathering of sulphides to sulphate on land is complete. Sulphate availability also depends on the inventory of sulphur in continental rocks and on volcanic outgassing rates (Canfield, 2004). The availability of Fe depends on the fluxes of Fe from continental and volcanic sources, and these have likely changed through time, as will be explored more fully below. The relationship between these variables and their control on marine chemistry is shown in Figure 9.3.

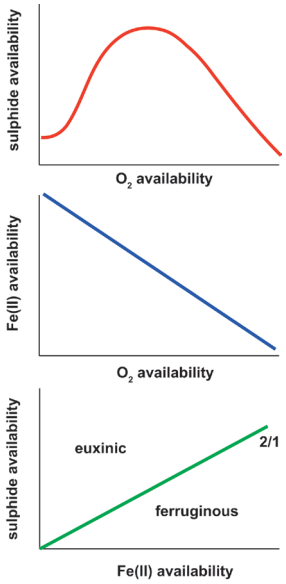

Figure 9.3 Cartoon showing expected relationship, between O_2 availability and the availability of sulphide and Fe(II) in the oceans. Also shown is the relationship between highly reactive Fe availability and sulphide availability and how their combination defines either euxinic or ferruginous conditions in anoxic waters.

Archean Oxygen Levels. Therefore, fully understanding the Archean Fe cycle requires some knowledge of the levels of atmospheric oxygen. This would be helped with some understanding of when cyanobacteria, the first oxygen-producing phototrophs, evolved. This later point is the subject of a great deal of debate in the scientific community, with widely divergent opinions based mostly on reasonable but different views of the geologic record. It is nearly impossible to prove that cyanobacteria were not present, so most of the debate rests on what is sufficient evidence to prove that they were. I prefer not to delve into this debate here, but the interested reader can consult a number of recent papers for

updates (Buick, 2008; Canfield, 2005; Kirschvink and Kopp, 2008; Rasmussen *et al.*, 2008; Waldbauer *et al.*, 2011). Rather, we will take our cues from the geologic record of Fe and sulphur geochemistry. This record has certainly been influenced by oxygen, and as we shall see, can therefore inform on the likely presence of cyanobacteria and oxygen production at the Earth surface.

The sulphur isotope record has played prominently into this discussion, particularly the record of the rare sulphur isotopes ^{33}S and ^{36}S. These data were brought to the forefront of discussion in the year 2000 by my good friend James Farquhar, who, seemingly out of nowhere, documented so-called mass-independent behaviour for sedimentary sulphur compounds before about 2.3 to 2.4 billion years ago, and mass-dependent behaviour for sulphur compounds of younger age (Fig. 9.4) (Farquhar *et al.*, 2000). Indeed, mass-dependent fractionations are the expectation through most known biological and geochemical processes, so the mass-independent signal required some explanation. James determined experimentally that atmospheric reactions of gaseous volcanic sulphur compounds in the near UV range could cause such fractionations (Farquhar *et al.*, 2001), and atmospheric models suggested that oxygen concentrations of 10^{-5} PAL or less would be needed for the fractionations associated with these reactions to be delivered to the Earth surface for preservation in the geologic record (Pavlov and Kasting, 2002). The loss of the mass-independent-fractionation (MIF) signal in the geologic record marks the Great Oxidation Event (GOE) as described above and a fundamental change in the chemistry of the Earth surface.

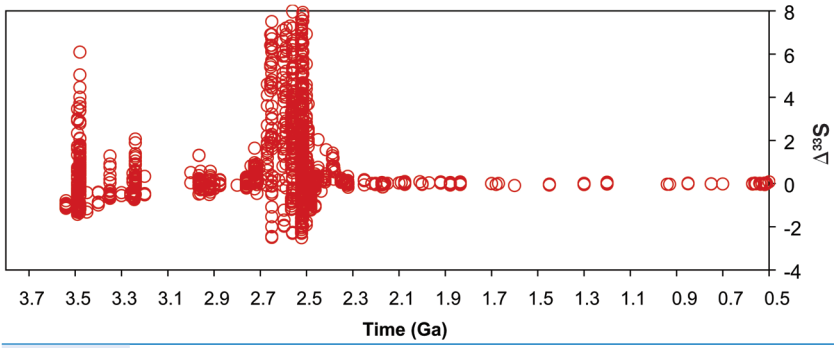

Figure 9.4 $\Delta^{33}S$ over time. This parameter represents the deviation on $\delta^{33}S$ from an expected mass fractionation law, and values ranging from zero express mass independent fractionations (data from Farquhar *et al.*, 2010).

Archean Fe Cycle. So what about the Fe cycle? The geologic record seems to indicate two things. The first is that Fe(II) was dissolved in seawater in excess of sulphide during much of the Archean. This is observed in the deposition of banded iron formations (BIFs) through much of the Archean (Fig. 9.5), which required a dissolved source of Fe(II) in their formation. BIF deposition however,

has been correlated to periods of extreme mantle activity, which may have contributed to an enhanced supply of Fe(II) to the oceans (Bekker *et al.*, 2010; Isley, 1995). The question is whether the record of BIF deposition can be taken to represent marine chemical conditions throughout the Archean? This may be difficult to know given a somewhat spotty record of preserved Archean sedimentary rocks, but fortunately, BIFs are not the only rocks which can inform on the nature of Archean ocean chemistry. Many Archean shales are also enriched in Fe(II) relative to normal crustal rocks e.g. (Kump and Holland, 1992; Reinhard *et al.*, 2009; Kendall *et al.*, 2011; Scott *et al.*, 2011), providing further evidence for the mobilisation of Fe(II) and the enhanced deposition of Fe in Archean sediments. Therefore, taken together, BIFs and Fe-enriched shales are telling us the same thing about Archean ocean chemistry: marine waters were enriched in dissolved Fe(II). The accumulation of Fe(II) and its mobilisation in Archean seawater makes sense in a low-oxygen atmosphere where the oxidation of sulphide to sulphate is incomplete and there is insufficient oxygen to ventilate the deep ocean.

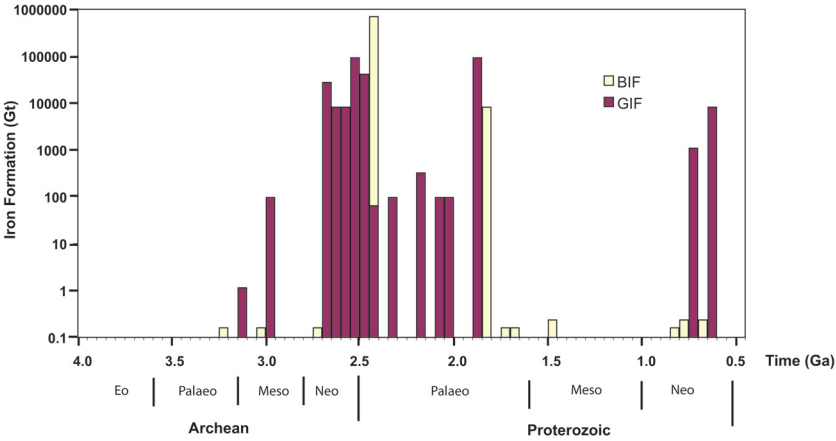

Figure 9.5 Distribution of the volume of banded iron formations (BIF) and granular iron formations (GIF) through time (redrafted from Bekker *et al.*, 2010).

Archean Euxinic Conditions. This brings me to the second aspect of Archean ocean chemistry. In the later parts of the Archean, there IS evidence for periodic marine sulphidic conditions. These insights are mostly provided by Tim Lyons, Ariel Anbar, their colleagues and students. Tim is yet another former Bob Berner student, and a graduate student colleague of mine. Ariel received his PhD at Caltech with the legendary Gerry Wasserburg, and both together and on their own, Tim and Ariel have been powerful forces in unravelling the early history of ocean and atmospheric chemistry. To date, Tim, Ariel and their students have found strong evidence for sulphidic conditions in several instances in the late Archean. We begin with the well-studied 2.5 billion year old Mount McRae Shale from the Hamersley Basin, Western Australia (Reinhard *et al.*, 2009). The McRae

Shale is an organic rich and pyrite-rich shale unit found within a thick sequence of the Hamersley Group that mostly comprises banded iron formation. Geochemical studies have documented a clear euxinic signal within the upper portion of the shale, while the middle and lower portions document ferruginous conditions. This episode of marine euxinia is correlated with other evidence for Earth surface oxygenation (Anbar *et al*., 2007; Garvin *et al*., 2009). This led to the suggestion that a relatively short-lived period of elevated atmospheric oxygen levels enhanced the oxidative weathering of sulphides to sulphate on land, increasing the flux of sulphate to the oceans. This allowed the rates of sulphide production by sulphate reduction to exceed the delivery flux of Fe(II) (with respect to FeS_2) to the water column overlying the deposition of the McRae Shale. It is not known whether euxinia at this time was local or widespread, but ferruginous conditions returned with the deposition of the overlying Brockman Iron Formation.

A second incidence of water column euxinia was found associated with deposition of the 2.66 billion year old Jeerinah Formation of the Hamersley Province, Western Australia (Kendall *et al*., 2011). In this case, the Roy Hill Shale represents a 50 meter thick euxinic interval immediately overlaying the Warrie Member, which is an organic-rich shale/turbidite unit, seemingly deposited under ferruginous water column conditions (Scott *et al*., 2011). With this incidence of euxinia, the authors do not see the same persuasive evidence for Earth surface oxygenation (such as elevated Mo concentrations) as observed for the McRae Shale, and they argue that an elevated volcanic source of sulphur could have provided, at least locally, a sufficient flux of sulphur to overwhelm the Fe(II) supply and allow for euxinic conditions.

The last incidence of marine euxinia was found in 2.46 to 2.59 billion year old shales of the Nauga and Klein Naute Formation from the Campbellrand-Malmani platform in South Africa (Kendall *et al*., 2011). A clear euxinic signal is observed in the Klein Naute Formation, and similar to the somewhat earlier Roy Hill Shale, geochemical data provide no pervasive indication of Earth surface oxygenation. The authors, however, argue for mild surface-water and atmospheric oxygenation from Fe speciation results and geochemical behaviour of Re and Mo, in the underlying Nauga Formation. These signals, at least to my eye, are subtle, but if real, marine surface waters at this time were oxidised enough to inhibit the introduction of either Fe(II) or sulphide from deeper waters. This would, perhaps, not be so surprising in a world with active cyanobacterial oxygen production in the upper photic zone of the ocean.

Interactions Between the Iron, Carbon and Phosphorus Cycles. Harking back to Bob Garrels (Garrels *et al*., 1973), it would seem natural that if ferruginous conditions were a dominant feature of Archean ocean chemistry, that these conditions would influence both the ecology of the ancient oceans and the dynamics of the carbon cycle. By analogy with Lake Matano (see Section 8.4) and the physiology of known Fe-oxidising phototrophs (Hegler *et al*., 2008), one can imagine an active population of anoxygenic phototrophs in the lower reaches of the marine photic zone with a good supply for Fe(II) from below (Kappler *et al*., 2005). Dynamic Fe and carbon cycles such as described in Section 9.3 would have

resulted. Before oxygenic photosynthesis, such an Fe cycle may have dominated the carbon cycle on the Earth. The carbon cycle, however, would have been considerably accelerated after the evolution of cyanobacteria and their ability to use H_2O as an electron donor. With water available, only light and nutrients would limit rates of primary production (Canfield *et al.*, 2006).

One might expect to see such a transition in the geologic record, especially in the dynamics of the carbon cycle. Carbon isotopes have been typically used to gain such insights, with the idea being that biologically produced organic carbon is distinctly fractionated from inorganic carbon during carbon fixation, and the burial of the resulting ^{13}C-depleted carbon in sediments leaves the inorganic carbon remaining in seawater ^{13}C-enriched. The magnitude of this enrichment depends on the fractionation (Δ_{org}) between the organic carbon ($\delta^{13}C_{carb}$) and inorganic carbon ($\delta^{13}C_{inorg}$) and the proportion of the total carbon entering the ocean (C_{in}) leaving as organic carbon (f_{org}). In this simple analysis, the remaining carbon leaves as carbonate rocks (see Bjerrum and Canfield, (2004) for a somewhat more sophisticated analysis). The expectation is that the higher values of f_{org} accompany more active primary production and organic carbon burial. The mass balance equation expressing this relation is given as:

$$f_{org} = \frac{(\partial^{13}C_{carb} - \partial^{13}C_{in})}{\Delta_{org}} \tag{9.2}$$

When we look at the isotope record (Fig. 9.6), no clear signals emerge as to major reorganisations of the carbon cycle during the Archean. The record, or course, is spotty, and neither the organic carbon nor its isotopic composition are very well preserved (Des Marais, 2001). But still, no major jumps are observed in f_{org}, especially positive ones. Thus, there is no indication of a shift from a world dominated by Fe cycling, where we can estimate that f_{org} would be less than 10% of today's value of 0.2, to a world where oxygenic photosynthesis was the main driver of the carbon cycle, providing f_{org} values in the range of 0.15 to 0.3 as we observe after the GOE (Des Marais, 2001) (see Section 9.2). Indeed, the f_{org} values through the Archean are similar to those through much of the Proterozoic where we know oxygenic photosynthesis was well established. This point was first recognised by Manfred Schidlowski (Schidlowski *et al.*, 1979).

The isotope record, therefore, does not give a clear signal of life before oxygen, but that does not mean that Fe cycling was unimportant. In chemically stratified sulphidic basins today, anoxygenic photosynthesis can contribute up to 80% of the total carbon fixation in the system, even though oxygenic photosynthesis is the ultimate source of energy (Canfield *et al.*, 2005). We showed in our textbook "Aquatic Geomicrobiology" (Canfield *et al.*, 2005) that the importance of anoxygenic photosynthesis in stratified systems depends on the efficiency with which organic carbon is exported from the surface layer into the anoxic water and the efficiency with which the redox active species (S or Fe) are recycled to their reduced form below the photic zone (Canfield *et al.*, 2005). These details are perhaps beyond the present discussion, but they make the point that an active Archean Fe cycle is not incompatible with the presence of oxygenic photosynthesis.

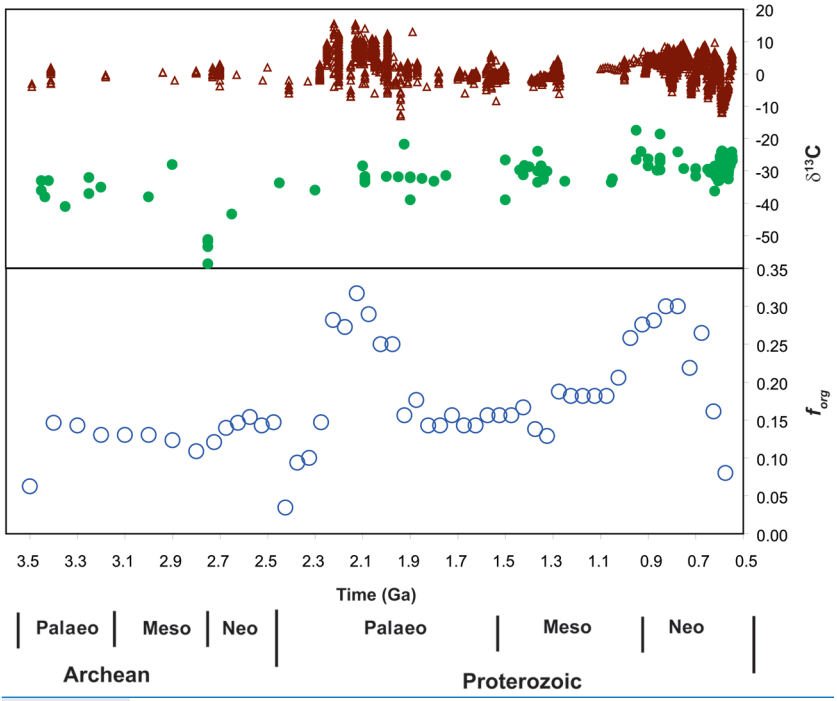

Figure 9.6 Isotopic composition of inorganic carbon and organic carbon over time. In the upper panel, closed triangles represent the isotopic composition of inorganic carbon, whereas the closed circles represent the isotopic composition of organic carbon. Data taken from compilation in Canfield (2012). With additional data from Des Marais (2001). Note that only well-preserved organic carbon is represented (see Des Marais, 2001).

Even though Archean values of f_{org} are higher than we would expect for "life before oxygen", they are still low compared to the Phanerozoic range of 0.2 to 0.3 (Hayes *et al.*, 1999). My colleague Christian Bjerrum and I worried greatly about this, and, as explored in Section 8.3, we concluded that perhaps the Fe cycle may have acted to regulate the concentration of phosphorus to lower values than we have at present. We used the affinity of phosphate for modern hydrothermal Fe(oxyhydr)oxide particles, combined with the P content of BIFs, to estimate that during times of BIF formation, phosphate levels may have been only 7 to 25% of modern values. In our view, this would help explain the low f_{org} values, and maybe also why oxygen was not abundant and available in the Archean atmosphere. The link to oxygen availability comes because the burial of organic matter is the ultimate source of oxygen into the atmosphere (Berner, 2004; Garrels and Perry, 1974). In any event, we were unaware at the time that silica could severely influence the extent of phosphate absorption onto Fe(oxyhydr)oxides (Konhauser *et al.*, 2007), and since silica levels were likely much higher in the Archean, our

concentration estimates, ultimately, may be too low. As pointed out in Section 8.3 though, the Fe cycle may have regulated Si concentration to values lower than expected for saturation with solid Si dioxide phases, so it will be exciting to see how this story develops.

Final Thoughts. The Archean ocean was mostly dominated by Fe(II)-rich conditions leading to the deposition of BIFs and Fe-enriched shales. While water-column Fe-cycling may have been quite important, there is no present indication for the operation of an Archean "Fe World" where anoxygenic phototrophic Fe oxidation dominated primary production. In the late Archean, euxinic conditions also occurred, sometimes in association with elevated atmospheric oxygen levels which enhanced pyrite weathering on land and the sulphate flux to the oceans. During other times, euxinia may have developed from enhanced local sources of volcanogenic sulphur. On balance, though, ferruginous conditions seem to dominate. As far as we know now, thick stratigraphic intervals of BIFs and Fe-rich (relatively sulphide poor) shales have far more extensive stratigraphic representation than shales displaying euxinic conditions, which so far occupy only about 100 meters of known stratigraphic section.

9.5 Birth of An Idea

In the summer of 1986, I attended, together with Rob, my first Gordon Conference in Chemical Oceanography. This was organised by Bob Berner. I came with great excitement bearing a poster outlining some of my first thoughts on the reactivity of Fe phases towards sulphide. I don't recall my poster gathering much attention, but I do remember meeting many of my scientific heroes, and in particular, I remember a talk by Jorge Sarmiento. Jorge was challenged by Bob to come up with a model explaining the main features of the oxygen distribution of the oceans, and this he did with great originality. He started with a simple two-box model and showed that if all the deep water phosphorus was used in primary production, which we imagine to be the case in most regions of the oceans, then the deep ocean would become completely anoxic. This, of course, was completely at odds with the observations. So what was wrong here?

Jorge went on to explain that not all the P at high latitudes in the oceans is used. Since this water was down-welled, forming the deep water masses of the oceans, some so-called "preformed" phosphorus was just cycled around and did not really support primary production. The idea of preformed nutrients goes back to Alfred Redfield (Redfield *et al.*, 1963), but apparently nobody thought before to construct a whole ocean model of oxygen control utilising this concept. Therefore, Jorge introduced a third box in his model including the high latitude box supplying the preformed nutrients to the deep ocean. With this box in place, the simple 3 box model could be used to explain the average intensity of oxygen draw down in the deep ocean, and to explore the processes controlling it (Sarmiento *et al.*, 1988).

By this time, I was becoming interested in the evolution of Earth surface chemistry through time and especially the history of atmospheric oxygen. This was not an official research topic of mine, but I used all of my graduate school course term papers to educate myself on various aspects of the subject. After hearing Jorge, it occurred to me that atmospheric oxygen levels of about half of today's or lower should drive major anoxia in the deep ocean. This is seen in Figure 9.7, where Jorge's model is used to generate predictions on deep water oxygen concentrations with different assumptions about atmospheric oxygen levels and marine phosphorus concentrations (that is, deep water values minus the "preformed" value). If you follow this diagram, an initial high-latitude oxygen concentration of about 150 μM will become fully depleted (giving a deep water concentration of 0 μM) when the present concentration of available phosphorus (P_D-P_H) is reached. Therefore, other factors being equal, reducing atmospheric oxygen to 40 to 50% of today's level would be sufficient to encourage wide-scale ocean anoxia. Deep ocean anoxia after the "GOE" (the GOE was recognised well before it was eloquently defined by rare sulphur isotopes; Cloud, 1972; Holland, 1984a; Holland, 1984b) did not fit with the contemporary thinking on the evolution of marine chemistry (Holland, 1984a), where the ocean deeps were believed to have become well oxygenated after the GOE. One of the drivers of this reasoning was the substantial loss of BIFs from the geologic record in approximate association with the GOE (more on this below).

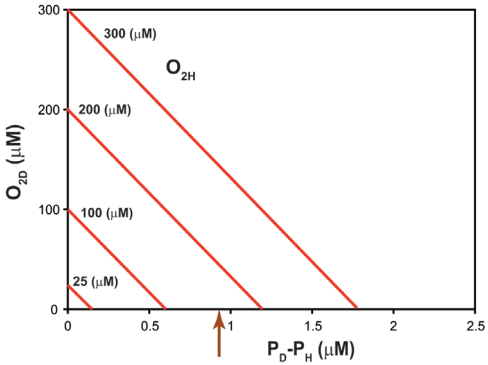

Figure 9.7 Relationship between bottom-water oxygen concentrations (O_{2D}) and available deep water phosphorus concentration (P_D-P_H) as a function of different oxygen concentrations down-welled from high-latitude surface water (O_{2H}). The available deep water phosphorus concentration represents the difference between the actual concentration measured in deep water (P_D) and the concentration of "preformed" phosphorus down-welled from high latitudes (P_H). The arrow represents today's value (redrawn from Canfield, 1998).

The next step came during my time at the Max Planck for Marine Microbiology in Bremen in 1994-1996. Here, I was interested in many things including new studies on the processes controlling S isotope fractionation in nature (Canfield and Thamdrup, 1994; Habicht and Canfield, 1996; Habicht *et al.*, 1998) and further studies on the importance of different electron acceptors in carbon mineralisation. In my spare time, though, I was scouring the literature and compiling a record of sulphur isotope compositions through time, as a compliment to our new work on fractionation systematics. Andreas Teske, a bright young

graduate student of Bo Barker Jørgensen, caught wind of what I was doing, and revealed that he, in his spare time, was constructing molecular clocks with the aim of timing the emergence of various sulphur metabolisms. With Andreas as a new partner, I redoubled my efforts to make an exhaustive compilation of sulphur isotope trends. Our combined efforts resulted in a paper (Canfield and Teske, 1996) of which I will say little of here, but one conclusion was that oxygen levels appeared to rise in the Neoproterozoic to values exceeding, apparently for the first time, about 10% of PAL. This conclusion seemed to confirm earlier suspicions that there was a late Precambrian increase in atmospheric oxygen levels (Berkner and Marshall, 1965; Knoll, 1992). The compilation also revealed clear patterns in sulphur isotope behaviour, one of which was a large jump in fractionations at around 2.3 billion years ago, remarkably close to the GOE (Fig. 9.8). This was also previously recognised by Eion Cameron (Cameron, 1982).

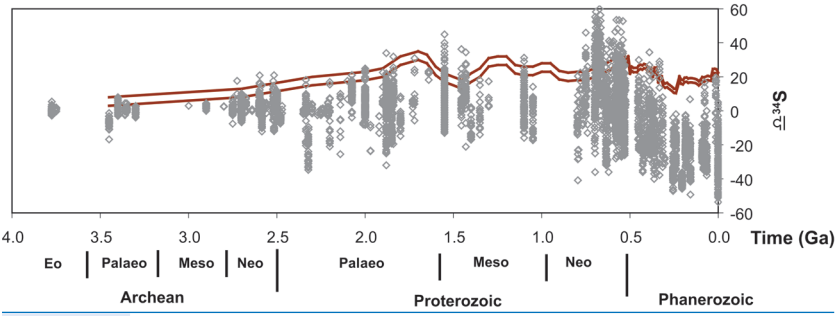

Figure 9.8 Isotopic composition, $\delta^{34}S$, of sulphur through time. Sulphides given as data in symbols, while sulphate values are represented by the parallel red lines (data from Canfield and Farquhar, 2009).

Now the pieces were ready to complete the puzzle. The pieces included:

(a) an increase in sulphate concentration in apparent association with the GOE, implying enhanced oxidative weathering of sulphides on land and an enhanced source of sulphate to the oceans,

(b) an indication that after the GOE oxygen did not rise to modern levels, and was perhaps as low as 10% of PAL or less,

(c) if oxygen levels were lower than about 50% PAL, then Jorge Sarmiento's model suggested substantial deep water anoxia and finally,

(d) the disappearance of BIFs is roughly timed with the GOE and an increase in the sulphate concentrations of the oceans.

The logical conclusion was that the increase in sulphate availability as a result of the GOE stimulated rates of sulphate reduction to the point where sulphide production exceeded the delivery of Fe(II) to the deep anoxic ocean, causing a

transition from ferruginous to sulphidic marine conditions (see Section 9.2). This seemed to make sense and was consistent with available constraints, but there was hardly a stitch of direct evidence to back it up.

At about the same time I came to this conclusion, I moved from the Max Planck to my current residence at the University of Southern Denmark in Odense. While in the process of building a new lab, I had some slow time and thought I would try and write this idea down and to pitch it to *Nature* magazine. The paper went through a whole year of 3 drawn-out rounds of review. In particular, one reviewer was completely unconvinced, and met every new round of responses with a fresh round of objections. At loggerheads, I asked for a tie-breaker review and this was positive, so the paper went through (Canfield, 1998). It landed with a relative thud, being cited only a few times in its first couple of years. It did have one fan though. Andy Knoll from Harvard University seemed to like the idea, and he felt that it could explain some aspects of biological evolution. He subsequently called this Proterozoic period of sulphidic conditions the "Canfield Ocean" (Fig. 9.9). For better or worse, the name has stuck. As we shall see below, subsequent work has begun to redefine the nature and evolution of Proterozoic ocean chemistry and what the "Canfield Ocean" really looked like.

Figure 9.9 What do you have in the Canfield Ocean?

9.6 The Proterozoic Eon

The Proterozoic Eon encompasses an enormous stretch of Earth history, from the end of the Archean at 2.5 Ga, to the beginning of the Phanerozoic Eon nearly 2 billion years later at 0.542 Ga. It is subdivided into 3 Eras; the Palaeoproterozoic from 2.5 to 1.6 Ga, the Mesoproterozoic from 1.6 to 1.0 Ga, and the Neoproterozoic from 1.0 to 0.542 Ga. Through this incredible Eon, eukaryote evolution ran its major course, beginning, likely, with the expansion of new eukaryotic lineages that first evolved in the Archean (Waldbauer *et al.*, 2009), through the development of multicellularity, to the evolution of animals near the end (Knoll, 2003).

Biologically at least, the beginning and end of the Proterozoic were completely different worlds. Geochemically, the GOE didn't quite usher in the Proterozoic, but at 2.4 to 2.3 billion years ago, it came close. We have already discussed in general terms how the GOE might have influenced the evolution of ocean chemistry and the Fe and S cycles. In the following sections, we will look more closely at the geochemical evidence for the evolution of the Fe cycle through the Proterozoic and its relationship with the evolution of other biogeochemical cycles, particularly oxygen and sulphur.

The GOE. We begin with the obvious question: can we observe any effects of the GOE on ocean chemistry? While the question seems straightforward, the answer, so far, remains somewhat illusive. The GOE occurs, most likely, between the 2nd and 3rd of three recognised glaciation events during the ~2.2. to 2.4 Ga Huronian glacial epoch (Bekker *et al*., 2004). Most studies of the GOE have focused on the MIF sulphur isotope fractionations, in order to constrain its timing, and carbon isotopes, to understand how the GOE may have influenced the carbon cycle (Bekker *et al*., 2004; Bekker and Kaufman, 2007; Guo *et al*., 2009). While some of this work is outside of the present discussion, studies have revealed a marked increase in the isotope fractionation between pyrite and sulphate sulphur immediately following the loss of the sulphur MIF signal (Bekker *et al*., 2004; Cameron, 1982; Guo *et al*., 2009). Therefore, the idea remains intact that the oxygenation following the GOE led to more oxidative weathering of pyrite on land and to an increase in the sulphate concentration of the oceans. Unfortunately, there is very little direct geochemical evidence, such as iron speciation studies, for example, on the extent of marine oxygenation or marine concentrations of Fe(II) and sulphide either immediately before, during, or immediately after the GOE.

One piece of indirect geochemical evidence comes from the temporal distribution of known BIF volume (Fig. 9.5). This shows a marked decrease in BIF abundance just before the GOE, with some sporadic and relatively small BIF occurrences until about 1.9 Ga, where a short-lived, but major, episode of BIF deposition occurs. These patterns are consistent with the broad features of the "Canfield Ocean" model, where increased sulphate availability from the GOE would have increased rates of sulphate reduction, titrating a substantial amount of the available Fe(II) as pyrite. This would have reduced the concentrations of Fe(II) in the deep waters (assuming that they remained anoxic), diminishing, in turn, the prospects for BIF deposition. Sulphidic water-column conditions could have ensued, at least locally, during some times in this time interval. Taken together, reduced Fe(II) availability is indicated, but this scenario lacks direct geochemical observations of water column chemistry, and must therefore be viewed as speculative. Luckily, not all times in the Proterozoic lack detailed and appropriate geochemical observations, so we continue by asking, where is the sulphide?

Where is the Sulphide? Shortly after publication of the "Canfield Ocean" model, Yanan Shen joined our lab as a postdoc, and we, together with Andy Knoll, used the iron speciation protocols described earlier (Section 3.6), to explore the

chemical nature of 1.73 Ga Wollogorang and 1.64 Ga Reward Formations, both from McArthur Basin in Northern Australia. The McArthur Basin represents an ancient intracratonic seaway, with access to the open ocean, but it cannot be considered an open ocean setting. These sediments became our first target as previous studies had speculated that they may have deposited under euxinic conditions (Jackson *et al.*, 1987; Large *et al.*, 1998; Southgate *et al.*, 1997). Our results (Fig. 3.10) clearly showed that both the Wollogorang and Reward Formations deposited in sulphidic waters (Shen *et al.*, 2002). Indeed, the geochemical signals for these sediments proved very similar to those from the modern Black Sea (Shen *et al.*, 2002). After moving to a postdoc position at Harvard with Andy Knoll, Yanan continued to work on the somewhat younger, 1.4 to 1.5 Ga, sediments from the Roper Group, Northern Australia. These sediments were carefully collected with respect to palaeowater depth, and basin location such that inner shelf sediments could be distinguished from distal shelf sediments, and these from basinal sediments. In what one might view as a test of methodology, shallow-water sediments displayed an oxic signal, and only the basinal sediments proved euxinic based on iron speciation (Shen *et al.*, 2003). This euxinic signal, combined with those from the underlying McArthur Basin sediments, demonstrate that euxinic basinal conditions persisted for over 250 million years in this part of the world (Shen *et al.*, 2003). Therefore, extensive periods of mid-Proterozoic sulphidic conditions could be identified, but it is not at all certain that these basins represented open ocean conditions, so the nature of open ocean chemistry remained equivocal.

As an added bonus to this work, and as a small aside, the isotopic compositions of pyrite in McArthur Basin sediments were very close to contemporaneous seawater sulphate, particularly in the lower Reward Formation (Shen *et al.*, 2002), suggesting that sulphate concentrations were significantly reduced from seawater concentrations in the euxinic bottom waters. This does not happen in modern euxinic settings because marine sulphate concentrations are too high. After modelling the likely maximum extent of sulphate drawdown one might expect in a marine basin, we concluded that the maximum marine sulphate concentration at 1.6 Ga was in the range of 0.5 to 2.5 mM, compared to today's value of 28 mM. Soon after making these calculations, I presented this idea at an institute seminar at the department of Earth and Planetary Sciences at Harvard University. After I mentioned the calculation results, the eminent geochemist Dick Holland jumped out of his chair and yelled "Boooo"! Luckily, other work has reached similar conclusions (e.g. Hurtgen *et al.*, 2002; Kah *et al.*, 2004), and the idea that Proterozoic seawater contained low concentrations of sulphate (although generally higher than in the Archean; Canfield and Farquhar, 2009) is now rather well accepted.

A BIF/sulphide Transition. Shortly after finishing the McArthur work, Simon Poulton, a former PhD student with my co-author Rob, joined my lab as a postdoc. We wished to continue with Yanan's work, and our target became the 1.8 to 1.9 Ga sediments from Animikie Basin of Northern Minnesota and Southern Ontario. These sediments contain the last major phase of BIF deposition before the Neoproterozoic some 1 billion years later (and discussed in more detail below)

(Fig. 9.5). This episode of BIF deposition, however, comes nearly 400 million years after the GOE, and its initiation is not well understood. There is some growing evidence that these BIFs may have deposited during a transient return to low oxygen conditions. This evidence comes from the nature of the deposits themselves. For example, the Gunflint BIF is deposited in a shallow water setting (Fralick and Barrett, 1995), and therefore, Fe(II) would have been transported long distances over a broad continental shelf in order to form this BIF. Given the rapid kinetics of inorganic Fe(II) oxidation with oxygen (see Section 8.2), such long-distance transport of Fe(II) could only be accomplished under very low atmospheric oxygen conditions (Canfield, 2005). Other evidence comes from the lack of fractionated Cr isotopes in these BIFs, which indicates a lack of oxidative weathering of Cr on land (Frei *et al*., 2009). We speculate that the oxidative weathering of sulphide on land may have been equally influenced, reducing the flux of sulphate to the oceans, encouraging BIF deposition. While it seems that oxygen may have dipped to very low values during the deposition of these BIFs, there are no reports of MIF sulphur anomalies in the rocks, somewhat at odds with the other evidence for low atmospheric oxygen. This mystery will not be solved here, but it seems reasonable that fluctuations in atmospheric oxygen may have followed the GOE and that these could have influenced the nature of ocean chemistry.

In any event, Simon and I were intrigued by the disappearance of these BIFs and the resulting transition in ocean chemistry. Together with Phil Fralick from Lakehead University, we sampled a beautiful drill core intercepting the Gunflint Fe Formation and its transition into the overlying black shales of the Rove Formation. Fe speciation results revealed a clear transit from banded iron formation, into a transitional zone of likely alternating ferruginous/sulphidic conditions and finally into an euxinic zone (Fig. 9.10) (Poulton *et al*., 2004). To the best of our knowledge, these sediments deposited in a setting open to the global ocean, and therefore, we seemed to have captured a chemical transition as predicted by the original "Canfield Ocean" model.

Mo Isotope Proxy. At about this same time, Ariel Anbar, Tim Lyons and colleagues were developing a different tool for assessing the extent of sulphidic marine conditions. This is based on the geochemical behaviour of Mo and its isotopes. To make a long story short, Mo may be actively removed in sulphidic settings without a significant fractionation, providing free sulphide concentrations are high enough (estimated at about 11μM). In contrast, it is slowly removed in oxygenated environments onto Mn oxides (and probably also Fe(oxyhydr) oxides), but with significant fractionation (Arnold *et al*., 2004; Goldberg *et al*., 2009). Therefore, one can, in principle, access the isotopic composition of ancient seawater Mo from euxinic sediments, and furthermore, the more fractionated this Mo is compared to the river input value, the more important is the oxic removal pathway. Results indicate that through most of the Proterozoic (Fig. 9.11), Mo was considerably less fractionated than today, indicating less oxic and more sulphidic removal for Mo than either today or through most of the Phanerozoic. This would be broadly consistent with the "Canfield Ocean" model. The devil is in the details

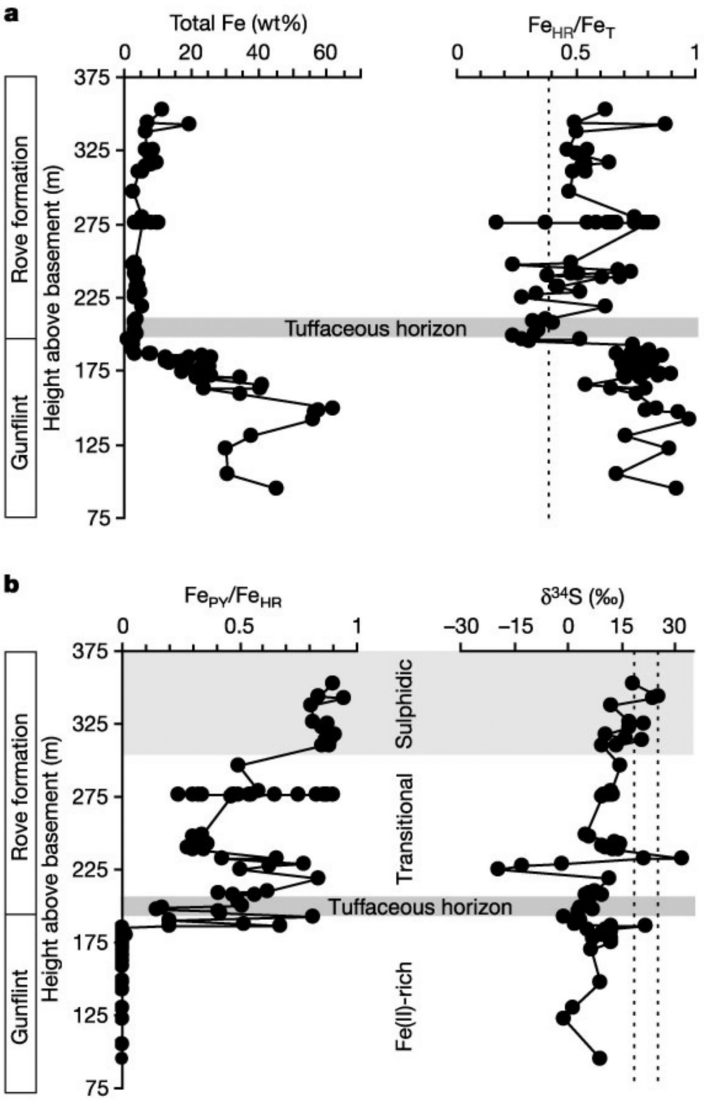

Figure 9.10 Iron speciation results and $\delta^{34}S$ for the Gunflint/Rove transition (from Poulton *et al.*, 2004, with permission from Nature).

though, and my former student and postdoc Tais Dahl has taken to modelling the Mo cycle. His models suggests that while sulphidic removal may have been some 40 to 80 times more important during the Proterozoic than today, sufficient

removal might be accomplished if only some 2 to 4 % of the global seafloor became overlain with sulphidic waters (Dahl *et al.*, 2011). The model is relatively insensitive, however, to what happens in the slowly depositing sediment of the deep ocean and the continental slope (Dahl *et al.*, 2011). In any event, these models are potentially powerful tools in unravelling the nature of ancient ocean chemistry, but they are still in their infancy, and it will be critical to refine them as better constraints and modelling techniques become available.

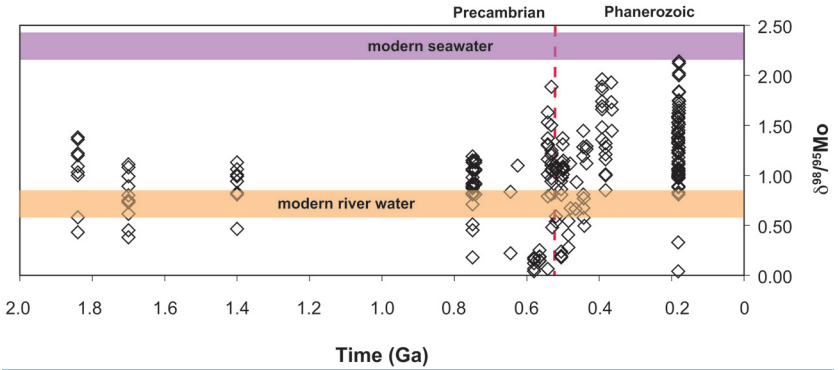

Figure 9.11 The isotopic composition of Mo through time. Data comes mostly from euxinic basin, but not every sample represents euxinic deposition. Maximum values are likely closest to contemporaneous seawater. Redrawn from data in Dahl *et al.* (2010), with additional data from Dahl *et al.* (2011) and Kendall *et al.* (2011).

An Evolving Picture of the "Canfield Ocean". To summarise what we have discussed so far, the original "Canfield Ocean" seems to accurately describe the relationship between the GOE providing an enhanced sulphate flux to the ocean, and a decrease in the importance of BIFs as a removal pathway of Fe. It also seems to have correctly identified extensive anoxic deep ocean waters after the GOE. Furthermore, sulphidic ocean conditions have been found in a variety of middle Proterozoic marine settings, and Mo isotope evidence suggests enhanced removal of Mo by sulphidic pathways in the Proterozoic compared to today. Yet, the Mo isotope evidence does not require globally expansive regions of sulphidic water, and the Fe and S mass balance arguments presented in Section 9.2 suggest that ocean-wide sulphidic conditions may be difficult to maintain given the relative fluxes of highly reactive iron and sulphur to the oceans. Furthermore, Slack *et al.* (2007) identified Fe (oxyhydr)oxide-containing 1.74 Ga deep water marine volcanogenic exhalites, which would be inconsistent with the expectation of sulphidised Fe if the water receiving the exhalites was sulphidic. Clearly, the original "Canfield Ocean" model, while apparently correct in many details, overestimated the extent of sulphidic marine waters after the GOE.

Our own appreciation of a more complex redox structure for the middle Proterozoic ocean has developed from a number of directions. Soon after analysing sediments from the Gunflint/Rove transition, we realised that enough

additional core material was available to explore the nature of ocean chemistry in the Animikie Basin over 100's of kilometres extending from the shallow continental shelf into deep waters. This study was possible because of Simon Poulton's tenacity and patience and because of the excellent sedimentological context painstakingly assembled by Phil Fralick over the years. In all, the study took 4 years to assemble, but the result was a remarkable insight into the structure of water-column chemistry (Poulton *et al.*, 2010). After the cessation of BIF deposition, sulphidic conditions developed over the shelf, as we had previously identified, and they extended out some 100 km from the palaeoshoreline. Further out in deeper water, though, ferruginous conditions developed (Fig. 9.12). We did not, however, observe the deposition of BIFs, and except for some minor occurrences (Bekker *et al.*, 2010; Wilson *et al.*, 2010), BIFs are absent from the geologic record for the next billion years, as mentioned above. Therefore, while ferruginous conditions are observed in deep marine waters, the Fe(II) concentrations appear to be insufficiently high to promote BIF deposition. It is possible, and indeed probable, that expanded sulphidic conditions represented a strong sink for highly reactive iron, reducing the concentrations of Fe(II) in marine waters, but not enough to remove the Fe(II) completely. Therefore, we speculate that these middle Proterozoic ferruginous waters contained much less Fe(II) than the Archean counterparts.

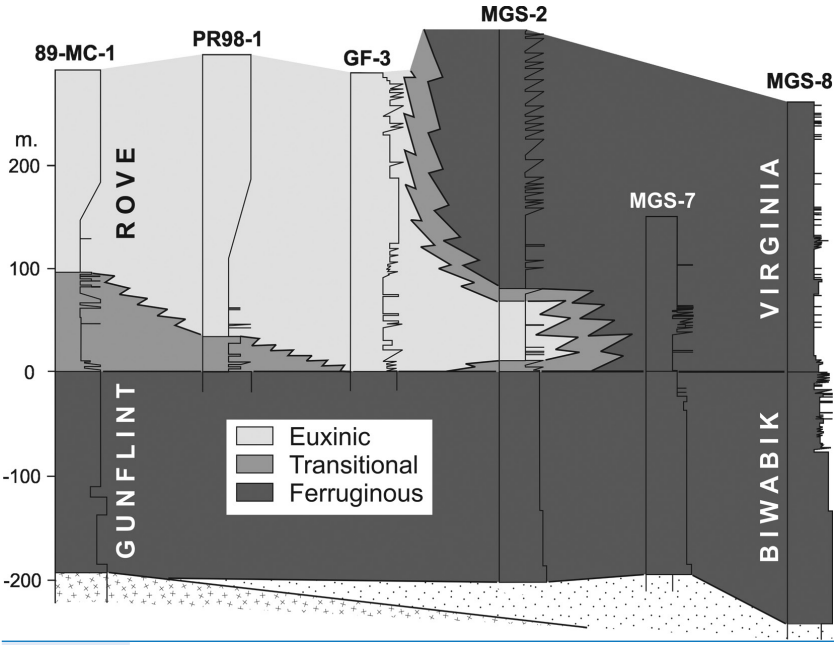

Figure 9.12 Distribution of ferruginous and euxinic conditions through the Animikie Basin (from Poulton *et al.*, 2010, with permission from Nature Geoscience).

Overall, Simon's work points to a more nuanced picture of the "Canfield Ocean" (Poulton *et al.*, 2010). Sulphidic conditions were concentrated near shore (but probably not everywhere near shore), where an increased organic carbon flux drove sulphide production by sulphate reduction to exceed the delivery flux of highly reactive iron from settling particles and from the mixing and upwelling of Fe(II) from the deep ocean. Further offshore, as the organic carbon flux waned, the intensity of sulphate reduction decreased allowing Fe(II) to persist. This would be more consistent with the Mo isotope evidence and other evidence, as described above, for the nature of ocean chemistry. This evolving picture of Proterozoic ocean chemistry has recently been presented by Simon and myself (Poulton and Canfield, 2011) (Fig. 9.13), and is supported by very recent work from Tim Lyon's group identifying several other instances of ferruginous conditions during the middle Proterozoic (Planavsky *et al.*, 2011).

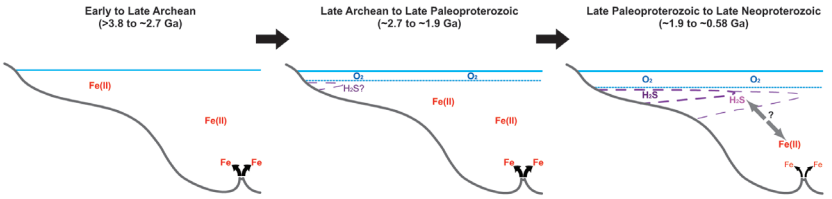

Figure 9.13 Model of the distributions of ferruginous and euxinic conditions through the Precambrian (from Poulton and Canfield, 2011, with permission from Elements).

Bottom Water Oxygen? It is possible that the ocean had even more structure than indicated in Figure 9.13. Dick Holland has highlighted the potential consequences of a prokaryote-dominated world on the marine carbon cycle (Holland, 2006). Small prokaryote cells should settle more slowly than the much larger eukaryotic algae (even enhanced with carbonate and silicate hard parts in some cases). Because of this, in the prokaryote-dominated middle Proterozoic, we would expect cells from the upper water column to have decomposed preferentially higher up in the water column than today. Therefore, less organic carbon would sink deeply, providing less of an oxygen sink to deeper water. We have started modelling this in 1-D ocean models (not yet published), and, with slower sinking organic matter, oxygen could persist in the deep ocean even with 10% PAL, consistent with Holland's predictions. This part of the deep ocean would be something like an oxygenated biological desert, with little metabolisable organic matter.

The Neoproterozoic Era. So much can be said about the Neoproterozoic, its episodes of massive glaciation, its large carbon isotope fluctuations and its history of biological evolution. I will not, unfortunately, cover these themes here, except as they may pertain to the evolution of marine Fe chemistry, which is a truly rich story in itself. Indeed, our emerging appreciation for the nature of Neoproterozoic chemistry has very much informed our understanding of middle Proterozoic ocean chemistry as outlined above.

The story begins with the original "Canfield Ocean" model, which posited that sulphidic ocean water conditions gave way to oxygenated conditions sometime in the late Neoproterozoic. At the time the "Canfield Ocean" model was originally presented, there was absolutely no information by which to test this hypothesis. While the middle Proterozoic was an initial priority, I was also deeply interested in the Neoproterozoic, and in 2004, I jumped at the invitation by Gerry Ross of the Geologic Survey of Canada (at the time) to join them on a trip to Castle Creek, British Columbia to explore Neoproterozoic rocks of the Windermere Supergroup. The rocks at Castle Creek are post Marinoan glaciation (younger than 630 Ma) and represent an exposed delta of low metamorphic grade conveniently flipped on their side. The section exposes rocks deposited in environments ranging from the deep basin well onto the face of the delta proper. These rocks also appeared to have deposited on a passive margin with open access to the ocean. Perfect! The strategy was simple; collect rocks every 10 meters starting at the lowest possible exposure in the section, representing the deepest depositional environment, and walk up section, and up the face of the delta, for as far as snow, ice and topography allowed. In this way we covered nearly two kilometres of vertical section.

In the field, the rocks did not appear sulphide rich, and rather, if anything was obvious, it was distinctly iron banded, particularly higher up in the section. Fe speciation results confirmed this and revealed what appeared to be oxic conditions in the Kaza Formation, representing the deep basin, giving way to ferruginous conditions in shallower water on the delta proper (Fig. 9.14). All of this was surprising. We seemed to have an early indication of deep water oxygenation (although the exact dating is poor) as well as the apparent development of a ferruginous oxygen-minimum zone (OMZ) off the delta front. I still struggle with this later observation as it is very different to the nitrate-rich OMZs we find today in the global ocean (Cline and Richards, 1972; Codispoti, 1983). Indeed, as explored in Section 8.6, it is well known that microorganisms actively react Fe(II) with nitrate (and nitrite), and therefore, Fe(II) and nitrate simply do not coexist. Therefore, the presence of an Fe(II)-rich OMZ requires an extreme paucity of nitrate in the water column. This idea requires much further development.

The results from Castle Creek (Canfield *et al*., 2008) suggested that Neoproterozoic ocean chemistry was very different from what might have been expected, and to get the story right, Simon Poulton and I began a massive campaign[3] to collect and analyse all of the Neoproterozoic shales we could identify. In the end, it took us almost 3 years to analyse over 700 samples from 34 geologic formations. The results, however, were pretty clear, and are summarised in Figure 9.15 (Canfield *et al*., 2008). The Neoproterozoic was dominated by deep water ferruginous conditions. Sulphidic conditions were sporadic, and/or rare during this Era.

3. With thanks to many good colleagues for supplying samples and lending support including, especially, Andy Knoll, Guy Narbonne and Harold Strauss.

We identified deep water oxygenation just after the Gaskiers Glaciation at 580 Ma (Canfield *et al.*, 2007), although we may have also seen an earlier incidence depending on the age of the Castle Creek deposits.

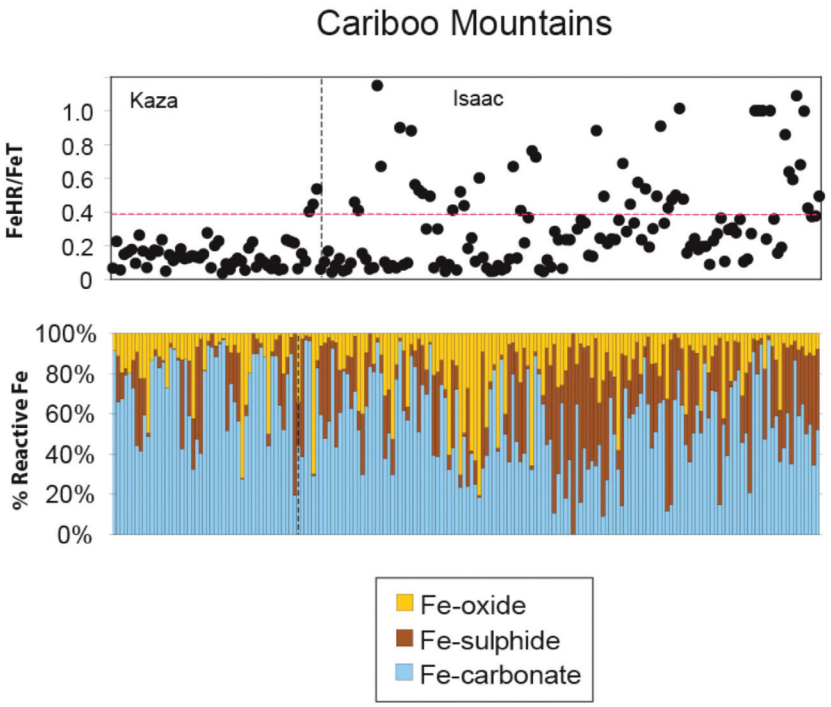

Figure 9.14 Iron speciation results from the Neoproterozoic Cariboo Creek section of the Windermere Supergroup. The FeHR/FeT results indicate anoxic conditions in the Isaac Formation, and the distribution of highly reactive Fe suggests that the anoxic waters were ferruginous (data from Canfield *et al.*, 2008).

Many others have subsequently contributed to this story. Yanan Shen reported a similarly timed transition to oxic conditions for sediments from Northwestern Canada (Shen *et al.*, 2008), and Tim Lyons and his group identified intermittent sulphidic conditions in outer-shelf sediments from the Yangtze platform, with persistently ferruginous conditions in deeper waters (Li *et al.*, 2010). They furthermore argued for a persistent "wedge" of sulphidic waters off the Yangtze Platform shelf, extending in time from the Marinoan glaciation until the end of the Neoproterozoic, but cycling in and out of view at their sampling location they sampled due to fluctuating sea level (Li *et al.*, 2010). A somewhat similar picture has also emerged from further detailed study of the 0.8 Ga Chuar Group from the Grand Canyon Area, USA. Our initial exploration of these sediments revealed a

strongly euxinic horizon in the Walcott member, but we did not explore deep in the section. Dave Johnston from Harvard, however, did look further down section and found a strong indication of persistent ferruginous conditions, suggesting that the euxinic conditions we first observed were a transient phenomenon (Johnston *et al.*, 2010).

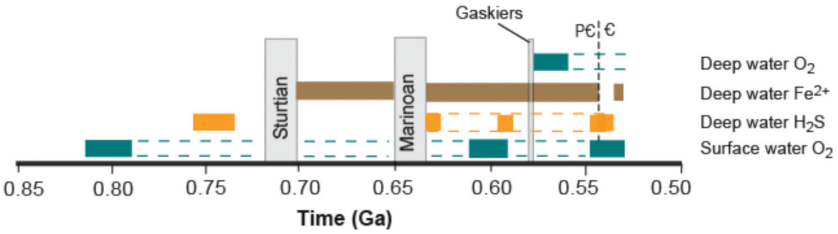

Figure 9.15 Cartoon depicting water chemistry through the Neoproterozoic (modified from Canfield *et al.*, 2008 with additional insights from Li *et al.*, 2010).

Overall, ferruginous deep water conditions seem to dominate the Neoproterozoic. These conditions are a persistent expression of the type of water chemistry indicated by the occasional deposition of Neoproterozoic BIFs (Fig. 9.5). Neoproterozoic BIFs are found in association with glacial deposits and are believed to have precipitated from Fe(II) accumulated in the deep ocean over long periods during extensive ice cover (Hoffman *et al.*, 1998; Kirschvink, 1992), when sub-glacial Fe sources would have been important (Section 6.3) as well as sources from hydrothermal input. Clearly, ferruginous conditions were more widespread than the episodes of BIF deposition would suggest, but outside of these specific time windows of BIF deposition, concentrations of Fe(II) were likely much lower than the concentrations accumulated during Neoproterozoic glaciation.

How do the Middle Proterozoic and Neoproterozoic Compare? The question becomes, are these persistent Neoproterozoic ferruginous conditions similar to or different from those in the middle Proterozoic? Also, was there a greater (or lesser) expression of sulphidic conditions during the middle Proterozoic than the Neoproterozoic? Our picture of Proterozoic ocean chemistry is evolving rapidly, but there is still too little information, particularly through the middle Proterozoic, to answer these questions precisely. An impression based on the available Fe speciation results might indicate that sulphidic conditions were more common in the middle Proterozoic, at least before about 1.3 Ga, than we find in the Neoproterozoic. This is because we can indentify long-term euxinia in both the Animikie Basin and the MacArthur Basin, representing the time window from about 1.84 Ga to 1.36 Ga. In contrast, in the Neoproterozoic, which is much more heavily sampled, anything approaching long-term euxinia is only found on the Yangtze Platform in the time window from 0.635 to 0.542 Ga. But even here, direct evidence only demonstrates periodic euxinia. This view, of course, could easily change with more detailed sampling and new geochemical insights.

One potential insight could come from Mo isotopes (Fig. 9.12). The data is very spotty, but there is really very little difference in the isotopic composition of Mo from about 1.84 Ga until just before the Cambrian-Precambrian boundary. Many factors can influence the isotopic composition of Mo (Dahl *et al.*, 2011; Kendall *et al.*, 2011), but taken at face value, this record might suggest that the average extent of euxinic conditions has changed little from when the last middle Proterozoic BIFs deposited about 1.85 billion years ago and for the next 1.3 billion years.

We can speculate further, but it is probably most constructive to leave with two potential working hypotheses:

(a) Broadly speaking, the relative intensities of ferruginous and euxinic conditions has remained similar from the middle Proterozoic and through the Neoproterozoic, and

(b) ferruginous conditions became more extensive in the Neoproterozoic compared to the middle Proterozoic.

The first may be viewed as the null hypothesis and later requires either an increased flux of highly reactive Fe into the oceans during the Neoproterozoic, or a reduced flux of sulphur (Canfield *et al.*, 2008). In an earlier contribution, I suggested that the subduction of pyrite generated in a sulphidic middle Proterozoic ocean could have reduced the surface inventory of sulphur, ultimately reducing the flux of sulphate to the oceans (Canfield, 2004; Canfield *et al.*, 2008). Following this model, a more ferruginous Neoproterozoic ocean would be the natural consequence of more sulphidic middle Proterozoic conditions. This is an attractive view, but requires the substantial subduction of pyrite during the middle Proterozoic. In our emerging view of middle Proterozoic ocean chemistry, it is not certain that pyrite formation occurred in sediments susceptible to subduction, so this model requires further evaluation.

Dave Johnston has offered an alternative explanation. In his view, the answer lies in the relative fluxes of Fe (oxyhydr)oxides and metabolisable carbon into the anoxic basin (Johnston *et al.*, 2010). If the carbon flux is insufficient to drive the complete reduction of the Fe(oxyhydr)oxides, then, following the natural progression of electron acceptor use in carbon mineralisation (Froelich *et al.*, 1979), the system will not proceed to sulphate reduction, and Fe reduction and ferruginous conditions should dominate. This hypothesis is, therefore, predominantly a thermodynamic one, but based on the relative fluxes of metabolisable organic carbon and Fe(oxyhydr)oxides into the deep ocean. In coastal marine sediments (shelf and slope), however, over which euxinic conditions have been observed to develop, the flux of metabolisable organic carbon is almost always well in excess of the Fe(oxyhydr)oxide flux (Fig. 3.4). This data has not been compiled for water column fluxes, but in a given environment, the flux of metabolisable carbon through the water column will be higher than the flux to the sediment, so the problem gets worse. Indeed, because of this, ferruginous conditions are rare in the modern world of high marine sulphate levels as explored in Section 9.2.

Note that Dave's hypothesis, as least as I understand it, is different from what Simon, Phil and I proposed as an explanation for the controls on the distribution of ferruginous vs. sulphidic conditions (Poulton *et al.*, 2009). We argued, as did Dave, that the organic carbon flux may be decisive in driving an anoxic water column to sulphidic conditions. However, as supported by recent observations in Lake Matano (Crowe *et al.*, 2008; Fig. 8.4), in our model, sulphate reduction will occur under ferruginous conditions as long as it can be sustained. The critical point, then, is whether sulphate reduction rates (controlled by both organic carbon flux and sulphate availability) can out-titrate the Fe delivered to the water-column region of interest. In our view, Fe can be delivered from a combination of sources including adjacent ferruginous areas of the water column or from depositing Fe (oxyhydr)oxides (see Section 4; Fig. 9.13). Our argument, therefore, is based on the balance of sulphide and iron fluxes. It is not based on thermodynamic arguments, which, to fuel prolonged periods of ferruginous conditions, would require, as I understand it anyway, unrealistically low export fluxes of metabolisable organic carbon to the ocean depths, at least as a general condition. What Dave suggests, however, could apply in some situations of low metabolisable organic carbon flux. Furthermore, perhaps I have misunderstood something in Dave's arguments, and our two models may be closer than I appreciate.

9.7 The Phanerozoic Eon

The Phanerozoic is the final Eon in Earth history, extending from the end of the Neoproterozoic Era at 0.542 Ga, until now. It is divided into 3 Eras whose boundaries are palaeontologically defined and can alter in age with advances in dating and stratigraphic resolution. The Eras include the Palaeozoic (542 Ma to 251 Ma), the Mesozoic (251 Ma to 66.5 Ma) and the Cenozoic (66.5 Ma until present). The Phanerozoic is, of course, the age of animals and plants, and during this time, the Earth gained the character we are familiar with today. Whereas various geochemical lines of evidence, discussed above, suggest a late Neoproterozoic rise in atmospheric oxygen concentrations, these levels did not likely reach modern values. Indeed, the Phanerozoic may have begun with oxygen in the range of only 20% of so of PAL. Lower-than-today early Phanerozoic atmospheric oxygen concentrations are consistent with some (Bergman *et al.*, 2004), but not all (Berner, 2006; Berner and Canfield, 1989) biogeochemical carbon models. Lower early Phanerozoic oxygen levels, however, would also be consistent with Mo isotope evidence (Fig. 9.12), which suggests more removal of Mo into anoxic settings compared to today (Dahl *et al.*, 2010). Both models and Mo isotopes therefore support a middle Proterozoic rise in oxygen levels in the middle Palaeozoic, to values approaching those of today (Bergman *et al.*, 2004; Berner, 2006; Dahl *et al.*, 2010).

Early Views on Phanerozoic Ocean Redox Structure. Our understanding of the history of Phanerozoic redox chemistry has evolved considerably over the last 30 years or so. In a classic early consideration of the subject, William

Berry and Pat Wilde (Berry and Wilde, 1978) analysed the time distribution of black shales, and concluded that anoxic ocean conditions were widespread during the early Palaeozoic, yielding to a greater oxygenation of the deep ocean in the later Paleozoic. This view is quite similar to that revealed recently from the molybdenum isotope record, as explained above. Berry and Wilde did not discuss the chemical nature of the anoxic waters, and it seems that they had something like a modern oxygen-minimum zone in mind. In one of the most elegant geochemical papers of which I am aware, Bob Berner and Rob Raiswell (Berner and Raiswell, 1983) explored with models, and by analogy with modern environments, the Phanerozoic history of the carbon and sulphur cycles. They forwarded many novel ideas in this paper, but of relevance here, they concluded that, in particular, euxinic conditions were widespread in the early Palaeozoic, diminishing in intensity in the Devonian. Sound familiar? Indeed, this work prompted Rob to develop tools, including the use of C/S ratios and DOP (see Sections 3.4 and 3.5) to specifically explore the redox nature of ancient seawater, where many specific instances of Palaeozoic euxinia were revealed (Raiswell and Al-Biatty, 1989; Raiswell and Berner, 1985; Raiswell *et al*., 1988; Raiswell *et al*., 2001). These ranked among the very first applications of palaeo-redox indicators to the geologic record.

Further Thoughts on Phanerozoic Redox History. Recent work by Tim Lyons and his group has reinforced earlier discussions of early Palaeozoic euxinia by identifying widespread sulphidic conditions in association with the Cambrian SPICE (Steptoean Positive Carbon Isotope Excursion) anomaly (Gill *et al*., 2011). Paul Wignall has also highlighted a view linking the end-Permian mass extinction to the mixing of sulphidic ocean deep water into shallow depths, poisoning animal communities in the sea and on the land (Wignall and Twitchett, 1996). Others have described a period of "superanoxia" starting in the end Permian and continuing into the early Triassic, where in deep sea sections from Southwest Japan and British Columbia, red clays and cherts give way to black shales (Isozaki, 1997). Lee Kump of Penn State has taken this idea further and has modelled the circumstances under which sulphide could have been released from the oceans to the atmosphere (Kump *et al*., 2005).

Euxinic intervals are also well-known and well-studied in the Cretaceous where black shales were deposited in a series of so-called ocean anoxic events (OAEs) (Jenkyns, 1980, 2010). Black shale deposition is mainly known from the proto-north and proto-south Atlantic, where, especially in the proto-north Atlantic, circulation may have been quite restricted. These intervals of black shale deposition have long been linked to euxinic conditions, and this is supported by the presence of biomarkers for sulphide-utilising anoxygenic phototrophic bacteria in black shale intervals (Damste and Koster, 1998; Kuypers *et al*., 2002) together with enrichments in redox sensitive trace metals, including Mo (Kuypers *et al*., 2004).

Fe speciation protocols have recently been applied by Simon Poulton and his group to further explore the nature of bottom water chemistry during the 85 Ma Coniacian-Santonian Ocean Anoxic Event (OAE 3) (März *et al*., 2008) in the Demerara rise of the semi-restricted proto-North Atlantic. The Fe speciation data are a bit noisy, but when combined with the distribution of other elements, in particular P, V and Cd, the picture emerges of euxinic conditions alternating with non-sulphidic, possibly ferruginous conditions. While the sulphidic conditions dominate, the return to ferruginous conditions reflect periodically limited sulphide production in the water column. This could have resulted from periodic draw-down in sulphate concentrations due to, perhaps, changes in basin restriction, or to changes in the depth of the chemocline in the basin (März *et al*. 2008).

The expanded application of Fe speciation protocols have revealed further instances of Phanerozoic ferruginous conditions. In particular, we uncovered evidence for ferruginous waters in the earliest Cambrian of the Yangtze Platform (Fig. 9.15) (Canfield *et al*., 2008). So clearly, some ferruginous water column conditions also accompanied the early age of animals in the Phanerozoic. In other work, my PhD student Emma Hammarlund found an interval of ferruginous conditions associated with the deposition of the 505 Ma Wheeler shale (Fig. 9.16) (Hammarlund, 2007), a site of soft-bodied fossil preservation contemporaneous with the famous Burgess Shale. Therefore, ferruginous conditions may have been more widely distributed in the Phanerozoic than we realise. As the Fe speciation techniques commonly used in Precambrian rocks are further applied to Phanerozoic sections we will better understand the balance between euxinic and ferruginous conditions through the Phanerozoic.

Why so Much Sulphide? Still, the available evidence suggests that when anoxic, Phanerozoic waters tended towards euxinic conditions. This is in stark contrast to the preceding Neoproterozoic, where ferruginous conditions seem to have dominated. Why should this be so? We have some difficult explaining to do.

I will not pretend to solve this problem here, but I will offer some suggestions. Going back to the basics: ferruginous conditions dominate when the flux of highly reactive iron exceeds the delivery flux of sulphide (through sulphate reduction) in the 1 to 2 proportion needed to make pyrite (Fig. 9.3). In the Neoproterozoic, ferruginous conditions dominated because sulphate reduction occurred in an environment where the sulphide produced was overwhelmed by the highly reactive iron flux. As described in Section 9.2, this preferentially occurs in areas of high sedimentation on the continental shelf receiving a high flux of highly reactive iron. In contrast, in the deep sea, the ratio between the potential supply of sulphate to drive sulphate reduction and highly reactive Fe delivery is more evenly balanced and can easily tip in favour of euxinic conditions if the waters go anoxic (Table 9.1). Logically then, one could conclude that in the Neoproterozoic, sulphate reduction tended to occur in ocean areas with an excess of highly reactive Fe, whereas the opposite was true in the Phanerozoic. I can think of several reasons why this could be true.

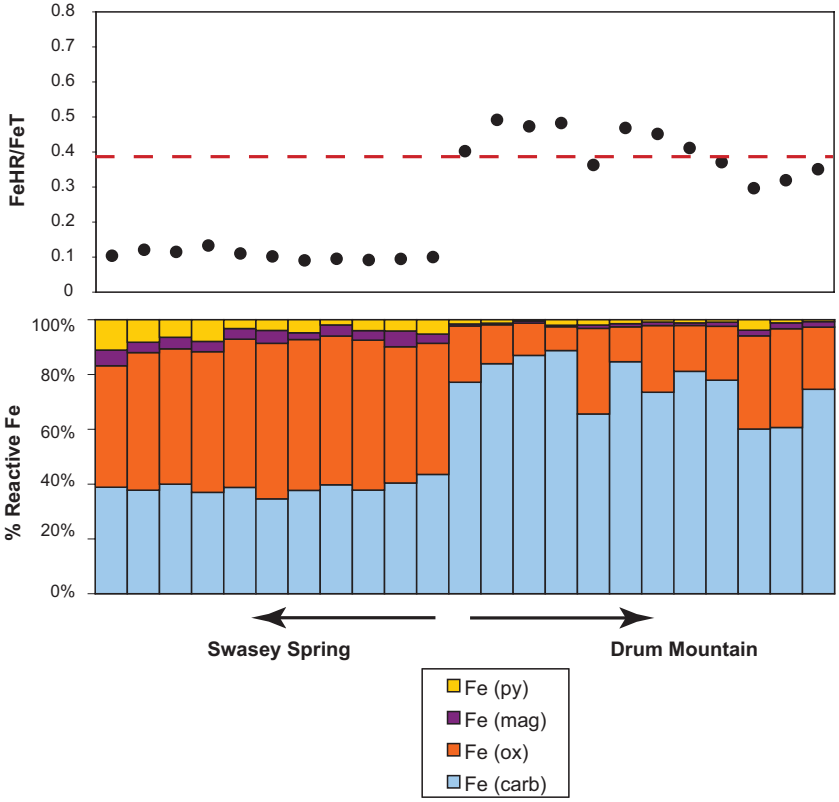

Figure 9.16 Fe speciation results from the Wheeler Formation (data from Hammarlund, 2007).

First, with lower levels of atmospheric oxygen, it is possible that the marine redox-cline was located rather far up onto the continental shelf. This would have exposed a greater proportion of the highly reactive iron flux to the oceans to anoxic marine waters encouraging ferruginous conditions. Indeed, described in Section 9.2, there is enough highly reactive iron delivered to the continental shelves to remove all of the sulphate flux to the oceans as pyrite, with plenty of highly reactive Fe to spare. This balance between the flux of highly reactive iron and rates of sulphide formation by sulphate reduction, however, will also depend on regional conditions of highly reactive iron delivery rates, and sulphate and organic carbon availability, as described in Section 9.6. These will change from place to place in the oceans allowing euxinic conditions in some locations, but not as a general condition. This was our model for the development of sulphidic conditions in the Proterozoic oceans as described above.

As oxygen concentrations increased at the end of the Precambrian, the marine chemocline deepens, removing the access of deeper anoxic waters to the excess highly reactive Fe on the shelf (except as a much smaller flux of pore-water Fe lost from the sediments to the over lying oxic waters; see Section 4.5). Increased oxygenation would have had another effect. The associated reduction in volume of anoxic waters (as suggested by Mo isotopes) would have reduced the anoxic sink for sulphide, allowing for more sulphate to be reduced to sulphide in the smaller volume of anoxic waters remaining. This happens today. There is so much sulphate available in seawater that the small amounts of modern-day anoxic water have a near limitless supply of sulphate through exchange with the large marine reservoir.

Another contributing factor may have been the evolution of animal grazers. Graham Logan and colleagues cleverly deduced some years ago that the packaging of organic matter in animal faecal material (as well as skeletonised algal hard parts somewhat later) may have accelerated the transport of metabolisable organic matter to the ocean depths and by doing so, reorganised biogeochemical cycles (Logan *et al.*, 1995). Borrowing this idea, it seems plausible that animal evolution could have enhanced the efficiency of organic matter transport out of the upper photic zone for rapid delivery to depth into outer shelf and continental slope environments. Here, the sulphide produced by the decomposition of this elevated flux of organic matter by sulphate reduction may have been able outpace the lower availability of highly reactive Fe in this setting. Indeed, Berry and Wilde (Berry and Wilde, 1978) highlight that Palaeozoic black shale deposits develop primarily on continental slopes. Futhermore, many of the examples of Phanerozoic euxinia described above are also from deep water settings.

Yet another biological factor may have been the evolution of bioturbating animals. Bioturbation has the effect of mixing the sediment, encouraging sulphide oxidation and limiting the amount of pyrite (Section 3.4 and Berner and Westrich, 1985; Canfield and Farquhar, 2009) that can form. If less sulphur is buried in continental shelf sediments, more sulphate becomes available for sulphate reduction elsewhere, such as in euxinic environments. This would further enhance the availability of sulphate to a more limited volume of anoxic waters as generated through elevated oxygen levels.

Therefore, it seems that a number of factors have combined to contribute to the apparent dominance of anoxic euxinic conditions (as opposed to ferruginous conditions) through the Phanerozoic. These factors include aspects of both atmospheric oxygenation and biological evolution. Whether there are links between these two is a frontier area of research. It is possible, though, that these factors could have combined in different magnitudes as the intensity of bioturbation intensified through time and as atmospheric oxygen levels increased with a different history. More intense utilisation of Fe speciation protocols should provide the data base by which to elucidate the history of Phanerozoic ocean chemistry, the basis by which these ideas and others can be tested.

Furthermore, these ideas need to be validated with careful biogeochemical modelling.

9.8 Summary

Throughout Earth's history, the redox chemistry of the oceans has been controlled by the interplay, mainly, between the cycles of oxygen, sulphur and iron. The evolution of this interplay is shown in Figure 9.17. Early in the Archean, there is little evidence for any pervasive oxygenation of the Earth surface, and if present, oxygen was presumably low enough in concentration to hinder the weathering of sulphide on land to sulphate. The oceans were anoxic (save possibly for some oxygen-containing oases if cyanobacteria were present) and dominated by Fe cycling (field "a" in Fig. 9.17). Many geochemical indicators point to the periodic late Archean oxygenation of the Earth surface. Ocean redox seemed to respond with the occasional establishment of euxinic conditions. Still, euxinia seemed to have been rare and ferruginous conditions dominated (field "b" in Fig. 9.17). During the Great Oxidation Event, atmospheric oxygen increased, promoting effective weathering of sulphide to sulphate on land. We have few observations on the nature of ocean redox associated with and immediately after this event, but a reduction in BIF deposition is indicated, promoted, most likely, by an increase in the sequestration of highly reactive Fe by the sulphide produced from elevated rates of sulphate reduction.

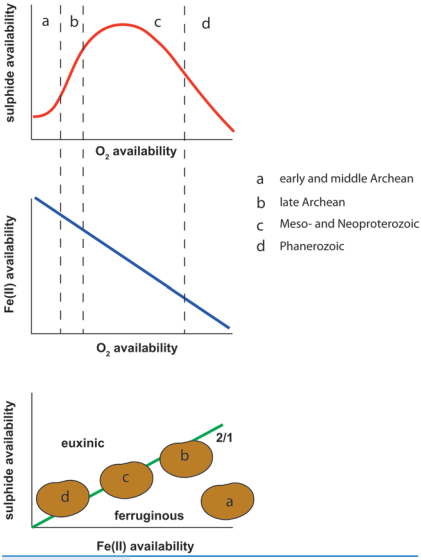

Figure 9.17 Cartoon illustrating how the viability of sulphide and Fe availability through time has influenced ocean chemistry. For further details, see text, especially Section 9.8.

There are numerous indications of euxinic intervals after the deposition of the last major episode of BIF at 1.84 Ga. The emerging view, however, is that euxinic conditions were concentrated either in restricted basins or as wedges of sulphidic water extending from the continental shelf, but giving way to ferruginous deep water conditions further offshore. Although ferruginous waters may have dominated the oceans by volume, euxinic conditions acted as an important sink for highly reactive Fe (and other redox-sensitive trace metals), limiting the concentrations of Fe(II)

in the ferruginous waters, and thereby limiting the deposition of BIF. It is possible that oxygenated deep waters were also present during the middle Proterozoic (field "c" in Fig. 9.17).

It is an open question whether Neoproterozoic chemistry was much different from the preceding middle Proterozoic (field "c" in Fig. 9.17). Mo isotope evidence suggests that they may be similar, but the paucity of observed euxinic intervals in the Neoproterozoic may suggest that this time in Earth history was, indeed, more ferruginous than the time before. It is not completely clear why this should be so, but pyrite subduction through the middle Proterozoic could have decreased the surface inventory of sulphur, increasing the excess of highly reactive Fe over sulphide.

There is evidence for a late Neoproterozoic oxygenation of the surface environment, which likely reduced the overall extent of anoxia in the global ocean. Where anoxic, the Phanerozoic ocean was dominantly euxinic, in stark contrast to the apparently dominant ferruginous conditions of the Neoproterozoic (field "d" in Fig. 9.17). This is indeed a puzzle, but elevated oxygen levels may have increased the depth of the chemocline, restricting the access of highly reactive Fe to deeper anoxic waters. An expansion of oxic conditions also reduced the overall volume of anoxic waters, allowing a greater sulphate supply to drive sulphate reduction in the lower volume of anoxic water. Furthermore, the evolution of animals allowed rapid export of faecal material to depths in the ocean where the highly reactive Fe flux is limited. Therefore, rates of sulphate reduction may have been accelerated in highly reactive-Fe-poor depths of the ocean, tipping the balance towards euxinic conditions. The evolution of bioturbation by animals may have also limited sulphur removal as pyrite on continental shelves, increasing the availability of sulphate for sulphate reduction in anoxic areas of the ocean.

10. CONCLUSIONS

We have presented a journey through the evolution of our understanding of the Fe biogeochemical cycle both past and present. This journey is both personal and professional as seen through the eyes of two colleagues who have worked together, on and off, for nearly 30 years. A starting point to this journey, in both cases, was the lab of Bob Berner in New Haven, Connecticut, whose inspiration and insights were pivotal to the both of us. This story would not be possible without him.

Through our careers we have seen profound changes in both our understanding of the Fe cycle and the methods used to explore it. Burettes and glass pipettes have long given way to more sophisticated tools, allowing us to ask and answer questions nearly inconceivable 30 years ago. Then, we filtered water through a 0.45 μm filter and thought we obtained "dissolved" Fe. Now, we realise that while some this "dissolved" Fe may consist of aqueous ionic or complexed Fe species, a major portion in many cases consists of nanoparticulate or colloidal material. The size, mineralogy, crystallinity and composition of this material proves central to our understanding of its bioavailabilty to primary producing algae as well as the transport potential of this Fe to distant regions of the global ocean. This understanding comes from a combination of advanced technologies including: ultrafiltration, competitive ligand exchange and high resolution microscopy.

We also now appreciate that there are multiple sources of Fe to the global ocean completely unrecognised only 10 years ago. These include hydrothermal activity, sub-glacial runoff (a direct source of Fe(II) to the oceans), as well as glacial rock flour and other ice-entombed particles, which are liberated to the oceans as the glaciers melt. Combined, these glacial sources represent bioavailable sources of iron contributing to a possible negative feedback against global warming. This is because elevated sources of iron to the iron-limited regions of the global ocean, derived from glacial melting, should stimulate primary production and the export, ultimately, of CO_2 into the deep ocean. This should lower temperature and encourage more glaciation.

Marine sediments of the continental shelf represent another newly recognised source of Fe to the global ocean. A small amount of the porewater iron accumulated in sediments of the continental margins is mixed or diffused into the overlying water. Here, it can either be anoxically transported in the chemocline, or oxidised into colloidal/nanoparticulate Fe (oxyhydr)oxides, for transport to distant parts of the ocean. Some of this Fe will be bioavailable depending on its speciation, crystallinity and mineralogy. All of these newly recognised Fe sources are combined with the "classic" Fe sources of riverine runoff and aeolian dust deposition to represent the modern Fe cycle.

Fe interacts with the biogeochemical cycling of many elements including phosphorus, carbon, oxygen and nitrogen. We have shown that each of these interactions, in different ways, is of direct relevance for our understanding of

issues ranging from the biogeochemical cycling of the earliest Earth's ecosystems, to the control on primary production through to time. These interactions also define our understanding of the chemistry of modern and ancient oxygen minimum zones. We have highlighted here interactions between the iron, sulphur and oxygen cycles. Thirty years ago, our ideas as to how these cycles interacted were vague at best. Our current understanding has come from many directions, but key has been the development of chemical extraction techniques, allowing us to partition Fe into various mineralogical classes. These insights, coupled with experimental work and field observations, have allowed us to understand how Fe and sulphur interact over a range of different time scales. This, in turn, provides the foundation for our ability to define the "highly reactive Fe" content of sediments. These insights, combined with parallel work defining the "degree of pyritisation" (DOP) of sediments, have given us some of the first, and indeed the most robust, palaeoenvironmental indicators.

We can now distinguish sediments deposited into different types of sedimentary environments including normal marine, euxinic, and anoxic ferruginous, based on their proportions of highly reactive Fe, the distribution of mineral types comprising highly reactive Fe phases, and different DOP contents. These palaeoenvironmental indicators have been widely applied, and have both defined and redefined the evolution of ocean chemistry through time. Generally, the specifics of ocean chemistry have depended on the interactions between the cycles of iron, sulphur and oxygen, and these interactions have changed through time. In the Archean Eon, oxygen was limiting, inhibiting the oxidative weathering of sulphides to sulphate. Thus, there was a limited flux of sulphur to the oceans and ferruginous conditions dominated except during transient periods of oxygenation or with locally elevated sulphur sources (volcanic sources for example) giving occasional euxinic conditions.

After the general oxygenation of the atmosphere 2.3 to 2.4 billion years ago, the sulphate flux to the oceans increased. Oxygen was not sufficiently high to ventilate the oceans as today, leaving vast volumes of anoxic water, in which sulphidic marine conditions became more prevalent than in the Archean. Sulphidic conditions were, however, probably locally restricted, and ferruginous conditions dominated otherwise. Such mixed sulphidic-ferruginous ocean conditions, in variable proportions, seem to have defined the remainder of the Proterozoic, although oxygenated deep waters have also been identified in the later part of this Eon. Moving into the Phanerozoic Eon, the oceans were apparently predominantly euxinic when anoxic, although some instances of ferruginous conditions have also been identified. The enhanced significance of euxinic conditions in the Phanerozoic seems to be related to a combination of factors including an increase in atmospheric oxygen levels leading to an overall reduction in the volume of anoxic water, the evolution of bioturbation encouraging sulphide oxidation in sediments and increases in particle export rates by eukaryotic grazers.

While the progress over the last 30 years has been breathtaking, we still identify many frontier areas for further work. We believe the next major challenge in understanding the modern Fe cycle will be to distinguish between the behaviour of aqueous species and mixtures of colloidal/nanoparticulate iron (oxyhydr)

oxides and associated organic matter. This will require the routine adoption of techniques delivering improved separation of aqueous and colloidal/nanoparticulate iron inorganic and organic species in natural systems. This is a major hurdle, but a smaller number of highly selective data will be more insightful than many more measurements of lesser selectivity.

Improved separation, on its own, will not suffice. Equal analytical attention must be paid to both aqueous and colloidal/nanoparticulate species. Many techniques are already available to characterise colloidal/nanoparticulate phases both chemically and mineralogically, but applying these will require a new era of cross-disciplinary collaboration between oceanographers, geochemists and mineralogists. Powerful forces drive us towards specialisation including the disciplinary nature of academic departments, research funding and the way research publication is organised. Our progress in understanding the modern iron biogeochemical cycle will reflect how well we are able to achieve cross-disciplinary integration. Natural system research should not be limited by phase boundaries. We also feel that our understanding of the modern Fe cycle is hampered by a poor quantification of many of the important Fe fluxes, including those from icebergs, sub-glacial melt and marine sediments. More focus on the consequences of these fluxes to fuel global primary production should also be a priority.

We have begun to define the evolution of ocean chemistry through time, but through most of Earth history, the data are spotty or missing altogether. There is almost no information, for example, through the Mesoproterozoic, and modern Fe speciation techniques have only recently been applied to the Phanerozoic. We are, of course, limited by the available rock record, but redoubled efforts to identify new promising sedimentary sequences and dedicated efforts to drill them will bring us far. The speciation techniques we use are themselves a convenient way to explore different classes of Fe minerals in sediments, but they lack mineralogical rigor. We welcome advancements in the techniques to bring mineralogy more in focus.

As explored through the text, the evolution of the Fe cycle cannot be understood in isolation as it interacts with the cycling of many other elements, but in particular, oxygen and sulphur. Progress, therefore, depends on our understanding of the evolution of these cycles as well. Progress is being made, but our ideas are still primitive as how ocean chemistry is controlled. Modelling will be central to exploring the coupling between these biogeochemical cycles, and it will probably not be long before full-blown 3-D ocean-atmosphere biogeochemical cycling models will be developed to unravel these interactions. We look forward to these developments, and as explored above for the modern Fe cycle, progress will require multi-disciplinary engagement.

Overall, science is limited mostly by good ideas. We have enjoyed our exploration of the Fe cycle and its evolution, and we hope we have contributed something tangible to the discussion. However, a new generation of Earth scientists is moving through the ranks. We expect that when they re-write this story 30 years from now, our ideas today will seem as primitive as those we faced 30 years ago.

REFERENCES

Aguilar-Islas, A.M., Wu, J., Rember, R., Johansen, A.M., Shank, L.M. (2010) Dissolution of aerosol-derived iron in seawater: Leach solution chemistry, aerosol type, and colloidal iron fraction. *Marine Chemistry* 120, 25-33.

Ahmed I.A., Benning L.G., Kakonyi G., Sumoondur A., Terril N., and Shaw S. (2010) The formation of green rust sulfate: situ and time-resolved scattering and electrochemistry. *Langmuir* 26, 6593–6603.

Aller, R.C., Blair, N.E. (2006) Carbon remineralization in the Amazon-Guianas tropical mobile mudbelt: A sedimentary incinerator. *Continental Shelf Research* 26, 2241-2259.

Aller, R.C., Mackin, J.E., Cox, R.T.Jr. (1986) Diagenesis of Fe and S in Amazon inner shelf muds: Apparent dominance of Fe reduction and implications for the genesis of ironstones. *Continental Shelf Research* 6, 263-289.

Aller, R.C., Blair, N.E., Xia, Q., Rude, P.D. (1996) Remineralisation rates, recycling, and storage of carbon in Amazon shelf sediments. *Continental Shelf Research* 16, 753-786.

Aller, R.C., Hannides, A., Heilbrun, C., Panzeca, C. (2004) Coupling of early diagenetic processes and sedimentary dynamics in tropical shelf environments: the Gulf of Papua deltaic complex. *Continental Shelf Research* 24, 2455-2486.

Allnutt, F.C.T., Bonner, W.D. (1987) Evaluation of reductive release as a mechanism for iron uptake from ferrioxamine B by *Chlorella vulgaris*. *Journal of Plant Physiology* 85, 751-756.

Amin, S.A., Green, D.H., Hart, M.C., Kupper, F.C., Sunda, W.G., Carrano, C.J. (2009) Photolysis of iron-siderophore chelates promotes bacterial-algal mutualism. *Proceedings of the National Academy of Sciences of the United States of America* 106, 17071-17076.

Anbar, A.D., Knoll, A.H. (2002) Proterozoic ocean chemistry and evolution: A bioinorganic bridge? *Science* 297, 1137-1142.

Anbar, A.D., Duan, Y., Lyons, T.W., Arnold, G.L., Kendall, B., Creaser, R.A., Kaufman, A.J., Gordon, G.W., Scott, C., Garvin, J., Buick, R. (2007) A whiff of oxygen before the Great Oxidation Event? *Science* 317, 1903-1906.

Anderson, T.F., Raiswell., R. (2004) Sources and mechanism for the enrichment of highly reactive iron in euxinic Black Sea sediments. *American Journal of Science* 304, 203-233.

Andreae, M.O., Crutzen, P.J. (1997) Atmospheric aerosol: Biogeochemical sources and role in atmospheric chemistry. *Science* 276, 1052-1058.

Aplin, A.C., MacQuaker, J.H.S. (1993) C-S-Fe geochemistry of some modern and ancient anoxic marine muds and mudstones. *Philosophical Transactions of the Royal Society* 344, 89-100.

Appelo, C.A.J., Postma, D. (2007) Geochemistry, Groundwater and Pollution. Balkema, London.

Ardelan, M.V., Holm-Hansen, O., Hewes, C.D., Reiss, C.S., Silva, N.S., Dulaiova, H., Steinnes, E., Sakshaug, E. (2010) Natural iron enrichment around the Antarctic Peninsula in the Southern Ocean. *Biogeosciences* 7, 11-25.

Arimoto, R.W., Balsam, C., Schloesslin (2002) Visible spectroscopy of aerosol particles collected on filters: iron-oxide minerals. *Atmospheric Environment* 36, 89-96.

Arnold, G.L., Anbar, A.D., Barling, J., Lyons, T.W. (2004) Molybdenum isotope evidence for widespread anoxia in mid-Proterozoic oceans. *Science* 304, 87-90.

Atherton, M.P., Brotherton, M.S., Raiswell, R. (1971) A comparison of automatic and manual wet chemical analysis of rocks. *Chemical Geology* 7, 285-293.

Aumont, O., Bopp, l. (2006) Globalizing results from ocean in situ fertilization studies. *Global Biogeochemical Cycles* 20, GB2017.

Avila, A., Queralt-Mitjans, I., Alarcon, M. (1997) Mineralogical composition of African dust delivered by red rains over northeastern Spain. *Journal of Geophysical Research* 102, 21977-21996

Baker, A.R., Jickells, T.D. (2006) Mineral particle size as a control on aerosol iron solubility. *Geophysical Research Letters* 33, L17608.

Balistrier, L., Brewer, P.G., Murray, J.W. (1981) Scavenging residence times of trace metals and surface chemistry of sinking particles in the deep ocean. *Deep-Sea Research* 28A, 101-121.

Balzano, S., Statham, P.J., Pancost, R.D., Lloyd, J.R. (2009) Role of microbial populations in the release of iron to the water column from marine aggregates. *Aquatic Microbial Ecology* 54, 291-303.

Banwart, S., Davies, S., Stumm, W. (1989) The role of oxalate in accelerating the dissolution of hematite (α-Fe_2O_3) by ascorbate. *Colloids and Surfaces* 39, 303-309.

Barbeau, K. (2006) Photochemistry of organic Fe(III) complexing ligands in oceanic systems. *Photochemistry and Photobiology* 82, 1505-1516.

Barbeau, K., Moffett, J.W. (2000) Laboratory and field studies of colloidal iron dissolution as mediated by phagotrophy and photolysis. *Limnology and Oceanography* 45, 827-835.

Barbeau, K., Moffett, J.W., Caron, D.A., Croot, P.L., Erdner, D.L. (1996) Role of protozoan grazing in relieving iron limitations of plankton. *Nature* 380, 61-64.

Barbeau, K., Rue, E.L., Trick, C.G., Bruland, K.W., Butler, A. (2003) Photochemical reactivity of siderophores produced by marine heterotrophic bacteria and cyanobacteria based on characteristic Fe(III) binding groups. *Limnology and Oceanography* 48, 1069-1078.

Bekker, A., Kaufman, A.J. (2007) Oxidative forcing of global climate change: A biogeochemical record across the oldest Paleoproterozoic ice age in North America. *Earth and Planetary Science Letters* 258, 486-499.

Bekker, A., Holland, H.D., Wang, P.-L., Rumble III, D., Stein, H.J., Hannah, J.L., Coetzee, L.L., Beukes, N.J. (2004) Dating the rise of atmospheric oxygen. *Nature* 427, 117-120.

Bekker, A., Slack, J.F., Planavsky, N., Krapez, B., Hofmann, A., Konhauser, K.O., Rouxel, O.J. (2010) Iron Formation: The Sedimentary Product of a Complex Interplay among Mantle, Tectonic, Oceanic, and Biospheric Processes. *Economic Geology* 105, 467-508.

Bennett, S.A., Achterberg, E.P., Connelly, D.P., Statham, P.J., Fones, G.R., German, C.R. (2008) The distribution and solubilisation of dissolved Fe in deep-sea hydrothermal plumes. *Earth and Planetary Science Letters* 270, 157-167.

Benning, L. G., Waychunas, G.A. (2007) Nucleation, growth and aggregation of mineral phases: mechanisms and kinetics. In: Brantley, S., Kubicki, J., White, A. (Eds.) Kinetics of Water-Rock Interactions. Springer-Verlag, New York pp. 259-335.

Benning, L.G., Wilkin, R.T., Barnes, H.L. (2000) Reaction pathways in the FeS system below 100°C. *Chemical Geology* 167, 25-51.

Berelson, W.M., McManus, J., Coale, K.H., Johnson, K.S., Burdige, D., Kilgoe, T., Colodner, D., Chavez, F., Kudela, R., Boucher, J. (2003) A time series of benthic flux measurements from Monterey Bay, CA. *Continental Shelf Research* 33, 457-481.

Berg, P., Rysgaard, S., Thamdrup, B. (2003) Dynamic modeling of early diagenesis and nutrient cycling: a case study in an Arctic marine sediment. *American Journal of Science* 303, 905-955.

Bergquist, B.A., Wu, J., Boyle, E.A. (2007) Variability in oceanic dissolved iron is dominated by the colloidal fraction. *Geochimica et Cosmochimica Acta* 71, 2960-2974.

Bergman, N.M., Lenton, T.M., Watson, A.J. (2004) COPSE: A new model of biogeochemical cycling over Phanerozoic time. *American Journal of Science* 304, 397-437.

Berkner, L.V., Marshall, L.C. (1965) On the origin and rise of oxygen concentration in the Earth's atmosphere. *Journal of the Atmospheric Sciences* 22, 225-261.

Berman-Frank, I., Cullen, J.T., Shaked, Y., Sherrell, R.M., Falkowski, P.G. (2001) Iron availability, cellular iron quotas, and nitrogen fixation in *Trichodesmium*. *Limnology and Oceanography* 46, 1249-1260.

Berner, R.A. (1964) An idealized model of dissolved sulfate distribution in recent sediments. *Geochimica et Cosmochimica Acta* 28, 1497-1503.

Berner, R.A. (1970) Sedimentary pyrite formation. *American Journal of Science* 268, 1-23.

Berner, R.A. (1971) Principles of Chemical *Sedimentology*. McGraw-Hill, New York.

Berner, R.A. (1974) Kinetic models for the early diagenesis of nitrogen, sulfur, phosphorus and silicon in anoxic marine sediments. In: Goldberg, E.D. (Ed.) The Sea, vol. 5. Wiley-Interscience, New York, pp. 427-450.

Berner, R.A. (1980) Early Diagenesis: A Theoretical Approach. Princeton University Press.

Berner, R.A. (1982) Burial of organic carbon and pyrite sulfur in the modern ocean: its geochemical and environmental significance. *American Journal of Science* 282, 451-478.

Berner, R.A. (2004) The Phanerozoic Carbon Cycle: CO_2 and O_2. Oxford University Press, Oxford.

Berner, R.A. (2006) GEOCARBSULF: A combined model for Phanerozoic atmospheric O_2 and CO_2. *Geochimica et Cosmochimica Acta* 70, 5653-5664.

Berner, R.A., Raiswell, R. (1983) Burial of organic carbon and pyrite sulfur in sediment over Phanerozoic time: a new theory. *Geochimica et Cosmochimica Acta* 47, 855-862.

Berner, R.A., Raiswell, R. (1984) C/S method for distinguishing freshwater from marine sedimentary rocks. *Geology* 12, 365-368.

Berner, R.A., Westrich, J.T. (1984) The role of sedimentary organic matter in bacterial sulfate reduction: The G model tested. *Limnology and Oceanography* 29, 236-249.

Berner, R.A., Westrich, J.T. (1985) Bioturbation and the early diagenesis of carbon and sulfur. *American Journal of Science* 285, 193-206.

Berner, R.A., Canfield, D.E. (1989) A new model for atmospheric oxygen over Phanerozoic time. *American Journal of Science* 289, 333-361.

Berry, W.B.N., Wilde, P. (1978) Progressive ventilation of the oceans – an explanation for the distribution of the lower Paleozoic black shales. *American Journal of Science* 278, 257-275.

Beukes, N.J., Klein, C. (1992) Models for iron-formation deposition. In: Schopf, J.W., Klein, C. (Eds.) The Proterozoic Biosphere: a multidisciplinary study. Cambridge University Press, Cambridge, pp. 147-151.

Bigham, J.M., Schwertmann, U., Traina, S.J., Winland, R.L.,Wolf, M. (1996) Schwertmannite and the chemical modelling of iron in acid sulfate waters. *Geochimica et Cosmochimica Acta* 60, 2111-2121.

Bjerrum, C.J., Canfield, D.E. (2002) Ocean productivity before about 1.9 Gyr ago limited by phosphorus adsorption onto iron oxides. *Nature* 417, 159-162.

Bjerrum, C.J., Canfield, D.E. (2004) New insights into the burial history of organic carbon on the early Earth. *Geochemistry Geophysics Geosystems* 5, 9.

Blain, S., Queguiner, B., Armand, L., Belviso, S., Bombled, B., Bopp, L., Bowie, A., Brunet, C., Brussard, C., Carlotti, F., Christaki, U., Corbiere, A., Durant, I., Ebersbach, F., Fuda, J-L., Garcia, N., Gerringa, L., Griffiths, B., Guigue, C., Guillerm, C., Jacquet, S., Jeandel. C., Laan, P., Lefevre, D., Monaco C.L., Malits, A., Mosseri, J., Obernosterer, I., Park, Y-H., Picheral, M., Pondaven, P., Remenyi, T., Sandroni, V., Sarthou, G., Savoye, N., Scouarnec, L., Souhaut, M., Thuiller, D., Timmermans K., Trull, T., Uitz, J., van Beek, P., Veldhuis, M., Vincent, D., Violler, E., Vong, L., Wagener, T. (2007) The effect of natural iron fertilization on carbon sequestration in the Southern Ocean. *Nature* 446, 1070-1074.

Blankenship, R.E. (1992) Origin and early evolution of photosynthesis. *Photosynthesis Research* 33, 91-111.

Blankenship, R.E. (2001) Molecular evidence for the evolution of photosynthesis. *Trends in Plant Science* 6, 4-6.

Blankenship, R.E., Hartman, H. (1998) The origin and evolution of oxygenic photosynthesis. *Trends in Biochemical Sciences* 23, 94-97.

Bligh, M, Waite, T.D. (2011) Formation, reactivity, and aging of ferric oxide particles formed from Fe(II) and Fe(III) sources: implications for iron bioavailability in the marine environment. *Geochimica et Cosmochimica Acta* 75, 7741-7758.

Bonneville, S., Van Cappellen, P.V., Behrends, T. (2004) Microbial reduction of iron (III) oxyhydroxides: effects of mineral solubility and availability. *Chemical Geology* 212, 255-268.

Borer, P., Sulzberger, B., Reichard, P.U., Kraemer, S.M. (2005) Effect of siderophores on the light-induced dissolution of colloidal iron (III) (hydr)oxides. *Marine Chemistry* 93, 179-193.

Bottrell, S.H., Tranter, M. (2002) Sulphide oxidation under partially anoxic conditions at the bed of Haut Glacier d'Arolla, Switzerland. *Hydrological Processes* 16, 2363-2368.

Boudreau, B.P. (1984) On the equivalence of nonlocal and radial-diffusion models for porewater irrigation. *Journal of Marine Research* 42, 731-735.

Boudreau, B.P (1997) Diagenetic Models and Their Implementation. Springer, Berlin.

Boyd, E.S., Skidmore, M., Mitchell, A.C., Bakermans, C., Peters, J.W. (2011) Methanogenesis in subglacial sediments. *Environmental Microbiology Reports* 2, 685-692.

Boyd, P.W. (2008) Implications of large-scale iron fertilization of the oceans: Introduction and synthesis. *Marine Ecology Progress Series* 364, 213-218.

Boyd, P.W., Elwood, M.J. (2010) The biogeochemical cycle of iron in the ocean. *Nature Geoscience* 3, 675-682.

Boyd, P.W., Watson, A.J., Law, C.S., Abraham, E.R., Trull, T., Murdoch, R., Bakker, D.C.E., Bowie, A.R., Buessler, K.O., Chang, H., Charette, M., Croot, P., Downing, K., Frew, R., Gail, M., Hadfield, M., Hall., J., Harvey, M., Jameson, G., LaRoche, J., Liddicoat, M., Ling, R., Maldonado, M.T., McKay, R.M., Nodder, S., Pickmere, S., Pridmore, R., Rintoul, S., Safi, K., Sutton, P., Strzepek, R., Tanneberger, K., Turner, S., Waite, A., Zeldis, J. (2000) A mesoscale phytoplankton bloom in the polar Southern Ocean stimulated by iron fertilization. *Nature* 407, 695-702.

Boyd, P.W., Mackie, D.S., Hunter, K.A. (2010a) Aerosol iron deposition to the surface ocean – Modes of iron supply and biological responses. *Marine Chemistry* 120, 128-143.

Boyd, P.W., Ibisanmi, E., Sander S., Hunter K.H. Jackson, G.A. (2010b) Remineralisation of upper ocean particles: implications for iron biogeochemistry. *Limnology and Oceanography* 55, 1271-1288.

Boye, M., Nishioka, J., Croot, P., Laan, P., Timmermans, K.R., Strass, V.H., Takeda, S., de Baar, H.J.W. (2010) Significant proportion of dissolved organic Fe complexes in fact is Fe colloids. *Marine Chemistry* 122, 20-27.

Breitbarth, E., Achterberger, E.T., Ardelan, M. V., Baker, A.R., Bucciarelli, E., Chever, F., Croot, P.L., Duggan, S., Gledhill, M., Hasselhov, M., Hoffmann, L.J., Hunter, K.A., Hutchins, D.A., Ingri, J., Jickells, T., Lohan, M. C., Nielsdottir, M.C.,

Sarthou, G., Schoemann, V., Trapp, J. M., Turner, D.R. and Ye, Y. (2010) Iron biogeochemistry across marine systems-progress from the past decade. *Biogeosciences* 7, 1075-1097.

Broecker, W.S. (1974) Chemical Oceanography. Harcourt Brace Jovanovich, New York.

Bromfield, S.M. (1954) Reduction of ferric compounds by soil bacteria. *Journal of General Microbiology* 10, 1-6.

Brown, G.H. (2002) Glacier meltwater hydrochemistry. *Applied Geochemistry* 17, 855-883.

Brown, G.H., Tranter, M., Sharp, M.J., Davies, T.D., Tsiouris, S. (1994) Dissolved oxygen variations in Alpine glacial meltwaters. *Earth Surface Processes and Landforms* 10, 247-253.

Buessler, K.O., Livingston, H.D., Casso, C. (1991) Mixing between oxic and anoxic waters in the Black Sea as traced by Chernobyl cesium isotopes. *Deep-Sea Research*, 38, S725-745.

Buick, R. (2008) When did oxygenic photosynthesis evolve? *Philosophical Transactions of the Royal Society B* 363, 2731-2743.

Buseck, P.R., Adachi, K. (2008) Nanoparticles in the atmosphere. *Elements* 4, 389-394.

Butler, A. (1998) Acquisition and utilization of transition metal ions by marine organisms. *Science* 281, 207-210.

Calvert, S.E., Pedersen, T.F. (1993) Geochemistry of recent oxic and anoxic marine-sediments-implications for the geological record. *Marine Geology* 113, 67-88.

Cameron, E.M. (1982) Sulphate and sulphate reduction in early Precambrian oceans. *Nature* 296, 145-148.

Canfield, D.E. (1988) Sulfate reduction and the diagenesis of iron in anoxic marine sediments. Unpub. PhD thesis, Yale, 248p.

Canfield, D.E. (1989) Reactive iron in marine sediments. *Geochimica et Cosmochimica Acta* 53, 619-632.

Canfield, D.E. (1993) Organic matter oxidation in marine sediments. In: Wollast, R., Chou, L., Mackenzie, F. (Eds.) Interactions of C, N, P and S Biogeochemical cycles. NATO Advanced Research Workshop, Berlin, pp. 333-363.

Canfield, D.E. (1994) Factors influencing organic carbon preservation in marine sediments. *Chemical Geology* 114, 315-329.

Canfield, D.E. (1998) A new model for Proterozoic ocean chemistry. *Nature* 396, 450-453.

Canfield, D.E. (2004) The evolution of the Earth surface sulfur reservoir. *American Journal of Science* 304, 839-861.

Canfield, D.E. (2005) The early history of atmospheric oxygen: Homage to Robert M. Garrels. *Annual Review of Earth and Planetary Science* 33, 1-36.

Canfield, D.E. (2012) Proterozoic atmospheric oxygen. In: Farquhar, J. (Ed.) Treatise on Geochemistry, Atmosphere-History, 2nd ed. Elsevier, Amsterdam (in press).

Canfield, D.E., Berner, R.A. (1987) Dissolution and pyritization of magnetite in anoxic marine sediments. *Geochimica et Cosmochimica Acta* 51, 645-659.

Canfield, D.E., Raiswell, R. (1991) Pyrite Formation and Fossil Preservation. In: Allison, P. A., Briggs, D. E. G. (Eds.) Taphonomy: Releasing the Data Locked in the Fossil Record. New York, Plenum, pp. 337-387.

Canfield, D.E., Thamdrup (1994) The production of ^{34}S-depleted sulfide during bacterial disproportionation of elemental sulfur. *Science* 206, 1073-1075.

Canfield, D.E., Teske, A. (1996) Late Proterozoic rise in atmospheric oxygen concentration inferred from phylogenetic and sulphur-isotope studies. *Nature* 382, 127-132.

Canfield, D.E., Raiswell, R. (1999) The evolution of the sulfur cycle. *American Journal of Science* 299, 697-723.

Canfield, D.E., Farquhar, J. (2009) Animal evolution, bioturbation, and the sulfate concentration of the oceans. *Proceedings of the National Academy of Sciences of the United States of America* 106, 8123-8127.

Canfield, D.E., Green, W.J., Gardner, T.J., Ferdelman, T. (1984) Elemental residence times in Action Lake, Ohio. *Archives of Hydrobiology* 100, 501-519.

Canfield, D.E., Raiswell, R., Bottrell, S. (1992) The reactivity of sedimentary iron minerals toward sulfide. *American Journal of Science* 292, 659-683.

Canfield, D.E., Thamdrup, B., Hansen, J.W. (1993) The anaerobic degradation of organic matter in Danish coastal sediments: Iron reduction, manganese reduction and sulfate reduction. *Geochimica et Cosmochimica Acta* 57, 3867-3883.

Canfield, D.E., Green, W.J., Nixon, P. (1995) Pb-210 and stable lead through the redox transition zone of an Antarctic lake. *Geochimica et Cosmochimica Acta* 59, 2459-2468.

Canfield, D.E., Lyons T.W,. Raiswell R. (1996) A model for iron deposition to euxinic Black Sea sediments. *American Journal of Science* 296, 818-834.

Canfield, D.E., Thamdrup, B., Fleischer, S. (1998) Isotope fractionation and sulfur metabolism by pure and enrichment cultures of elemental sulfur disproportionating bacteria. *Limnology and Oceanography* 43, 253-264.

Canfield, D.E., Habicht, K.S., Thamdrup, B. (2000) The Archean sulfur cycle and the early history of atmospheric oxygen. *Science* 288, 658-661.

Canfield, D.E., Kristensen, E., Thamdrup, B. (2005) Aquatic Geomicrobiology. Academic Press.

Canfield, D.E., Rosing, M.T., Bjerrum, C. (2006) Early anaerobic metabolisms. *Philosophical Transactions of the Royal Society B* 361, 1819-1834.

Canfield, D.E., Poulton, S.W., Narbonne, G.M. (2007) Late-Neoproterozoic deep-ocean oxygenation and the rise of animal life. *Science* 315, 92-95.

Canfield, D.E., Poulton, S.W., Knoll, A.H., Narbonne, G.M., Ross, G., Goldberg, T., Strauss, H. (2008) Ferruginous conditions dominated later Neoproterozoic deep water chemistry. *Science* 321, 949-952.

Cassar, N., Bender, M.L., Barnett, B.A., Fan, S., Moxim, W.J., Levy, II H., Tilbrook, B. (2007) The Southern Ocean biological response to aeolian iron deposition. *Science* 317, 67-70.

Chatellier, X., West, M.M., Rose, J., Fortin, D., Leppard, G.G., Ferris, F.G. (2004) Characterization of iron-oxides formed by oxidation of ferrous iron in the presence of various bacterial species and inorganic ligands. *Geomicrobiology Journal* 21, 99-112.

Chen, M., Wang, W-X. (2001) Bioavailability of natural colloid-bound iron to marine plankton: influences of colloidal size and aging. *Limnology and Oceanography* 46, 1956-1967.

Chen, M., Dei, R.C.H., Wang, W-X., Guo, L. (2003) Marine diatom uptake of iron bound with natural colloids of different origins. *Marine Chemistry* 81, 177-189.

Chester, R. (2003) Marine Chemistry. 2nd edition, Unwin Hyman, London.

Chisholm, S.W., Morel, F.M.M. (1991) What controls phytoplankton production in nutrient-rich areas of the open ocean? *Limnology and Oceanography* 36, 1507-1511.

Chisholm, S.W., Falkowski, P.G., Cullen, J.J. (2001) Dis-crediting ocean fertilization. *Science* 294, 309-310.

Church, J.A., Gregory, J.M,, Huybrechts, P., Kuhn, M., Lambeck, K., Nhuan, M.T., Quin, D., Woodworth, P.L. Changes in Sea Level, in Houghton, J.T., Ding, Y., Griggs, D.J., Noguer, P.J., van der Linden, M., Dai, X., Maskell, K., Johnson, C.A. (Eds.) Climate Change 2001: The Scientific Basis, Contribution of Working Group I to the Third Assessment Report of the Intergovernmental Panel on Climate. Cambridge, Cambridge University Press. pp. 639-693.

Clarke, F.W. (1924) Data on Geochemistry. US Geological Survey Bulletin, v.770.

Cline, J.D., Richards, F.A. (1972) Oxygen deficient conditions and nitrate reduction in the Eastern tropical North Pacific Ocean. *Limnology and Oceanography* 17, 885-900.

Cloud, P.E., Jr. (1972) A working model of the primitive Earth. *American Journal of Science* 272, 537-548.

Codispoti, L.A. (1983) Nitrogen in upwelling systems. In: Carpenter, E.J., Capone, D.G. (Eds.), Nitrogen in the Marine Environment. Academic Press, Inc., New York.

Cornell, R.M. and Schwertmann, U. (2003) The Iron Oxides: Structure, Properties, Reactions, Occurrences and Uses. Wiley, New York.

Croal, L.R., Johnson, C.M., Beard, B.L., Newman, D.K. (2004) Iron isotope fractionation by Fe(II)-oxidizing photoautotrophic bacteria. *Geochimica et Cosmochimica Acta* 68, 1227-1242.

Croot, P.L., Streu, P., Baker, A.R. (2004) Short residence time for iron in surface seawater impacted by atmospheric dry deposition from Saharan dust events. *Geophysical Research Letters* 31, L23S08.

Crowe, S.A., Jones, C., Katsev, S., Magen, C., O'Neill, A.H., Sturm, A., Canfield, D.E., Haffner, G.D., Mucci, A., Sundby, B., Fowle, D.A. (2008) Photoferrotrophs thrive in an Archean Ocean analogue. *Proceedings of the National Academy of Sciences of the United States of America* 105, 15938-15943.

Cruse, A.M., Lyons, T.W. (2004) Trace metal records of regional paleoenvironmental variability in Pennsylvanian (Upper Carboniferous) black shales. *Chemical Geology* 206, 319-345.

Crusius, J., Schroth, A.W., Gasso, S., Moy, C.M., Levy, R.C., Gatica, M. (2011) Glacial flour dust storms in the Gulf of Alaska: Hydrologic and meteorological controls and their importance as a source of bioavailable iron. *Geophysical Research Letters* 38, L06602.

Cuffey, K.M., Conway, H., Gades, A.M., Raymond, C.F. (1999) Interfacial water in polar glaciers and glacier sliding at -17°C. *Geophysical Research Letters* 26, 751-754.

Cullen, J.T., Bergquist, B.A., Moffett, J.W. (2006) Thermodynamic characterization of the partitioning of iron between soluble and colloidal species in the Atlantic Ocean. *Marine Chemistry* 98, 295-303.

Dahl, T.W., Canfield, D.E., M.T., R., Frei, R., Gordon, G.W., Knoll, A.H., Anbar, A.D. (2011) Molybdenum evidence for expansive sulfidic water masses in ~750 Ma oceans. *Earth Planetary Science Letters* 311, 264-274.

Dahl, T.W., Hammarlund, E.U., Anbar, A.D., Bond, D.P.G., Gill, B.C., Gordon, G.W., Knoll, A.H., Nielsen, A.T., Schovsbo, N.H., Canfield, D.E. (2010) Devonian rise in atmospheric oxygen correlated to the radiations of terrestrial plants and large predatory fish. *PNAS* 107, 17911-17915.

Dai, M., Martin, J.M. (1995) First data on trace metal level and behavior in two major Arctic river estuarine systems (Ob and Yenisey) and in the adjacent Kara Sea. *Earth Planetary Science Letters* 131, 127-141.

Dai, W., Qian, T., Trenbeth, K.E., Milliman, J.D. (2009) Change in continental freshwater discharge 1948-2004. *International Journal of Climatology* 22, 2773-2791.

Dalsgaard, T., Thamdrup, B., Canfield, D.E. (2005) Anaerobic ammonium oxidation (anammox) in the marine environment. *Research in Microbiology* 156, 457-464.

Damste, J.S.S., Koster, J. (1998) A euxinic southern North Atlantic Ocean during the Cenomanian/Turonian oceanic anoxic event. *Earth Planetary Science Letters* 158, 165-173.

Das, S., Hendry, J., Essilfie-Dughan, J. (2011) Transformation of two-line ferrihydrite to goethite and hematite as a function of pH and temperature. *Environmental Science & Technology* 45, 268-275.

David, L.A., Alm, E.J. (2011) Rapid evolutionary innovation during an Archaean genetic expansion. *Nature* 469, 93-96.

Davidson, L.E., Shaw, S., Benning, L.G. (2008) The kinetics and mechanisms of schwertmannite transformation to goethite and hematite under alkaline conditions. *American Mineralogist* 93, 1326-1337.

Davis, C.C., Chen, H.W., Edwards, M. (2002) Modeling silica sorption to iron hydroxide. *Environmental Science & Technology* 36, 582-587.

De Baar, H.J.W., de Jong, J.T.M. (2001) Distribution, Sources and Sinks of Iron in Seawater. In: Turner D.R., Hunter K.A. (Eds) The Biogeochemistry of Iron in Seawater. Wiley, New York, pp. 123-253.

Decastro, A.F., Ehrlich, H.L. (1970) Reduction of iron oxide minerals by a marine bacillus. Antonie Van Leeuwenhoek *Journal of Microbiology and Serology* 36, 317-327.

Deer, W.A., Howie R.A., Zussman, J. (1992) An Introduction to the Rock Forming Minerals. 2nd edition, Pearson Education Limited, England.

Des Marais, D.J. (2000) Evolution: When did photosynthesis emerge on Earth? *Science* 289, 1703-1705.

Des Marais, D.J. (2001) Isotopic evolution of the biogeochemical carbon cycle during the Precambrian. In: Valley, J.W., Cole, D.R. (Eds.) Stable Isotope Geochemistry Reviews in Mineralogy & Geochemistry. The Mineralogical Society of America, Washington, pp.555-578.

Drobner, E., Huber, H., Wachtershauser, G., Rose, D., Stetter, K.O. (1990) Pyrite formation linked with hydrogen evolution under anaerobic conditions. *Nature* 346, 742.

Druschel, G.K., Emerson, D., Sutka, R., Suchecki, P., Luther, G.W. (2008) Low-oxygen and chemical kinetic constraints on the geochemical niche of neutrophilic iron(II) oxidizing microorganisms. *Geochimica et Cosmochimica Acta* 72, 3358-3370.

Duan, Y., Severmann, S., Anbar, A., Lyons, T.W., Gordon, G.W., Sageman, B.B. (2010) Isotopic evidence for Fe cycling and repartitioning in ancient oxygen-deficient setting: Examples from black shales of the mid-to-late Devonian Appalachian basin. *Earth Planetary Science Letters* 290, 244-253.

Eady, R.R. (1996) Structure-function relationships of alternative nitrogenases. *Chemical Reviews* 96, 3013-3030.

Edwards, R., Sedwick, P. N. (2001) Iron in East Antarctic snow: Implications for atmospheric iron deposition and algal production in Antarctic waters. *Geophysical Research Letters* 28, 3907-3910.

Edwards, R., Sedwick, P.N., Morgan, V., Boutron, C.F., Hong, S. (1998) Iron in ice cores from Law Dome, East Antarctica: implications for past deposition of aerosol iron. *Annals of Glaciology* 27, 365-370.

Ehrenreich, A., Widdel, F. (1994) Phototrophic oxidation of ferrous minerals-a new aspect in the redox microbiology of iron. In: Stal, L.J., Caumette, P. (Eds.) Microbial Mats. Springer-Verlag, Berlin, pp. 393-402.

Einsele, W. (1938) Ûber chemische und kolloidchemische vorgange in eisen-phosphate-system unter limnochemischen und limnogeologischen gesichtpunkten. *Archives of Hydrobiology Plankton* 33, 361-387.

Elderfield, H., Schlutz, A. (1996) Mid-ocean ridge hydrothermal fluxes and the chemical composition of the oceans. *Earth Planetary Science Letters* 24, 191-224.

Elrod, V.A., Berelson, W.M., Coale, K.H., Johnson, K.S. (2004) The flux of iron from continental shelf sediments: A missing source for global budgets. *Geophysical Research Letters* 31, L12307.

Emerson, D., Revsbech, N.P. (1994a) Investigation of an iron-oxidizing microbial mat community located near Aarhus, Denmark: field studies. *Applied and Environmental Microbiology* 60, 4022-4031.

Emerson, D., Revsbech, N.P. (1994b) Investigation of an iron-oxidizing microbial mat community located near Aarhus, Denmark: laboratory studies. *Applied and Environmental Microbiology* 60, 4032-4038.

Emerson, D., Fleming, E.J., McBeth, J.M. (2010) Iron-Oxidizing Bacteria: An Environmental and Genomic Perspective. *Annual Review of Microbiology* 64, 561-583.

Engelbrecht, J.P., Derbyshire, E. (2010) Airbourne mineral dust. *Elements* 6, 241-246.

Erel, Y., Pehkonen, S.O., Hoffmann, M.R. (1993) Redox chemistry of iron in fog and stratus cloud. *Journal of Geophysical Research* 98, 18423-18434.

Esteve-Nunez, A., Sosnik, J., Visconti, P., Lovley, D.R. (2008) Fluorescent properties of c-type cytochromes reveal their potential role as an extracytoplasmic electron sink in *Geobacter sulfurreducens*. *Environmental Microbiology* 10, 497-505.

Eusterhues, K., Rennert, T., Knicker, H., Kogel-Knaber, I., Totsche, K.U., Schwertmann, U. (2011) Fractionation of organic matter with ferrihydrite: coprecipitation versus adsorption. *Environmental Science & Technology* 45, 527-533.

Ewing, R.C. (2009) Is geochemistry important? *Elements* 5, 205.

Fairburn *et al.* (1951) A co-operative investigation of precision and accuracy in chemical, spectrochemical and modal analyses of silicate rocks. *U.S. Geological Survey Bulletin* 980.

Fairchild, I.J., Bradby, L., Spiro, B. (1993) Carbonate diagenesis in ice. *Geology* 21, 903-904.

Falkovich, A.H., Ganor, E., Levin, Z., Formenti, P., Rudich, Y. (2001) Chemical and mineralogical analysis of individual mineral dust particles. *Journal of Geophysical Research (Atmospheres)* 106, 18029-18036.

Falkowski, P.G. (1997) Evolution of the nitrogen cycle and its influence on the biological sequestration of CO_2 in the ocean. *Nature* 387, 272-275.

Fan, S-M., Moxim, W.J., Levy II, H. (2006) Aeolian input of bioavailable iron to the ocean. *Geophysical Research Letters* 33, L07602.

Farquhar, J., Bao, H.M., Thiemens, M. (2000) Atmospheric influence of Earth's earliest sulfur cycle. *Science* 289, 756-758.

Farquhar, J., Savarino, J., Airieau, S., Thiemens, M.H. (2001) Observation of the wavelength-sensitive mass-dependent sulfur isotope effects during SO_2 photolysis: Implications for the early atmosphere. *Journal of Geophysical Research* 106, 32829-32839.

Farquhar, J., Wu, N.P., Canfield, D.E., Oduro, H. (2010) Connections between Sulfur Cycle Evolution, Sulfur Isotopes, Sediments, and Base Metal Sulfide Deposits. *Economic Geology* 105, 509-533.

Feely, R.A., Trefry, J.H., Lebon, G.T., German, C.R. (1998) The relationship between P/Fe and V/Fe ratios in hydrothermal precipitates and dissolved phosphate in seawater. *Geophysical Research Letters* 25, 2253-2256.

Ferris, F.G. (2005) Biogeochemical properties of bacteriogenic iron oxides. *Geomicrobiology Journal* 22, 79-85.

Field, C.B., Behrenfeld, M.J., Randerson J.T., Falkowski, P. (1998) Primary production of the biosphere: Integrating terrestrial and oceanic components. *Science* 281, 237-240.

Fischer, W.W., Knoll, A.H. (2009) An iron shuttle for deepwater silica in Late Archean and early Paleoproterozoic iron formation. *Geological Society of America Bulletin* 121, 222-235.

Fralick, P., Barrett, T.J. (1995) Depositional controls on iron formation associations in Canada. *Special Publications International Association of Sedimentologists* 22, 137-156.

Frei, R., Gaucher, C., Poulton, S.W., Canfield, D.E. (2009) Fluctuations in Precambrian atmospheric oxygenation recorded by chromium isotopes. *Nature* 461, 250-U125.

Froelich, P.N., Klinkhammer, G.P., Bender, M.L., Luedtke, N.A., Heath, G.R., Cullen, D., Dauphin, P., Hammond, D., Hartman, B., Maynard, V. (1979) Early oxidation of organic matter in pelagic sediments of the eastern equatorial Atlantic: suboxic diagenesis. *Geochimica et Cosmochimica Acta* 43, 1075-1090.

Gaiero, D.M., Depetries, P.J., Probst, J-L., Bidart, S.M., Leleyter, L. (2004) The signature of river – and wind-bourne materials exported from Patagonia to the southern latitudes: a view from REEs and implications for paleoclimatic interpretations. *Earth Planetary Science Letters* 219, 357-376.

Gao, Y., Fan, S-M., Sarmiento, J.L. (2003) Aeolian iron input to the ocean through precipitation scavenging: A modeling perspective and its implication for natural iron fertilization in the ocean. *Journal of Geophysical Research* 108, 4221.

Garrels, R.M. (1960) Mineral Equilibria, Harper Geoscience.

Garrels, R.M., Mackenzie, F.T. (1971) Evolution of Sedimentary Rocks. Norton and Co., New York.

Garrels, R.M., Perry, E.A. (1974) Cycling of carbon, sulfur, and oxygen through geologic time. In: Goldberg, E.D. (Ed.), The Sea, vol.5. Wiley-Interscience, New York, pp. 303-336.

Garrels, R.M., Mackenzie, F.T., Hunt, C. (1971) Chemical Cycles and the Global Environment. William Kaufman, California.

Garrels, R.M., Perry, E.A., Jr., Mackenzie, F.T. (1973) Genesis of Precambrian iron-formations and the development of atmospheric oxygen. *Economic Geology* 68, 1173-1179.

Garvin, J., Buick, R., Anbar, A.D., Arnold, G.L., Kaufman, A.J. (2009) Isotopic evidence for an aerobic nitrogen cycle in the latest Archean. *Science* 323, 1045-1048.

Gilbert, B., Ono, R.K., Ching, K.A., Kim, C.S. (2009) The effects of nanoparticle aggregation processes on aggregate structure and metal uptake. *Journal of Colloid and Interface Science* 339, 285-295.

Gill, B.C., Lyons, T.W., Young, S.A., Kump, L.R., Knoll, A.H., Saltzman, M.R. (2011) Geochemical evidence for widespread euxinia in the Later Cambrian ocean. *Nature* 469, 80-83.

Glaccum, R.A., Prospero, J.M. (1980) Saharan aerosols over the tropical North Atlantic-mineralogy. *Marine Geology* 37, 295-321.

Glass, J.B., Wolfe-Simon, F., Anbar, A.D. (2009) Coevolution of metal availability and nitrogen assimilation in cyanobacteria and algae. *Geobiology* 7, 100-123.

Gledhill, M., van den Berg, C.M.G. (1994) Determination of the complexation of Fe(III) with natural organic complexing ligands in seawater using cathodic stripping voltammetry. *Marine Chemistry* 47, 41-54.

Gledhill, M., van den Berg, C.M.G. (1995) Measurement of the redox speciation of iron in seawater by catalytic cathodic stripping voltammetry. *Marine Chemistry* 50, 51-61.

Goldberg, T., Poulton, S.W., Archer, C., Vance, D., Thamdrup, B. (2009) Controls on Mo isotope fractionations in modern anoxic marine sediments – A key to paleoredox research. *Geochimica et Cosmochimica Acta* 73, A445-A445.

Goldhaber, M.B., Kaplan, I.R. (1974) The sulfur cycle. In: Goldberg, E.D. (Ed.) The Sea, vol.5. Wiley-Interscience, New York, pp. 569-655.

Gralnick, J.A., Newman, D.K. (2007) Extracellular respiration. *Molecular Microbiology* 65, 1-11.

Granger, J., Price, N.M. (1999) The importance of siderophores in iron nutrition of heterotrophic marine bacteria. *Limnology and Oceanography* 44, 541-555.

Green, W.J., Canfield, D.E., Steinly, B.A. (1985) Spatial variations in and controls on the calcite saturation index in Acton Lake, Ohio. *Freshwater Biology* 15, 525-533.

Guo, Q.J., Strauss, H., Kaufman, A.J., Schroder, S., Gutzmer, J., Wing, B., Baker, M.A., Bekker, A., Jin, Q.S., Kim, S.T., Farquhar, J. (2009) Reconstructing Earth's surface oxidation across the Archean-Proterozoic transition. *Geology* 37, 399-402.

Habicht, K.S., Canfield, D.E. (1996) Sulphur isotope fractionation in modern microbial mats and the evolution of the sulphur cycle. *Nature* 382, 342-343.

Habicht, K.S., Canfield, D.E., Rethmeier, J. (1998) Sulfur isotope fractionation during bacterial reduction and disproportionation of thiosulfate and sulfite. *Geochimica et Cosmochimica Acta* 62, 2585-2595.

Hammarlund, E.U. (2007) The Ocean Chemistry at Cambran Deposits with Exceptional Preservation, and The Influence of Sulphate on Soft-Tissue Decay, Institute of Biology. University of Southern Denmark, Odense, p. 64.

Hartman, H. (1984) The evolution of photosynthesis and microbial mats: A speculation on the banded iron formations. In: Microbial Mats: Stromatolites. Alan R. Liss Inc., New York, pp. 449-453.

Hassler, C.S., Schoemann, V., Nichols, C.M., Butler, E.C.V., Boyd, P.W. (2011) Saccharides enhance iron bioavailability to Southern Ocean phytoplankton. *Proceedings of the National Academy of Sciences of the United States of America* 108, 1076-1081.

Hayes, J.M., Strauss, H., Kaufman, A.J. (1999) The abundance of ^{13}C in marine organic matter and isotopic fractionation in the global biogeochemical cycle of carbon during the past 800 Ma. *Chemical Geology* 161, 103-125.

Haygood, M.G., Holt, P.D., Butler, A. (1993) Aerobactin production by a planktonic marine *Vibrio* sp. *Limnology and Oceanography* 38, 1091-1097.

Hegler, F., Posth, N.R., Jiang, J., Kappler, A. (2008) Physiology of phototrophic iron(II)-oxidizing bacteria: implications for modern and ancient environments. *Fems Microbiology Ecology* 66, 250-260.

Heising, S., Schink, B. (1998) Phototrophic oxidation of ferrous iron by a *Rhodomicrobium vannielii* strain. *Microbiology-Uk* 144, 2263-2269.

Hines, M.E., Bazylinski, D.A., Tugel, J.B., Lyons, W.B. (1991) Anaerobic microbial biogeochemistry in sediments from two basins in the Gulf of Maine: evidence for iron and manganese. Estuarine, *Coastal and Shelf Science* 32, 313-324.

Hochella, M.F. (2008) Nanogeoscience: From origins to cutting-edge applications. *Elements* 4, 373-379.

Hoffman, P.F., Kaufman, A.J., Halverson, G.P., Schrag, D.P. (1998) A Neoproterozoic snowball Earth. *Science* 281, 1342-1346.

Hohmann-Marriott, M.F., Blankenship, R.E. (2011) Evolution of Photosynthesis. *Annual Review of Plant Biology* 62, 515-548.

Holland, H.D. (1984a) The Chemical Evolution of the Atmosphere and Oceans. Princeton Series in Geochemistry, Princeton University Press, Princeton, N.J.

HOLLAND, H.D. (1984b) Early Proterozoic Atmospheric Change. In: Bengtson (Ed.), Early life on Earth. Columbia University Press, New York, pp. 237-244.

HOLLAND, H.D. (2004) The geologic history of seawater. In: Holland, H.D., Turekian, K.K. (Eds.) Treatise on Geochemistry. Elsevier, Amsterdam, pp.583-625.

HOLLAND, H.D. (2006) The oxygenation of the atmosphere and oceans. *Philosophical Transactions of The Royal Society of London B* 361, 903-915.

HOMOKY, W.B., SEVERMANN, S., MILLS, P.A., STATHAM, P.J., FONES, G.R. (2009) Pore-fluid Fe isotopes reflect the extent of benthic Fe redox recycling: Evidence from continental shelf and deep-sea sediments. *Geology* 37, 751-754.

HOMOKY, W.B., HEMBURY, D.J., HEPBURN, L.E., MILLS, R.A., STATHAM, P.J., FONES, G.R., PALMER, M.R. (2011) Iron and manganese diagenesis in deep sdea volcanogenic sediments and the origins of pore water colloids. *Geochimica Cosmochimica Acta*, 75, 5032-5048.

HOPKINSON, B.M., MOREL, F.M.M. (2009) The role of siderophores in iron acquisition by photosynthetic marine microorganisms. *Biometals* 22, 659-669.

HOROWITZ, A.J., ELRICK, K.A. (1997) The relation of stream sediment surface area, grain-size and composition to trace element chemistry. *Applied Geochemistry* 2, 437-451.

HOWARD, A.G. (2010) On the challenge of quantifying man-made nanoparticles in the aquatic environment. *Journal of Environmental Monitoring* 12, 135-142.

HOWARTH, R.W., MARINO, R., COLE, J.J. (1988) Nitrogen fixation in fresh-water, estuarine, and marine ecosystems. 2. Biogeochemical controls. *Limnology and Oceanography* 33, 669-687.

HUBBARD, A., LAWSON, W., ANDERSON, B., HUBARD, B., BLATTER, H. (2004) Evidence for subglacial ponding across Taylor glacier, Dry Valleys, Antarctica. *Annals of Glaciology* 39, 79-84.

HUDSON, R.J.M., MOREL, F.M.M. (1990) Iron transport in marine phytoplankton: kinetics of cellular and medium coordination reactions. *Limnology and Oceanography* 35, 1002-1020.

HUDSON, R.J.M., COVAULT, D.T., MOREL, F.M.M. (1992) Investigation of iron coordination reactions in seawater using ^{59}Fe radiometry and ion pair solvent extraction of amphiphilic iron complexes. *Marine Chemistry* 38, 209-235.

HUNGER, S., BENNING, L. G. (2007) Greigite: the intermediate phase on the pyrite formation pathway. *Geochemical Transactions* 8, 1-20.

HURTGEN, M.T., LYONS, T.W., INGALL, E.D., CRUSE, A.M. (1999) Anomalous enrichments of iron monosulfide in euxinic marine sediments and the role of H_2S in iron sulfide transformations: Examples from Effingham inlet, Orca Basin, and the Black Sea. *American Journal of Science* 299, 556-588.

HURTGEN, M.T., ARTHUR, M.A., SUITS, N.S., KAUFMAN, A.J. (2002) The sulfur isotopic composition of Neoproterozoic seawater sulfate: implications for a snowball Earth? *Earth Planetary Science Letters* 203, 413-429.

HUTCHINS, D.A., WITTER, A.E., BUTLER, A., LUTHER III, G.W. (1999) Competition among marine phytoplankton for different chelated iron species. *Nature* 400, 858-861.

Hyacinthe, C., Van Cappellen, P. (2004) An authigenic iron phosphate phase in estuarine sediments: composition, formation and chemical reactivity. *Marine Chemistry* 91, 227-251.

Ingall, E.D., Jahnke, R.A. (1997) Influence of water column anoxia on the elemental fractionation of carbon and phosphorus during sediment diagenesis. *Marine Geology* 139, 219-229.

Ingall, E.D., Bustin, R.M., Van Cappellen, P. (1993) Influence of water column anoxia on the burial and preservation of carbon and phosphorus in marine shales. *Geochimica et Cosmochimica Acta* 57, 303-316.

Isley, A.E. (1995) Hydrothermal plumes and the delivery of iron to banded iron formations. *The Journal of Geology* 103, 169-185.

Isley, A.E., Abbott, D.H. (1999) Plume-related mafic volcanism and the deposition of banded iron formation. *Journal of Geophysical Research* 104, 15461-15477.

Isozaki, Y. (1997) Permo-Triassic boundary superanoxia and stratified superocean: records from lost deep sea. *Science* 276, 235-238.

Jackson, M.J., Muir, M.D., Plumb, K.A. (1987) Geology of the southern McArthur Basin, Northern Territory. Bureau of Mineral Resources, *Geology & Geophysics* 220, 173-.

Jambor, J.L., Dutrizac, J.E. (1998) Occurrence and constitution of natural and synthetic ferrihydrite, a widespread iron oxyhydroxide. *Chemical Reviews* 98, 2549-2585.

James, H.L. (1966) Chemistry of the iron-rich sedimentary rocks. *U.S. Geological Survey Professional Papers* 440-W1-W61.

Janney. D.E., Cowley, J.M., Buseck, P. (2000) Structure of synthetic 2-line ferrihydrite by electron nanodiffraction. *American Mineralogist* 85, 1180-1187.

Janney. D.E., Cowley, J.M., Buseck, P. (2001) Structure of 6-line ferrihydrite by electron nanodiffraction. *American Mineralogist* 86, 327-335.

Jenkyns, H.C. (1980) Cretaceous Anoxic Events – from Continents to Oceans. *Journal of the Geological Society* 137, 171-188.

Jenkyns, H.C. (2010) Geochemistry of oceanic anoxic events. *Geochemistry Geophysics Geosystems* 11, 30.

Jensen, H.S., Mortensen, P.B., Andersen, F.O., Rasmussen, E., Jensen, A. (1995) Phosphorus cycling in a coastal marine sediment, Aarhus Bay, Denmark. *Limnology and Oceanography* 40, 908-917.

Jensen, M.M., Thamdrup, B., Ryesgaard, S., Holmer, M., Fossing, H. (2003) Rates and regulation of microbial iron reduction in sediments of the Baltic-North Sea transition. *Biogeochemistry* 65, 295-317.

Jickells, T.D., Spokes, L. (2001) Atmospheric Iron Inputs to the Oceans. In: Turner, D.R., Hunter, K.A. (Eds.) The Biogeochemistry of Iron in Seawater. Wiley, New York, pp. 85-121.

Jickells, T.D., An, Z.S., Anderson, K.K., Baker, A.R., Bergametti, G., Brooks, N., Cao, J.J., Boyd, P.W., Duce, R.A., Hunter, K.A., Kawahata, H., Kubilay, N., LaRoche, J., Liss, P.S., Mahowald, N., Prospero, JM., Ridgewell, A.J., Tegen, I., Torres, R. (2005) Global iron connections between desert dust, ocean biogeochemistry, and climate. *Science* 308, 67-73.

Joerger, R.D., Bishop, P.E. (1988) Bacterial alternative nitrogen-fixation systems. *Critical Reviews in Microbiology* 16, 1-14.

Johnson, K.S., Coale, K.H., Elrod, V.A., Tindale, N.W. (1994) Iron photochemistry in the equatorial Pacific. *Marine Chemistry* 46, 319-334.

Johnson, K.S., Chavez, F.P., Friederich, G.E. (1999) Continental-shelf sediment as a primary source of iron for coastal plankton. *Nature* 398, 697-700.

Johnston, D.T., Poulton, S.W., Dehler, C., Porter, S., Husson, J., Canfield, D.E., Knoll, A.H. (2010) An emerging picture of Neoproterozoic ocean chemistry: Insights from the Chuar Group, Grand Canyon, USA. *Earth Planetary Science Letters* 290, 64-73.

Jones, A.M., Collins, R.N., Rose, J., Waite, T.D. (2009) The effect of silica and natural organic matter on the Fe(II)-catalysed transformation and reactivity of iron minerals. *Geochimica et Cosmochimica Acta* 73, 4409-4422.

Jones, C., Crowe, S.A., Sturm, A., Leslie, K.L., MacLean, L.C.W., Katsev, S., Henny, C., Fowle, D.A. and Canfield, D.E. (2011) Biogeochemistry of manganese in ferruginous Lake Matano, Indonesia. *Biogeosciences* 8, 2977-2991.

Jones, J.G. (1983) A note on the isolation and enumeration of bacteria which deposit and reduce ferric iron. *Journal of Applied Bacteriology* 54, 305-310.

Jones, J.G., Gardener, S., Simon, B.M. (1983) Bacterial reduction of ferric iron in a stratified eutrophic lake. *Journal of General Microbiology* 129, 131-139.

Jørgensen, B.B. (1977) The sulfur cycle of a coastal marine sediment (Limfjorden, Denmark). *Limnology and Oceanography* 22, 814-832.

Journet, E., Desboeufs, K.V., Caquineau, S., Colin, J-L. (2008) Mineralogy as a critical factor in dust iron solubility. *Geophysical Research Letters* 35, L07805.

Kah, L.C., Lyons, T.W., Frank, T.D. (2004) Low marine sulphate and protracted oxygenation of the Proterozoic biosphere. *Nature* 431, 834-838.

Kakegawa, T., Kawai, H., Ohmoto, H. (1999) Origins of pyrites in the ~2.5 Ga Mt. McRae Shale, the Hamersley district, Western Australia. *Geochimica et Cosmochimica Acta* 62, 3205-3200.

Kappler, A., Newman, D.K. (2004) Formation of Fe(III)-minerals by Fe(II)-oxidizing photoautotrophic bacteria. *Geochimica et Cosmochimica Acta* 68, 1217-1226.

Kappler, A., Straub, K.L. (2005) Geomicrobiological cycling of iron. *Molecular Geomicrobiology* 59, 85-108.

Kappler, A., Pasquero, C., Konhauser, K., Newman, D.K. (2005) Deposition of banded iron formations by phototrophic Fe(II)-oxidizing bacteria. *Geology* 33, 865-868.

Kashefi, K., Lovley, D. (2003) Extending the upper temperature limit for life. *Science* 310, 934.

Kasten, S., Jorgensen, B.B. (2000) Sulfate reduction in marine sediments. In: Zabel, M. (Ed.) Marine Geochemistry. Springer-Verlag, pp. 263-281.

Kendall, B., Gordon, G.W., Poulton, S.W., Anbar, A.D. (2011) Molybdenum isotope constraints on the extent of late Paleoproterozoic ocean euxinia. *Earth Planetary Science Letters* 307, 450-460.

Kharecha, P., Kasting, J., Siefert, J. (2005) A coupled atmosphere-ecosystem model of the early Archean Earth. *Geobiology* 3, 53-76.

Kirschvink, J.L. (1992) Late Proterozoic Low-Latitude Global Glaciation: The Snowball Earth. In: Schopf, J.W., Klein, C. (Eds.) The Proterozoic Biosphere. The Press Syndicate of the University of Cambridge, Cambridge, pp.51-58.

Kirschvink, J.L., Kopp, R.E. (2008) Palaeoproterozoic ice houses and the evolution of oxygen-mediating enzymes: the case for a late origin of photosystem II. *Philosophical Transactions of the Royal Society B* 363, 2755-2765.

Klotz, M.G., Stein, L.Y. (2008) Nitrifier genomics and evolution of the nitrogen cycle. *Fems Microbiology Letters* 278, 146-156.

Knoll, A.H. (1992) Biological and biogeochemical preludes to the Ediacaran radiation. In: Lipps, J.H., Signor, P.W. (Eds.) Origin and Early Evolution of the Metazoa. Plenum Press, New York, pp.53-84.

Knoll, A.H. (2003) Life on a Young Planet. The First Three Billion Years of Evolution on Earth. Princeton University Press, Princeton and Oxford.

Konhauser, K.O., Lalonde, S.V., Amskold, L., Holland, H.D. (2007) Was there really an Archean phosphate crisis? *Science* 315, 1234-1234.

Kostka, J.E., Luther, G.W. III (1994) Partitioning and speciation of solid phase iron in saltmarsh sediments. *Geochimica et Cosmochimica Acta* 58, 1701-1710.

Kostka, J.E., Nealson, K.H. (1995) Dissolution and reduction of magnetite by bacteria. *Environmental Science and Technology* 29, 2535-2540.

Kostka, J.E., Haefele, E., Viehweger, R., Stucki, J.W. (1999) Respiration and dissolution of Iron (III)-containing clay minerals by bacteria. *Environmental Science & Technology* 33, 3127-3133.

Krachler, R., Jirsa, F., Ayromlou, A. (2005) Factors influencing the dissolved iron input by rivers to the open ocean. *Biogeosciences* 2, 311-315.

Kraemer, S.M. (2006) Iron oxide dissolution and solubility in the presence of siderophores. *Aquatic Science* 3, 3-18.

Kraemer, S.M., Butler, A., Borer, P., Cervini-Silva, J. (2005) Siderophores and the dissolution of iron-bearing minerals in marine systems. *Reviews in Mineralogy and Geochemistry* 59, 53-84.

Krauskopf, K.B. (1957) Separation of manganese and iron in sedimentary processes. *Geochimica et Cosmochimica Acta* 12, 61-84.

Krauskopf, K.B. (1979) Introduction to Geochemistry, 2nd ed. McGraw-Hill, New York.

Kuma, K, Matsunaga, K. (1995) Availability of colloidal ferric oxides to coastal marine phytoplankton. *Marine Biology* 122, 1-11.

Kuma, K., Nakabayashi, S., Suzuki, Y., Matsunaga, K. (1992) Dissolution rate and solubility of hydrous ferric oxide in seawater. *Marine Chemistry* 38, 133-143.

Kump, L.R., Holland, H.D. (1992) Iron in Precambrian rocks: Implications for the global oxygen budget of the ancient Earth. *Geochimica et Cosmochimica Acta* 56, 3217-3223.

Kump, L.R., Seyfried, W.E. (2005) Hydrothermal Fe fluxes during the Precambrian: Effect of low oceanic sulfate concentrations and low hydrostatic pressure on the composition of black smokers. *Earth Planetary Science Letters* 235, 654-662.

Kump, L.R., Pavlov, A., Arthur, M.A. (2005) Massive release of hydrogen sulfide to the surface ocean and atmosphere during intervals of oceanic anoxia. *Geology* 33, 397-400.

Kupka, D., Rzhepishevska, O.I., Dopson, M., Lindstrom, E.B., Karnachuk, O.V., Tuovinen, H. (2007) Bacterial oxidation of ferrous iron at low temperatures. *Biotechnology and Bioengineering* 97, 1470-1478.

Kuypers, M.M.M., Pancost, R.D., Nijenhuis, I.A., Damste, J.S.S. (2002) Enhanced productivity led to increased organic carbon burial in the euxinic North Atlantic basin during the late Cenomanian oceanic anoxic event. *Paleoceanography* 17, 13.

Kuypers, M.M.M., Lourens, L.J., Rijpstra, W.R.C., Pancost, R.D., Nijenhuis, I.A., Damste, J.S.S., (2004) Orbital forcing of organic carbon burial in the proto-North Atlantic during oceanic anoxic event 2. *Earth Planetary Science Letters* 228, 465-482.

Lafon, S., Rajot, J-L., Alfaro, S.C., Guadichet, A. (2004) Quantification of iron oxides in desert aerosol. *Atmospheric Environment* 38, 1211-1218.

Lafon, S., Sokolik, I.N., Rajot, J.L., Caquineau, S, Gaudichet, A. (2006) Characterization of iron oxides in mineral dust aerosols: Implications for light absorption. *Journal of Geophysical Research* 111, D21207.

Lam, P., Kuypers, M.M.M. (2011) Microbial Nitrogen Cycling Processes in Oxygen Minimum Zones, Annual Review of Marine Science, Vol 3. Annual Reviews, Palo Alto, pp. 317-345.

Lam, P.J., Bishop, J.K.B. (2008) The continental margin is a key source of iron to the HNLC North Pacific Ocean. *Geophysical Research Letters* 35, L07608.

Lam, P.J., Bishop, J.K.B., Henning, C.C., Marcus, M.A., Waychunas, G.A., Fung, I.Y. (2006) Wintertime phytoplankton bloom in the subarctic Pacific supported by continental margin iron. *Global Biogeochemical Cycles* 20, GB1006.

Lam, P.J., Ohnemus, D.C., Marcus, M.A. (2012) The speciation of marine particulate iron adjacent to active and passive continental margins. *Geochimica et Cosmochimica Acta* (doi:10.1016/j.gca.2011.11.044).

Lancelot, C., de Montey, A., Goose, H., Becquefort, S., Schoemann, V., Basquer, B., Vancoppenolle, M (2009) Spatial distribution of the iron supply to phytoplankton in the Southern Ocean: a model study. *Biogeosciences* 6, 2861-2878.

Landing, W.M., Bruland, K.W. (1987) The contrasting biogeochemistry of iron and manganese in the Pacific Ocean. *Geochimica et Cosmochimica Acta* 51, 29-43.

Lannuzel, D., Schoemann, V., de Jong, J., Tison, J-L., Chou, L. (2007) Distribution and biogeochemical behavior of iron in the East Antarctica sea ice. *Marine Chemistry* 106, 18-32.

Lannuzel, D., Schoemann, V., de Jong, J., Chou, L., Deille, B., Becquevort, S., Tison, J-L. (2008) Iron study during a time series in the western Weddell pack ice. *Marine Chemistry* 108, 85-95.

Large, R.R., Bull, S.W., Cooke, D.R., McGoldrick, P.J. (1998) A genetic model for the H.Y.C. deposit, Australia: Based on regional sedimentology, geochemistry, and sulfide-sediment relationships. *Economic Geology* 93, 1345-1368.

Laruelle, G.G., Roubeix, V., Sferratore, A., Brodherr, B., Ciuffa, D., Conley, D.J., Durr, H.H., Garnier, J., Lancelot, C., Phuong, Q.L.T., Meunier, J.D., Meybeck, M., Michalopoulos, P., Moriceau, B., Longphuirt, S.N., Loucaides, S., Papush, L., Presti, M., Ragueneau, O., Regnier, P., Saccone, L., Slomp, C.P., Spiteri, C., Van Cappellen, P. (2009) Anthropogenic perturbations of the silicon cycle at the global scale: Key role of the land-ocean transition. *Global Biogeochemical Cycle* 23, 17.

Lasaga, A.C., Berner, R.A. (1998) Fundamental aspects of quantitative models for geochemical cycles. *Chemical Geology* 145, 161-175.

Lavender, K.L., Owens, W.B., Davis, R.E. (2005) The mid-depth circulation of the subpolar North Atlantic Ocean as measured by sub-surface floats. *Deep-Sea Research* I 52, 767-785.

Lazaro, F.J., Gutierrez, L., Barron, V., Gelado, M.D. (2008) The speciation of iron in desert dust collected in Gran Canaria (Canary Islands): Combined chemical, magnetic and optical analysis. *Atmospheric Environment* 42, 8987-8896.

Lefevre, N., Watson, A.J. (1999) Modeling the geochemical cycle of iron in the oceans and its impact on atmospheric CO_2 concentrations. *Global Biogeochemical Cycles* 13, 727-736.

Lerman, A. (1979) Geochemical Processes: Water and Sediment Environments, Wiley, New York.

Leventhal, J., Taylor, C. (1990) Comparison of methods used to determine degree of pyritization. *Geochimica et Cosmochimica Acta* 54, 2621-2625.

Levitus S., Burgett, R., Boyer T.P. (1994) World Ocean Atlas vol.3

Li, C., Love, G.D., Lyons, T.W., Fike, D.A., Sessions, A.L., Chu, X. (2010) A stratified redox model for the Ediacaran ocean. *Science* 328, 80-83.

Libes, S. 2009. Introduction to Marine Biogeochemistry. Academic Press, Elsevier, Amsterdam.

Lin, S., Morse, J.W. (1991) Sulfate reduction and iron sulfide mineral formation in Gulf of Mexico anoxic sediments. *American Journal of Science* 291, 55-89.

Lin, H., Rauschenberg, S., Hexel, C.R., Shaw, T.J., Twining, B.S. (2011) Free-drifting icebergs as sources of iron to the Weddell Sea. *Deep-Sea Research II* 58, 1392-1406.

Lisitzin, A.P. (2002) Sea-Ice and Iceberg Sedimentation in the Ocean: Recent and Past. Springer-Verlag, Berlin.

Liu, L., Yu, L.L., Pearl, D.K., Edwards, S.V. (2009) Estimating Species Phylogenies Using Coalescence Times among Sequences. *Systems Biology* 58, 468-477.

Liu, X., Millero, F.J. (1999) The solubility of iron hydroxide in sodium chloride solution. *Geochimica et Cosmochimica Acta* 63, 3487-3497.

Logan, G.A., Hayes, J.M., Hieshima, G.B., Summons, R.E. (1995) Terminal Proterozoic reorganization of biogeochemical cycles. *Nature* 376, 53-56.

Longmuir, I.S. (1954) Respiration rate of bacteria as a function of oxygen concentration. *Biochemistry Journal* 57, 81-87.

Loscher, B.M., de Jong, J.T.M., de Baar, H.J.W., Veth, C., Dehairs, F. (1997) The distribution of iron in the Antarctic Circumpolar Current. *Deep-Sea Research II*, 143-187.

Lovley, D.R., Phillips, E.J.P. (1986) Organic matter mineralization with reduction of ferric iron in anaerobic sediments. *Applied and Environmental Microbiology* 51, 683-689.

Lovley, D.R., Phillips, E.J.P. (1988) Novel mode of microbial metabolism; organic carbon oxidation coupled to dissimilatory reduction of iron and manganese. *Applied and Environmental Microbiology* 6, 145-155.

Lovley, D.R., Coates, J.D., BluntHarris, E.L., Phillips, E.J.P., Woodward, J.C. (1996) Humic substances as electron acceptors for microbial respiration. *Nature* 382, 445-448.

Lovley, D.R., Holmes, D.E., Nevin, K.P. (2004) Dissimilatory Fe(III) and Mn(IV) reduction. *Advances in Microbial Physiology* 49, 219-286.

Lyons, T.W. (1997) Sulfur isotope trends and pathways of iron sulfide formation in the Upper Holocene sediments of the anoxic Black Sea. *Geochimica et Cosmochimica Acta* 61, 3367-3382.

Lyons, T.W., Berner, R.A. (1992) Carbon-sulfur-iron systematics of the uppermost deep-water sediments of the Black Sea. *Chemical Geology* 99, 1-27.

Lyons T.W., Severmann S (2006) A critical look at iron paleoredox proxies based on new insights from modern euxinic marine basins. *Geochimica et Cosmochimica Acta* 70, 5698-5722.

Lyons, T.W., Werne, J.P., Hollander, D.J., Murray, J.W. (2003) Contrasting sulfur geochemistry and Fe/Al and Mo/Al ratios across the last oxic-to-anoxic transition in the Cariaco Basin, Venezuela. *Chemical Geology* 195, 131-157.

Lyons, T.W., Reinhard, C.T., Scott, C. (2009) Redox redux. *Geobiology* 7, 489-494.

Mackey, D.J., O'Sullivan, J.E., Watson, R.J. (2002) Iron in the western Pacific: A riverine or hydrothermal source for iron in the Equatorial Undercurrent. *Deep-Sea Research* 40, 877-893.

Mackie, D.S., Boyd, P.W., Hunter, K.A., McTainsh, G.H. (2005) Simulating the cloud processing of iron in Australian dust: pH and dust concentration. *Geophysical Research Letters* 32, L06809.

Maher, B.A., Prospero, J.M., Mackie, D., Gaiero, D., Hesse, P.P., Balkanski, Y. (2010) Global connections between aeolian dust, climate and ocean biogeochemistry at the present day and at the last glacial maximum. *Earth-Science Reviews* 99, 61-97.

Mahowald, N.M., Muhs, D.R., Levis, S., Rasch, P.J., Yoshioka, M., Zender, C.S., Luo, C. (2006) Change in atmospheric mineral aerosols in response to climate: Last glacial period, preindustrial, modern, and doubled carbon dioxide climates. *Journal of Geophysical Research* 111 D10202.

Maldonado, M.T., Price, N.M. (2001) Reduction and transport of organically bound iron by *Thalassiosire oceanica* (Bactillariophyceae). *Journal of Phycology* 37, 298-309.

Martin JH (1990) Glacial-interglacial CO_2 change: the iron hypothesis. *Paleoceanography* 5, 1-11.

Martin, J.H., Gordon, R.M. (1988) Northeast Pacific iron distributions in relation to phytoplankton productivity. *Deep-Sea Research* 35, 177-196.

Martin, J.H., Gordon, M., Fitzwater, S.E. (1990) Iron in Antarctic waters. *Nature* 345, 156-158.

Marz, C., Poulton, S.W., Beckmann, B., Kuster, K., Wagner, T., Kasten, S. (2008) Redox sensitivity of P cycling during marine black shale formation; Dynamics of sulfidic and anoxic, non-sulfidic bottom waters. *Geochimica Cosmochimica Acta* 72, 3703-3717.

Mawji, E., Gledhill, M., Milton, J.A., Tarran, G.A., Ussher, S., Thompson A., Wolff, G.W., Worsfold, P.J., Achterberg, E.P. (2008) Hydroxamate siderophores: occurrence and importance in the Atlantic Ocean. *Environmental Science & Technology* 42, 8675-8680.

Maynard, J.B. (2010) The Chemistry of Manganese Ores through Time: A Signal of Increasing Diversity of Earth-Surface Environments. *Economic Geology* 105, 535-552.

McKibben, M.A., Barnes, H.L. (1986) Oxidation of pyrite in low-temperature acidic solutions – rate laws and surface textures. *Geochimica et Cosmochimica Acta* 50, 1509-1520.

McKibben, M.A., Tallant, B.A., del Angel, J.K. (2008) Kinetics of inorganic arsenopyrite oxidation in acidic aqueous solutions. *Applied Geochemistry* 23 121-135.

McManus, J., Berelson, W.M., Coale, K.H., Kilgore, T.E. (1997) Phosphorus regeneration in continental margin sediments. *Geochimica et Cosmochimica Acta* 61, 2891-2907.

Measures, C.I. (1999) The role of entrained sediments in sea ice in the distribution of aluminium and iron in the surface waters of the Arctic Ocean. *Marine Chemistry* 68, 59-70.

Meguro, H., Toba, Y., Murkami, H., Kimura, N. (2004) Simultaneous remote sensing of chlorophyll, sea ice and sea surface temperature in the Antarctic waters with special reference to the primary production from ice algae. *Advances in Space Research* 33, 1168-1172.

Meskhidze, N., Chameides, W.L., Nenes, A., Chen, G. (2003) Iron mobilization in mineral dust; Can anthropogenic SO_2 emissions affect ocean productivity? *Geophysical Research Letters* 30, 2085.

Michel, F.M., Ehm, L., Aritao, S.M., Lee, P.L., Chupas, P.J., Liu, G., Strongin, D.R., Schoonen, M.A.A., Phillips, B.L., Parise, J.B., (2007) The structure of ferrihydrite: a nanocrystalline mineral. *Science* 216, 1726-1729.

Mikucki, J.A., Pearson, A., Johnston, D.T., Turchyn, A.V., Farquhar, J., Schrag, D.P., Anbar, A., Prisco, J.C., Lee, P.A. (2009) A contemporary microbially maintained subglacial ferrous 'ocean'. *Science* 324, 397-400.

Miller, A.-F., Orme-Johnson, W.H. (1992) The Dependence on Iron Availability of Allocation of Iron to Nitrogenase Components in *K. pneumoniae* and *E. coli*. *Journal of Biological Chemistry* 267, 9398-9408.

Miller, W.L., King, D.W., Lin, J., Kester, D.R. (1995) Photochemical cycling of iron in coastal seawater. *Marine Chemistry* 50, 63-77.

Millero, F.J., Sotolongo, S., Izaguirre, M. (1987) The oxidation kinetics of Fe(II) in seawater. *Geochimica et Cosmochimica Acta* 51, 793-801.

Millero, F.J., Yao, W., Aicher, J. (1995) The speciation of Fe(II) and Fe(III) in natural waters. *Marine Chemistry* 50, 21-39.

Moffett, J.W. (2001) Transformation among Different Forms of Iron in the Ocean. In: Turner, D.R., Hunter, K.A. (Eds.) The Biogeochemistry of Iron in Seawater. Wiley, New York, pp. 343-372.

Moore, J.K., Braucher, O. (2008) Sedimentary and mineral dust sources of dissolved iron to the world ocean. *Biogeosciences* 5, 631-656.

Moore, J.K., Doney, S.C., Lindsay, K. (2004) Upper ocean ecosystem dynamics and iron cycling in a global three-dimensional model. *Global Biogeochemical Cycles* 18, GB4028.

Monteiro, F.M., Dutkiewicz, S., Follows, M.J. (2011) Biogeographical controls on the marine nitrogen fixers. *Global Biogeochemistry Cy* 25, 8.

Morel, F.M.M., Price, N.M. (2003) The biogeochemical cycles of trace metals in the oceans. *Science* 300, 944-947.

Morse J.W., Emeis, K.C. (1990) Controls on C/S ratios in hemipelagic sediments. *American Journal of Science* 290, 1117-1135.

Morse, J.W., Berner, R.A. (1995) What determines sedimentary C/S ratios? *Geochimica et Cosmochimica Acta* 59, 1073-1077.

Mortimer, C.H. (1941) The exchange of dissolved substances between mud and water in lakes. *Journal of Ecology* 29, 280-329.

Mosley, L.M., Hunter, K.A., Ducker, W.A. (2003) Forces between colloidal particles in natural waters. *Environmental Science & Technology* 37, 3303-3308.

Munch, J.C., Ottow, J.C.G. (1982) Effect of cell contact and Fe(III)-oxide form on bacterial iron reduction. *Zeitschrift für Pflanzenernährung und Bodenkunde* 145, 66-77.

Myers, C.R., Myers, J.M. (1992) Localization of cytochromes to the outer-membrane of ananerobically grown *Shewanella putrefaciens* MR-1 *Journal of Bacteriology* 174, 3429-3438.

Neubauer, S.C., Emerson, D., Megonigal, J.P. (2002) Life at the energetic edge: Kinetics of circumneutral iron oxidation by lithotrophic iron-oxidizing bacteria isolated from the wetland-plant rhizosphere. *Applied and Environmental Microbiology* 68, 3988-3995.

Nevin, K.P., Lovley, D.R. (2000) Lack of production of electron-shuttling compounds or solubilization of Fe(III) during reduction of insoluble Fe(III) oxide by *Geobacter metallireducens*. *Applied and Environmental Microbiology* 66, 2248-2251.

Nevin, K.P., Lovley, D.R. (2002) Mechanisms for accessing insoluble Fe(III) oxide during dissimilatory Fe(III) reduction by *Geothrix fermentans*. *Applied and Environmental Microbiology* 68, 2294-2299.

Newman, D.K., Kolter, R. (2000) A role for excreted quinones in extracellular electron transfer. *Nature* 405, 94-97.

Nicholson, R.V., Gillham, R.W., Reardon, E.J. (1988) Pyrite oxidation in carbonate-buffered solution: 1. Experimental kinetics. *Geochimica et Cosmochimica Acta* 52, 1077-1085.

Nielsen, L.P., Risgaard-Petersen, N., Fossing, H., Christensen, P.B., Sayama, M. (2010) Electric currents couple spatially separated biogeochemical processes in marine sediment, *Nature* 463, 1071-1074.

Nishioka, J., Ono, T., Saito, H., Nakatsuka, T., Takeda, S., Yoshimura, T., Suzuki, K., Kuma, K., Nakabayashi, S., Tsumune, D., Mitsudera, H., Johnson, W.K., Tsuda, A. (2007) Iron supply to the western subarctic Pacific: Importance of iron export from the Sea of Okhotsk. *Journal of Geophysical Research* 112, C10012.

Nodwell, L.M., Price, N.M. (2001) Direct use of inorganic colloidal iron by marine thixotrophic phytoplankton. *Limnology and Oceanography* 46, 765-777.

Nordstrom, D.K., Southam, G. (1997) Geomicrobiology of sulfide mineral oxidation. In: Banfield, J.F., Nealson, K.H. (Eds.) Geomicrobiology: Interactions between Microbes and Minerals. Mineralogical Society of America, Washington, pp. 361-390.

Ntarlagiannis, D., Atekwana, E.A., Hill, E.A., Gorby, Y. (2007) Microbial nanowires: Is the subsurface "hardwired"? *Geophysical Research Letters* 34, 5.

Obuekwe, C.O., Westlake, D.W.S. (1982) Effect of medium composition on cell pigmentation, cytochrome content, and ferric iron reduction in a *Pseudomonas* sp. isolated from crude oil. *Canadian Journal of Microbiology* 28, 989-992.

Ohle, W. (1937) Kolloidgele als nahrstoffregulatoren der gewasser. *Naturwissenschaften* 25, 471-474.

Olson, J.M. (1978) Precambrian evolution of photosynthetic and respiratory organisms. *Evolutionary Biology* 11, 1-37.

Oremland, R.S., Taylor, B.F. (1978) Sulfate reduction and methanogensis in marine sediments. *Geochimica et Cosmochimica Acta* 42, 209-214.

Ottow, J.C.G. (1968) Evaluation of iron-reducing bacteria in soils and physiological mechanism of iron-reduction in *Aerobacter aerogenes*. *Zeitschrift Für Allgemeine Mikrobiologie* 8, 441-443.

Pattyn, F. (2010) Antarctic subglacial conditions inferred from a hybrid ice sheet/ice stream model. *Earth Planetary Science Letters* 295, 451-461.

Pavlov, A.A., Kasting, J.F. (2002) Mass-independent fractionation of sulfur isotopes in Archean sediments: Strong evidence for an anoxic Archean atmosphere. *Astrobiology* 2, 27-41.

Pilskaln, C.H., Lehmann, C., Paduan, J.B., Silver, M.W. (1998) Spatial and temporal dynamics in marine aggregate abundance, sinking rate and flux: Monterey Bay, central California. *Deep-Sea Research II* 45, 1803-1837.

Planavsky, N.J., McGoldrick, P., Scott, C.T., Li, C., Reinhard, C.T., Kelly, A.E., Chu, X., Bekker, A., Love, G.D., Lyons, T.W. (2011) Widespread iron-rich conditions in the mid-Proterozoic ocean. *Nature* 477, 448-451.

Postma, D. (1985) Concentrations of Mn and separation from Fe in sediments -1. Kinetics and stoichiometry of the reaction between birnessite and dissolved Fe(II) at 10 °C. *Geochimica et Cosmochimica Acta* 49, 1023-1033.

Poulton, S.W. (2003) Sulfide oxidation and iron dissolution kinetics during the reaction of dissolved sulfide with ferrihydrite. *Chemical Geology* 202, 79-94.

Poulton S.W., Raiswell R. (2002) The low-temperature geochemical cycle of iron: from continental fluxes to marine sediment deposition. *American Journal of Science* 302, 774-805.

Poulton, S.W., Canfield, D.E. (2005) Development of a sequential extraction procedure for iron; implications for iron partitioning in continentally derived particulates. *Chemical Geology* 214, 209-221.

Poulton S.W., Raiswell R. (2005) Chemical and physical characteristics of iron oxides in riverine and glacial meltwater sediments. *Chemical Geology* 218, 203-221.

Poulton, S.W., Canfield, D.E. (2011) Ferruginous conditions: a dominant feature of the ocean through earth's history. *Elements* 7, 107-112.

Poulton, S.W., Canfield, D.E., Fralick, P. (2004) The transition to a sulfidic ocean ~1.84 billion years ago. *Nature* 431, 173-177.

Poulton, S.W., Krom, M.D., Raiswell R. (2004) A revised scheme for the reactivity of iron (oxyhydr)oxide minerals towards dissolved sulfide. *Geochimica et Cosmochimica Acta* 68, 3703-3715.

Poulton, S.W., Fralick, P.W., Canfield, D.E. (2010) Spatial variability in oceanic redox structure 1.8 billion years ago. *Nature Geoscience* 3, 486-490.

Pyzik, A.J., Sommer, S.E. (1981) Sedimentary iron monosulfides: kinetics and mechanism of formation. *Geochimica et Cosmochimica Acta* 45, 687-698.

Raiswell, R. (1984) Chemical models of solute acquisition in glacial meltwaters. *Journal of Glaciology* 30, 49-57.

Raiswell, R. (2011a) Iron transport from the continents to the open ocean: The aging-rejuvenation cycle. *Elements* 7, 101-106.

Raiswell, R. (2011b) Iceberg-hosted nanoparticulate Fe in the Southern Ocean: Mineralogy, origin, dissolution kinetics and source of bioavailable Fe. *Deep-Sea Research* 58, 1364-1375.

Raiswell, R., Thomas, A.G. (1984) Solute acquisition in glacial meltwaters. I. Fjallssjokull (S.E. Iceland): bulk meltwaters with closed-system characteristics. *Journal of Glaciology* 30, 35-43.

Raiswell, R., Berner, R.A. (1985) Pyrite formation in euxinic and semi-euxinic sediments. *American Journal of Science* 285, 710-724.

Raiswell, R., Berner, R.A. (1987) Organic carbon losses during burial and thermal maturation of normal marine shales. *Geology* 15, 853-856.

Raiswell, R., Berner, R.A. (1986) Pyrite and organic matter in normal marine shales. *Geochimica et Cosmochimica Acta* 50, 1967-1976

Raiswell, R., Al-Biatty, H.J. (1989) Depositional and diagenetic C-S-Fe signatures in early Paleozoic normal marine shales. *Geochimica et Cosmochimica Acta* 53, 1147-1152.

Raiswell R., Canfield, D.E. (1996) Rates of reaction between silicate iron and dissolved sulfide in Peru Margin sediments. *Geochimica et Cosmochimica Acta* 60, 2777-2787.

Raiswell, R., Canfield, D.E. (1998) Sources of iron for pyrite formation in marine sediments. *American Journal of Science* 298, 219-245.

Raiswell, R., Anderson, T.F (2005) Reactive Iron Enrichment in Sediments Deposited beneath Euxinic Bottom Waters: Constraints on Supply by Shelf Recycling. In: McDonald, I., Boyce, A.J., Butler, I., Herrington, R.J., Polya, D. (Eds.) Mineral Deposits and Earth Evolution. *Geological Society of London Special Publications* 218, 179-194.

Raiswell, R., Buckley, F., Berner, R.A., Anderson, T.F. (1988) Degree of pyritization of iron as a paleoenvironmental indicator. *Journal Sedimentary Petrology* 58, 812-819.

Raiswell, R., Canfield., D.E., Berner, R.A. (1994) A comparison of iron extraction methods for the determination of degree of pyritization and recognition of iron-limited pyrite formation. *Chemical Geology* 111, 101-111.

Raiswell, R., Newton, R., Wignall, P.B. (2001) An indicator of water-column anoxia: Resolution of biofacies variations in the Kimmeridge Clay (Upper Jurassic, U.K.). *Journal of Sedimentary Research* 71, 286-294.

Raiswell R., Tranter M., Benning L.G., Siegert M., De'ath R., Huybrechts P., Payne T. (2006) Contributions from glacially derived sediment to the global iron oxyhydroxide cycle: implications for iron delivery to the oceans. *Geochimica et Cosmochimica Acta* 70, 2765-2780.

Raiswell, R., Benning, L.G., Tranter, M., Tulaczyk, S. (2008a) Bioavailable iron in the Southern Ocean: The significance of the iceberg conveyor belt. *Geochemical Transactions* 9, 7.

Raiswell, R., Benning, L.G., Davidson, L, Tranter, M. (2008b) Nanoparticulate bioavailable iron minerals in icebergs and glaciers. *Mineralogical Magazine* 72, 345-348.

Raiswell, R., Newton, R., Bottrell, S.H., Coburn, P., Briggs, D.E.G., Bond, D.P.G., Poulton, S.W. (2008c) Turbidite depositional influences on the diagenesis of Beecher's Trilobite Bed and the Hunsruck Slate: sites of soft tissue pyritization. *American Journal of Science* 308, 105-129.

Raiswell, R., Benning, L.G., Davidson, L., Tranter, M., Tulaczyk, S. (2009) Schwertmannite in wet, acid and oxic microenvironments beneath polar and polythermal glaciers. *Geology* 37, 431-434.

Raiswell, R., Vu, H.P., Brinza, L., Benning, L.G. (2010) The determination of labile Fe in ferrihydrite by ascorbic acid extraction: methodology, dissolution kinetics and loss of solubility with age and de-watering. *Chemical Geology* 278, 70-79.

Raiswell, R., Reinhardt, C.T., Derkowski, A., Owens, J., Bottrell, S.H., Anbar, A.D., Lyons, T.W. (2011) Formation of syngenetic and early diagenetic iron minerals in the late Archean Mt. McRae Shale, Hamersley Basin, Australia: new insights on the patterns, controls and paleoenvironmental implications of authigenic mineral formation. *Geochimica et Cosmochimica Acta* 75, 1072-1087.

Rasmussen, B., Fletcher, I.R., Brocks, J.J., Kilburn, M.R. (2008) Reassessing the first appearance of eukaryotes and cyanobacteria. *Nature* 455, 1101-U1109.

Raymond, J., Segre, D. (2006) The effect of oxygen on biochemical networks and the evolution of complex life. *Science* 311, 1764-1767.

Redfield, A.C., Ketchum, B.H., Richards, F.A. (1963) The influence of organisms on the composition of seawater. In: Hill, N.M. (Ed.) The Sea. Academic Press, London, pp.26-77.

Reed, D.C., Slomp, C.P., Gustafsson, B.G. (2011) Sedimentary phosphorus dynamics and the evolution of bottom-water hypoxia: A coupled benthic-pelagic model of a coastal ecosystem. *Limnology and Oceanography* 56, 1075-1092.

Reguera, G., McCarthy, K.D., Mehta, T., Nicoll, J.S., Tuominen, M.T., Lovley, D.R. (2005) Extracellular electron transfer via microbial nanowires. *Nature* 435, 1098-1101.

Reinhard, C.T., Raiswell, R., Scott, C., Anbar, A.D., Lyons, T.W. (2009) A late Archean sulfidic sea stimulated by early oxidative weathering of the continents. *Science* 326, 713-716.

Rentz, J.A., Kraiya, C., Luther, G.W., Emerson, D. (2007) Control of ferrous iron oxidation within circumneutral microbial iron mats by cellular activity and autocatalysis. *Environmental Science & Technology* 41, 6084-6089.

Rickard, D. (1997) Kinetics of pyrite formation by the H_2S oxidation of Fe(II) monosulfide in aqueous solutions between 25°C and 125°C: the rate equation. *Geochimica et Cosmochimica Acta* 61.

Rickard, D., Luther, G.W. III (2007) Chemistry of iron sulfides. *Chemical Reviews* 107, 514-562.

Rickard, D., Schoonen, M.A.A., Luther, G.W. (1995) Chemistry of Iron Sulfides in Sedimentary Environments, in Vairavamurthy, M.A., Schoonen, M.A.A. (Eds.) Geochemical Transformations of Sedimentary Sulfur, *American Chemical Society Symposium Series* 612, 168-193.

Rich, H.W., Morel, F.M.M. (1990) Availability of well-defined iron colloids to the marine diatom *Thalassiosira weissflogii*. *Limnology and Oceanography* 35, 652-662.

Rignot, E., Bamber, J.L., van en Broeke, M.R., Davis, C., Li, Y., van den Berg, W.J., van Meijigaard, E. (2008) Recent Antarctic ice mass loss from radar interferometry and regional climate modeling. *Nature Geoscience* 1, 106-111.

Riley, J.P. (1958) The rapid analysis of silicate rocks and minerals. *Analytica Chimica Acta*, 19, 413-428.

Roden, E.E. (2003) Fe(III) oxide reactivity toward biological versus chemical reduction. *Environmental Science & Technology* 37, 1319-1324.

Roden, E. E. (2004) Analysis of long-term bacterial vs. chemical Fe(III) oxide reduction kinetics. *Geochimica et Cosmochimica Acta* 68, 3205-3216.

Roden, E.E., Urrutia, M.M. (2002) Influence of biogenic Fe(II) on bacterial crystalline Fe(III) oxide reduction. *Geomicrobiology Journal* 19, 209-251.

Roden, E.E., Urrutia, M.M., Mann, C.J. (2000) Bacterial reductive dissolution of crystalline Fe(III) oxide in continuous-flow column reactors. *Applied and Environmental Microbiology* 66, 1062-1065.

Ronov, A.B., Migdisov, A.A. (1971) Geochemical history of crystalline basement and sedimentary cover of the Russian and North American Platforms. *Sedimentology* 16, 173-183.

Rose, A.L., Waite, T.D. (2003) Kinetics of hydrolysis and precipitation of ferric iron in seawater. *Environmental Science & Technology* 37, 3897-3903.

Rose, A.L., Waite, T.D. (2007) Reconciling kinetic and equilibrium observations of iron(III) solubility in aqueous solutions with a polymer based model. *Geochimica et Cosmochimica Acta* 71, 5605-5619.

Rue, E.L., Bruland, K.W. (1995) Complexation of iron(III) by natural organic ligands in the Central North Pacific as determined by a new competitive ligand equilibration/adsorptive cathodic stripping voltammetric method. *Marine Chemistry* 50, 117-138.

Rue, E.L., Bruland, K.W. (1997) The role of organic complexation on ambient iron chemistry in the equatorial Pacific Ocean and the response of a mesoscale iron addition experiment. *Limnology and Oceanography* 42, 901-910.

Ruttenberg, K.C. (1992) Development of a Sequential Extraction Method for Different Forms of Phosphorus in Marine-Sediments. *Limnology and Oceanography* 37, 1460-1482.

Ruttenberg, K.C. (1993) Reassessment of the Oceanic Residence Time of Phosphorus. *Chemical Geology* 107, 405-409.

Ruttenberg, K.C. (2003) The global phosphorus cycle. In: Schlesinger, W. H. (Ed) Treatise on Geochemistry 8. Elsevier, Honolulu, pp. 585-643.

Sander, S., Mosley, L.M., Hunter, K.H. (2004) Investigation of interparticle forces in natural waters: effects of adsorbed humic acids on iron oxide and alumina surface properties. *Environmental Science & Technology* 38, 4791-4796.

Sarmiento, J.L., Herbert, T.D., Toggweiler, J.R. (1988) Causes of anoxia in the world ocean. *Global Biogeochemical Cycles* 2, 115-128.

Schidlowski, M., Appel, P.W.U., Eichmann, R., Junge, C.E. (1979) Carbon isotope geochemistry of the 3.7×10^9 -yr-old Isua sediments, West Greenland: implications for the Archean carbon and oxygen cycles. *Geochimica et Cosmochimica Acta* 43, 189-199.

Schieber, J. (1995) Anomalous iron distribution in shales as a manifestation of 'non-clastic' supply to sedimentary basins: relevance for pyritic shales, base-metal mineralization, and oolitic ironstone deposits. *Mineralium Deposita* 30, 294-302.

Schoonen, M.A.A. (2004) Mechanisms of Sedimentary Pyrite Formation. In: Amend, J.P., Edwards, K.J., Lyons, T.W (Eds.) Sulfur Biogeochemistry-Past and Present. Geological Society of America Special Paper 379, 117-134.

Schroth, A.W., Crusius, J., Sholkovitz, E.R., Bostick, B.C. (2009) Iron solubility driven by speciation in dust sources to the ocean. *Nature Geoscience* 2, 337-340.

Schwertmann, U., Fischer, W.R. (1973) Natural 'amorphous' ferric hydroxide. *Geoderma* 10, 237-247.

Schwertmann, U., Carlson, L. (2005) The pH-dependent transformation of schwertmannite to goethite at 25°C. *Clay Minerals* 40, 63-66.

Schwertmann, U., Stanjek, H., Becher, H.-H. (2004) Long-term in vitro transformation of 2-line ferrihydrite to goethite/hematite at 4, 10, 15 and 25°C. *Clay Minerals* 39, 433-438.

Scott, C., Lyons, T.W., Bekker, A., Shen, Y., Poulton, S.W., Chu, X., Anbar, A.D. (2008) Tracing the stepwise oxygenation of the Proterozoic ocean. *Nature* 452, 456-U455.

Scott, C.T., Bekker, A., Reinhard, C.T., Schnetger, B., Krapez, B., Rumble, D., Lyons, T.W. (2011) Late Archean euxinic conditions before the rise of atmospheric oxygen. *Geology* 39, 119-122.

Scott, D.T., McKnight, D.M., Blunt-Harris, E.L., Kolesar, S.E., Lovley, D.R. (1998) Quinone moieties act as electron acceptors in the reduction of humic substances by humics-reducing microorganisms. *Environmental Science & Technology* 32, 2984-2989.

Sedwick, P.N., DiTullio, G.R. (1997) Regulation of algal blooms in Antarctic shelf waters by the release of iron from melting sea ice. *Geophysical Research Letters* 24, 2515-2518.

Severmann, S., Lyons, T.W., Anbar, A., McManus, J., Gordon, G. (2009) Modern iron isotope perspective on the benthic iron shuttle and the redox evolution of the ancient oceans. *Geology* 36, 487-490.

Sharp, M., Parkes, J., Cragg, B., Fairchild, I.J., Lamb, H., Tranter, M. (1999) Widespread bacterial populations at glacier beds and their relationship to rock weathering and carbon cycling. *Geology* 27, 107-110.

Shaw, T.J., Hexel, C.R., Sherman, A.D., Smith, Jr., K.L., Kingelberger, S. (2011a) ^{234}Th-based carbon export around free-drifting icebergs in the Southern Ocean. *Deep-Sea Research II* 58, 1384-1391.

Shaw, T.J., Raiswell, R., Hexel, C.R., Vu, H.P., Moore, W.S., Dudgeon, R., Smith, K.L. (2011b) Input, composition and potential impact of terrigenous material from free-drifting icebergs in the Weddell Sea. *Deep-Sea Research II* 58, 1376-1383.

Shen, Y., Canfield, D.E., Knoll, A.H. (2002) Middle Proterozoic ocean chemistry: evidence from the McArthur Basin, Northern Australia. *American Journal of Science* 302, 81-109.

Shen, Y., Knoll, A.H., Walter, M.R. (2003) Evidence for low sulphate and anoxia in a mid-Proterozoic marine basin. *Nature* 423, 632-635.

Shen, Y., Zhang, T., Hoffman, P.F. (2008) On the coevolution of Ediacaran oceans and animals. *Proceedings of the National Academy of Sciences of the United States of America* 105, 7376-7381.

Shen, Z., Caquineau, S., Cao, J., Zhang, X., Han, Y., Gaudichet, A., Gomes, L. (2009) Mineralogical characteristics of soil dust from source regions in northern China. *Particuology* 7, 507-512.

Shi, Z. Krom, M.D., Bonneville, S., Baker, A.R., Jickells, T.D., Benning, L.G. (2009) Formation of iron nanoparticles and increase in iron reactivity in mineral dust during simulated cloud processing. *Environmental Science & Technology* 43, 6592-6596.

Shi, Z., Bonneville, S., Krom, M.D., Carslaw, K.S., Jickells, T. D, Benning, L.G. (2011a) Dissolution kinetics of iron in mineral dust at low pH during simulated atmospheric processing. *Atmospheric Chemistry and Physics Discussions* 11, 995-1007.

Shi, Z., Krom, M.D., Bonneville, S., Baker, A.R., Bristow, C., Drake, N., Mann, G., Carlsaw, K., McQuaid, J.B., Jickells, T., Benning, L.G. (2011b) Influence of chemical weathering and aging of iron oxides on the potential solubility of Saharan dust during simulated cloud processing. *Global Biogeochemical Cycles* 25, GB2010.

Siefert, R.L., Pehkonen, S.O., Erel, Y., Hoffmann, M.R. (1994) Iron photochemistry of aqueous suspensions of ambient aerosols with added organic acids. *Geochimica et Cosmochimica Acta* 58, 3271-3279.

Siever, R. (1992) The silica cycle in the Precambrian. *Geochimica et Cosmochimica Acta* 56, 3265-3272.

Singer, P.C., Stumm, W. (1970) Acid mine drainage: the rate determining step. *Science* 167, 1121-1123.

Skidmore, M.L., Foght, J.M., Sharp., M.J. (2000) Microbial life beneath a High Arctic glacier. *Applied and Environmental Microbiology* 66, 3214-3220.

Skidmore, M.L., Tranter, S., Tulaczyk, S., Lanoil, B. (2010) Hydrochemistry of ice stream beds-evaporitic or microbial effects? *Hydrological Processes* 24, 517-523.

Slack, J.F., Grenne, T., Bekker, A., Rouxel, O.J., Lindberg, P.A. (2007) Suboxic deep seawater in the late Paleoproterozoic: Evidence from hematitic chert and iron formation related to seafloor-hydrothermal sulfide deposits, central Arizona, USA. *Earth Planetary Science Letters* 255, 243-256.

Slomp, C.P., Malschaert, J.F.P., Lohse, L., Van Raaphorst, W. (1997) Iron and manganese cycling in different sedimentary environments on the North Sea continental margin. *Continental Shelf Research* 17, 1083-1117.

Smith, E.E., Shumate, K.S. (1970) Sulfide to Sulfate Reaction Mechanism. Department of the Interior, Federal Water Quality Administration, Washington DC, p. 115.

Smith, K.L., Robison, B.H., Helly, J.J., Kaufmann, R.S., Ruhl, H.A., Shaw, T.J., Twining, B.S., Vernat, M. (2007) Free-drifting icebergs: Hot spots of chemical and biological enrichment in the Weddell Sea. *Science* 317, 478-483.

Smith, K.L., Sherman, A.D., Shaw, T., Murray, A., Vernet, M., Cefarelli, A. (2011) Carbon export associated with free-drifting icebergs in the Southern Ocean. *Deep-Sea Research II* 58, 1485-1496.

Sørensen, J. (1982) Reduction of ferric iron in anaerobic, marine sediment and interaction with reduction of nitrate and sulfate. *Applied and Environmental Microbiology* 43, 319-324.

Southgate, P.N., Jackson, M.J., Winefield, P. (1997) Sequence stratigraphy of the upper McArthur Group: Teena Dolomite to looking glass formations. *Australian Geological Survey Organisation Record* 1997/12, unpaginated.

Spokes, L.J., Jickells, T.D. (1996) Factors controlling the solubility of aerosol trace metals in the atmosphere and on mixing into seawater. *Aquatic Geochemistry* 1, 355-374.

Starkey, R.L., Halvorson, H.O. (1927) Studies on the transformations of iron in nature. II. concerning the importance of micro-organisms in the solution and precipitation of iron. *Soil Science* 24, 381-402.

Statham, P.J., Skidmore, M., Tranter, M. (2007) Inputs of glacially derived dissolved and colloidal iron to the coastal ocean and implications for primary productivity. *Global Biogeochemical Cycles* 22 GB3013.

Steigenberger, S., Statham, P.J., Volker, C., Passow, U. (2010) The role of polysaccharides and diatom exudates in the redox cycling of Fe and the photoreduction of hydrogen peroxide in coastal seawater. *Biogeosciences* 7, 109-119.

Stibal, M., Tranter, M., Benning, L.G., Rehák, J. (2008) Microbial primary production on an Arctic glacier is insignificant in comparison to allochthonous organic carbon input. *Environmental Microbiology* 10, 2172-2178.

Stolp, B., Hasselhov, M. (2007) Changes in size distribution of fresh water nanoscale colloidal matter and associated elements on mixing with seawater. *Geochimica et Cosmochimica Acta* 71, 3292-3301.

Stolper, D.A., Revsbech, N.P., Canfield, D.E. (2010) Aerobic growth at nanomolar oxygen concentrations. *Proceedings of the National Academy of Sciences of the United States of America* 107, 18755-18760.

Straub, K.L., Benz, M., Schink, B., Widdel, F. (1996) Anaerobic, nitrate-dependent Microbial oxidation of ferrous iron. *Applied and Environmental Microbiology* 62, 1458-1460.

Straub, K.L., Rainey, F.A., Widdel, F. (1999) *Rhodovulum iodosum* sp. nov, and *Rhodovulum robiginosum* sp. nov., two new marine phototrophic ferrous-iron-oxidizing purple bacteria. *International Journal of Systemic Bacteriology* 49, 729-735.

Straub, K.L., Schonhuber, W.A., Buchholz-Cleven, B.E.E., Schink, B. (2004) Diversity of ferrous iron-oxidizing, nitrate-reducing bacteria and their involvement in oxygen-independent iron cycling. *Geomicrobiology Journal* 21, 371-378.

Stumm, W., Lee, G.F. (1961) Oxygenation of ferrous iron. *Industrial and Engineering Chemistry* 53, 143-146.

Stumm, W., Morgan J.J. (1970) Aquatic Chemistry. Wiley-Interscience, New York.

Sulzberger, B., Laubscher, H. (1995) Reactivity of various types of iron (III) (hydr)oxides towards light-induced dissolution. *Marine Chemistry* 50, 103-115.

Sunda, W.G. (2001) Bioavailability and Bioaccumulation of Iron in Seawater. In: Turner, D.R., Hunter, K.A. (Eds.) The Biogeochemistry of Iron in Seawater. Wiley, New York, pp. 41-84.

Tagliabue, A., Bopp, L., Aumont, O. (2009) Evaluating the importance of atmospheric and sedimentary iron sources to Southern Ocean biogeochemistry. *Geophysical Research Letters* 36, L13601.

Tagliabue, A., Bopp, L., Dutay, J-C., Bowie, A.R., Chever, F., Jean-Babtise, P., Bucciarelli, E., Lannuzel, D., Remeny, T., Sarthou, G., Aumont, A., Gehlen, M., Jeandel, C. (2010) Hydrothermal contribution to the oceanic dissolved iron inventory. *Nature Geoscience* 3, 252-256.

Takai, Y., Kamura, T. (1966) The mechanism of reduction in waterlogged paddy soil. *Folia Microbiologica* 11, 304-312.

Taylor, K.G., Macquaker, J.H.S. (2011) Iron minerals in marine sediments record chemical environments. *Elements* 7, 113-118.

Taylor, S.R., McLennan, S.M. (1985) The Continental Crust: Its Composition and Evolution. Blackwell, Oxford.

Thamdrup, B. (2000) Microbial manganese and iron reduction in aquatic sediments. *Advances in Microbial Ecology* 16, 41-84.

Thamdrup, B., Canfield, D.E. (1996) Pathways of carbon oxidation in continental margin sediments off central Chile. *Limnology and Oceanography* 41, 1629-1650.

Towe, K.M., Bradley, W.F. (1967) Mineralogical constitution of colloidal 'hydrous ferric oxide'. *Journal of Colloid and Interface Science* 24, 384-392.

Tranter, M. (2005) Sediment and Solute Transport in Glacial Meltwater Streams. In: Anderson, M., (Ed.), Encyclopedia of Hydrological Sciences. Wiley, New York, Chapter 169, pp. 1-13.

Tranter, M.T., Brown, G.H., Raiswell, R., Sharp, M.J., Gurnell, A.M. (1993) A conceptual model of solute acquisition by Alpine meltwaters. *Journal of Glaciology* 39, 573-561.

Tranter, M., Brown, G.H., Hodson, A., Gurnall, A.M., Sharp, M.J. (1994) Variations in nitrate concentration of glacial runoff in Alpine and sub-Polar Environments. IAMAP/IAHS Joint International Meeting Yokohama, Japan. *International Association of Hydrology Science Publication* 223, 299-311.

Tranter, M., Huybrechts, P., Munhoven, G., Sharp, M.J., Brown, G.H., Jones, I.W., Hodson, A.J., Hodgkins, R., Wadham, J.L. (2002) Glacial bicarbonate, sulphate and base cation fluxes during the last glacial cycle, and their potential impact on atmospheric CO_2. *Chemical Geology* 190, 33-44.

Tsikos, H., Matthews, A., Erel, Y., Moore, J.M. (2010) Iron isotopes constrain biogeochemical redox cycling of iron and manganese in a Palaeoproterozoic stratified basin. *Earth Planetary Science Letters* 298, 125-134.

Turner, J.T. (2002) Zooplankton fecal pellets, marine snow and sinking phytoplankton blooms. *Aquatic Microbial Ecology* 27, 57-102.

Usher, C.R., Michel, A.E., Grassian, V.H. (2003) Reactions on mineral dust. *Chemical Reviews* 103, 4883-4940.

Van Cappellen, P., Ingall, E.D. (1997) Redox stabilization of the atmosphere and oceans and marine productivity. *Science* 275, 406-408.

Van den Berg, C.M.G. (1995) Evidence for organic complexation of iron in seawater. *Marine Chemistry* 50, 139-157.

Van der Zee, C., Roberts, D.,R., Rancourth, D.G., Slomp, C.P. (2003) Nanogoethite is the dominant reactive oxyhydroxide phase in lake and marine sediments. *Geology* 31, 993-996.

Van Niel, C.B. (1931) On the morphology and physiology of the purple and green sulphur bacteria. *Archives of Microbiology* 3.

Velde, B. (2003) Green Clay Minerals. In: Mackenzie, F. T. (Ed) Treatise on Geochemistry 7. Elsevier, Amsterdam, pp. 309-324.

Velicogna, I., Wahr, J. (2006) Measurements of time-variable gravity show mass loss in Antarctica. *Science* 311, 1777-1779.

Vernadsky, V.I. (1998) The Biosphere. Springer-Verlag New York Inc., New York..

Vilge-Ritter, A., Rose, J., Maison, A., Bottero, J-Y., Laine, J-M. (1999) Chemistry and structure of aggregates formed with Fe-salts and natural organic matter. *Colloids and Surfaces 147A*, 297-308.

Visser, F., Gerringa, L.J.A., Van der Gaast, S.J., de Baar, H.J.W., Timmermans, K.R. (2003) The role of reactivity and content of iron of aerosol dust on growth rates of two Antarctic diatom species. *Journal of Phycology* 39, 1085-1094.

Voelker, B.M., Sedlack, D.L. (1995) Iron reduction by photoproduced superoxide in seawater. *Marine Chemistry* 53, 93-102.

Wächtershäuser, G. (1988) Pyrite formation, the first energy source for life: a hypothesis. *Systematic and Applied Microbiology* 10, 207-210.

Wadham, J.L., Bottrell, S.H., Tranter, M., Raiswell, R. (2004) Stable isotope evidence for microbial sulphate reduction at the bed of a polythermal high Arctic glacier. *Earth Planetary Science Letters* 219, 341-355.

Wadham, J.L., Tranter, M., Skidmore, M., Hodson, A.J., Priscu, J., Lyons, W.B., Sharp, M., Wynn, P., Jackson, M. (2010a) Biogeochemical weathering under ice: size matters. *Global Biogeochemical Cycles* 24, GB3025.

Wadham, J.L., Tranter, M., Hodson, A.J., Hodgkins, R., Bottrell, S., Copper, R., Raiswell, R. (2010b) Hydro-biogeochemical coupling beneath a large polythermal Arctic glacier: implications for subice sheet biogeochemistry. *Journal of Geophysical Research* 115, F04017.

Wadham, J.L., De'ath, R., Moneiro, F., Ridgewell, A., Raiswell, R., Tulaczyk, S. (2012) The potential role of the Antarctic Ice Sheet in *Global Biogeochemical Cycles*. *Transaction of the Royal Society of Edinburgh* (in review).

Wagener, T., Pulido-Villena, E., Guieu, C. (2008) Dust iron dissolution in seawater: Results from a one-year time-series in the Mediterranean Sea. *Geophysical Research Letters* 35, L16601.

Wagener, T., Guieu, C., Leblond, N. (2010) Effects of dust deposition on iron cycle in the surface Mediterranean Sea: results from a mesocosm seeding experiment. *Biogeosciences* 7, 3769-3781.

Waite, T.D. (2001) Thermodynamics of the Iron System in Seawater. In: Turner, D.R., Hunter, K.A. (Eds.) The Biogeochemistry of Iron in Seawater. Wiley, New York, pp. 291-339.

Waite, T.D., Morel, F.M.M. (1984) Photoreductive dissolution of colloidal iron oxides in natural waters. *Environmental Science & Technology* 18, 860-868.

Waite, T.D., Szymczak, R., Espey, Q.J., Furnas, M.J. (1995) Diel variations in iron speciation in northern Australian shelf waters. *Marine Chemistry* 50, 79-91

Waldbauer, J.R., Newman, D.K., Summons, R.E. (2011) Microaerobic steroid biosynthesis and the molecular fossil record of Archean life. *Proceedings of the National Academy of Sciences of the United States of America* 108, 13409-13414.

Waldbauer, J.R., Sherman, L.S., Sumner, D.Y., Summons, R.E. (2009) Late Archean molecular fossils from the Transvaal Supergroup record the antiquity of microbial diversity and aerobiosis. *Precambrian Research* 169, 28-47.

Wang, Y., Van Cappellen, P. (1996) A multicomponent reactive transport model of early diagenesis: Application to redox cycling in coastal marine sediments. *Geochimica et Cosmochimica Acta* 60, 2993-3014.

Wang, H.M., Bigham, J.M., Tuovinen, O.H. (2006) Formation of schwertmannite and its transformation to jarosite in the presence of acidophilic iron-oxidizing microorganisms. *Materials Science and Engineering* C 26, 588-592.

Waychunas, G.A. (2001) Structure, aggregation and characterization of nanoparticles. *Reviews in Mineralogy and Geochemistry* 44, 105-166.

Waychunas, G.A., Zhang, H. (2008) Structure, chemistry and properties of mineral nanoparticles. *Elements* 4, 381-387.

Waychunas, G.A., Kim, C.S., Banfield, J.F. (2005) Nanoparticulate iron oxide minerals in soils and sediments: unique properties and contaminant scavenging mechanisms. *Journal of Nanoparticle Research* 7, 409-433.

Wells, M.J., Goldberg, E.D. (1991) Occurrence of small colloids in seawater. *Nature* 353, 342-344.

Wells, M.J., Goldberg, E.D. (1992) Marine sub-micron particles. *Marine Chemistry* 40, 5-18.

Wells, M.J., Goldberg, E.D. (1994) The distribution of colloids in the North Atlantic and southern Oceans. *Limnology and Oceanography* 39, 286-302.

Wells M.L., Mayer L.M. (1991) The photoconversion of colloidal iron oxyhydroxides in seawater. *Deep-Sea Research* 38, 1379-1395.

Wells M.L., Zorkin N.G., Lewis A.G. (1983) The role of colloid chemistry in providing a source of iron to phytoplankton. *Journal of Marine Research* 41, 731-746.

Wells, M.L., Mayer, L.M., Guillard, R.R.L. (1991) A chemical method for estimating the availability of iron to phytoplankton in seawater. *Marine Chemistry* 33, 23-40.

Werne, J.P., Sageman, B.B., Lyons, T.W., Hollander, D.J. (2002) An integrated assessment of a 'type euxinic'deposit: evidence for multiple controls on black shale depsosition in the Midle Devonian Oatka Greek Formation. *American Journal of Science* 302, 110-143.

Westrich, J.T., Berner, R.A. (1984) The role of sedimentary organic matter in bacterial sulfate reduction: the G model tested. *Limnology and Oceanography* 29, 236-249.

Whitney, P.R. (1975) Relationship of manganese-iron oxides and associated heavy metals to grain size in stream sediments. *Journal of Geochemical Exploration* 4, 251-263.

Whittaker, S., Bidle, K.D., Kustka, A.B., Falkowski, P.G. (2011) Quantification of nitrogenase in *Trichodesmium* IMS 101: implications for iron limitation of nitrogen fixation in the ocean. *Environmental Microbiology Reports* 3, 54-58.

Widdel, F., Schnell, S., Heising, S., Ehrenreich, A., Assmus, B., Schink, B. (1993) Ferrous iron oxidation by anoxygenic phototrophic bacteria. *Nature* 362, 834-835.

Wignall, P.B. (1994) Black Shales. Oxford, Clarendon Press.

Wignall, P.B., Hallam, A. (1991) Biofacies, Stratigraphic Distribution and Depositional Models of British on-shore Jurassic Black Shales, in Tyson, R.V., Pearson, T.H., (Eds.), Modern and Ancient Continental Shelf Anoxia, *Geological Society of London Special Publications* 58, 291-309.

Wignall, P.B., Twitchett, R.J. (1996) Oceanic anoxia and the end Permian mass extinction. *Science* 272, 1155-1158.

Wijsman, J.W.M., Middleberg, J.J., Heip, C. H.R. (2001) Reactive iron in Black Sea sediments: implications for iron cycling. *Marine Geology* 172, 167-180.

Williams, D.B., Carter, D.B. (2009) Transmission Electron Microscopy: A Textbook for Materials. 2nd edition, Springer, Berlin.

Williamson, M.A., Rimstidt, J.D. (1994) The kinetics and electrochemical rate-determining step of aqueous pyrite oxidation. *Geochimica et Cosmochimica Acta* 58, 5443-5454.

Wilson, J.P., Fischer, W.W., Johnston, D.T., Knoll, A.H., Grotzinger, J.P., Walter, M.R., McNaughton, N.J., Simon, M., Abelson, J., Schrag, D.P., Summons, R., Allwood, A., Andres, M., Gammon, C., Garvin, J., Rashby, S., Schweizer, M., Watters, W.A. (2010) Geobiology of the late Paleoproterozoic Duck Creek Formation, Western Australia. *Precambrian Research* 179, 135-149.

Witter, A.E., Hutchins, D.A., Butler, A., Luther, G.W. III (2000) Determination of conditional stability constants and kinetic constants for strong model Fe-binding ligands in seawater. *Marine Chemistry* 69, 1-17.

Wu J, Luther G.W. III (1994) Size-fractionated iron concentrations in the water column of the Northwest Atlantic Ocean. *Limnology and Oceanography* 38, 119-1129.

Wu, J., Luther, G.W. III (1995) Compexation of Fe(III) by natural organic ligands in the Northwest Atlantic Ocean by a competitive ligand equilibration method and a kinetic approach. *Marine Chemistry* 50, 159-177.

Wu J, Luther G.W. III (1996) Spatial and temporal distribution of iron in the surface water of the northwestern Atlantic Ocean. *Geochimica et Cosmochimica Acta* 60, 2729-2742.

Wu, J., Boyle, E.A., Sunda, W.G., Wen, L. (2001) Soluble and colloidal iron in oligotrophic North Atlantic and North Pacific. *Science* 293, 847-849.

Wu, J., Wells, M.L., Rember, R. (2011) Dissolved iron anomaly in the deep tropical-subtropical Pacific: Evidence for long-range transport of hydrothermal iron. *Geochimica et Cosmochimica Acta* 75, 460-468.

Yde, J.C., Finster K.W., Raiswell, R., Steffansen, J.P., Heinemeier, J., Olsen, J., Gunnlaugsson, H.P., Nielsen, O.B. (2010) Basal ice microbiology at the margin of the Greenland Ice sheet. *Annals of Glaciology* 51, 71-79.

Yoshida, T., Hayash, K., Ohmoto, H. (2002) Dissolution of iron hydroxides by marine bacterial siderophore. *Chemical Geology* 184, 1-9.

Yoshida, M., Kuma, K., Iwade, S., Isoda, Y., Takata, H., Yamada, M. (2006) Effect of aging time on the availability of freshly precipitated ferric hydroxide to coastal marine diatoms. *Marine Biology* 149, 379-392.

Yu, J.Y., Park, M., Kim, J. (2002) Solubilities of synthetic schwertmannite and ferrihydrite. *Geochemical Journal* 36, 119-132.

Yucel, M., Gartman, A., Chan, C.S., Luther, G.W. III (2011) Hydrothermal vents as a kinetically stable source of iron-sulphide-bearing nanoparticles to the ocean. *Nature Geoscience* 4,367-371.

Zerkle, A.L., House, C.H., Cox, R.P., Canfield, D.E. (2006) Metal limitation of cyanobacterial N2 fixation and implications for the Precambrian nitrogen cycle. *Geobiology* 4, 285-297.

Zhu, X., Prospero, J.M., Millero, F.J., Savoie, D.L., Brass, G.W. (1992) The solubility of ferric iron in marine mineral aerosol solutions at ambient relative humidities. *Marine Chemistry* 38, 91-107.

Zhu, X., Prospero, J.M., Savoie, D.L., Millero, F.J., Zika, R.G.,Salzman, E.S. (1993) Photoreduction of Fe(III) in marine mineral aerosol solutions. *Journal of Geophysical Research* 98, 9039-9046.

Zhu, X.R., Prospero, J.M., Millero, F.J. (1997) Diel variability of soluble Fe(II) and soluble total Fe in North African dust in trade winds at Barbados. *Journal of Geophysical Research (Atmos)* 102, 21297-21305.

SUPPLEMENTARY INFORMATION

SI-1

Bioavailablity of Iron in Seawater

In general aqueous iron occurs mainly as Fe(III) organic complexes, which are capable of supplying bioavailable Fe (Butler, 1998; Hutchins *et al.*, 1999). Uncomplexed Fe(III) (and Fe(II) produced by reduction) is more readily bioavailable than their equivalent organic complexes (Sunda, 2001). However, the cells of most organisms are impermeable to highly charged or polar species and membrane transporters are necessary for Fe uptake into the cell. Different organisms have developed different strategies to acquire iron; in general eukaryotic phytoplankton directly take up inorganic iron using membrane transporters that bind with labile Fe species whilst prokaryotes excrete siderophores that bind with Fe(III) which is then transported into the cell by membrane proteins (Sunda, 2001).

Iron Uptake by Eukaryotic Organisms. Eukaryotic phytoplankton are thought to take up Fe either by photochemical reduction (external to the cell) and/or by the reduction of colloids adsorbed to the cell surface (Allnutt and Bonner, 1987; Hudson and Morel, 1990; Maldonado and Price, 2001). Eukaryotic organisms do not produce siderophores, but they are able to

access Fe-siderophore complexes via their membrane transporter systems (Maldonado and Price, 2001; 1999; Amin *et al.*, 2009). Most experimental work has shown that the addition of ferrihydrite enhances the growth of diatoms in seawater at pH ~8, where the initial cultures initially contained no aqueous Fe species. These results are valuable because diatoms form algal blooms in HNLC areas (Maher *et al.*, 2010). However, growth rates decreased with aged ferrihydrite, and other iron minerals (goethite, haematite) have been found to be only poorly bioavailable (Wells *et al.*, 1983; Rich and Morel, 1990), probably because of their lower solubilities and dissolution rates in seawater (Kuma and Matsunaga, 1995). Yoshida *et al.* (2006) studied the effects of ferrihydrite aging on iron uptake by coastal diatoms. Decreasing cell yields with more aged material were attributed to age-related chemical and structural changes that affected the ability to supply bioavailable Fe by dissolution (Fig. SI-1). Solubility measurements of ferrihydrite showed that the aqueous Fe content of solutions in contact with ferrihydrite decreased over 20 days due to the progressive growth of larger and more stable particles, consistent with the aggregation observed by Gilbert *et al.* (2009), Raiswell *et al.* (2010) and Bligh and Waite (2011).

There is thus good evidence that synthetic ferrihydrite can support plankton growth, but do natural ferrihydrites behave in the same way? Visser *et al.* (2003) found that iron present as ferrihydrite in soil dust, and the iron dissolved from the dust, were able to increase the growth rate of diatoms. The ferrihydrite was not completely bioavailable and, more surprisingly, neither was the dissolved iron completely utilised. However dissolved Fe was measured on solutions passing a 0.2 µm filter and may thus contain colloids which were not readily bioavailable. Experimental work suggests that iron-bearing colloids harvested from seawater are only partially bioavailable to eukaryotic organisms. Chen and Wang (2001) carried out experimental studies of diatom growth in seawater spiked with colloids/nanoparticles harvested from seawater and separated into two size fractions (approximately <5 nm and 5 nm to 0.2 µm), each labelled with ^{56}Fe. Uptake of iron from the smaller size fraction exceeded that from the larger, but both fractions were used less readily than Fe present as low molecular weight aqueous complexes. No data were presented on the colloid composition but Chen *et al.* (2003) used the same approach to follow the variations in uptake between colloids harvested from coastal, oceanic and estuarine environments. Over a 35 day period, uptake increased to maximum levels of ~20% from the coastal colloids and ~15% from the oceanic material, as compared to ~25% from the low molecular weight Fe complexes. The estuarine colloids were only weakly bioavailable (~8%), and uptake remained uniform with time. Experiments in which three different saccharides (poorly defined, polyfunctional carbohydrate compounds) were added to eukaryotic plankton assemblages produced an increase in iron uptake by forming highly bioavailable species (probably by adsorption

rather than complexing) with iron and by increasing the solubility of colloidal iron. (Hassler *et al*, 2010). These relatively weak iron-saccharide species are easily able to exchange iron with the more strongly-binding iron transporters used by eukaryotes to supply Fe(III) to the cell surface, where reduction to Fe(II) is followed by entry into the cell (see Supplementary Information SI-2).

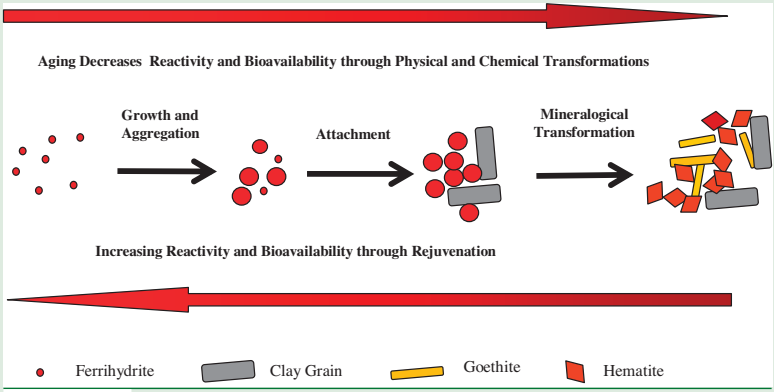

Figure SI-1 The aging-rejuvenation cycle (from Raiswell, 2011a, with permission from Elements). Aging may be inhibited by adsorbed organic matter.

In addition to these processes it has been suggested that colloidal iron is rapidly recycled where phytoplankton are grazed by heterotrophic protozoans but detailed mechanisms are poorly understood (Breitbarth *et al*., 2010). Ingested iron minerals are subjected to low pH processing in the gut that enhances bioavailability. Nodwell and Price (2001) showed that some species of mixotrophic flagellates were able to use goethite, haematite and magnetite but not ferrihydrite, whilst other species could only use ferrihydrite. In all cases uptake appeared to involve ingestion and thus represents the direct use of colloidal iron by eukaryotic organisms. Barbeau *et al*. (1996) have also shown that ingestion by grazing decreased the grain-size of colloidal ferrihydrite, increased the labile Fe content and increased the bioavailability to marine diatoms (Fig. SI-1). Faecal aggregates may also supply Fe(II) where microbial reduction of Fe (oxyhydr)oxides occurs inside organic C-bearing marine aggregates (Balzano *et al*., 2009), although rapid sinking of aggregates would suggest that this source is more effective for deep waters than surface waters. To summarise; it seems clear that eukaryotes can, at least partially, take up Fe from natural and synthetic ferrihydrite and from natural Fe-bearing organic colloids.

Iron Uptake by Prokaryotic Organisms. Siderophore transport systems are utilised by prokaryotic organisms to chelate and solubilise aqueous iron species and iron minerals. Siderophores are low molecular weight organic ligands with a high affinity and specificity for iron chelation. The stability constants of Fe(III) siderophores are 10^{23} to 10^{52}, significantly higher than for common laboratory complexing agents such as EDTA (which has a stability constant of 10^{20}). Siderophores can be synthesised by many prokaryotic organisms, including cyanobacteria (Haygood *et al.*, 1993; Sunda, 2001). However, organisms that are unable to produce siderophores may still be able to take up iron bound to siderophores produced by other organisms (Granger and Price, 1999).

The influence of siderophores on iron dissolution and complexation has been studied using thermodynamic models (Kraemer *et al.*, 2005). These models show that the solubility of ferrihydrite and goethite increases with increasing concentrations of the siderophore desferrioxamine B (DFOB) in seawater at pH 8, but significant (order of magnitude) increases in the solubility of ferrihydrite only occurred at siderophore concentrations above ~1 nM. Kraemer *et al.* (2005) also show that variations in siderophore stability constant (log K_{Fe3+L} from 18 to 25) have little effect on ferrihydrite solubility but large effects on goethite and haematite solubility. Experimental work described below has supported the modelling results. Yoshida *et al.* (2002) showed that siderophores extracted from marine organisms increased both the dissolution rate and solubility of ferrihydrite aged for 24 hrs. Dissolution rates increased as siderophore concentrations increased but rates slowed with increasing pH and the dissolution rates at pH 8 were too slow to measure over 100 days. Siderophore concentrations were not directly measured but were in the micromolar range. This implies that there would be limited kinetic enhancement of siderophore-controlled dissolution of aged ferrihydrite in seawater with much lower concentrations of siderophores (Kraemer, 2006). Fresh ferrihydrite (aged for 1 minute) is however dissolved an order of magnitude more readily by the siderophore DFOB at pH 8 than material aged for 24 hrs (Rose and Waite, 2003). Overall, siderophores are clearly able to produce Fe from iron (oxyhydr)oxides that is bioavailable to prokaryotic organisms but fresh ferrihydrite may represent a more viable resource in seawater than aged ferrihydrite.

SI-2

Filterable Iron and Complexed Iron in Seawater

More than 99% of the *filterable* Fe(III) in the 0.2-0.4 µm size fraction is bound to organic ligands (Gledhill and van den Berg, 1994; van den Berg, 1995; Rue and Bruland, 1995). Two distinct classes of iron-binding organic ligands with different affinities for Fe^{3+} have been recognised, where iron affinity is defined by the stability constant K_{Fe3+L}. A strong iron-binding ligand (termed L_1 with a log K_{Fe3+L1} ~23) is confined to the upper ocean where it is found at a mean concentration of ~0.44 nM. These log K_{Fe3+L1} values have been shown (Witter *et al*., 2000) to approximate to those of siderophores (log K_{Fe3+L} = ~21-24) with which they share some structural similarities, notably the presence of hydroxymate Fe-binding functional groups (Mawji *et al*., 2008). Siderophores are believed to be produced by prokaryotic organisms to aid the acquisition of iron and, consistent with this, the L_1 ligand has been observed to be produced over several days in response to iron fertilisation experiments (Rue and Bruland, 1997). The weaker ligand (log K_{Fe3+L2} = ~21) is found throughout the water column with an average concentration of ~1.5 nM and may also comprise different siderophores (Rue and Bruland, 1995; Amin *et al*., 2009; Boyd *et al*., 2010b). Together these ligands exert a profound effect on iron speciation such that >99.9% of the *filterable* Fe(III) appears to be complexed. This, it seemed, was the reason why iron Fe(III) was kept in solution in seawater rather than being precipitated as iron (oxyhydr)oxides.

There has, however, been a recent, unexpected twist to this elegant story that defines the role of organic ligands. Studies of organic complexation have utilised seawater filtered through 0.2-0.45µm which includes colloids and nanoparticles as well as aqueous species. Size-fractionated studies (Wu and Luther 1994; 1996) of seawater from the Northwest Atlantic showed that concentrations of iron occurring in the colloidal size range (0.2-0.4 µm) exceeded those in the <0.2µm fraction (assumed to be mainly aqueous species but actually also including nanoparticles). Wu and Luther (1995) also found that the <0.4 µm fraction at the same sites contained iron that was non-labile towards competitive ligand exchange (indicating an apparent log $K_{Fe3+L} > 23$). This Fe was thought to be either strongly complexed (with stability constants greater than the ligand used for exchange) or present as inorganic colloidal Fe (oxyhydr)oxides. This suggests that a significant proportion of *filterable* Fe was neither aqueous nor complexed – but nanoparticulate Fe (oxyhydr)oxides.

Distinguishing between aqueous and nanoparticulate species has required the isolation of small diameter size fractions in which aqueous species predominate. Wu *et al.* (2001) measured the concentrations of organic ligands in a <0.02 µm fraction of surface seawater from the North Atlantic and North Pacific. Ligand concentrations in this fraction (~0.1 nM) were much lower than previously measured on *filterable* fractions (see above) and somewhat lower than the concentrations of Fe in the <0.02 µm and 0.02-0.2 µm fractions (0.1 to 0.4 nM). These results (see also Bergquist *et al.*, 2007) also indicate that a significant proportion of the *filterable* Fe is neither aqueous nor complexed, but is an inorganic Fe colloid or nanoparticulate.

Consistent with this, Cullen *et al.* (2006) found a relatively small proportion (5-35%) of the *filterable* Fe (<0.4 µm) in the surface waters of the Atlantic Ocean in the <0.02µm fraction compared to 65-95% in the colloidal fraction (0.02 µm to 0.4 µm). Rather lower proportions of colloidal iron (~40%) occurred in the deep water samples. These proportions seem to be reversed in the Southern Ocean where Boye *et al.* (2010) found that aqueous Fe and ligands (<0.03 µm) dominated in surface waters, but the colloidal fraction (0.03-0.2 µm) was still significant and comprised 37-51% of the <0.2 µm fraction (and increased with depth). Temporal and spatial variability in the distribution of Fe between the aqueous and colloidal forms (Wu and Luther, 1994) may be partly controlled by the equilibrium partitioning of Fe between soluble and colloidal ligands (Cullen *et al.*, 2006), in turn responding to biological uptake of the aqueous species and/or the loss of colloidal Fe by scavenging (Wu *et al.*, 2001; Bergquist *et al.*, 2007). Nevertheless the simple fact is that colloid forms of Fe are clearly significant but are these colloids organic or inorganic?

Cullen *et al.* (2006) have shown that a significant fraction of the colloidal Fe (ranging from 40% in surface waters up to 100% in some deep water samples) was inert towards competitive ligand exchange and was suggested to be present as an (oxyhydr)oxide that must be present as both nanoparticles and colloids. Could this (oxyhydr)oxide phase also be bound to organic matter? Recent work suggests that saccharides are an important component of the L_2 pool and that Fe-saccharide colloids may be the major component of colloidal Fe in surface seawater (Hassler *et al.*, 2011). Saccharides are poorly-defined, polyfunctional compounds some of which have iron-binding stability constants that fall within the L_2 range. Saccharides are the dominant component in the colloidal size fraction of surface seawater and occur in relatively high concentrations (up to micromolar), enabling them to outcompete the stronger binding L_1 ligands and bind (via adsorption) to a higher proportion of the *filterable* iron.

The colloidal Fe in seawater is thus likely to be an (oxyhydr)oxide present as Fe-organic matter colloids and/or nanoparticles (Boye *et al.*, 2010). Identifying the role of nanoparticulate aggregates of organic matter and (oxyhydr)oxide minerals in the Fe biogeochemical cycle presents a huge challenge. What might be the nature of the relationship between the two components in a colloidal/nanoparticulate aggregate; are they coprecipitated or are the organics adsorbed on the mineral surfaces? The competitive ligand exchange studies suggest that the surface properties of a significant proportion of the colloidal/nanoparticulate Fe are controlled by organic matter but two end-member situations can be envisaged (Fig. 2.3). In one case we can envisage that the adsorbed organic matter covers all or most of the surface of an Fe (oxyhydr)oxide-organic matter aggregate, and is thus able to control the surface properties. Alternatively, a relatively small fraction of the aggregate surface may be organic matter, either because surface adsorption is discontinuous or because organic matter sub-units are coprecipitated with Fe (oxyhydr)oxide nanoparticles (Fig. 2.3). These end-members may exhibit different surface properties (and may exhibit different behaviour with respect to competitive ligand exchange) because aggregates coated with adsorbed organic matter have less mineral exposed at their surfaces. Furthermore organic matter coprecipitated with ferrihydrite differs in amount and composition from adsorbed organic matter (which can be relatively enriched in polysaccharides; Eusterhues *et al.*, 2011). Adsorbed fulvic acids are able to slow down the rate at which ferrihydrite transforms to more stable (oxyhydr)oxides by blocking dissolution sites or hindering the nucleation of the more stable phases (Jones *et al.*, 2009). Might the retardation effects on transformation (Vilge-Ritter *et al.*, 1999) be less efficient with discontinuous coatings or with coprecipitated organic matter? A more mineralogical-based approach to the *filterable* Fe fraction in seawater should be high on everyone's wish list.

SI-3

Origin of Fe (Oxyhydr)oxide Colloids/ Nanoparticles in Seawater

Wells and Goldberg (1992) examined organic, inorganic and clay colloids from surface seawater off the Californian coast and found that particles with diameters <120 nm (nanoparticles) were the most abundant. A number of particles in the 100-500 nm size range were shown by Energy

Dispersive X-ray Spectrometry to be composed almost exclusively of iron and occasionally weak diffraction patterns were observed although no determination of mineralogy was possible. Transmission Electron Microscopy showed these to be 50-100 nm aggregates of elliptical sub-units 2-5 nm in diameter; reminiscent of ferrihydrite (see Fig. SI-6a,b). Subsequent studies on the Scotian Shelf and in the Southern Ocean (Wells and Goldberg, 1994) found predominantly organic colloids comprised of 30-60 nm units that may be coalesced into larger aggregates.

Formation of Nanoparticulate Fe (Oxyhydr)oxides. Nanoparticles of Fe (oxyhydr)oxides are believed to form at high degrees of supersaturation. Aqueous Fe^{2+} rapidly oxidises and the Fe^{3+} forms octahedral Fe $(O, OH, OH_2)_6$ clusters that slowly aggregate to nanoparticles and then to colloids (Waychunas *et al.*, 2005). Aggregation is promoted by a decrease in the surface energies, however nanoparticles of these minerals persist in nature provided transformation kinetics are slow. There are at least three main mechanisms by which nanoparticles of Fe (oxyhydr)oxides may form in seawater. First, diffusion or physical re-working mixes porewater Fe(II) in reducing sediments into the overlying oxic waters, where the iron is oxidised to nanoparticulate Fe (oxyhydr)oxides (Raiswell *et al.*, 2008a). Second, they form by the oxidation of Fe^{2+}-bearing rock minerals such as carbonates, sulphides and silicates. Third, nanoparticulate (oxyhydr) oxides may form by the transformation of pre-existing nanoparticles. For example, ferrihydrite may be formed by the aging of schwertmannite and may itself be transformed to goethite and haematite (Bigham *et al.*, 1996; Schwertmann *et al.*, 2004; Davidson *et al.*, 2008).

Transformations between the Iron (Oxyhydr)oxides. Reactivity changes result from mineralogical transformations of the most reactive iron (oxyhydr)oxide nanoparticulates to more stable forms. The transformation of ferrihydrite to goethite has been studied by Schwertmann *et al.* (2004) who have shown that the time to transform 50% of ferrihydrite depends on pH and temperature (Fig. 2.4). The transformation at 5°C takes approximately 500 days at pH 8 and 1500 days at pH 7. Das *et al.* (2011) show comparable data over a wider range of pH (2 to 10) and temperature (25-100°C). However rates of transformation may vary considerably, for example due to the adsorption of foreign ions and organic matter (see Supplementary Information SI-2). Haematite and goethite are much more stable than ferrihydrite and their formation is likely on year-long timescales during immersion in seawater at surface temperatures.

SI-4

Properties of Nanoparticulate Fe Oxyhydr(oxides)

Surface Charge of Nanoparticulate Iron Oxyhydr(oxides). Surface charge on Fe (oxyhydr)oxide nanoparticles arises from the ionisation of surface groups, from double layer interactions and from van der Waals forces. Surface oxide and hydroxyl groups can undergo protonation (producing a positive surface charge in acid conditions) and deprotonation (producing a negative surface charge in alkaline conditions). Hence a point of zero charge (PZC) can be recognised, which is the pH at which there is no surface charge. Cornell and Schwertmann (2003) report the PZC of ferrihydrite as 7.8-7.9, lepidocrocite 6.7-7.3, haematite 7.5-9.5 and goethite 7.5-9.5. However, the surface charge of colloids and nanoparticles (irrespective of their composition) in natural systems appears to be controlled by the adsorption of other ions or films of organic matter (see Supplementary Information SI-2), the acidic functional groups of which convey a uniformly negative charge. This surface charge attracts a layer of oppositely charged ions (the counterions) from the surrounding solution, which together comprise the double layer. At low ionic strength, the influence of the double layer extends over distances many times larger than the nanoparticle diameter and this strong repulsion prevents close approach and aggregation. In solutions with a high ionic strength (such as seawater), the double layer is compressed and the layer of counterions may shrink inside the layer of adsorbed organic matter. The distance of closest approach may then be small enough to allow bonding interactions between the adsorbed organic matter on colliding nanoparticulates (Sander *et al.*, 2004). For example ferrihydrite nanoparticles coated with organic matter in river water at near-neutral pH are stabilised because strong repulsion occurs between the double layers on neighbouring nanoparticles (Mosley *et al.*, 2003). However the double layer is compressed on entering seawater and nanoparticles that are brought into close proximity may then aggregate (see below). Nanoparticles that approach to within 0.3 nm are influenced by bonding forces rather than electrostatic interactions (and/or van der Waals forces). Bonding forces are typically several orders of magnitude stronger than electrostatic or van der Waals forces (Waychunas, 2001; Benning and Waychunas, 2007). Note that organic matter coatings influence surface properties but ferrihydrite aggregates possess significant internal microporosity that may be unavailable to organic matter but may provide sites for the adsorption of ionic species.

Surface Area of Nanoparticulate Iron (Oxyhydr)oxides. Surface area has a dramatic effect on solubility because smaller particles have more surface energy and are thus less stable. Cornell and Schwertmann (2003)

have estimated the size effects on the solubility of goethite and haematite. Size effects become significant once particle size decreases below ~100nm, and below ~10 nm solubility is increased by more than an order of magnitude. The increased solubility of the smallest nanoparticles produces a phenomenon known as Ostwald ripening, by which the largest nanoparticles grow at the expense of the smaller nanoparticles (see for example Benning and Waychunas, 2007). The size distribution of a suite of nanoparticles may also evolve to larger sizes where aggregation results from collisions between nanoparticles. Collisions become increasingly likely where there are large concentrations of nanoparticles and where external forces impose movement or turbulence.

Reactivity and Solubility of Nanoparticulate Fe (Oxyhydr) oxides. The reactivity of ferrihydrite can be considered to be determined by the mineral structure at three size levels; the molecular structure or crystallinity (i.e. the coordination environment of Fe), the size of the nanoparticles (unaggregated), and the aggregate structure (Bligh and Waite, 2011). At the molecular level the changes in ferrihydrite reactivity with time (often termed aging) have been suggested to occur because there is increased coordination of Fe by bridging groups and because hydroxo-bridges are converted to stronger oxo-bridges (Rose and Waite, 2007). Bligh and Waite (2011) found that rapid changes in the reactivity of ferrihydrite (over 5 hours) were not accompanied by changes in crystal structure. Their data suggested that the crystal structure of ferrihydrite was established shortly after nucleation (within 90 minutes) and that there was then little further growth and no changes in crystal structure. The size of ferrihydrite nanoparticles lie in a relatively narrow size range (1-5nm; Schwertmann and Fischer, 1973; Janney *et al.*, 2000; Cornell and Schwertmann, 2003) which is rapidly established after initial nucleation (Bligh and Waite, 2011). Aging, it seems, is most likely a result of aggregation.

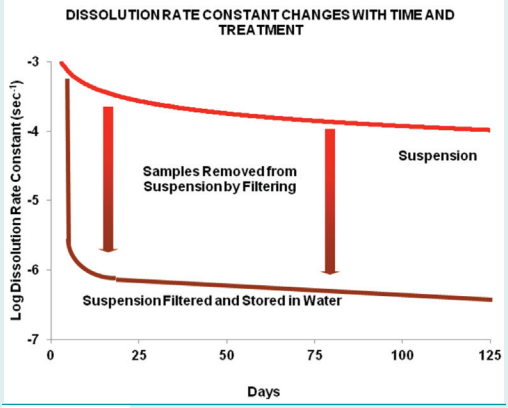

Figure SI-4 Variation in ferrihydrite reactivity with time and sample treatment, as shown by changes in the rate constant for dissolution in ascorbic acid (from Raiswell, 2011a, with permission from Elements).

Aggregation has a dramatic effect on solubility. Fe (oxyhydr)oxide nanoparticulate aggregates have a significant degree of internal microporosity which limits access of aqueous reactants to the interior of the aggregate and hence diminishes reactivity (Cornell and Schwertmann, 2003; Gilbert *et al*., 2009). For example, an 8% suspension of ferrihydrite in water at pH 6-6.5 re-organised into aggregates that became an order of magnitude less soluble in ascorbic acid in ~100 days (Fig. SI-4). Aggregation of the same suspension by wetting and drying (filtering followed by air-drying) produced more compact aggregates that were more than 3 orders of magnitude less soluble in ascorbic acid (Fig. SI-4). These observations, although based on laboratory systems, show how rapidly ferrihydrite nanoparticles lose solubility by aggregation.

SI-5

Iron Photochemistry

The Photochemistry of Fe Complexes. Fe(III) is the thermodynamically stable form of iron in seawater, but Fe(II) can be transiently present as a result of photochemical reactions. Once formed, Fe(II) is kinetically labile and highly bioavailable but may be stabilised in oxic seawater by organic ligands (Breitbarth *et al*., 2010). Many aqueous Fe(III) inorganic and organic complexes can be photoreduced to Fe(II). Organic complexes are considered, however, to be the most photoreactive both because these complexes are thought to predominate in seawater (see Supplementary Information SI-2) and also because the major inorganic hydroxyl complexes (see Table 2.1) are only weakly photoreactive (Waite, 2001). The photochemical behavior of Fe(III) associated with the L_1 and L_2 ligands is currently a major research focus and progress in this area has been reviewed by Barbeau (2006), who also provides a detailed discussion of photochemical reduction mechanisms. Photochemical reduction, it seems, can occur either by the direct photolysis of Fe(III) complexes or indirectly by reactions with other photochemically produced species, such as superoxides.

The direct photolysis of Fe(III) complexes with siderophores has shown varying behaviour; some siderophore Fe(III)-binding groups are photochemically reactive (α-hydroxy carboxylate groups; Borer *et al*., 2005), whilst others (hydroxymate and catacholate) are non-reactive (Barbeau, 2006). The siderophore vibrioferrin contains two α-hydroxy groups, and the Fe-vibrioferrin complex undergoes photolysis 10-20 times faster than other

siderophores (Amin *et al*., 2009). Siderophores with α-hydroxy carboxylate groups are produced by marine bacteria, which suggests that an active photoredox cycle can exist in seawater with bacterially-produced siderophores producing Fe(II) for uptake by plankton. This cycle may only supply a small proportion of the Fe required by plankton (Hopkinson and Morel, 2009) possibly because the relative proportion of reactive to unreactive siderophores is too small.

Indirect reactions with photochemically produced radicals are an alternative mechanism for the production of Fe(II). A variety of reactive oxygen species are known to be produced by the photochemical reactions of organic species, with superoxide (O_2^-) the most likely Fe(III) reducing agent (Barbeau, 2006). Two pathways are possible: one involves the reduction of an Fe(III)-ligand complex to form an Fe(II)-ligand complex, whilst the other requires the dissociation of Fe(III) from the ligand prior to reduction to Fe(II). Experimental work on these mechanisms has to date produced conflicting results (Barbeau, 2006).

A further level of complexity has been introduced by Steigenberger *et al*. (2010) who studied the influence of artificial saccharides and diatom exudates (which contain saccharides) on the half-life of Fe(II) in seawater. Irradiation of the artificial saccharides produced H_2O_2, which is capable of oxidising Fe(II) to Fe(III). However H_2O_2 is formed photochemically via a superoxide intermediate which is capable of reducing Fe(III), thus maintaining concentrations of Fe(II). With the diatom exudates, the net result of these conflicting photochemical effects was to increase steady state concentrations of Fe(II) in seawater.

The Photochemistry of Fe (Oxyhydr)oxides. A few early studies (Johnson *et al*., 1994; Miller *et al*., 1995; Waite *et al*., 1995) directly observed the photochemical behavior of *filterable* Fe by demonstrating the net accumulation of Fe(II) in irradiated seawater. Studies involving iron (oxyhydr) oxides have been carried out by Waite and Morel (1984) using an (oxyhydr) oxide (probably ferrihydrite) separated by ultrafiltration. Photoreductive dissolution was significantly enhanced by the addition of natural organics, but decreased with increasing pH and was not observed in natural seawater, possibly because the concentration of organics is low and/or because of the rapid re-oxidation of photoreduced species at pH ~8. Hudson *et al*. (1992) also concluded that photoreduction was enhanced by humic acids but was difficult to observe at pH 8 due to the re-oxidation effects. Wells and Mayer (1991) irradiated synthetic ferrihydrite and goethite in coastal and offshore seawater at pH 8 and observed that the extractable (or labile) fraction of these minerals increased over 10 hours in seawater. However, seawater pre-treated by UV radiation prevented the formation of labile Fe and hence the increased lability was thought to arise from photoreduction

of organic species. Aging caused significant decreases in the rate of labile Fe release, as might be expected for nanoparticulate material that aggregated with time.

Rates of photoreduction depend on the wavelength and intensity of the incident light, on the concentration and type of any reductants that are present, the concentration, surface area and crystallinity of the solid Fe(III) phases, and the pH and ionic strength of the media (Sulzberger and Laubscher, 1995). The efficiency of photoreduction is controlled by the rates of Fe(II) release from the mineral surface (and thus decrease with increasing thermodynamic stability) because slow detachment allows in situ re-oxidation. Hence, photoreduction is observed with lepidocrocite but not with more stable phases such as goethite and haematite. On the one hand, slow release severely limits the ability of photoreduction to supply bioavailable Fe, on the other hand, in situ oxidation means that approaches which rely on measurements of the net accumulation of Fe significantly underestimate rates of photoreduction because of the re-oxidation effects (Waite, 2001). It seems possible that release of photoreduced Fe(II) might be most rapid with fresh ferrihydrite. Indeed there are dramatic differences in the rate constants reported for the photoreduction of iron (oxyhydr) oxides (which range from 0.12 to 20 day^{-1}) that relate to pre-treatments that age and alter iron (oxyhydr)oxides (Moffett, 2001), consistent with the known effects of aggregation on reactivity (see Supplementary Information SI-4). Photochemical studies of different, mineralogically-characterised size fractions of iron in seawater would be important in assessing the relative contributions from photochemical reduction of the aqueous and nanoparticulate/colloidal components.

SI-6

Iron Mineralogy

Cornell and Schwertmann (2003) provide an excellent review of the properties of the major iron (oxyhydr)oxide minerals that are found as nanoparticulates in these systems, as summarised below.

Ferrihydrite. The precise composition of ferrihydrite is not known but the formula $Fe_4HO_8.4H_2O$ is thought to be more accurate than $Fe(OH)_3$ (Towe and Bradley, 1967; Jambor and Dutrizac, 1998). Ferrihydrite is metastable and can be formed by the rapid oxidation of Fe^{2+} which produces a poorly ordered structure. The degree of ordering is variable and the two

extremes of crystal ordering are referred to as 2-line and 6-line ferrihydrite, which differ mainly in the size of the crystal domain (Janney *et al.*, 2000; 2001). Further structural details are still emerging (Michel *et al.*, 2007). 2-line ferrihydrite is often referred to in the literature as amorphous or hydrous ferric oxide (AFO or HFO) but this phase is poorly crystalline rather than amorphous and thus the terms AFO and HFO have been here replaced as ferrihydrite (following Jambor and Dutrizac, 1998) even where this has not been explicitly recognised in the literature. Once formed ferrihydrite coalesces to form microporous aggregates and/or may alter to a variety of other iron minerals including goethite/haematite mixtures. It is important to recognise that all ferrihydrite is nanoparticulate and hereafter ferrihydrite will be described as nanoparticulate only for emphasis; otherwise nanoparticulate is used for other minerals only where appropriate. Ferrihydrite characteristically occurs as aggregates of sub-spherical to hexagonal nanoparticulates (Fig. SI-6a,b).

Lepidocrocite (γ-FeOOH). The Fe in lepidocrocite is in octahedral coordination with three O^{2-} and three OH^{-} as in goethite but the double chains are organised into a layer-like structure. Lepidocrocite is much less common in soils than goethite or haematite and the mineral is characteristically formed in environments that fluctuate between reducing and oxidising, where Fe(II) can be oxidised at neutral pH in the presence of excess dissolved oxygen (Chatellier *et al.*, 2004). Lepidocrocite commonly occurs as laths.

Goethite (α-FeOOH). The Fe in goethite is in octahedral coordination with each Fe^{3+} surrounded by three O^{2-} and three OH^{-} giving $FeO_3(OH)_3$ octahedra. The Fe ions are arranged in double rows separated by rows of vacant sites which give the structure a tunnel-like appearance. Goethite is the most common Fe (oxyhydr)oxide in soils where it forms by the oxidation of Fe^{2+} dissolved from Fe minerals, or by the transformation of ferrihydrite or lepidocrocite. Goethite frequently occurs as acicular or needle-shaped crystals (Fig. SI-6c).

Haematite (α-Fe_2O_3). Haematite consists of layers of $Fe^{3+}(O^{2-})_6$ octahedra organised into a compact structure which gives a high density and good crystallinity. Haematite is often found in association with goethite and is most commonly formed in sediments by the transformation of ferrihydrite. Common morphologies are rhombohedral, platy and rounded.

Schwertmannite. This mineral is a poorly-ordered ferric (oxy) hydroxyl-sulphate with a compositional range of $Fe_3O_8\,(OH)_{8-2x}\,(SO_4^{2-})_x.\,nH_2O$ where x = 1 to 1.75 and n = 8.17 to 8.62 (Yu *et al.*, 2002). Schwertmannite is commonly found in acid mine drainage where it forms by the oxidative weathering of pyrite at pH 2-5. At near-neutral pH ferrihydrite is the main weathering product (Bigham *et al.*, 1996). Pyrite is often As-bearing,

and the presence of As in schwertmannite (where it substitutes for sulphate as the arsenate ion) is consistent with a formation by pyrite oxidation. The substitution of As increases the susceptibility of pyrite to oxidation and arsenopyrite oxidises about three orders of magnitude faster than pyrite (McKibben *et al*, 2008). Schwertmannite commonly occurs as spheroidal aggregates with a spikey, 'pin-cushion' morphology (Fig. SI-6d).

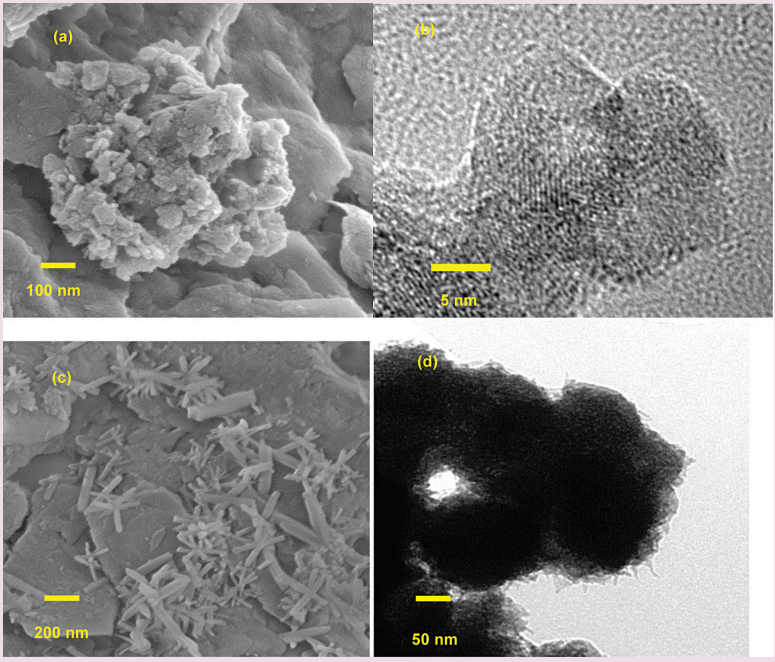

Figure SI-6 (a) SEM and (b) TEM microphotograph of ferrihydrite, (c) SEM microphotograph of goethite (d) SEM microphotograph of schwertmannite (from Raiswell, 2011a, with permission from Elements).

Brief details of other important iron minerals that are discussed in the following brief summaries are mainly taken from Deer *et al.* (1992).

Magnetite. Magnetite is one of the most common oxide minerals formed in igneous and metamorphic rocks. It is a mixed valence iron oxide with the formula $Fe^{2+}Fe^{3+}_2\,O_4$ that occurs as black or brownish-black grains with a metallic luster. The O^{2-} ions are arranged in a cubic lattice with the Fe ions occupying tetrahedral and octahedral sites.

Pyrite. Pyrite (FeS_2) is the most common sulphide mineral in marine sediments where it often occurs as spheroidal aggregates of microcrystalline pyrite grains (termed framboids) or as brassy-yellow aggregates of cubic crystals with a metallic luster (which are commonly referred to as 'fool's gold'). The structure consists of a face-centred cube with Fe^{2+} ions octahedrally coordinated with S_2^{2-} ions. Pyrite also occurs as pyritohedra and octahedra, as well as cubes.

Mackinawite. Mackinawite (FeS) is a black iron monsulphide with the Fe^{2+} ions in tetrahedral coordination with four equidistant S^{2-} ions. The precipitation of mackinawite occurs more rapidly than pyrite, the formation of which it commonly precedes (Benning *et al*, 2000), although mackinawite is not always a necessary precursor for pyrite formation (Rickard and Luther, 2007).

Greigite. Greigite ($Fe^{2+}Fe^{3+}_2 S_4$) is the sulphur analogue of magnetite and is a mixed valence iron sulphide that commonly occurs as dark, microscopic grains and is often used as a palaeomagnetic indicator mineral. The S^{2-} ions are arranged in a cubic lattice with the Fe ions occupying tetrahedral and octahedral sites, and is an important intermediate phase on the mackinawite to pyrite formation pathway (Hunger and Benning 2007).

Siderite. Siderite ($FeCO_3$) is one of the principle minerals in sedimentary iron ores and is typically found as light to dark-brown aggregates of rhombohedra, often with curved faces. The Fe^{2+} ions are octahedrally coordinated with CO_3^{2-} ions such that layers of metals ions alternate with layers of CO_3^{2-} ions.

Vivianite. Vivianite ($Fe_3(PO_4)_2.\ 8H_2O$) is found in sediments as microscopic, prismatic crystals or crusts and layers of fibrous to bladed crystals. The structure consists of single octahedra of $Fe(II)O_6$ and double octahedral of edge-shared Fe(II) and H_2O linked to phosphate ions.

Iron Silicates. Fe-bearing silicates of interest here can be classified according to their structure, which produces characteristic differences in basal spacing (Velde, 2003).

(a) The serpentine and kaolinite clay minerals have a basal spacing of 7 Å, and the main Fe-rich minerals are bertherine and greenalite.

(b) The mica, talc and illite minerals have basal spacings of 10 Å, and Fe-rich phases include stilpnomelane, glauconite, celadonite and minnesotaite.

(c) The smectite and chlorite minerals have a basal spacing of 14 Å, and the main Fe-rich minerals are nontronite, chamosite and clinochore.

SI-7

A Kinetic Model of Bioavailable Fe Supply to Seawater

Modelling is a valuable way to integrate the kinetic constraints on iron delivery rates (and rates of removal from the photic zone) into a global understanding of Fe bioavailability to primary producers. Here I present the development of an idealised, semi-quantitative kinetic model to evaluate how different mechanisms combine to control the supply of bioavailable Fe from sediments delivered to the ocean. Mechanisms include:

(a) iron input via dissolution, siderophore-aided dissolution, photochemical reduction and grazing.

(b) iron losses by sinking, scavenging and transformation to less bioavailable iron (oxyhydr)oxide minerals.

This model is based on information presented in the preceding Supplementary Information sections and is an extension of a model that I have recently published (Raiswell, 2011b). The model is used in the main text to estimate the supply of bioavailable iron from aeolian dust (see main text Section 5.5) and icebergs (see main text Section 6.4).

Model Assumptions. The model assumes:

(i) A solid phase (sediment or dust) is added to surface seawater at a constant rate of $\boldsymbol{S}$ kg day^{-1} and contains $\boldsymbol{f}$ kg kg^{-1} of iron present as ferrihydrite nanoparticles that are extractable by ascorbic acid (Kostka and Luther, 1994; Hyacinthe and Van Cappellen, 2004; Raiswell *et al*, 2010). Thus, nanoparticulate Fe is continuously added to surface seawater at a rate F_A where:

$$F_A = \boldsymbol{f} \times \boldsymbol{S} \text{ (kg day}^{-1}\text{)} \qquad \text{(SI-7.1)}$$

Sediment addition is accompanied by the delivery of instantaneously soluble (and bioavailable) Fe associated with the sediment at a concentration $\boldsymbol{c}$ kg kg^{-1}. Thus, soluble Fe is added at a rate F_{Sol}, where:

$$F_{Sol} = \boldsymbol{c} \times \boldsymbol{S} \text{ (kg day}^{-1}\text{)} \qquad \text{(SI-7.2)}$$

This approach is similar to that of Boyd *et al*. (2010a) whose model defines two forms of iron in aeolian dust; readily available and leachable.

(ii) The addition of sediment is accompanied by nanoparticles that are free-standing or attached to sediment grains. The surface charge characteristics of free-standing nanoparticles (and associated organic matter) in seawater produce rapid scavenging (see Supplementary Information SI-4). Attachment to organic and

inorganic sediment grains facilitates sinking through the water column under gravity and the resulting aggregates thus pass out of the photic zone where Fe can be utilised for photosynthesis. It is assumed that higher sediment concentrations encourage more attachment or irreversible scavenging of nanoparticles, which takes place at a rate that is proportional to the amount of nanoparticulate Fe in suspension, and thus follows first order kinetics. Nanoparticulate Fe may also become less reactive by transformation (to goethite/haematite) and by aging (which produces aggregation), which are also assumed to follow first order kinetics. Hence, the removal flux F_L for nanoparticulates is given by:

$$F_L = k_L \times M_t \quad \text{(SI-7.3)}$$

where k_L is the rate constant (in day^{-1}) for the loss of nanoparticulate Fe by either by sinking (due to scavenging or incorporation into faecal material), aging or transformation and M_t is the mass of nanoparticulate Fe at any time t.

(iii) Attached nanoparticles are assumed to become bioavailable through dissolution, photochemical reduction, grazing and siderophore-aided dissolution. It is assumed that, whatever the supply process, bioavailable Fe is instantaneously utilised by plankton rather than lost by reaction (including oxidation), scavenging to sediment particles, or rendered non-bioavailable by transformation. The rate of formation of bioavailable Fe (F_B) from nanoparticulate Fe (assumed equal to consumption by photosynthesis) is assumed to follow first order kinetics so that:

$$F_B = k_B \times M_t \quad \text{(SI-7.4)}$$

where k_B is the rate constant for the formation of bioavailable Fe (day^{-1}).

Now, the amount of nanoparticulate Fe remaining in the photic zone after t days is given by:

$$dM_t/dt = F_A - F_L - F_B = F_A - k_L \times M_t - k_{B.} \times M_t = F_A - K \times M_t \quad \text{(SI-7.5)}$$

where $K = k_L + k_B$. The solution to this differential equation is given by:

$$M_t = F_A\,(1 - e^{-Kt})\,/K \quad \text{(SI-7.6)}$$

where $M_t = 0$ when $t = 0$. Equation (SI-7.6) can be solved for M_t for different combinations of rate constants for the input and output processes and substituted back into equation (SI-7.4) to estimate the flux of bioavailable Fe being delivered. Hence,

$$F_B = k_{B.} \times F_A\,(1 - e^{-Kt})\,/K \quad \text{(SI-7.7)}$$

and integration of this equation over a specified time interval provides an estimate of the mass of bioavailable iron (B_i) that can be used to support productivity:

$$B_i = (k_B \times F_A /K) \int .dt - (k_B \times F_A /K) \int e^{-Kt}$$

$$= k_B \times F_A \times t /K + k_B \times F_A \times e^{-Kt} /K^2 + \text{Constant} \quad \text{(SI-7.8)}$$

However, $B_i = 0$ when $t = 0$ and the constant is therefore $- k_B \times F_A/K^2$ and equation (SI-7.8) becomes:

$$B_i = k_B \times F_A \times t /K - k_B \times F_A (1 - e^{-Kt})/K^2 \quad \text{(SI-7.9)}$$

Equation SI-7.9 represents the bioavailable Fe produced from Fe nanoparticulates but Fe is also supplied at a rate F_{Sol} (= $\boldsymbol{c}$. $\boldsymbol{S}$ kg day^{-1}) in a soluble form that is bioavailable. Thus, the total mass of bioavailable Fe is given by:

$$M_B = B_i + \boldsymbol{c} \times \boldsymbol{S} \times t. \quad \text{(SI-7.10)}$$

Estimation of Rate Constant Values for the Loss of Nanoparticulate Fe. Iron nanoparticles in seawater may be affected by a variety of processes that determine their residence time in surface waters, principally sinking under gravity, scavenging by attachment to sediment grains and scavenging by incorporation into faecal material. Free-standing nanoparticulates would sink at an exceedingly slow rate, but attachment to other sedimenting grains is likely in sediment-rich waters and is assumed to occur either before, or immediately after, delivery to seawater. The residence times for nanoparticles attached to sediment grains can be estimated from the rate at which such grains sink through the water column in the absence of turbulence. The iron (oxyhydr)oxide contents of riverine and marine sediments, and suspended sediments in glacial meltwaters, are highest in the <2 μm fraction (e.g. Horowitz and Elrick, 1987; Whitney, 1975; Poulton and Canfield, 2005; Poulton and Raiswell, 2005), which is assumed to be the principal host for nanoparticles in this model. Lerman (1979) estimates that spherical 2 μm diameter particles settle through seawater at ~35 m yr^{-1}, and discs (broadside down) settle approximately 4x more slowly (~10 m yr^{-1}). Hence 2 μm diameter particles have a mean residence time of 2.4 to 8.5 years in a 85 m photic zone, which equates to a first order rate constant k = 0.12-0.42 yr^{-1} or approximately 0.0003-0.001 day^{-1} (Table SI-7). Much lower first order rate constant values (0.00007 day^{-1}) are derived from the scavenging turnover time for *filterable* Fe (70 years; Libes, 2009) but rather higher rate constant values (0.008 day^{-1}) are derived from the residence time for particles in the ocean (0.365 yr^{-1}; Balistrieri *et al.*, 1981). Higher rate constants equate to faster losses of iron and an intermediate value of 0.001 day^{-1} will be used in the models presented here to quantify the removal of attached nanoparticulate Fe.

Nanoparticles in seawater may also be removed from surface waters by scavenging through impacts with coarser grains and organic matter (marine snow). The sinking rate for coarse particles is relatively fast, and Pilskaln *et al.* (1998) estimate that particles 500-5000 µm in diameter in surface waters (at 100 m depth) sink at rates of 13-25 m day^{-1} (see also Aumont and Bopp, 2006), equivalent to a first order rate constant of 0.2-0.4 day^{-1}. The models presented here will use a mean rate constant of 0.25 day^{-1} (Table SI-7), which is roughly consistent with the short residence times observed for iron (equivalent to first order rate constants of 0.02-0.17 day^{-1}) due to aggregation and sinking in near surface waters impacted by dry dust deposition (Croot *et al.*, 2004). However, sinking may be much faster for nanoparticles that are incorporated into faecal material. Libes (2009) has collated data that show the sinking rates of faecal pellets from copepods (5-22 m day^{-1}), euphasiids or krill (16-862 m day^{-1}), appendicularians (25-166 m day^{-1}) and chaetognaths (27-1313 m day^{-1}). The slowest sinking rates produce rate constants of 0.1 day^{-1} and the fastest sinking rates (krill and chaetognaths faecal pellets) produce maximum rate constants of 10-15 day^{-1}. Turner (2002) gives comparable sinking rates (16-370 m day^{-1}) for marine snow. A range of 0.1-12 day^{-1} is used for the rate constants of faecal pellet and organic matter scavenging in the following models (Table SI-7). Note that the release of dissolved iron from the remineralisation of faecal pellets (Balzano *et al.*, 2009) is assumed to be negligible within the photic zone, as also is the return of dissolved iron (from any source) from deeper waters to the photic zone by turbulence or upwelling.

Table SI-7 Rate constants for the formation and loss of bioavailable iron from the photic zone.

Process	Rate Constant (day^{-1}) for 0-5 °C	Rate constant (day^{-1}) for 10-12 °C	Rate Constant (day^{-1}) for 20-25 °C
Sinking and Scavenging: Fine grains (<2µm) Coarse grains (>2µm) Faecal Pellets	 0.001 0.25 0.1-12	 0.001 0.25 0.1-12	 0.001 0.25 0.1-12
Transformation	0.003	0.005	0.01
Dissolution	0.0007-0.003	0.0015-0.0057	0.003-0.0115
Siderophore-aided Dissolution	0.04-0.1	0.08-0.2	0.16-0.41
Photochemical Reduction and Grazing	0.1	0.1	0.1

In addition to physical processes that act to remove nanoparticulates from surface waters, transformation alters ferrihydrite to less reactive (oxyhydr)oxides. Schwertmann *et al.* (2004) estimate the half-life for the conversion of ferrihydrite to goethite/haematite mixtures as approximately 60 days at pH 8 and 24°C, equivalent to a rate constant of 0.01 day^{-1}. Cornell and Schwertmann (2003) state that the conversion rates are considerably slower at low temperatures. If rates approximately halve for each 10°C decrease in temperature, then the transformation rate constant at 10-12°C is 0.005 day^{-1} and at 5°C would be approximately 0.003 day^{-1} (Table SI-7).

Estimation of Rate Constant Values for the Formation of Bioavailable Fe. This section presents an amended set of the rate constants utilised by Raiswell (2011b) for estimating the production of bioavailable Fe from iron (oxyhydr)oxides by dissolution, siderophore-aided dissolution, photochemical reduction, and grazing. It is assumed that the uptake of bioavailable iron is controlled by rates of supply and not by the kinetics of the uptake processes acting at the cell surface that transport iron within the cell (but see Hudson and Morel, 1990).

(a) Dissolution. Kuma *et al.* (1992) and Kuma and Matsunaga (1995) give rate constants for the dissolution of ferrihydrite (aged for 1 week before dissolution) at the pH of seawater as 0.015 and 0.008 day^{-1} respectively at 20°C. These are first order rate constants with respect to particulate ferrihydrite concentrations, which are here assumed to be proportional to the mass of ferrihydrite (M_t) at any time t after dissolution is initiated. Rose and Waite (2003) found much higher dissolution rate constants for ferrihydrite by the siderophore DFOB in seawater at 25°C and in the absence of light (20 day^{-1} after aging for 1 minute, 0.4 day^{-1} after aging for one week). Rose and Waite (2003) argued that the smaller values found by Kuma *et al.* (1992) represent a mean value for the dissolution rate constant over the 12 days that the experimental data were collected. Thus, the Rose and Waite (2003) rate constants may more accurately reflect the instantaneous dissolution of fresh Fe nanoparticles immediately following their addition to seawater. The mean rate constant of 0.0115 day^{-1} (Kuma *et al.*, 1992; Kuma and Matsunaga, 1995) is preferred here (Table SI-7) as being more appropriate in the absence of siderophores and because the kinetic models presented here will explore rates of bioavailable Fe delivery over relatively long time spans (up to 100 or 365 days). However, Rose and Waite (2003) make a valuable point in arguing that rate constants decline with time and it is necessary to derive a time-dependant age correction for the mean rate constant used here.

Raiswell *et al.* (2010) showed that the rate constant for the dissolution of ferrihydrite by ascorbic acid declined as a power function of time ($t^{-0.6}$) over 100 days, and this time function is therefore applied to successive time increments of 0-10, 10-20, 20-50, 50-75 and 75-100 days. Using the end time in each increment suggests that the rate constant for the dissolution of ferrihydrite declines proportionately from 1 (0-10 days), 0.66 (10-20 days), 0.38 (20-50 days), 0.30 (50-75 days) to 0.25 (75-100 days) and thus range from a maximum of 0.0115 day^{-1} to a minimum of 0.003 day^{-1} in the 75-100 day interval (Fig. SI-7). Note that these data mainly reflect aggregation effects (Yoshida *et al.*, 2002; Kuma and Matsunaga, 1995; Raiswell *et al.*, 2010) and do not accommodate mineralogical transformations. Temperature corrections assume that the rate of dissolution doubles for each 10°C increase (Table SI-7).

(b) Siderophore-aided Dissolution. Siderophores may enhance photochemical reduction by assisting the efficient transfer of Fe(II) into solution (Borer *et al.*, 2005, see Supplementary Information SI-5), but only the influence on dissolution is considered here. Rose and Waite (2003) show that rate constants for the dissolution of ferrihydrite by DFOB decrease over 7 days and fit a power function of time ($t^{-0.37}$), reaching a minimum of 0.41 day^{-1}. This value is here assumed to represent a mean value for the time increment of 0-10 days and is here corrected for longer time intervals using the Rose and Waite (2003) power function. Applying this function to the end time in successive time increments of 0-10, 10-20, 20-50, 50-75 and 75-100 days gives values that decline in the following proportions relative to 0.41 day^{-1}; 1 (0-10 days), 0.77 (10-20m days), 0.55 (20-50 days), 0.48 (50-75 days) and 0.43 (75-100 days). These corrections produce rate constants that range from a maximum of 0.41 day^{-1} to a minimum of 0.16 day^{-1} in the 75-100 day interval, with temperature corrections applied as above (Fig. SI-7).

(c) Photochemical reduction of aqueous organic Fe^{3+} complexes can produce bioavailable Fe^{2+}, and organic complexes on the surface of Fe(III) minerals may also facilitate photochemical reduction. Efficient transfer of Fe^{2+} to solution requires that oxidation before release from the surface is prevented (Barbeau, 2006). Measurements of rates of photochemical reduction of iron (oxyhydr) oxides in seawater at pH 8 vary significantly with different experimental conditions and especially, for iron (oxyhydr)oxides, with different mineralogies and morphologies. Johnson *et al.* (1994) and Hudson *et al.* (1992) reported relatively high values for the first order rate constant of 20 day^{-1} and 7.2 day^{-1} respectively,

but substantially lower values of 0.05 to 0.43 day^{-1} were found by Wells *et al.* (1991), Voelker and Sedlack (1995) and Barbeau *et al.* (1996). Relatively high values provide good fits to experimental photochemical studies of seawater (Johnson *et al.*, 1994; Miller *et al.*, 1995), but Moffett (2001) preferred the lower values and suggests that these differences may partly arise because the (oxyhydr)oxides used by Wells *et al.* (1991), Voelker and Sedlack (1995) and Barbeau *et al.* (1996) were treated by heating or dialysis prior to experimentation, and were thus more crystalline and less reactive (see Supplementary Information SI-5).

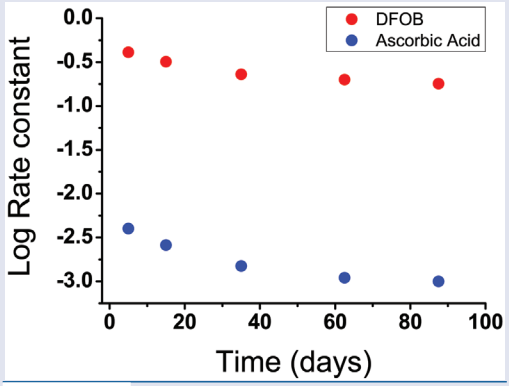

Figure SI-7 Variations in the logarithm of the rate constants (day^{-1}) with time (using midpoint values for each time increment) for the dissolution of ferrihydrite by ascorbic acid and DFOB. Data from Raiswell *et al.* (2010) and Rose and Waite (2003).

Wells *et al.* (1991) and Voelker and Sedlack (1995) determined rate constants for the maximum (noon-time) photochemical reduction of Fe in ferrihydrite as approximately 0.43 day^{-1}, but rates declined exponentially with depth as a result of light attenuation and were well below the maximum for most of the day (or on cloudy days or at night). Barbeau *et al.* (1996) compared the rates of photochemical reduction with rates of protozoan-mediated dissolution (for which a first order rate constant of 0.05 day^{-1} was estimated). This ferrihydrite was aged by heating to 50°C (which decreases reactivity) and is an order of magnitude smaller than the maximum rate constant for photochemical reduction. The models constructed here will assume a rate constant of 0.1 day^{-1} bearing in mind that photochemical reactions in the models

are assumed to occur throughout the day and that diminished photochemical reactivity occurs on cloudy days. This choice is rather arbitrary but it is clear that photochemical reduction is more rapid than simple dissolution. Activation energies for photochemical reactions are generally low and corrections of rate constants for temperature changes are small enough to be ignored in the present context (Appelo and Postma, 2007).

(d) Grazing. Protozoan grazing (see Supplementary Information SI-1) may be at least as effective at supplying bioavailable Fe as photochemical reduction when integrated temporally over the entire photic zone (Barbeau *et al.*, 1996; Barbeau and Moffett, 2000). Barbeau *et al.* (1996) estimated a first order rate constant of 0.05 day^{-1} for the protozoan-mediated dissolution of a ferrihydrite aged by heating to 50°C, suggesting that non-aged material would have a higher rate constant with roughly the same quantitative effects as photochemical reduction. There is much uncertainty in the rate constant data for photochemical reduction and grazing and the models will assume that a rate constant of 0.1 day^{-1} will demonstrate the combined effects of both processes. No temperature corrections are applied for the same reason. The loss processes that occur when grazing causes incorporation into faecel pellets can be modelled by using the range in rate constants (0.1-12 day^{-1}) for faecal pellet scavenging (see above).

The rate constants for the supply processes at 25°C range from 0.41 to 0.003 day^{-1} compared to 12 to 0.001 day^{-1} for the loss processes. Note that the values that will be used for k_L and k_B in the model calculations are each the sum of one or more processes. Although the model is described in terms of specific processes, it is in fact generic and essentially examines the impact of a range of any loss processes (with rate constants ranging from to 12 to 0.001 day^{-1}) on the production of bioavailable Fe by any supply processes (with rate constants 0.41 to 0.003 day^{-1}). The range of rate constant values for the removal processes are more than an order of magnitude larger than for the supply processes in order that the estimates for the rates of bioavailable Fe formation should be conservative. The model clearly requires improved data for the rate constants particularly for photochemical reduction, scavenging and the complex effects of grazing (on the removal and production of bioavailable Fe). However, the model will be used in main text Sections 5.5 and 6.4 to quantify the delivery of bioavailable Fe from aeolian dust and icebergs.

GLOSSARY

Used Numerical Terms

Terms	Description	Units
B_i	Mass of bioavailable Fe formed from nanoparticulate Fe	Mass
c	Sediment concentration	kg kg^{-1}
DOP	Degree of Pyritisation	No units
F	Flux into a reservoir	Mass $time^{-1}$
F_i	Input flux or fluxes	Mass $time^{-1}$
F_o	Output flux or fluxes	Mass $time^{-1}$
F_A	Flux of nanoparticulate Fe	Mass $time^{-1}$
F_B	Input flux of bioavailable Fe	Mass $time^{-1}$
F_L	Output flux of nanoparticulate Fe	Mass $time^{-1}$
FeA	Fe soluble in ascorbic acid	Percent
FeD	Fe soluble in dithionite	Percent

Terms	Description	Units
F_{sol}	Flux of soluble Fe	kg day^{-1}
f	Nanoparticulate Fe content	kg kg^{-1}
{H^+}	Hydrogen ion activity	Moles $litre^{-1}$
k	First order rate constant	$Time^{-1}$
k_L	First order rate constant for the output of nanoparticulate Fe	Day^{-1}
k_B	First order rate constant for the input of bioavailable Fe	Day^{-1}
K	Sum of k_L and k_B	Day^{-1}
M_B	Mass of bioavailable Fe plus soluble Fe	Mass
M	Mass in reservoir	Mass
M_o	Mass in reservoir at initially at t = 0	Mass
M_t	Mass in reservoir at time t	Mass
(O_2)	Concentration of dissolved oxygen	Moles $litre^{-1}$
R	Residence time	Time
S	Rate of sediment addition	kg day^{-1}

Used Terms and Definitions

Anaerobic	A metabolism not utilising oxygen.
Anoxic	Dissolved oxygen absent.
Anoxygenic photosynthesis	The photosynthetic production of organic biomass without the liberation of oxygen.
Aerobic	A metabolism utilising oxygen.
Benthic Chamber or Lander	An instrumented chamber installed at the sediment surface to measure the exchange of dissolved species between the sediment and the overlying seawater.
BIF	Banded Iron Formation. Laminated iron-rich (containing 15% Fe or more) chemical sedimentary rock predominantly found in the Precambrian.
Biogeochemical cycle	Describing the cycling of elements as promoted by combined geological and biological processes.

Bioturbation	The displacement and mixing of sediment grains and aqueous species by organisms.
Colloid	A particle having a diameter of 0.01 to 1 μm (10 to 1000 nm).
Competitive Ligand Exchange	Measures the speciation of a metal by exchange of a complexing ligand with another ligand of known affinity.
Concretion	A volume of sedimentary rock whose porosity is filled with mineral cement.
Cyanobacteria	Oxygen-producing photosynthetic prokaryote.
Diagenesis	The chemical, physical and biological changes that occur in a sediment after deposition but before metamorphism.
Diamictic	A lake which mixes twice during the year in response to water column instabilities resulting from seasonal temperature changes.
DFOB	Desferrioxamine B is a terrestrial siderophore.
Diatoms	A group of algae and one of the most common phytoplankton.
Dissimilatory	Oxidation or fermentation of organic compounds coupled to energy generation for the organism.
Eukaryote	An organism with complex structures enclosed within membranes including a nucleus and various organelles.
Euxinic	Dissolved sulphide present.
Filterable	All material (aqueous, nanoparticulate and colloidal) that passes a 0.2 or 0.45 μm filter.
f_{org}	The proportion of total carbon removed from ocean as organic matter.
Flagellates	Eukaryotic organisms that gain energy by grazing on, and consuming, NOM.
GIF	Granular Iron Formation. Fe-rich sedimentary rock consisting of well-sorted chemical sands lacking continuous even bedding.
GOE	Great Oxidation Event. Describing the significant oxidation of Earth atmosphere between 2.3 and 2.4 billion years ago.
Heterotrophic Organisms	Organisms that obtain energy by digesting organic matter.
Highly reactive iron	The sum of the iron present as (oxyhydr)oxides that are extracted by dithionite plus iron present as sulphides.

HNLC	High Nutrient (or Nitrate) Low Chlorophyll. Regions of the ocean where primary productivity is iron-limited.
Ligand	A molecule that binds to a metal ion to form a coordinate complex.
Metabolism	Set of chemical reactions yielding energy to sustain the life of an organism.
Microbial mat	An accumulation of microbes at a sediment surface, often in the presence of light.
MIF	Mass Independent Fractionation. Isotope fractionation patterns deviating from expected mass fractionation laws.
Molecular clock	Combining palaeontological constraints with molecular sequence data (such as DNA or RNA) to estimate the divergence time of organisms in geologic past.
Nanoparticle	A particle having a diameter of 5 nm to 100 nm.
Nitrogenase	Enzyme complex responsible for the reduction of N_2 to ammonium in some prokaryotes.
NOM	Natural Organic Matter, either marine or terrestrial.
Normal Marine	Marine depositional environment that is fully oxygenated with seawater salinity.
Oxic	Oxygen present.
Oxygenic photosynthesis	Oxygen production through photosynthesis.
PAL	Present Atmosphere Levels.
Photochemical Reduction	A compound that can absorb light which is used to excite an electron which is then used in reduction.
Phylogeny	Describing the evolutionary history of a group of organisms.
Phytoplankton	Free-living photosynthetic organisms that consume carbon dioxide and produce oxygen by photosynthesis.
Primary production	The production of organic biomass from carbon dioxide and water, principally through photosynthesis.
Prokaryote	Single-celled organisms lacking a membrane nucleus, and, with rare exceptions, membrane-bound organelles.
Protozoa	Eukaryotic organisms some of which can gain energy by consuming organic matter.
Redfield ratio	A C/N/P ratio of 106/16/1 representing the average composition of marine plankton as elucidated by Alfred Redfield.

Residence Time	The average amount of time a particle spends in a reservoir.
Reservoir	Reservoirs represent a part of a system which has distinct chemical or physical properties in which material is stored.
Saccharides	Components of marine organic matter (such as sugars) that have an atomic ratio of oxygen: hydrogen of 1:2. Polysaccharides are used to store energy or as structural components.
Siderophores	Low molecular weight chelating ligands with a very high affinity for iron that are secreted by microorganisms.
Stability Constant	An equilibrium constant for the formation of a complex.
Steady State	A reservoir is in a steady state when the addition of material is balanced by losses of material.

INDEX

Geochemical Perspectives is an official journal of the European Association of Geochemistry

The European Association of Geochemistry, EAG, was established in 1985 to promote geochemistry, and in particular, to provide a platform within Europe for the presentation of geochemistry, exchange of ideas, publications and recognition of scientific excellence.

Officers of the EAG Council

President	Bernard Bourdon, ENS Lyon, France
Vice-President	Chris Ballentine, University of Manchester, UK
Past-President	Eric H. Oelkers, CNRS Toulouse, France
Treasurer	Christa Göpel, IPG Paris, France
Secretary	Liane G. Benning, University of Leeds, UK
Goldschmidt Officer	Bernard Marty, CNRS Nancy, France
Goldschmidt Officer	Bernie Wood, University of Oxford, UK

www.eag.eu.com

ROBERT RAISWELL is an emeritus professor of sedimentary geochemistry in the School of Earth and Environment, University of Leeds. Rob's research focuses on the cycling of iron and sulphur in Earth surface environments, past and present. His current research topics include the formation and bioavailability of iron nanoparticles in modern marine and glacial environments and the use of iron minerals to deduce the depositional environments in early Earth history. Outside research, Rob is a keen traveller and has recently trekked in the mountain regions of Nepal, Peru, Arctic Canada, Ecuador, Tanzania and Mongolia. His favourite research sites are in the Polar regions and especially Antarctica (he subscribes to the widely-held view that Antarctica is as much an untreatable disease as a location). He was elected Fellow of the European Association of Geochemistry and the Geochemical Society in 2010.

DONALD E. CANFIELD is the professor of ecology and director of the Nordic Center for Earth Evolution (NordCEE) in the Institute of Biology, University of Southern Denmark. Don has worked at understanding the modern cycles of iron and sulphur, the evolution of these cycles, and their interface with other element cycles, through geologic time. Don's work spans the range of microbial ecology, biogeochemistry, and geology. He can be found at any given time (when not sorting papers) in the lab, with his hands deep in mud, or banging on a rock. His favourite current research sites include meromitic Lake Cadagno in Switzerland and the oxygen-minimum zone off the cost of Chile. He received the European Association of Geochemistry Urey Award in 2011.